AMESBURY TIDAL ENERGY PROJECT
(ATEP)

Integration of the Gorlov Helical Turbine
into an Optimized Hardware/Software System Platform

FINAL REPORT

Prepared by:

Verdant Power, LLC
And
GCK Technology, Inc.

April 30, 2005
(Rev 07.26.05)

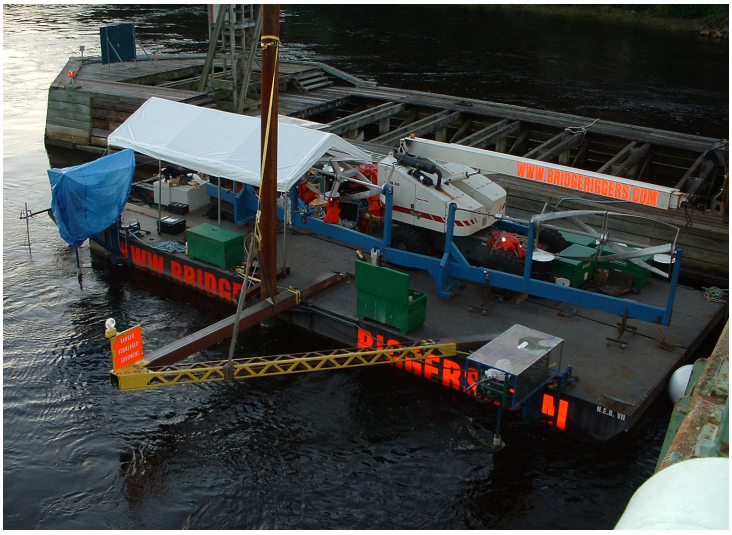

Funded by the Emerging Technology Demonstration Initiative
of the Renewable Energy Trust

MASSACHUSETTS
TECHNOLOGY
COLLABORATIVE

NOTICE

This report was prepared by Verdant Power, LLC in the course of performing work sponsored by the Renewable Energy Trust (RET), as administered by the Massachusetts Technology Collaborative (MTC), pursuant to grant number # ET-04-4. The opinions expressed in this report do not necessarily reflect those of MTC or the Commonwealth of Massachusetts, and reference to any specific product, service, process, or method does not constitute an implied or expressed recommendation or endorsement of it.

Further, MTC, the Commonwealth of Massachusetts, and the contractor make no warranties or representations, expressed or implied, as to the fitness for particular purpose or merchantability of any product, apparatus, or service, or the usefulness, completeness, or accuracy of any processes, methods or other information contained, described, disclosed, or referred to in this report. MTC, the Commonwealth of Massachusetts, and the contractor make no representation that the use of any product, apparatus, process, method, or other information will not infringe privately owned rights and will assume no liability for any loss, injury, or damage directly or indirectly resulting from, or occurring in connection with, the use of information contained, described, disclosed, or referred to in this report.

ABSTRACT

Verdant Power, LLC (VP) has conducted a study of the Gorlov Helical Turbine (GHT) hydropower turbine and associated systems pursuant to Agreement# ET-04-4.

The purpose of these studies was to empirically characterize the hydrodynamic performance of the 1-m diameter GHT, and develop balance-of-system designs including mechanical drivetrain and electrical generator systems to demonstrate the potential for GHT power generation.

The Gorlov Helical Turbine (GHT), developed by Dr. Alex Gorlov, was fabricated by GCK Technology, Inc. There have been GHT deployments in Massachusetts (Cape Cod), Maine, New York (Shelter Island), South Korea, and Brazil. Still, there has been a shortage of wide-range quantitative data that characterizes the performance of the GHT rotor. This information is essential to designing and implementing the balance-of-system mechanical and electrical components for an efficient "water-to-wire" system solution, and to making the economic projections required for commercial deployment of this technology.

In the present study, four GHT turbine systems were built and deployed in the Merrimack River in Amesbury, Mass. Dynamometry was performed on the GHT rotor and its power curve and efficiency were determined. Generator system versions were built, deployed and tested for water-to-wire efficiency and turbine interactions. Potential impacts on fish were monitored as part of the testing. Areas for performance improvement, potential economic deployment, and future research were identified.

KEYWORDS

hydro power	Gorlov Helical turbine	fish impact
renewable energy	underwater turbine	dynamometry
tidal energy	cross-flow turbine	power curve
distributed generation	Verdant Power	rotor efficiency
kinetic hydro power	Amesbury	load matching

Table of Contents

Figures

Tables

List of Abbreviations

Variable	Description	Typical Units
A	area	m^2, ft^2
C	is the blade chord	
Cp	Coefficient of Performance (= η_{rotor})	% (dimensionless)
D	rotor diameter	m, ft
η_{drive}	efficiency of the drivetrain, including shaft bearings and gearbox	%
η_{gen}	efficiency of the generator	%
η_{lm}	efficiency of the load-matching of the load to the rotor at a given **Vw**	%
$\eta_{w\text{-}w}$	Overall water-wire efficiency (= **Cp** * η_{lm} * η_{drive} * η_{gen})	%
N	number of blades in the rotor	(dimensionless)
PPPP	Peak Practical Power Point *This point is the greater of the power at the peak of the power curve fit, or if the rotor stalls before the peak of the curve, the highest power reasonably achieved prior to stall.*	**Ω** and P
R	electrical resistance	Ohms
Re	Reynolds Number *represents the ratio of the fluid's inertial and viscous forces*	(dimensionless)
σ	Solidity (= NC/**π**D)	% (dimensionless)
Ω	turbine rotation rate	rpm, rad/sec
Ω_{NL}	turbine rotation rate, at no load	rpm, rad/sec
Ω_{PP}	turbine rotation rate, at peak power	rpm, rad/sec
Vw	waterspeed *the magnitude of the velocity vector*	m/s, kn, fps
V	voltage	
V_{NL}	no-load voltage	
X	Tipspeed ratio **(= ΩR/Vw)**	(dimensionless)

PROJECT OVERVIEW

Over the period of the study, four turbines with GHT rotors were installed on a barge docked in the Merrimack River alongside the center fender of the Newburyport/Amesbury Bridge, and shown in the drawing, Figure 1 and photos, Figure 2 and Figure 3.

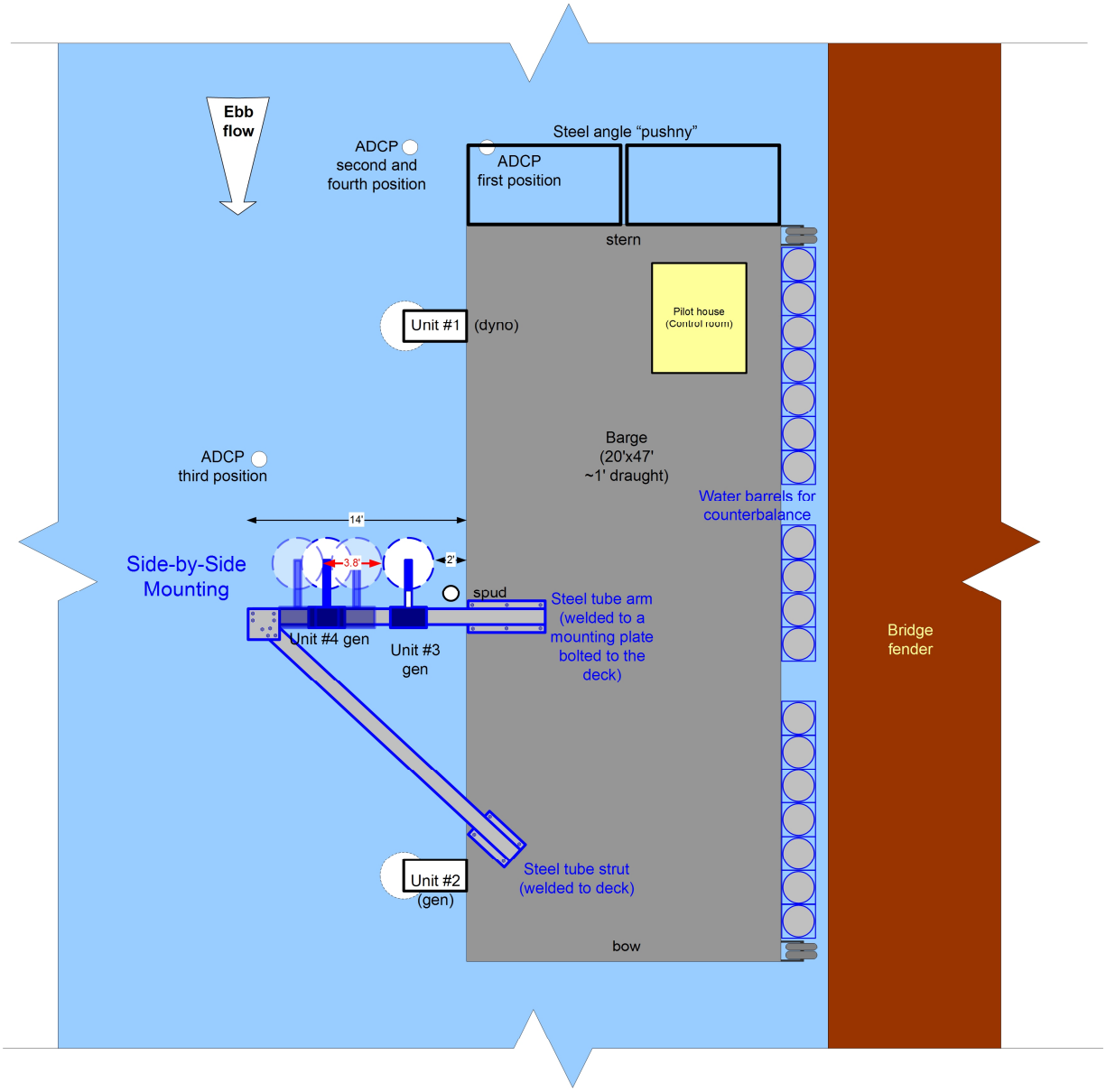

Figure 1 ATEP Barge Layout (Turbines #1 - #4)

The Merrimack River ATEP site has a depth of approximately 8 m (26 ft) and is partially tidal, with ebb tide currents reaching just over 1.5 m/s (2.9 kn) during the testing months of September and October. The site is described in detail in Appendix A, Site Selection and Characteristics.

Figure 2 View of the Bridge Fender from the Newburyport/Amesbury Bridge

The GCK rotors tested are nominally 1 meter in diameter and 2.5 meters in length overall, with a nominal 2.5 m^2 frontal area. They have a vertical axis with 3 blades made of aluminum airfoil-shaped extrusions with 5.5 inch (140mm) chords. The blades are inclined at 67 degrees from the horizontal, and mounted via spoke arms and central hubs to an aluminum hex-shaped shaft.

Based on information provided by GCK, VP used the nominal expected performance of the GHT rotor in the Merrimack River, as is shown in Table 1, to design and build frames, bearings, barge supports, and dynamometry and electrical generation loading systems.

Table 1. Nominal Expected Performance of the GHT Rotor

Merrimack River	**Waterspeed**		**Power, max**	**Torque**			**Rotor speed** (@max power)	
flow	kn	fps	kW	Nm	ft-lbs	in-lbs	rpm	rad/s
nominal	**4**	**6.8**	**3.6**	**408**	**301**	**3611**	**84**	**8.8**

The full range of Merrimack River conditions considered for the design of the turbine systems is contained in the Summary of Testing Protocols, Appendix D.

The rotors were assembled and mounted to the VP frames in the workshop of Larry's Marina, nearby, beginning on 8/2/04. The assembly of the turbines with the frames, designed and built by Verdant Power, is described in more detail in Appendix B.

Figure 3. ATEP Platform Tied Up to Newburyport/Amesbury Bridge Fender

TURBINE #1 – DYNAMOMETRY AND TURBINE #2 – GENERATION

The first deployment included two turbines, #1 and #2. Turbine #1 drove a prony brake and was instrumented to provide dynamometry data in order to fully characterize the behavior of the rotor at any possible loading. Turbine #2 drove a belt and pulley speed increaser and an electrical generator loaded by an adjustable resistive loadbank.

Turbine Frames

Verdant Power, LLC has patents pending on the technology described below:

The rotor support frames for the first two units were comprised of two submerged arms that support the rotor bearings, welded to a vertical column. These members are made substantially of welded steel plate with triangular cross-sections in order to minimize interference with the water flow.

The column is held to the barge within a clamp that holds the column in any vertical location from entirely above the water to fully submerged, at which point the top of the rotor is about 18" below the water surface. The triangular column is held captive to the outside of the barge clamp and held in vertical position by lockscrews. The inside of the barge clamp has upper and lower

pairs of arms that clamp from the bottom of the barge to the deck. Once secured, these are tack-welded in place for additional security.

The VP-designed bearings which hold the rotors are water-wetted – designed for use underwater without protection from the water. They are comprised of acetal plastic radial bushings and thrust washers secured to the rotor shaft by clamp blocks, and run against stainless steel races.

The initial deployment of the barge, with the first two turbines on board took place on 8/10/04.

Operation

As described in detail in the Summary of Testing Protocols, Appendix D, Turbine #1 was loaded variably via the brake from no-load until rotor stall at varying waterspeeds while torque and rotation rate data was taken.

Turbine #2 was operated to generate DC power and loaded by a loadbox with varying resistance while voltage and current data was recorded.

TURBINES #3 AND #4

ATEP GHT Units #3 and #4 were gearbox-driven generator units. They were mounted side-by-side on frames hung from an arm extending outward, perpendicular to the side of the barge, as shown in Figure 1. This allowed the turbines to be tested with variable spacing across the flow, from near-zero separation to a separation of over four feet (more than one turbine diameter of 1m). The purpose of the side by side mounting was to explore Dr. Gorlov's concept that two turbine rotors may interact synergistically when spaced closely across the flow.[1]

Structure

The side-by-side turbine frames were mounted from a cross arm extending 14ft (4.27m) over the water from the side of the barge. The cross arm and a diagonal stiffening strut were made from 10" x10" (254mm x 254 mm) steel tubes welded to angles welded to the barge deck. They are bolted together at the outboard end using steel plates which also held a turning block for the steel cable used to pull the turbine frames crosswise, a mounting for a guy to the raised starboard spud for stiffening and an operator safety line. Each piece of the assembly was moved into place using the barge lift.

Because the assembly extends significantly beyond the barge crosswise into the river, the U.S. Coast Guard and Amesbury Harbor Police required a warning sign and light on the end of the arm and two channel markers (buoys) so as to effectively close the adjacent channel under the swing bridge.

[1] Gorlov, Alex, **"Harnessing Power from Ocean Currents and Tides**." In *Sea Technology*, July 2004, pp. 40 - 43.

Turbine Frames

Turbine frames with an orientation 90 degrees from the first two were built, as their mounting on the cross arm was at right angles to the side of the barge as shown in Figure 1. Also, these two frames were designed to be mounted directly on the arm, as opposed to the first two turbine units which are mounted to the side of the barge using clamps. The frames themselves have single-sided arms supporting the rotor shaft bearings as before, but the frame arms point upstream, rather than across the stream, and because they do not present their sides to the flow, they were made using 4"x6" (1.2m x 1.8m) rectangular steel tube rather than triangular cross-sections made from plate. The bearing arms are welded to a new frame column that uses 4"x12" rectangular steel tubing aligned with the flow. The column has welded side members that rest on the 10"x10" (254mm x 254mm) cross arm, capturing it on three sides, and forming a clamp that can be repositioned and locked at different points along the cross arm using lock bolts.

One further change from units #1 and #2 was that both up and down thrust bearings (acetal plastic in stainless steel races) were located within the upper radial bearing housing rather than having one on each end. This allows free axial movement of the rotor from the top bearing downward, which would reduce any vertical vibration component, if any, from being transmitted from the rotor to the frame structure. (As it turned out, vertical driving forces were not the source of the vibrations found in units #1 and #2; see the Conclusions Section.)

Operation

Turbines #3 and #4 were operated to generate DC power and loaded by loadboxes with varying resistances while voltage and current data was recorded and power calculated.

As described in detail in the Summary of Testing Protocols, Appendix D, these turbines were started electrically, and the output of each turbine was tested with different crosswise spacings at different current speeds. Also, Turbine #3 was directly downstream from Turbine #1, and the simultaneous operational downstream interaction of the two was studied.

Testing was performed using the ebb tide current which is stronger and has less short-term fluctuation than the flood tide currents. Since the #3 and #4 turbine rotors are positioned upriver of the frame columns, they are also upstream during ebb, and meet the current prior to any flow interference from the frame columns.

RESULTS

DYNAMOMETRY

Turbine #1 with the dynamometry loading was used to fully characterize the performance of the GHT rotor and its power-optimal loading at every waterspeed encountered (between 0.589 and 1.541 m/s). Note that the maximum encountered waterspeeds, which are below historical averages for the waterway, are at the minimum range of waterspeed for which the GHT rotor is designed.

For this study, the testing is described in Summary of Testing Protocols, Appendix D, and the raw DACS data was processed and carefully selected according to ATEP Data Processing, Appendix E, to provide the basis for determining rotor performance. The dynamometry phase produced 10,499 valid data points as shown in the water data distribution shown in Figure 4.

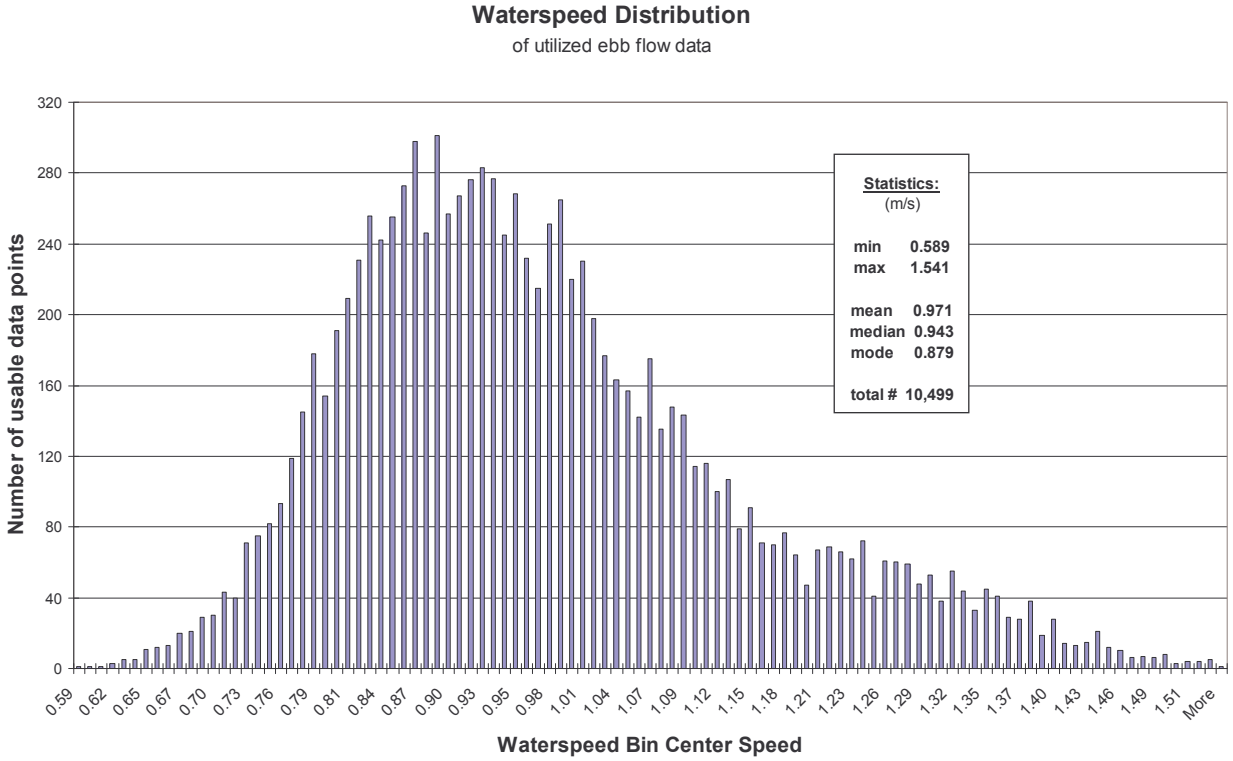

Figure 4. Waterspeed Distribution Histogram of Usable Datapoints

In order to determine the operating curve of the rotor at each waterspeed, this data was sorted by waterspeed. Thus, all of the data from the entire testing period was combined. This process essentially averages large amounts of data eliminating short-term variations due to waterspeed fluctuations, rotor momentum, and sensor noise. For each waterspeed, **Vw**, data within a narrow bin of waterspeeds is grouped, and a plot of power P vs. rotation rate, $\boldsymbol{\Omega}$, is made. The power of the turbine, $\mathbf{P_T}$, is the product of torque, $\boldsymbol{\tau}$, and $\boldsymbol{\Omega}$.

$$\mathbf{P = \tau\, \Omega}$$

Accordingly, a second-order polynomial curve fit[2] of this data indicates the rotor's operating curve at that waterspeed. These curves show the increase in torque and power and the decrease in rotor speed with increased brake load until rotor stall occurs.

Forty-three such operating curves were generated, at each 0.02 m/s from **V**= 0.66 m/s to 1.50 m/s. Two such graphs, for waterspeeds of 0.70 and 1.30 m/s are shown below in Figure 5 and Figure 6. The full set of 43 power curve graphs is contained in Appendix F.

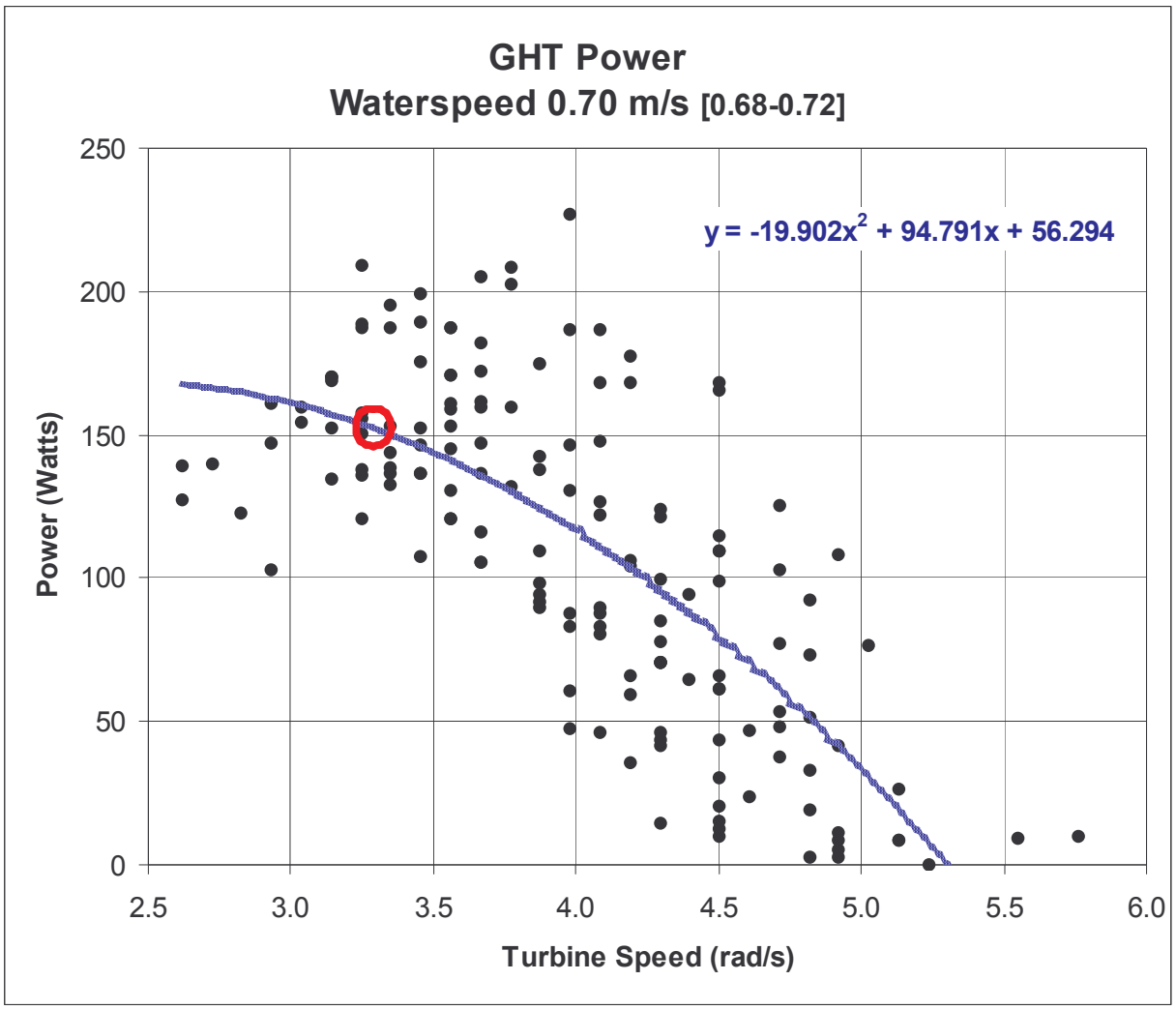

Figure 5. GHT Power Curve for V=0.70m/s

[2] Curve fits used Microsoft Excel least-squares regression functions.

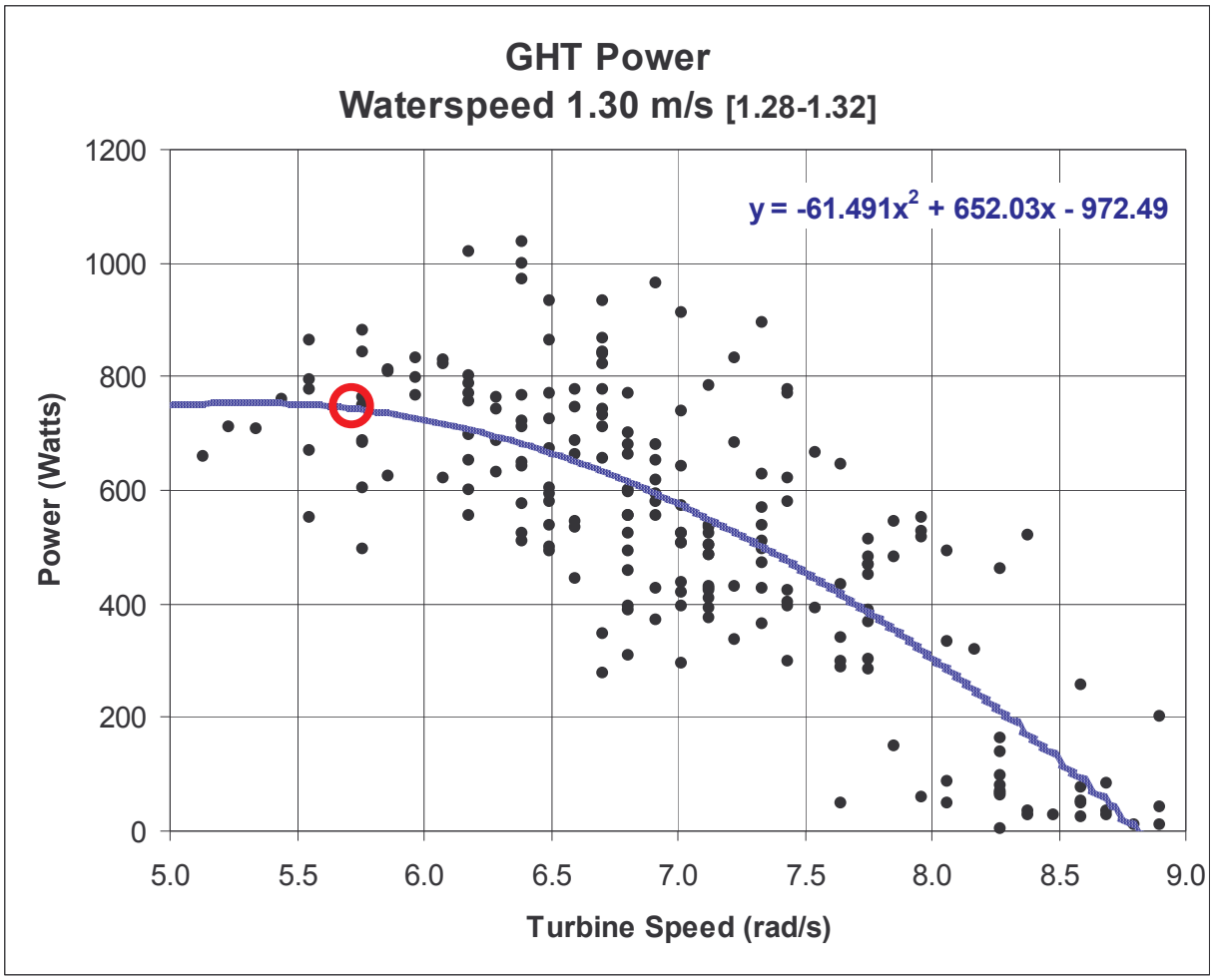

Figure 6. GHT Power Curve for V=1.30m/s

To each of these graphs, a red circle has been added indicating what we have termed the "Peak Practical Power Point" (**PPPP**). This point is either:

1) the power at the peak of the curve, or if the rotor stalled before the peak of the curve,
2) the highest power reasonably achieved prior to stall,

whichever is greater

The **τ**, and **Ω** at this point is the optimal operating point of the rotor at that waterspeed. The plot of all of these points relative to waterspeed is the overall operating curve of the rotor.

A table summarizing the GHT Dynamometry results is shown in Table 2.

Based on the rotor blades' flow-aligned chord length of 6 inches (0.15 m), the Reynolds numbers (**Re**) ranged from 90,000 at **Vw** = 0.6 m/s to 225,000 at **Vw** = 1.5 m/s. Therefore, at all waterspeeds the rotor flow was turbulent.

A number of rotor characteristics are derived from this data. Foremost, is the determination of the efficiency, or **Coefficient of Performance**, **Cp**, of the rotor. The **Cp** is defined as the ratio of mechanical power output of the rotor divided by power in the flowing water that is intercepted by the turbine.

$$\mathbf{Cp} = \mathbf{P_T}/\mathbf{P_W}$$

Where $\mathbf{P_W}$ is the power from the kinetic energy of the flowing water,

$$\mathbf{P_W} = 1/2\boldsymbol{\rho}\mathbf{A}\mathbf{V}^3$$

where $\boldsymbol{\rho}$ is the density of the water and **A** is the frontal area of the turbine. It should be noted that in this report, the nominal dimensions of the turbine (1m x 2.5m) were used[3].

The no-load rotation rate, $\boldsymbol{\Omega}_{NL}$, was also determined. Because a zero $\boldsymbol{\Omega}$ is not necessarily uniquely defined in terms of torque, data with zero $\boldsymbol{\Omega}$ was not included in the data sets. In order to find the no-load rotation rate, $\boldsymbol{\Omega}_{NL}$, at each waterspeed, the equation for the power curve was solved for the $\boldsymbol{\Omega}$ at **P** = 0. The results are shown in Table 2 and in the graph, in Figure 7.

The tipspeed ratio, **X**,

$$\mathbf{X} = \boldsymbol{\Omega}\mathrm{R}/\mathrm{V}$$

was calculated for the **PPPP**s and for the no-load condition. This is important information in general, for both rotor and balance-of-system design. The results are shown in Table 2.

[3] Since 1.0 meter is actually the diameter of the rotor blade centerline, the actual diameter was greater by about 3 cm. Adjusting for this factor would slightly decrease the Cp by about 3% (of the reported value). The height of the rotor is nominally and actually 2.5 m. Since the entire turbine which includes the frame, a larger frontal area could be used for the **Cp** calculation which would also decrease the Cp somewhat. A frame is, after all, necessary to hold a rotor in any practical application. Which value to use for the additional area could be the subject of much discussion. In this case, since the GHT rotor was of primary interest, the area of the VP frames was not included in the **Cp** calculation. Furthermore, the frames were designed to have the most minimal shapes required to hold the rotors with adequate strength and rigidity, and presented minimal resistance to the flow and neither detracting from nor augmenting the flow entering or leaving the rotor. Specifically, the frame arms that hold the rotor bearings extend above and below the rotor for a total height of 2.74 m (108 inches). Since they project crosswise to the stream (48 inches), the arms on frames #1 and #2 present more area to the flow than to the streamwise arms of frames #3 and #4. Additionally, the vertical frame columns for frames #1 and #2 that held the arms could be included in the area. (The columns for frames #3 and #4 were downstream of the rotor area.) The **Cp** results could be recalculated using justifiable modifications to the effective area, with slightly lowered **Cp** results.

Table 2 Summary of GHT Dynamometry Performance

	Summary GHT Performance											
	No Load			Practical Peak Power Points							Stall	
Waterspeed	Omega	Omega	X	Omega	Power	Torque	Omega	X	P_{water}	Cp	*estimate*	Waterspeed
m/s	rad/s	rpm	X=WR/V	rad/s	Watts	Nm	rpm		Watts	%	rpm	m/s
1.50	9.72	92.8	3.24	7.0	783	111.8	67	2.33	4219	18.6	64.9	1.50
1.48	9.42	90.0	3.18	6.8	841	123.7	65	2.30	4052	20.8	64.0	1.48
1.46	9.40	89.8	3.22	6.7	847	126.5	64	2.29	3890	21.8	62.1	1.46
1.44	9.55	91.2	3.32	6.7	847	126.5	64	2.33	3732	22.7	62.1	1.44
1.42	9.31	88.9	3.28	6.5	814	125.3	62	2.29	3579	22.8	60.2	1.42
1.40	9.09	86.8	3.25	6.4	788	123.1	61	2.29	3430	23.0	58.3	1.40
1.38	9.17	87.5	3.32	5.9	843	142.9	56	2.14	3285	25.7	54.4	1.38
1.36	9.10	86.9	3.35	5.7	845	148.2	54	2.10	3144	26.9	53.5	1.36
1.34	8.98	85.7	3.35	5.7	846	148.4	54	2.13	3008	28.1	53.5	1.34
1.32	8.80	84.1	3.33	5.5	804	146.1	53	2.08	2875	27.9	50.6	1.32
1.30	8.81	84.1	3.39	5.7	746	130.9	54	2.19	2746	27.2	53.5	1.30
1.28	8.66	82.7	3.38	5.5	712	129.4	53	2.15	2621	27.2	49.7	1.28
1.26	8.53	81.5	3.39	5.5	692	125.8	53	2.18	2500	27.7	48.7	1.26
1.24	8.51	81.3	3.43	5.3	666	125.7	51	2.14	2383	28.0	48.7	1.24
1.22	8.38	80.1	3.44	5.3	623	117.5	51	2.17	2270	27.4	48.7	1.22
1.20	8.31	79.3	3.46	5.2	584	112.4	50	2.17	2160	27.1	47.7	1.20
1.18	8.36	79.8	3.54	5.0	546	109.3	48	2.12	2054	26.6	46.8	1.18
1.16	8.25	78.8	3.56	4.9	505	103.1	47	2.11	1951	25.9	45.8	1.16
1.14	7.72	73.8	3.39	4.7	501	106.6	45	2.06	1852	27.1	43.9	1.14
1.12	7.57	72.3	3.38	4.7	457	97.3	45	2.10	1756	26.0	43.9	1.12
1.10	7.51	71.7	3.41	4.7	379	80.6	45	2.14	1664	22.8	42.0	1.10
1.08	7.30	69.7	3.38	4.8	349	72.6	46	2.22	1575	22.1	41.1	1.08
1.06	7.08	67.6	3.34	4.6	337	73.2	44	2.17	1489	22.6	40.1	1.06
1.04	7.00	66.8	3.36	4.5	305	67.7	43	2.16	1406	21.7	37.2	1.04
1.02	6.99	66.8	3.43	4.5	272	60.4	43	2.21	1327	20.5	34.4	1.02
1.00	6.84	65.3	3.42	4.4	259	58.8	42	2.20	1250	20.7	34.4	1.00
0.98	6.64	63.5	3.39	4.4	244	55.5	42	2.24	1176	20.7	32.5	0.98
0.96	6.58	62.8	3.43	4.2	230	54.7	40	2.19	1106	20.8	31.5	0.96
0.94	6.51	62.2	3.46	4.0	219	54.7	38	2.13	1038	21.1	31.5	0.94
0.92	6.33	60.4	3.44	4.0	210	52.6	38	2.17	973	21.6	34.4	0.92
0.90	6.05	57.7	3.36	4.1	208	50.8	39	2.28	911	22.9	30.6	0.90
0.88	5.96	57.0	3.39	4.0	195	48.8	38	2.27	852	22.9	28.6	0.88
0.86	5.97	57.0	3.47	3.9	181	46.3	37	2.27	795	22.7	29.6	0.86
0.84	5.84	55.8	3.48	3.9	173	44.4	37	2.32	741	23.4	27.7	0.84
0.82	5.71	54.5	3.48	3.8	165	43.3	36	2.32	689	23.9	26.7	0.82
0.80	5.64	53.8	3.52	3.6	159	44.2	34	2.25	640	24.9	26.7	0.80
0.78	5.52	52.8	3.54	3.5	155	44.3	33	2.24	593	26.1	26.7	0.78
0.76	5.45	52.0	3.58	3.3	152	46.2	32	2.17	549	27.8	27.7	0.76
0.74	5.39	51.4	3.64	3.3	154	46.8	32	2.23	507	30.5	28.6	0.74
0.72	5.34	51.0	3.71	3.3	158	47.9	32	2.29	467	33.9	28.6	0.72
0.70	5.30	50.6	3.79	3.3	152	46.2	32	2.36	429	35.5	27.7	0.70
0.68	5.20	49.7	3.82	3.4	144	42.5	32	2.50	393	36.7	27.7	0.68
0.66	5.27	50.4	4.00	3.1	139	44.9	30	2.35	359	38.8	27.7	0.66

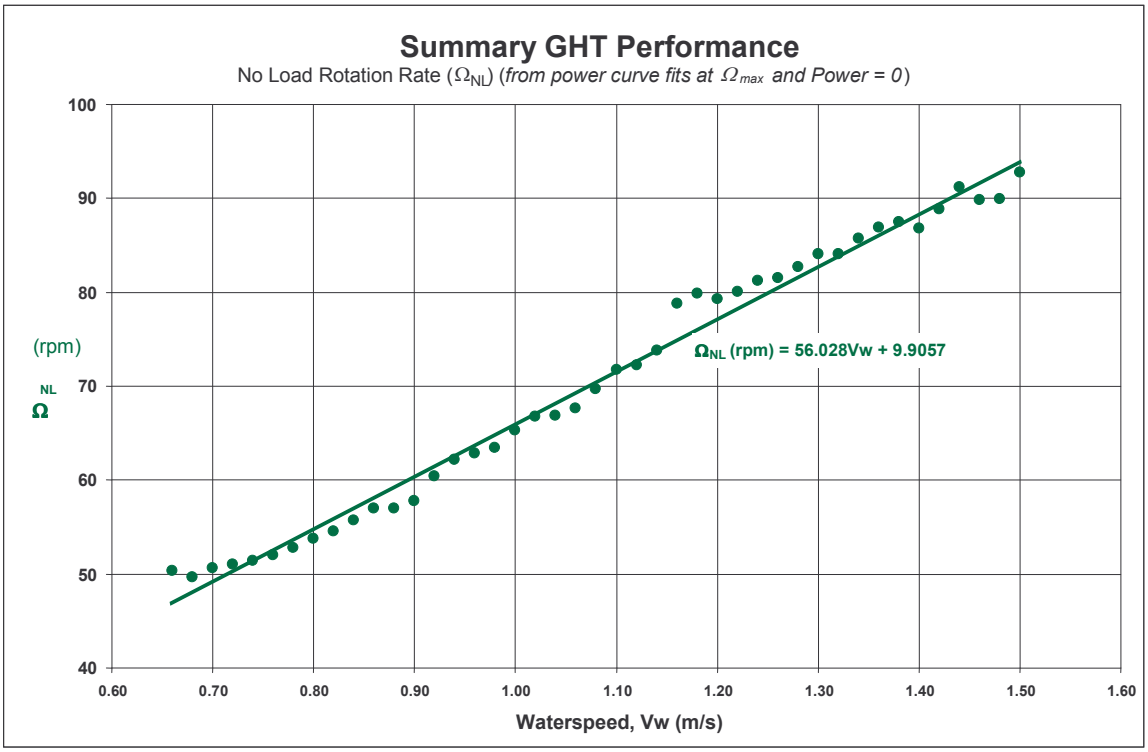

Figure 7. No-load Omega, Ω_{NL} vs.V Summary of GHT Performance

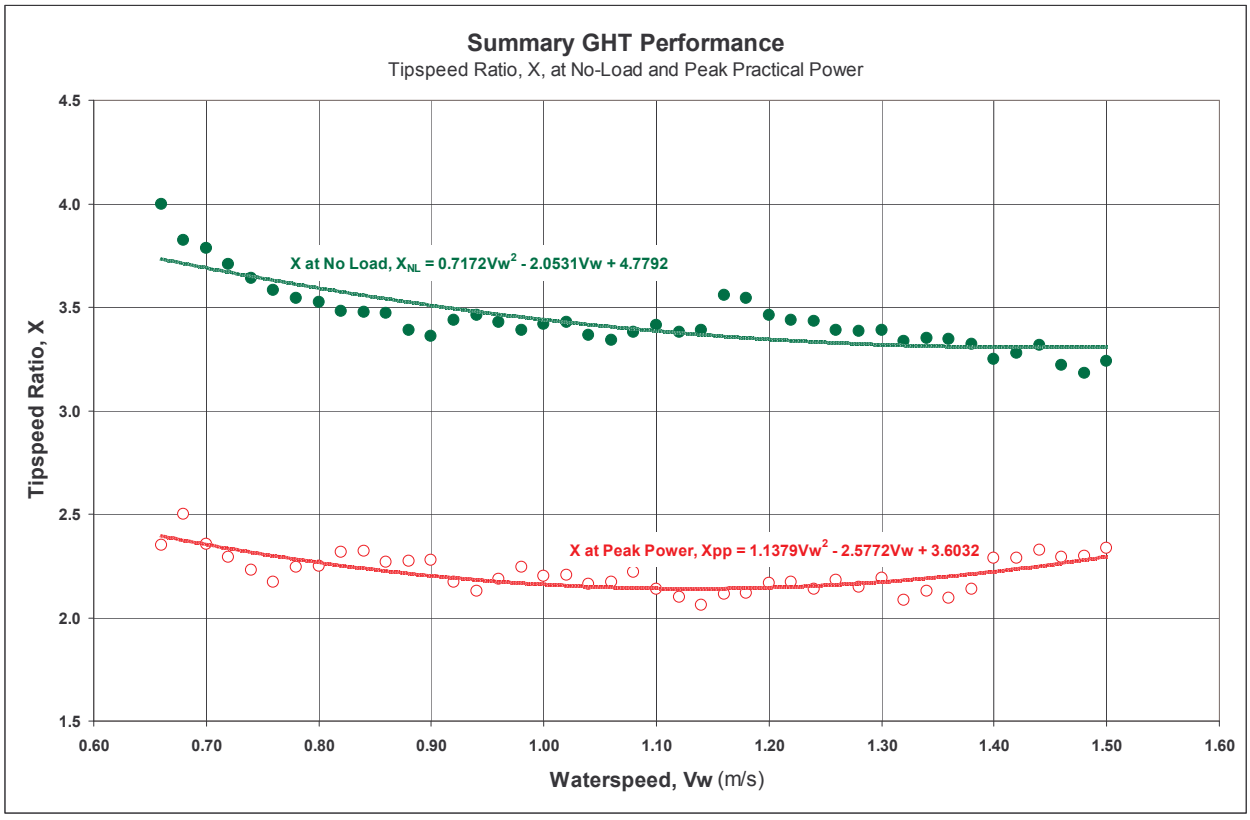

Figure 8. No-Load and Peak Power vs. V Summary of GHT Performance

Figure 8 is a summary graph of the turbine tipspeed ratio, **X** at both the no-load condition and at the peak practical power points. It should be borne in mind that because of the way the **PPPP**s were identified, the **Ω**, and therefore the **X,** is slightly higher in the middle range of **Vw** where the rotor stalled before reaching the peaks of the power curves.

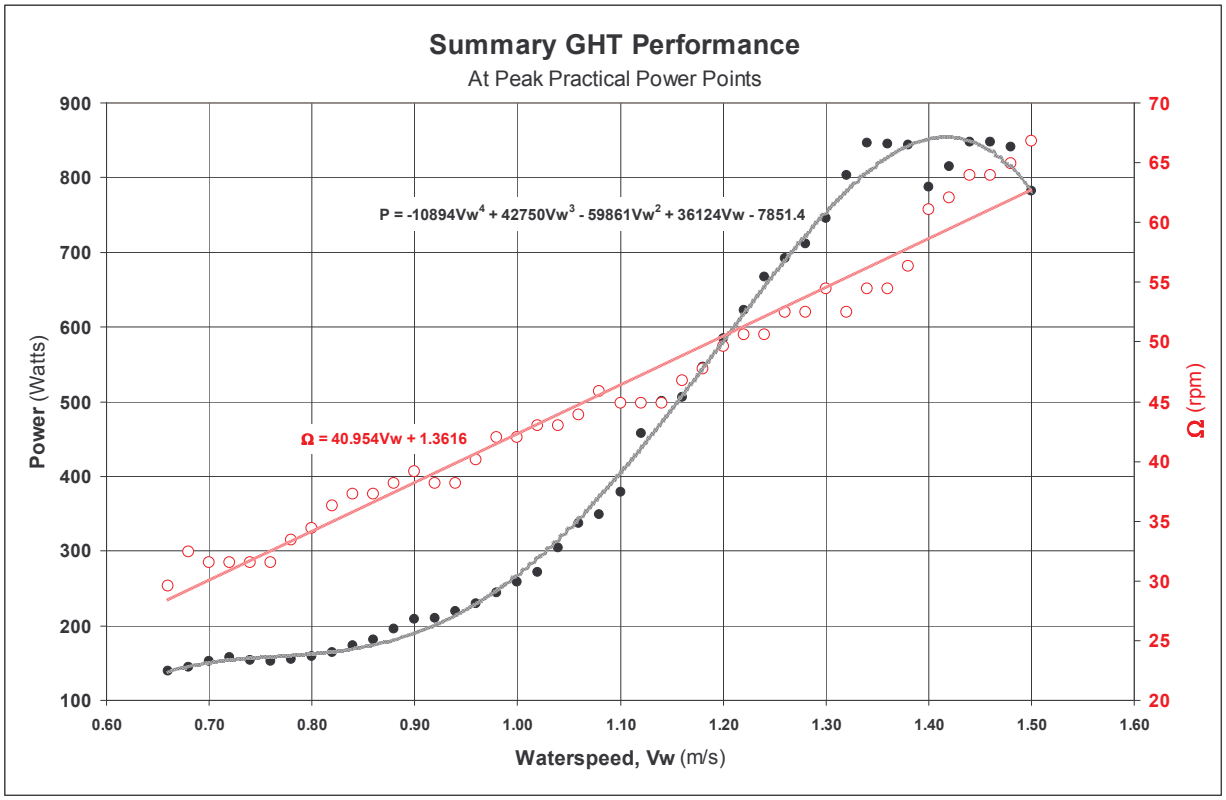

Figure 9. Ω and P vs. V Summary of GHT Performance

Figure 10 is a summary graph of the turbine power, $\mathbf{P_T}$, and efficiency, **Cp,** vs. Waterspeed, **Vw**, based on the power at the **PPPP**s. Note that the curve fits are purely descriptive (therefore can be of limited use to derive values within the tested range) and not theoretical. In particular, because we were not able to acquire data in the Merrimack above 1.5 m/s, we cannot know whether the power output and **Cp** would increase again after a plateau, making the downward curve of the curve fit above 1.4 m/s potentially misleading.

A peak **Cp** of about 28% is seen at about 1.33 m/s. These results are similar to those of the Nihon University study (for a helical rotor with a 60-degree inclination angle similar to the present rotor) at speeds 1 m/s and above. However, below 1 m/s, despite reduced power output, the **Cp** rose with decreasing **Vw**, reaching almost 39% at 0.66 m/s. Below this speed, the rotor would not start or reliably keep rotating while loaded, so it was not possible to examine its behavior at lower waterspeeds.

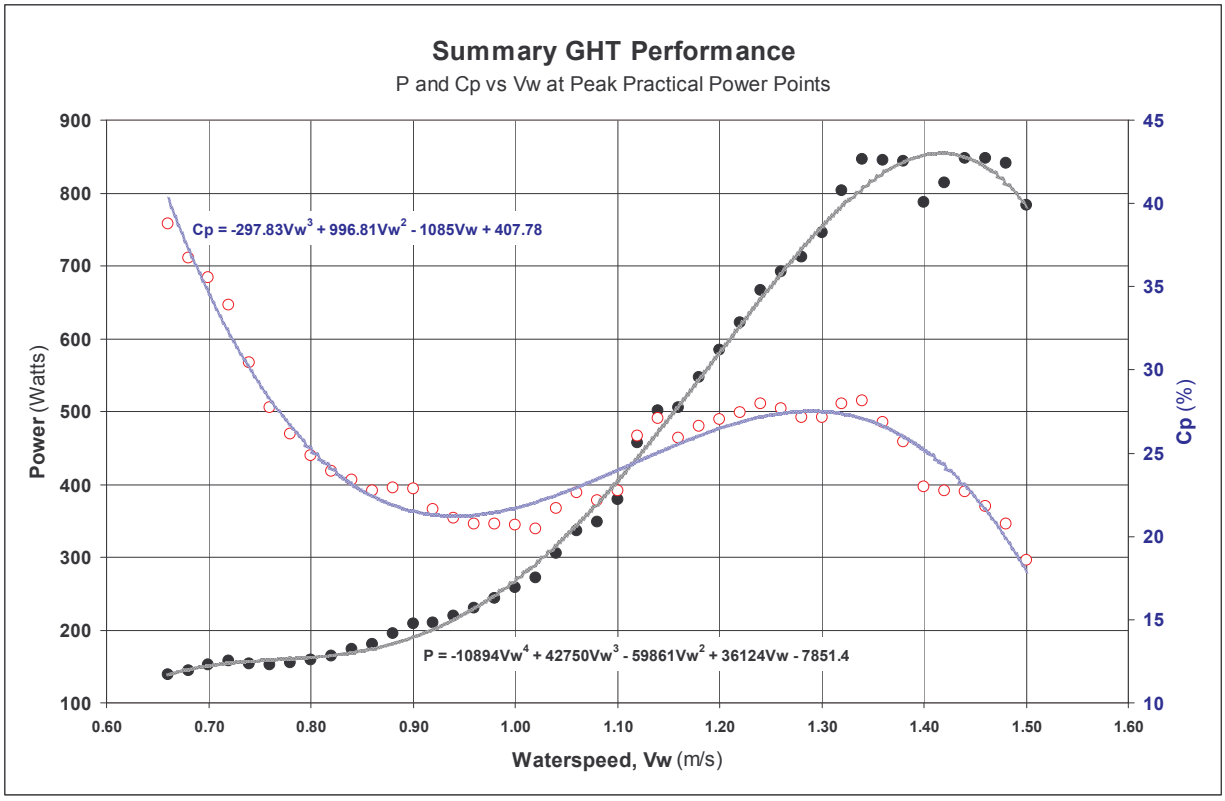

Figure 10. Power and Cp Summary of GHT Dynamometry Performance

A plot of **Cp** vs. **X** at **PPPP**, Figure 11, also indicated this property of the GHT rotor. The dramatic increase in **Cp** seen for very low waterspeeds was accompanied by an equally dramatic departure (clearly seen in Figure 11 where the low **Vw** data is highlighted) from the **Cp** vs. **X** relationship seen at higher speeds. The Nihon University study also found a strong **Cp** dependence on **V** for a given rotor, but did not show data for as wide a range of **Vw** and with the resolution we were able to measure. Overall, Figure 11 portrays almost a periodicity in the **Cp** vs. **Vw** relationship. This appears to be the result of a fundamental difference in the mode of operation of the rotor in the two different regimes of waterspeed contained in the range of 0.66 m/s to 1.5 m/s, relative to the absolute size and aspect ratio of the rotor.

One possible explanation for this is that at very low waterspeeds, where the flow leaving the upstream blade doesn't interfere very much with the flow meeting a downstream blade, the GHT could behave more like two separate rotors at once. That is, two blades are providing power from the same flow area. This would essentially allow the rotor to approach some fraction of twice the usual Betz limit for axial flow turbines. Such a phenomenon would deserve further study, especially using computational flow dynamics (CFD) but for the fact that the amounts of power available at such low speeds are probably not commercially significant.

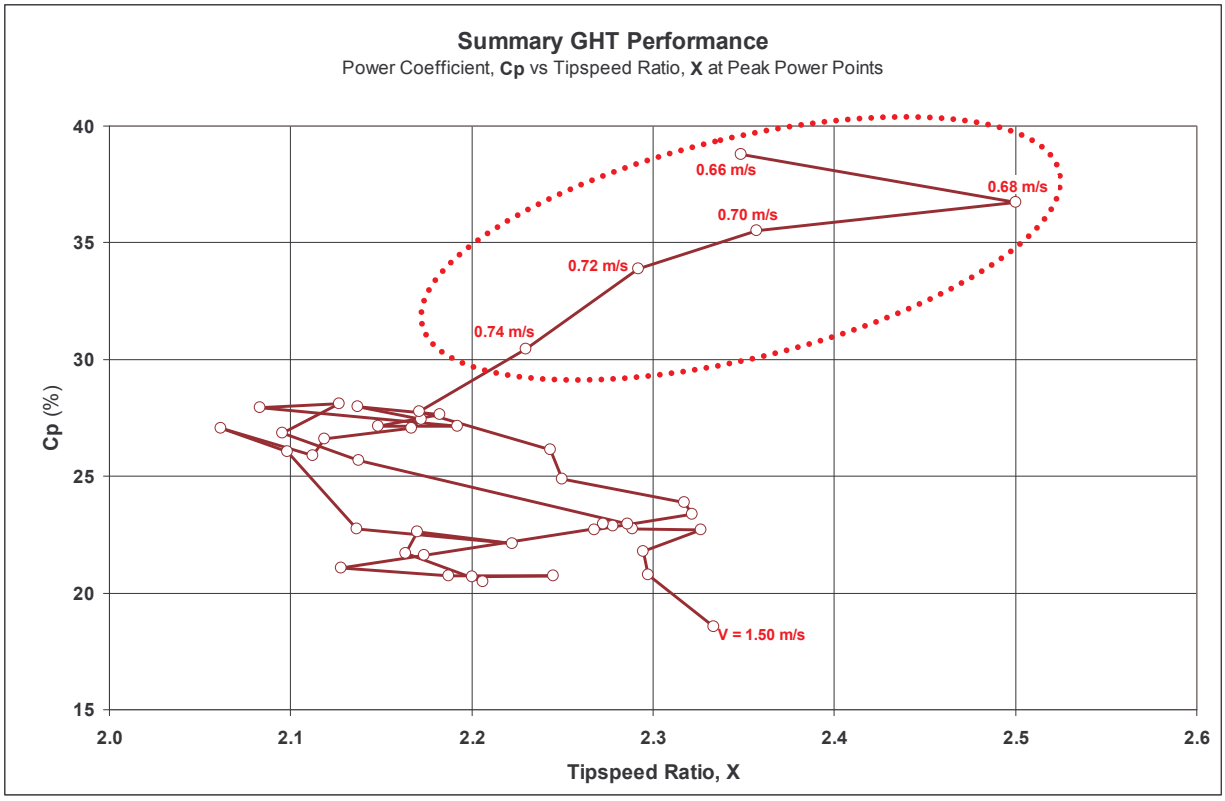

Figure 11. Cp vs. X Summary of GHT Performance

Meanwhile, the gradual reduction in **Cp** at waterspeeds above about 1.3 m/s we attribute to the rotor's upstream blade interfering increasingly with the flow impinging on the downstream blade, and/or creating vortices which create more drag or less lift on the blade sections at the sides of the rotor.

Altogether, we expect that the periodicity shown in the **Cp** vs. **Vw** graph is a function of the geometric relationships of the blade chord to the rotor diameter, and deserves further study aimed at increasing the overall **Cp** and flattening the curve so that the rotor can convert power efficiently at a wider range of practical waterspeeds. This relationship is expressed as the solidity, σ (= NC/πD), where N is the number of blades, **C** is the blade chord, and **D** is the rotor diameter.

The Nihon University study found a relationship between and both the maximum **Cp** and the **X** at which the **Cpmax** occurred. They found optimal values of σ between 0.3 and 0.4, with lowered **Cpmax** for values of σ both higher and lower. The lowest they examined was 0.2.

The GCK GHT rotors used in ATEP have a $\sigma = 0.14$ which may be too low to be optimal for maximizing **Cp** although it does result in higher speeds which reduces the gear ratio requirements of the drivetrain. On the other hand, it results in lower starting torques which is the main benefit of the helical rotor over straight-bladed rotors.

LOAD-MATCHING

The load-matching requirements of a practical turbine can be seen in Figure 12 and Figure 13 which show **Ω** and **τ** respectively vs. **Vw** at the **PPPP**s. These show the torque required to properly load the rotor for peak power and the resulting rotor speed. Developing a system with an active or passive load that closely follows this curve is critical to practical, efficient, and productive power conversion. The peak powers shown in Figure 13 can only be obtained if the load matching follows these relationships. As Figure 12 shows, the required **Ω** is closely approximated (with $R^2 = 0.9697$) by a simple linear curve fit as shown. This indicates that a relatively simple control system using only **Vw** and **Ω** data inputs could accurately and efficiently match the turbine rotor.

This strongly contrasts with the torques at peak power, τ_{PP}, which result in optimal load matching. As shown in Figure 13, which compares Ω_{PP} with τ_{PP}, a higher-order polynomial curve fit is required to approximate the torque.

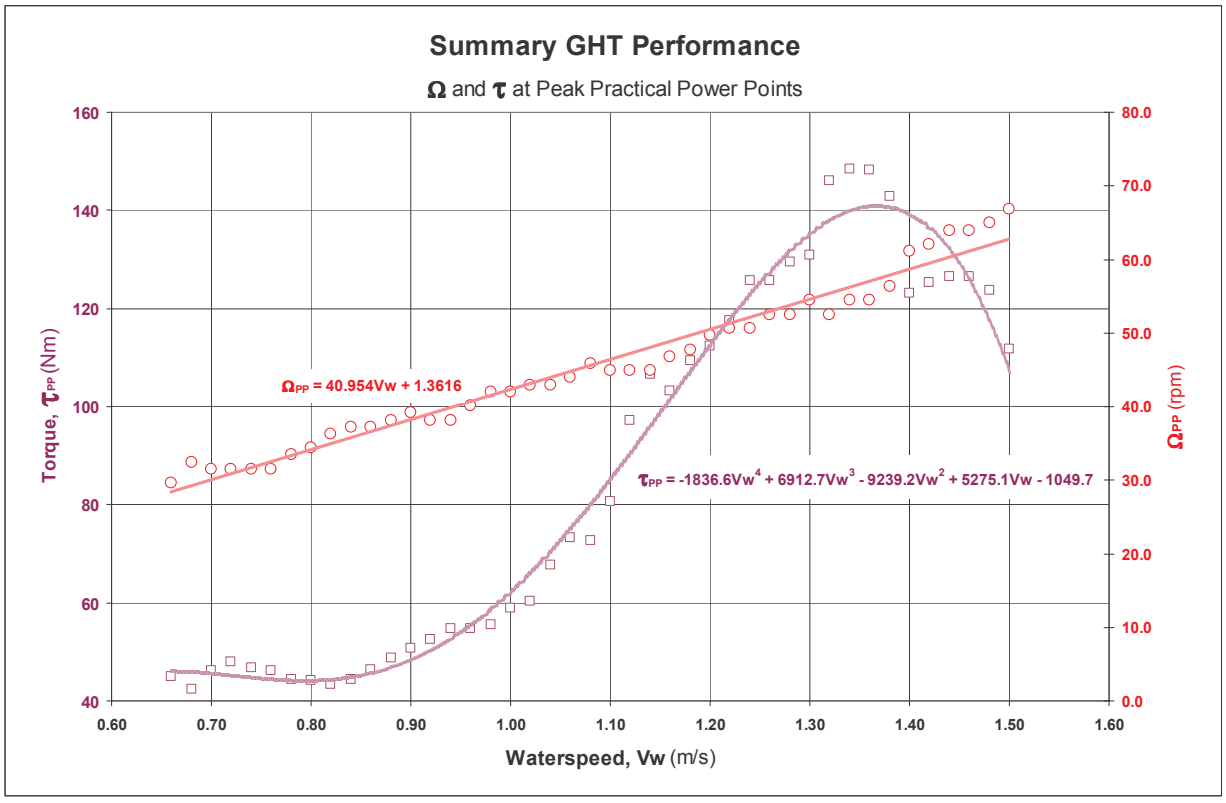

Figure 12. Ω_{PP} and τ_{PP} vs. Vw Summary of GHT Performance

A simple passive approach to load matching seems infeasible as shown clearly by the plot of τ_{PP} **vs.** Ω_{PP}. Since the torque required is not monotonic and there is not a unique value of τ for every value of Ω, no simple mechanical device could load the rotor in this manner. In order to track the waterspeed up and down in a tidal situation, it would also need to effectively retain the history of its position on the curve. However, as stated above, a relatively simple control system using only **Vw** and Ω data inputs, could accurately and efficiently match the turbine rotor. This will require a fast response time in the control system as the waterspeed can have significant sub-second fluctuations.

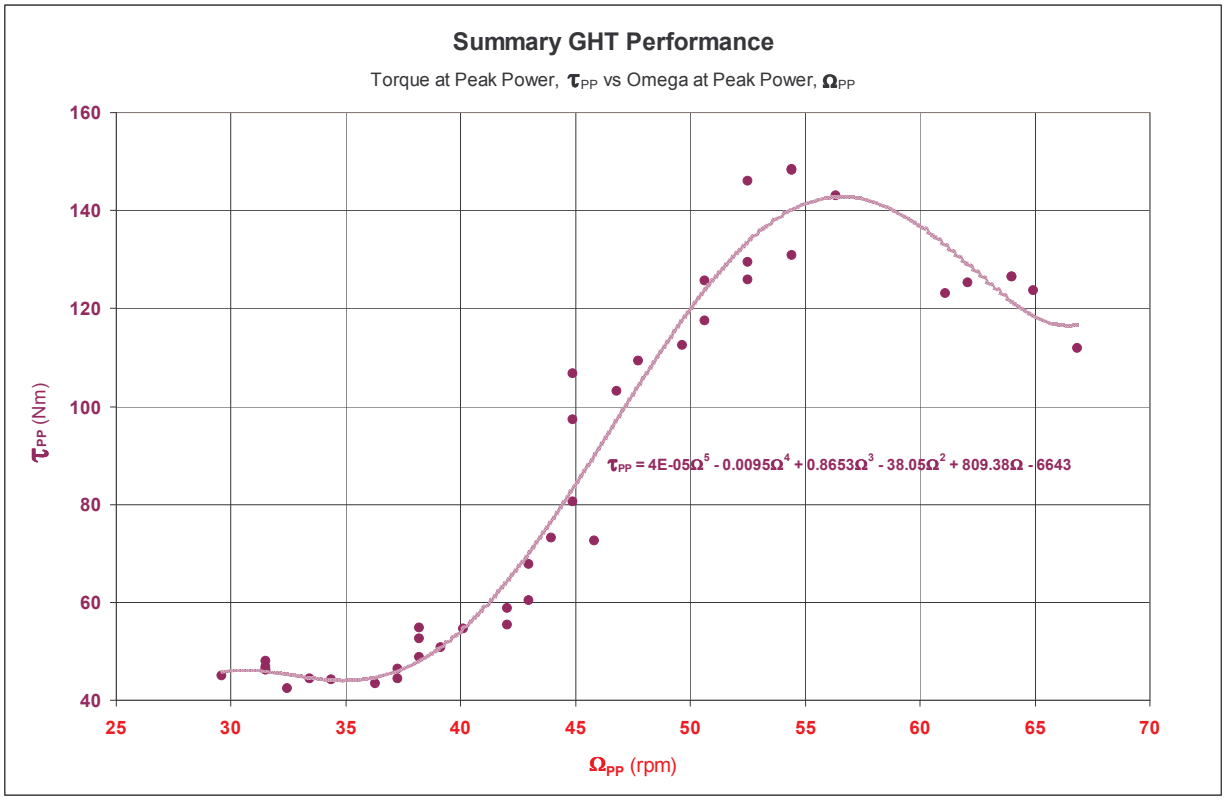

Figure 13. τ_{PP} **vs.** Ω_{PP} **Plot of GHT Performance**

Rather than design the loading system so that τ exactly matches the Ω at peak power, a practical loading system must avoid stalling initiated by flow fluctuations. Depending to a great degree on the individual site, waterspeeds generally fluctuate in the short term due to uneven structures in the flow that pass by the area of the turbine. An operating margin should be designed in to the system that will avoid stall. Otherwise, power production will be severely reduced, and the system could be subjected to the excess stresses of numerous undesirable start/stop cycles.

Therefore, care must be taken to keep the Ω at some reasonable operating margin above the rotor stall Ω. That is, the loading system should be designed to load the rotor less than the optimal amount so as to avoid stall in operation, even at the cost of some loss in turbine efficiency.

Figure 14 shows the estimated rotor stall speed, Ω_{stall} for each waterspeed along with Ω_{PP}. Figure 14 also shows an example of a design operating curve with an enhanced operating margin to increase what is probably a margin that is too narrow for practical operation. The specific losses at each waterspeed would need to be calculated and integrated to project the overall load matching efficiency that will be a component of the overall system efficiency.

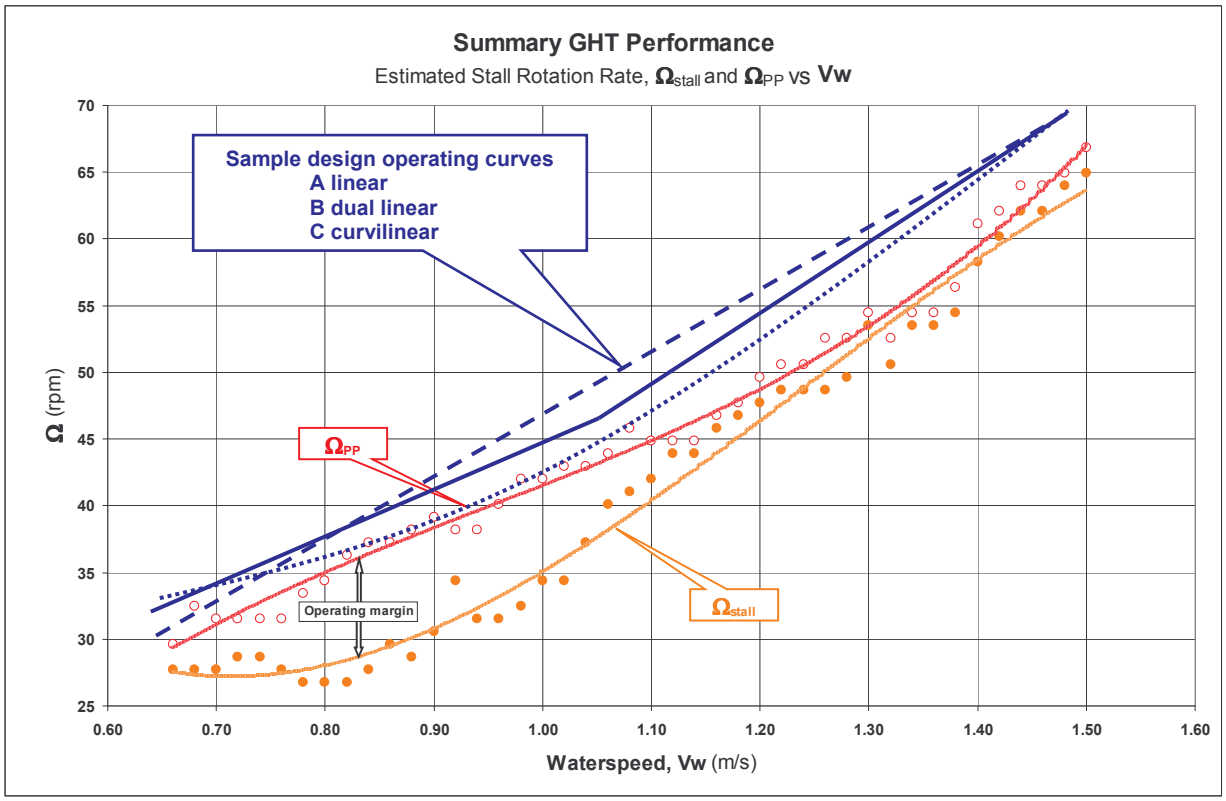

Figure 14. Ω_{PP} and Ω_{Pstall} vs. Vw Summary of GHT Performance

The load matching efficiency for the linear control line is shown in Figure 12. This is the simplest control strategy, and yields essentially a worst-case scenario. The implementation of more complex dual-mode linear or curvilinear control algorithms, as illustrated in Figure 14, could achieve higher load-matching efficiencies.

The most cost-effective control type can be determined by calculating the power loss from load-matching at each point by comparing the optimal Ω_{PP} with that given by the control Ω for each value of **Vw**. Weighting these by the expected site velocity distribution can give the overall energy penalty for each control strategy which can be compared to the life-cycle capital cost of each. Load matching is discussed further in the Conclusions and Recommendations section.

TURBINE #2 GENERATOR DATA

Turbine #2 was the first electrical generator version. In order to operate over a wide speed range and meet the other criteria described in Appendix C, Electrical System Documentation, a 18 kW peak power Ecycle permanent magnet brushless MG3-36 Motor/Generator was used. This unit provides a variable frequency, asynchronous 3-phase AC output which is normally rectified to variable-voltage DC. It has a voltage constant of 0.038 V/rpm, a torque constant 0.36 nm/A, and a rated efficiency of 95%.

Our "nominal" design point based on a waterspeed of about 2 m/s (4 kn) called for a gear ratio of 36:1 so that the nominal loaded **Ω** of 84 rpm would provide a generator speed of about 3000 rpm. The "typical" waterspeed of about 1 m/s (2 kn) would then give a loaded rotor **Ω** of about 42 rpm and a generator speed of 1720 rpm.

For the speed increasing and mounting for the Turbine #2 generator, VP designed and built a rotor frame top section with a relatively simple pulley and belt transmission. A diagram of the Turbine #2 transmission with generator is shown in Figure 15. This unit was designed to use the simplest gearing approach and utilize inexpensive, rugged and widely available components.

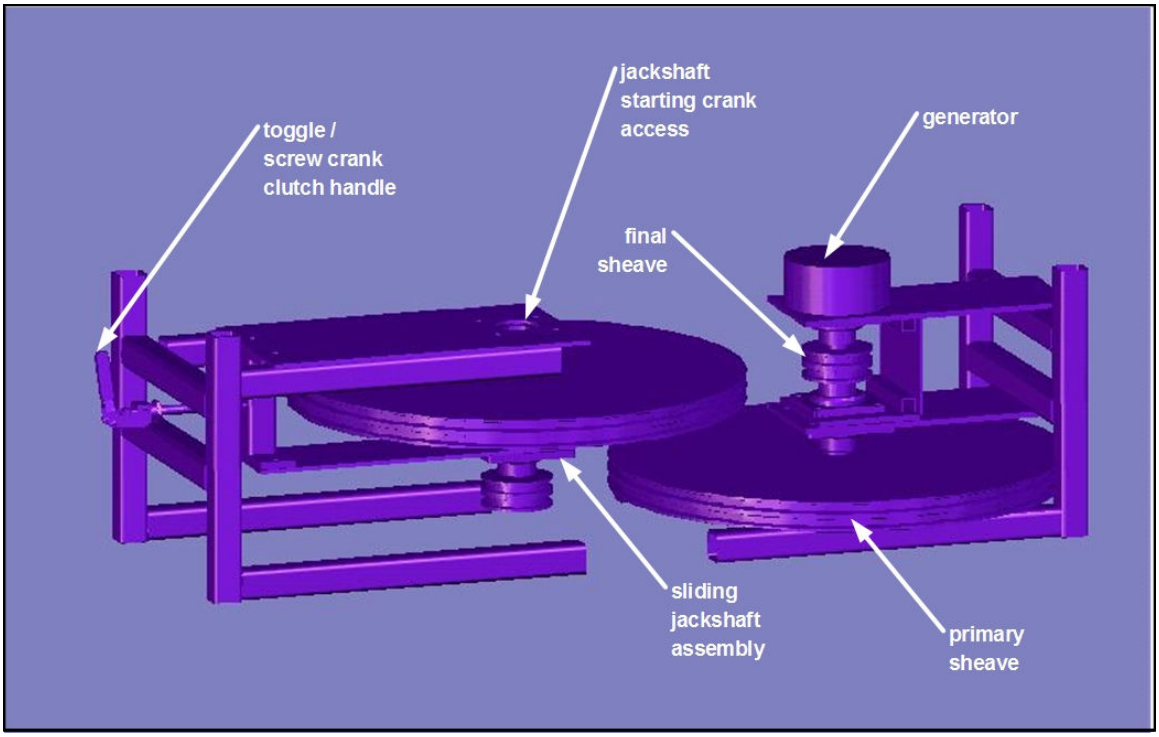

Figure 15. Turbine #2 Generator Transmission Assembly Diagram

Because it is necessary to be able to remove the load from the rotor for starting, a two-stage transmission assembly with dual opposing pairs of pulleys (sheaves**)** was designed, with one pair on a sliding jackshaft so that one assembly could provide both the speed increase and clutch functions. Standard dual-band type B vee-belts were used with matching dual-groove sheaves. With the large sheaves of 30-inch diameter, the final speed increase ratio of 39:1 was obtained.

The rotor shaft adapter and extension shaft was identical to that used for Turbine #1. Figure 16 is a photograph of the Turbine #2 transmission and generator while in operation.

The transmission also had to have a rotor starting capability, which was performed manually using a ratcheting crank on the jack shaft which was on the inboard end of the frame top and reachable by a crewmember on the barge deck. This proved difficult in practice, due to the speed at which even the intermediate-speed jackshaft had to be turned.

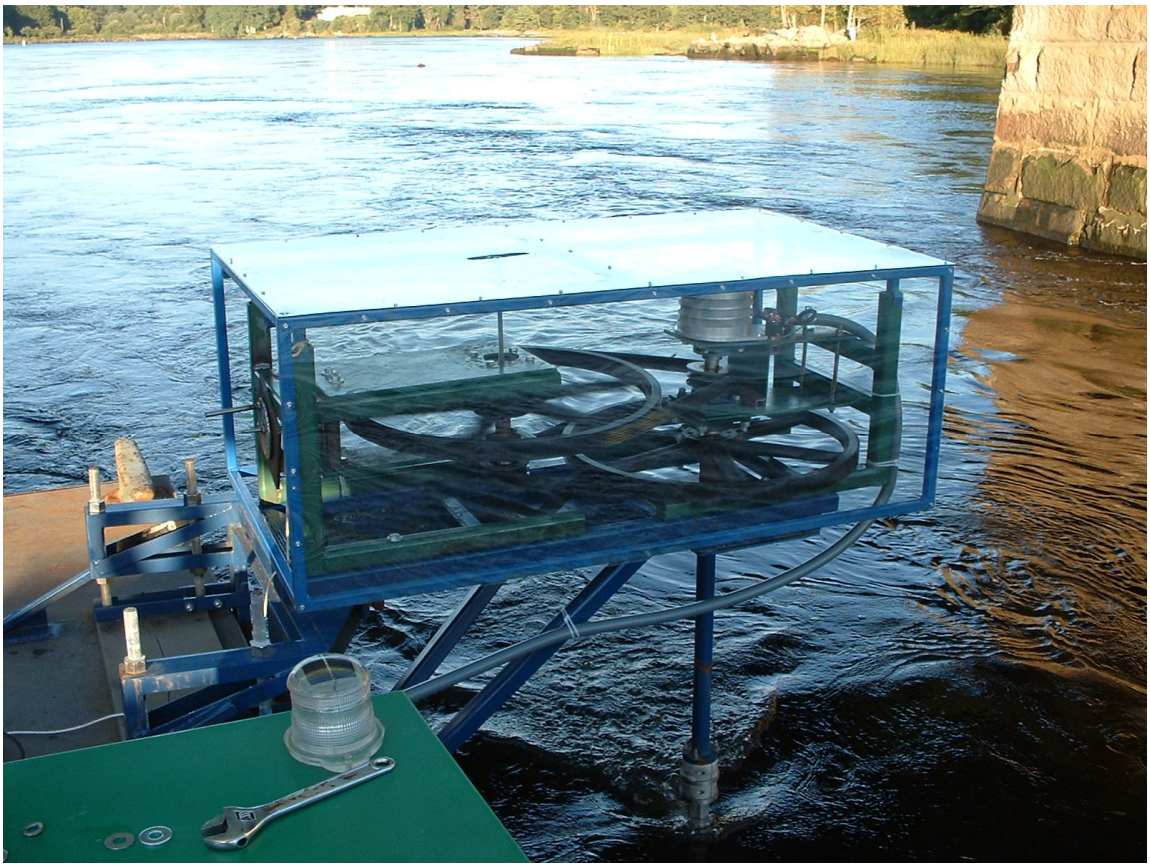

Figure 16. Turbine #2 Generator Transmission Assembly Photo

TURBINE #2 GENERATOR RESULTS

The data for Turbine #2 generation system was limited due to a number of factors. These included limited ability to start due to the manual starting coupled with limited water current speed range. Also, a requirement to curtail testing until thorough fish monitoring was established reduced the operating time and led to limited resistance values being tested.

The no-load generator voltage and turbine **Ω** is shown in Figure 17.

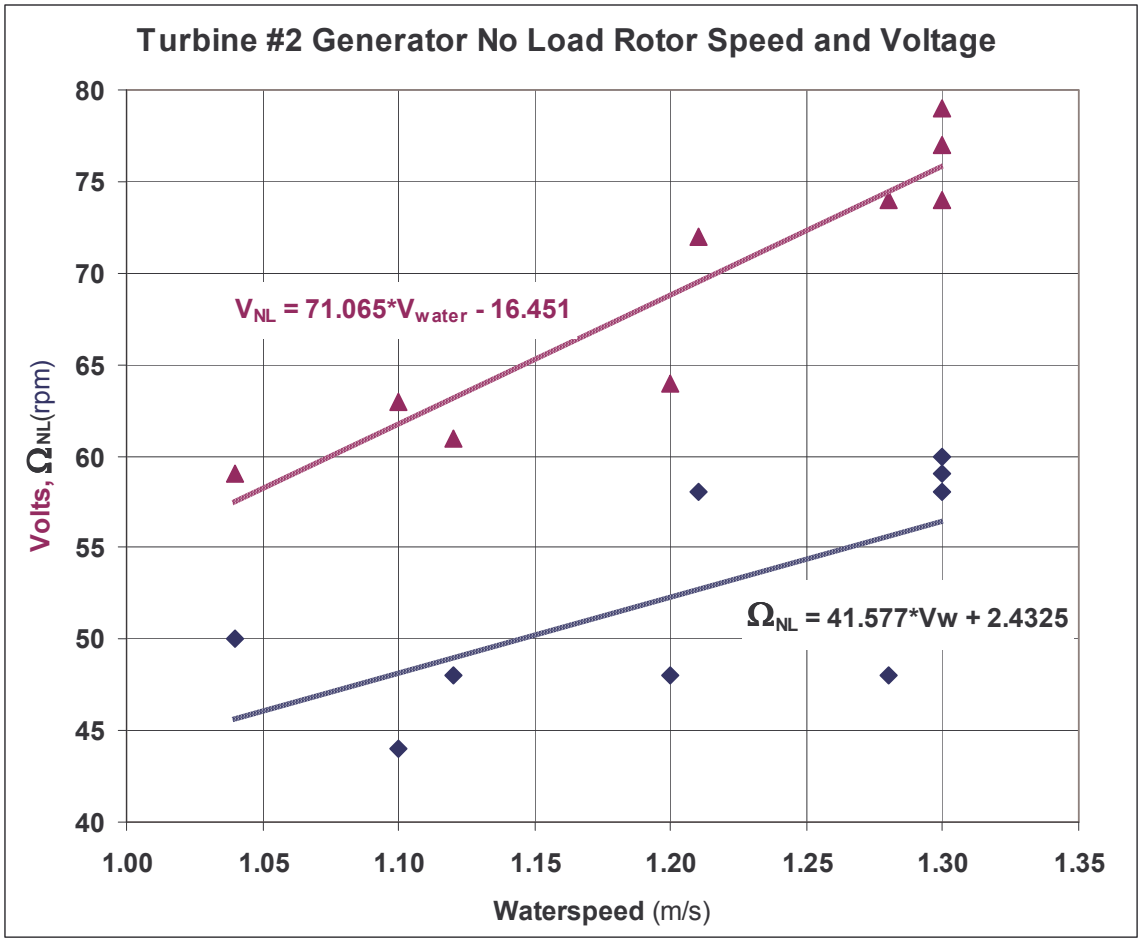

Figure 17. Turbine #2 No-Load Voltage, V_{NL} and Rotation Rate, Ω_{NL} vs Vw

Comparing the Turbine #2 no-load **Ω** (with transmission and open generator) with those from the Turbine #1 dynamometry in Figure 18 clearly shows the consistent transmission losses that were extracted from the shaft power prior to the generator. This high minimum residual torque load not only reduced power output but also effectively raised the minimum **Vw** at which Turbine #2 could sustain rotation.

At 1.20 m/s for example, the Turbine #2 rotor no-load speed is 52.3 rpm which is 27 rpm slower than the dynamometry of the Turbine #1 rotor at no load. The Turbine #1 dynamometry data at

1.20 m/s indicates that this level of slowing results from an applied torque of 105.8 Nm. Therefore, the transmission itself was significantly loading the Turbine #2 rotor prior to the generator. In fact, according to the dynamometry τ curve fit ($\tau = -1836.6Vw^4 + 6912.7Vw^3 - 9239.2Vw^2 + 5275.1Vw - 1049.7$), the torque load required for peak power at 1.20 m/s is 112.7 Nm, so the transmission loading on Turbine #2 at this waterspeed represents 94% of the optimal torque load. At this loading, the transmission itself is absorbing 99% of the peak power of 584 Watts that the rotor could deliver at that waterspeed.

As discussed in the conclusions, this transmission proved unsuccessful in terms of both its residual torque and low overall efficiency.

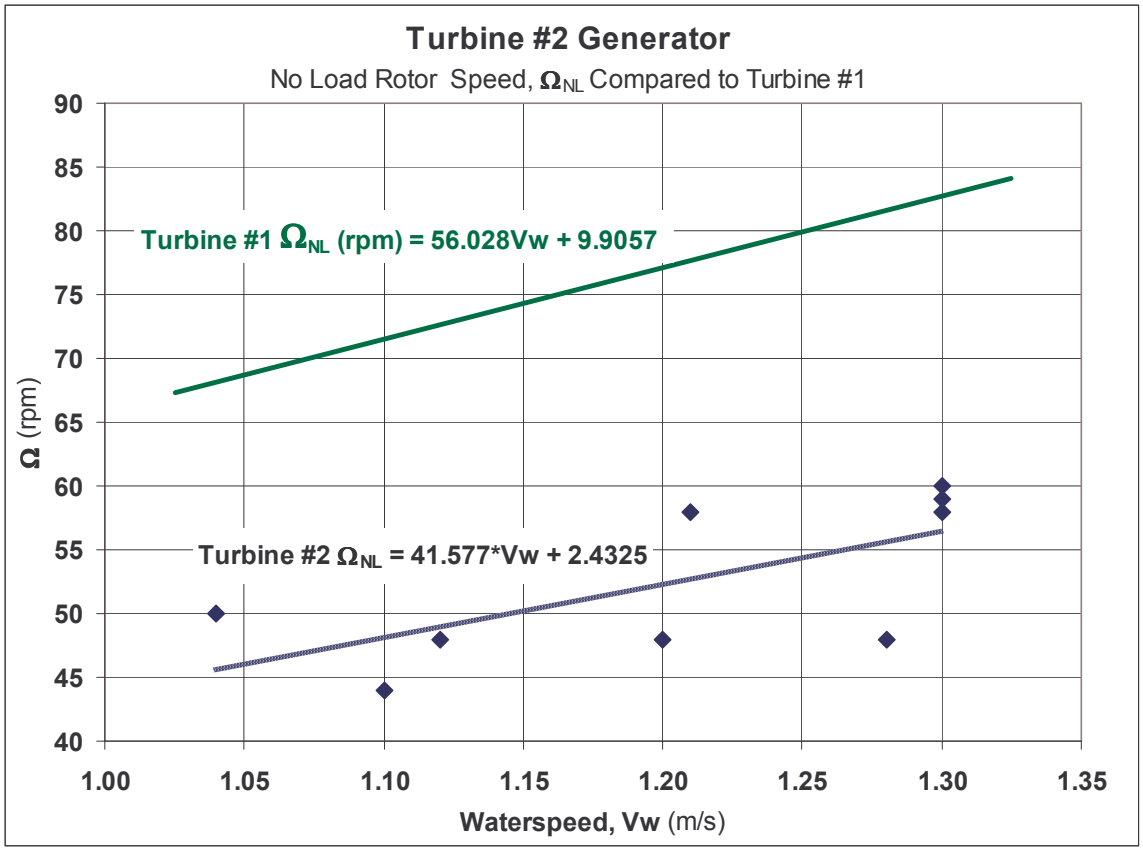

Figure 18. Turbine #2 and Turbine #1, Ω_{NL} vs Vw

The electrical generation tests for Turbine #2 were performed at three load resistance settings that were high enough to allow rotation, **R**= 9.1, 13.0, and 25.4 Ohms. Figure 19 through Figure 21 show the voltage, current, and power for those loads respectively, over the range of waterspeeds encountered.

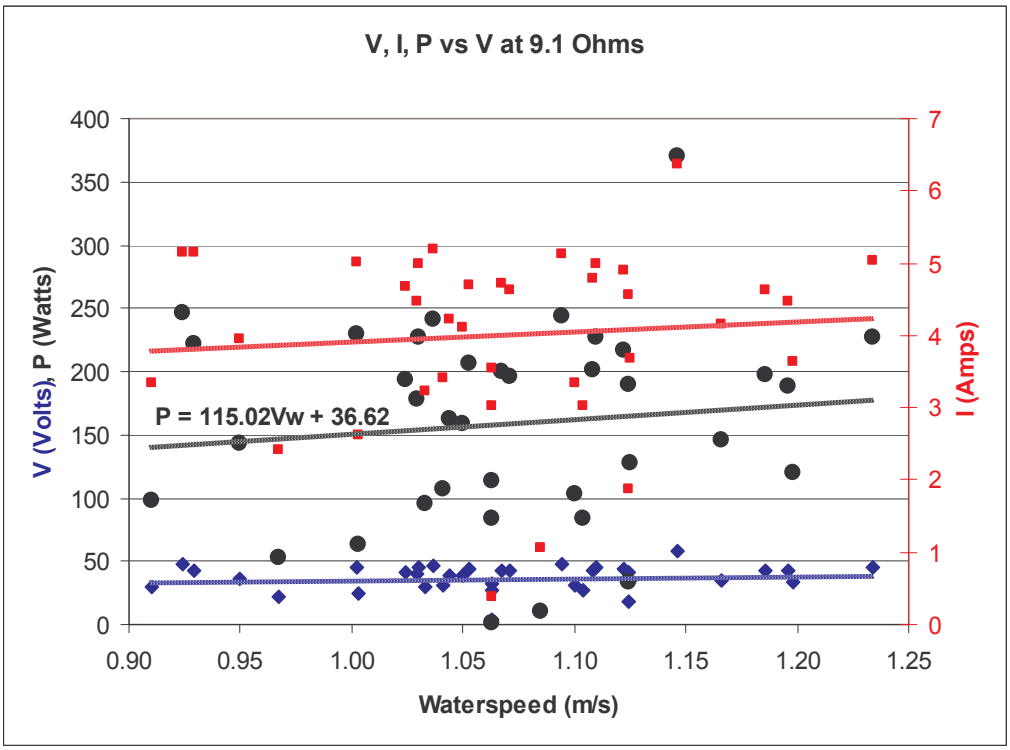

Figure 19. Turbine #2 Voltage, Current and Power vs Vw into 9.1 Ohm Load

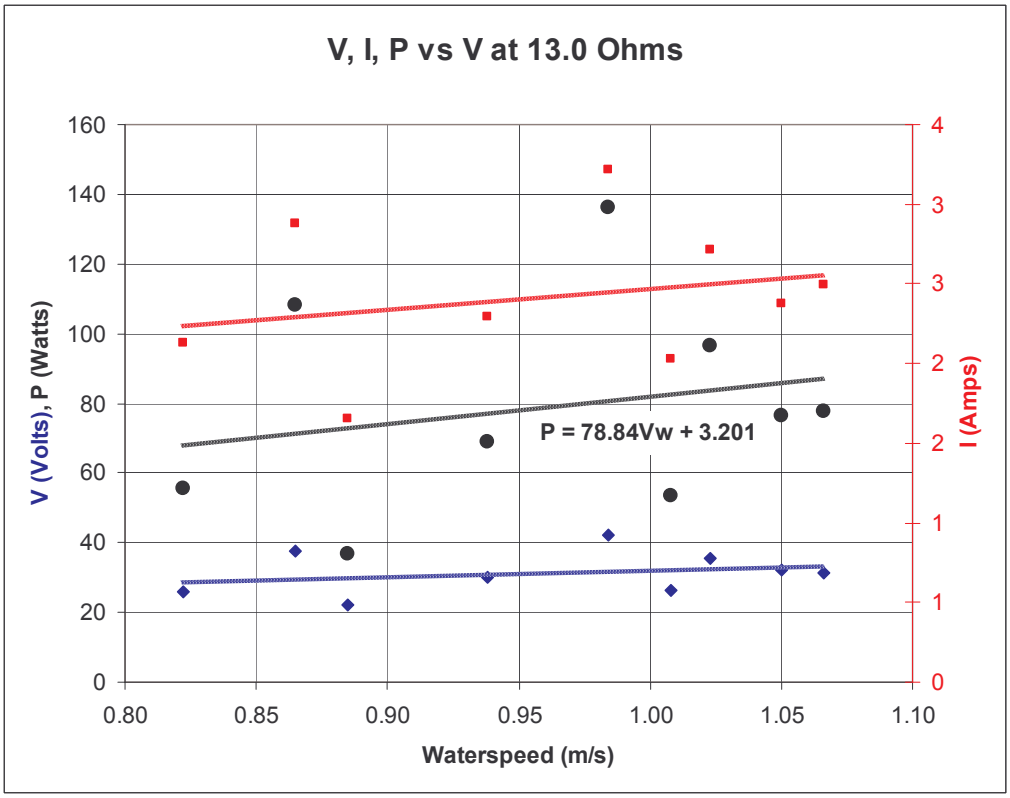

Figure 20. Turbine #2 Voltage, Current and Power vs Vw into 13 Ohm Load

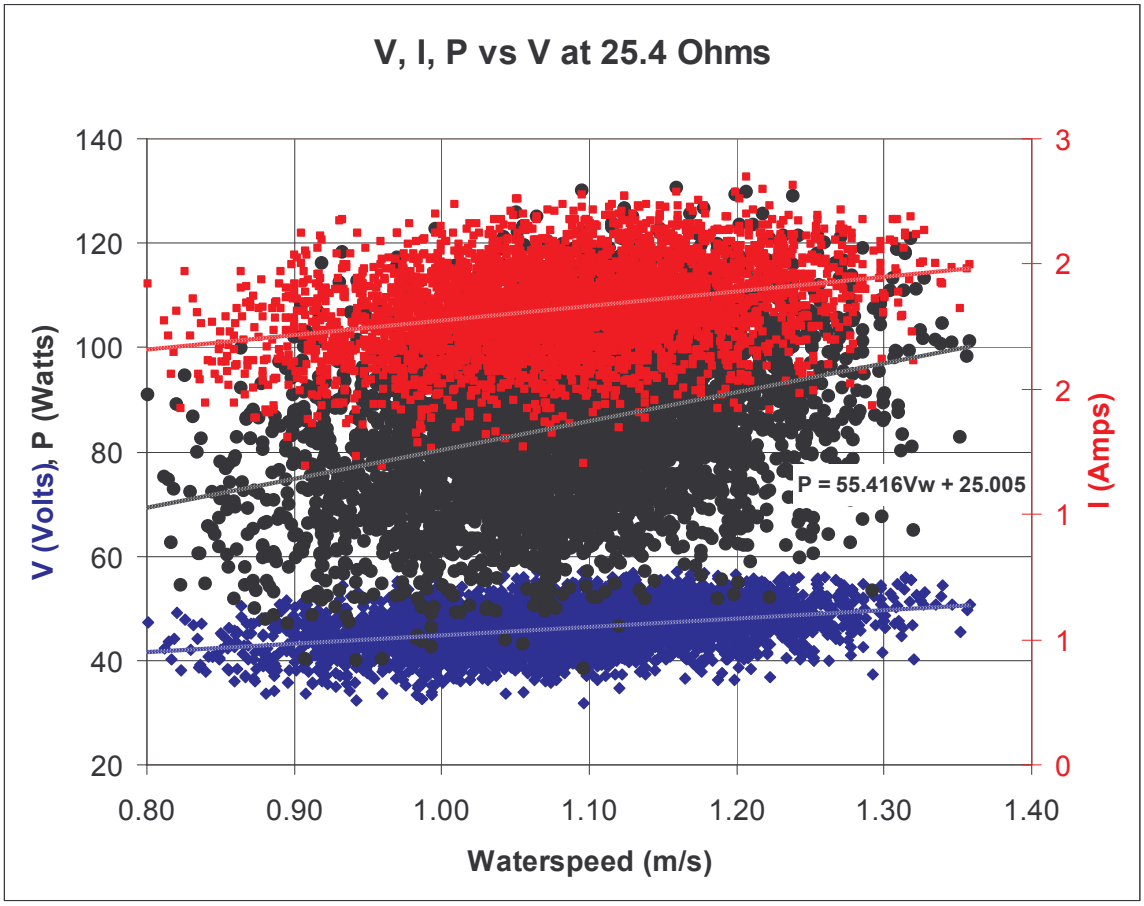

Figure 21. Turbine #2 Voltage, Current and Power vs Vw into 25.4 Ohm Load

Figure 22 summarizes the results of the Turbine #2 electrical generation tests. It is important to note that while 9.1 Ohms shows the highest power output, it is likely not the optimal resistance that would yield the highest possible power from the rotor – i.e., the best load-match. In this case, 9.1 Ohms is simply the best of the four fixed resistance values tested in this protocol, whereas, due to the persistent drivetrain load, the rotor stalled at lower resistances.

It should also be noted that the ideal load should ***change*** with **Vw** in order to maximize power. No fixed resistance can optimize the load-matching efficiency and power output of the rotor over a range of waterspeeds.

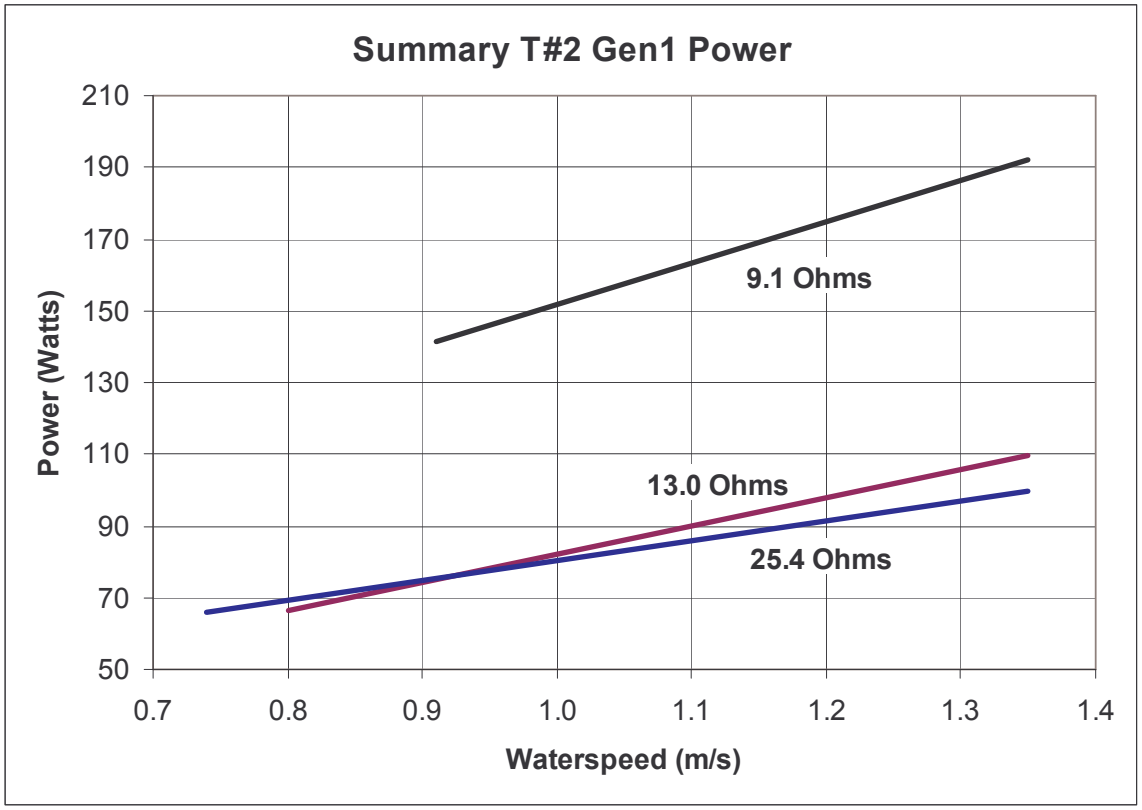

Figure 22. Summary of Turbine #2 Voltage, Current and Power vs Vw

Using the curve fit from the power output of Turbine #2 at 9.1 Ohms, Figure 23 shows the resultant overall water-to-wire efficiency, $\eta_{w\text{-}w}$, of the turbine. Figure 24 shows the same result plotted along with the basic potential efficiency of the rotor as determined by the dynamometry of Turbine #1.

The overall efficiency, or "water-to-wire" efficiency, $\eta_{w\text{-}w}$, is the product of all the component efficiencies including the rotor ($\eta_{rotor} = Cp$), drivetrain (η_{drive}), including bearings and gearing, load matching of the generator load to the rotor (η_{lm}), and generator, including electrical conversion components (η_{gen}):

$$\eta_{w\text{-}w} = Cp * \eta_{lm} * \eta_{drive} * \eta_{gen}$$

The energy losses from the inefficiencies in the drivetrain and generator are rejected as heat, while the less-than-perfect matching of the load results in capturing less and leaving more of the energy in the water flow than is possible for the rotor.

The $\eta_{w\text{-}w}$ values shown in Figure 23 include all the losses shown above, as illustrated in Figure 24.

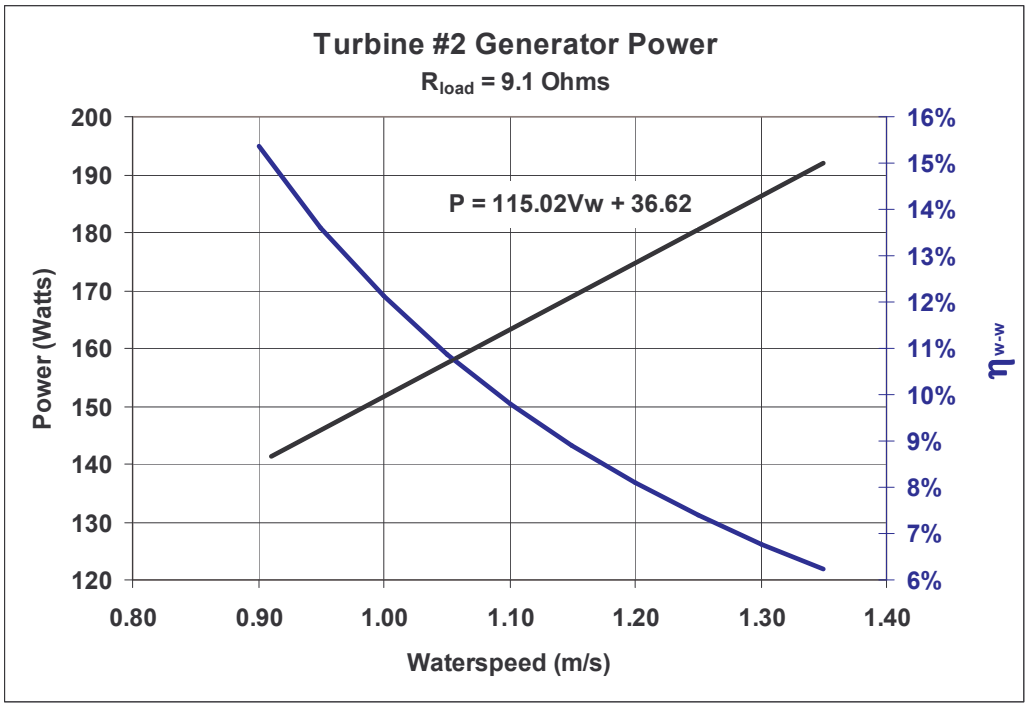

Figure 23. Turbine #2 Power and Cp vs Vw into 9.1 Ohm Load

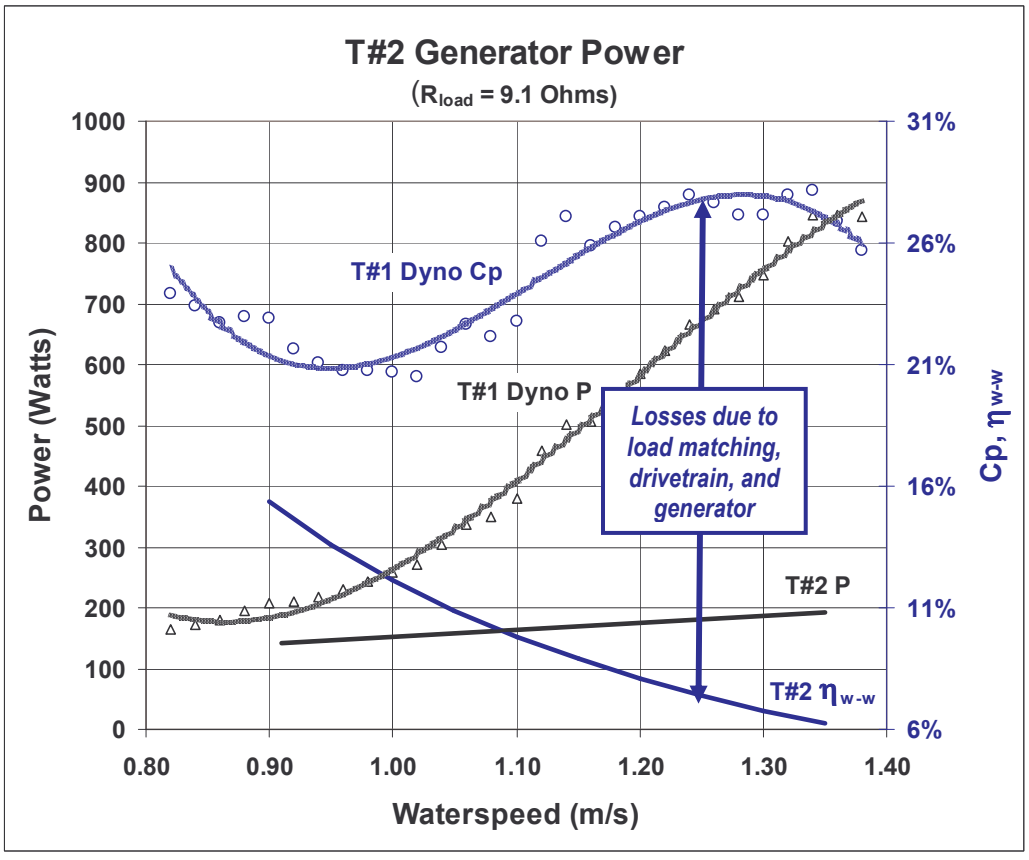

Figure 24. Turbine #2 Power and η_{w-w} Compared to Turbine #1 Dynamometry

Figure 25 uses the power curve for the GHT rotor at 1.02 m/s and the actual operating point of Turbine #2 1.02 m/s to illustrate the loss due to load matching.

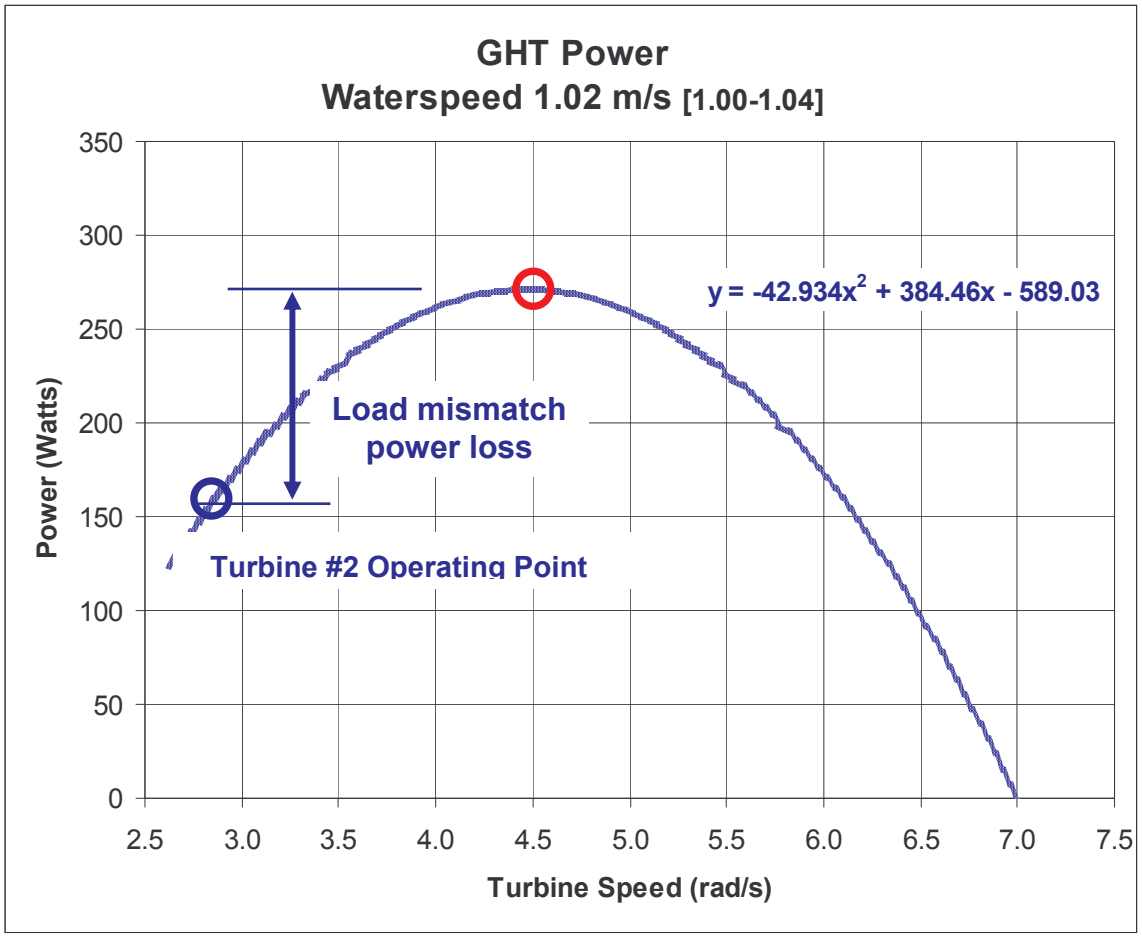

Figure 25. Turbine #2 Operating Point Compared to Dynamometry

In this case, due to the excessive residual loading of the rotor by the transmission, the available rotation speed and torque from the rotor to apply to the generator is limited, and the loading of the generator cannot be optimal. The overall $\eta_{w\text{-}w}$ is therefore a product of the contributing components to entire system, and not entirely due to the rotor.

TURBINES #3 AND #4, "SIDE-BY-SIDE" CROSSWISE SPACING

The GHT rotors in Turbines #3 and #4 drove 5 kW permanent magnet generators through vertical-axis planetary gearboxes, as described in Appendix B. These units were started electrically by using a drive circuit to operate the generators as motors.

They were tested first as individual generator units with their output rectified to DC and loaded by variable resistance loadboxes.

Secondly, they were tested while operating simultaneously to examine the performance with different crosswise spacings.

Finally, the behavior of Turbine #3 was examined relative to Turbine #1 from which it was directly downstream (during ebb flow).

As before, due to waterspeed fluctuations, and the strong power fluctuations due to the power being proportional to the cube of **Vw**, and the effects of rotor inertia, many data points were taken and curve fit, rather than using any instantaneous calculations.

Altogether, 3824 valid data points were used to develop the Power, voltage, resistance, **Vw** relationships below for Turbine #3 alone.

Examples of two such fits are shown in Figure 26 and Figure 27.

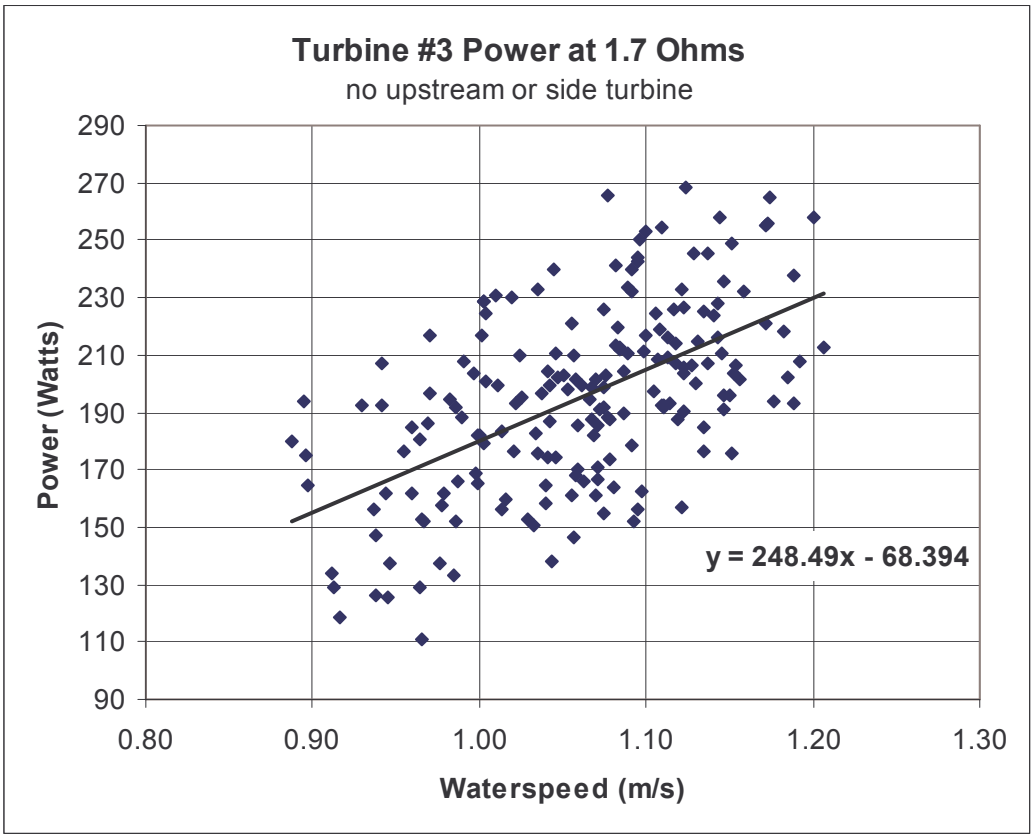

Figure 26. Turbine #3 Generator Power vs Vw at 1.7 Ohms Load

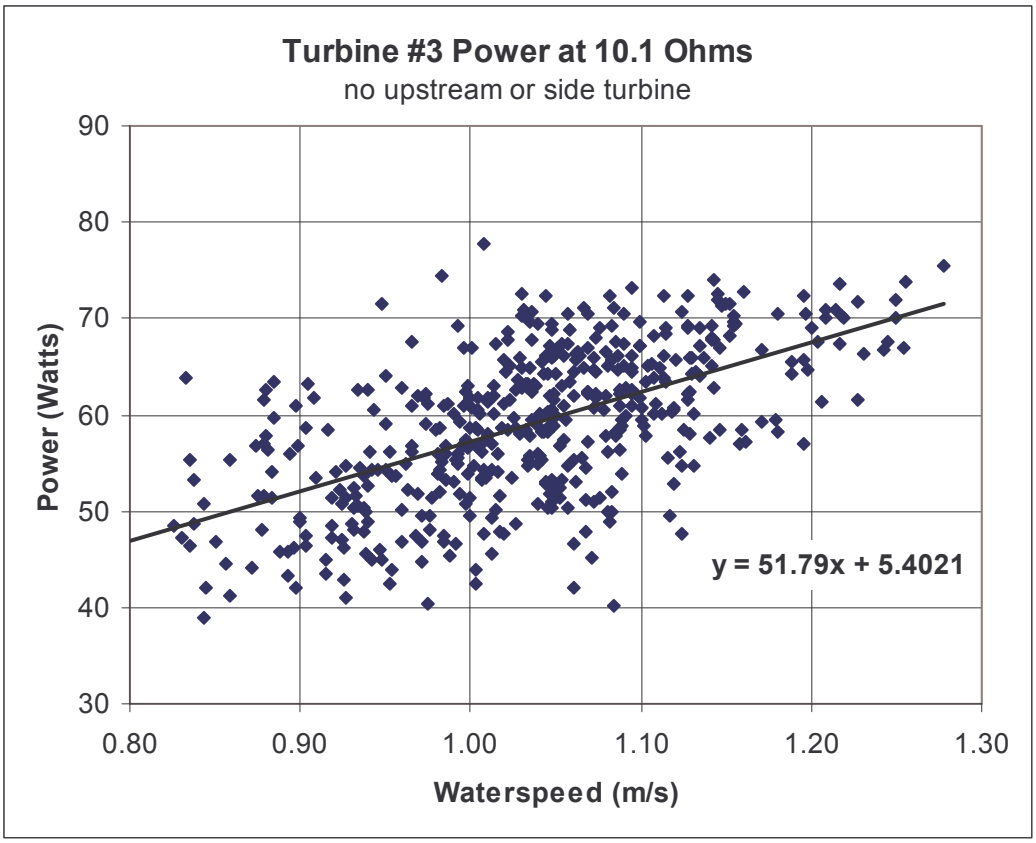

Figure 27. Turbine #3 Generator Power vs Vw at 10.1 Ohms Load

The power data for each load resistance setting was fit to a linear equation which is a reasonable approximation of what should be a relatively narrow section of a cubic curve since **Pw** varies with $\mathbf{Vw}^3$. A compilation of the power curve fits for the range of load resistance values is shown in Figure 28.

The same power vs. resistance tests were conducted on Turbine #4, with good agreement in performance, particularly at the most optimal power loading at 1.7 Ohms, as shown in Table 3, below and in Figure 29.

Table 3. Power Curve Fit Equations for Turbines #3 and #4

R (Ohms)	**Turbine**	**Power Curve**
1.7	**# 3**	**P** = 248.49**Vw** - 68.394
	# 4	**P** = 219.87**Vw** - 36.129
2.5	**# 3**	**P** = 132.26**Vw** - 1.2235
	# 4	**P** = 147.82**Vw** - 3.2145

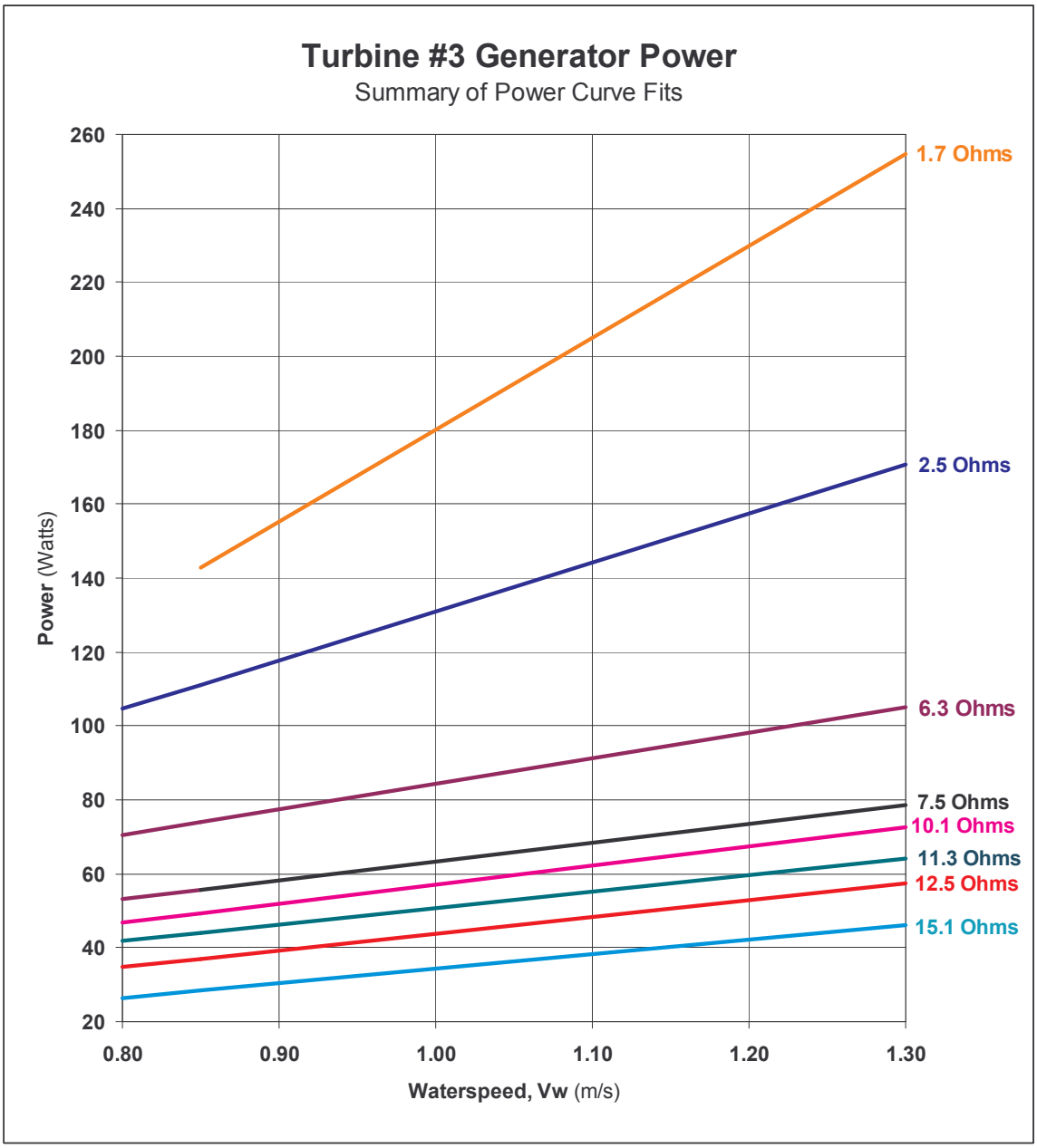

Figure 28. Turbine #3 Summary of Generator Power vs Vw

The overall efficiency, or "water-to-wire" efficiency, $\eta_{w\text{-}w}$, is the product of all the components efficiencies including the rotor (η_{rotor} = **Cp),** drivetrain, including bearings and gearing, load matching of the generator load to the rotor, generator

$$\eta_{w\text{-}w} = Cp * \eta_{lm} * \eta_{drive} * \eta_{gen}$$

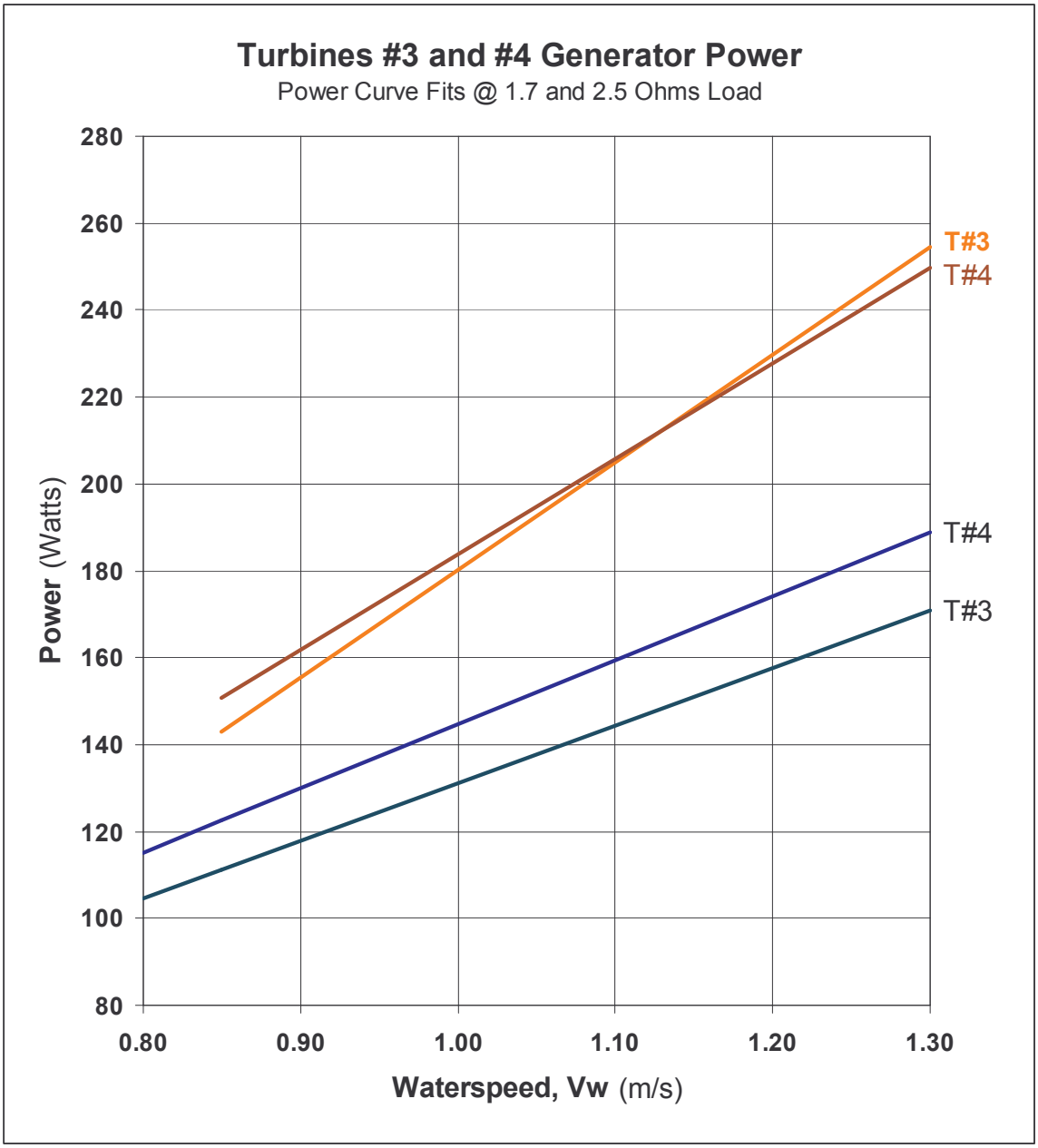

Figure 29. Comparison of Power Output of Turbines #3 and #4

The energy losses from the inefficiencies in the drivetrain and generator are rejected as heat, while the less-than-perfect matching of the load results in capturing less and leaving more of the energy in the water flow than is possible for the rotor.

The good overall agreement in performance between Turbine #3 and #4 shown above indicates a high likelihood that each turbine's subcomponents – rotor, bearings, gearbox, generator, and loadbank – performed similarly in the two units.

Meanwhile, the $\eta_{w\text{-}w}$ values shown in Figure 30 do include all the losses shown above, and are indicative of a non-optimized system.

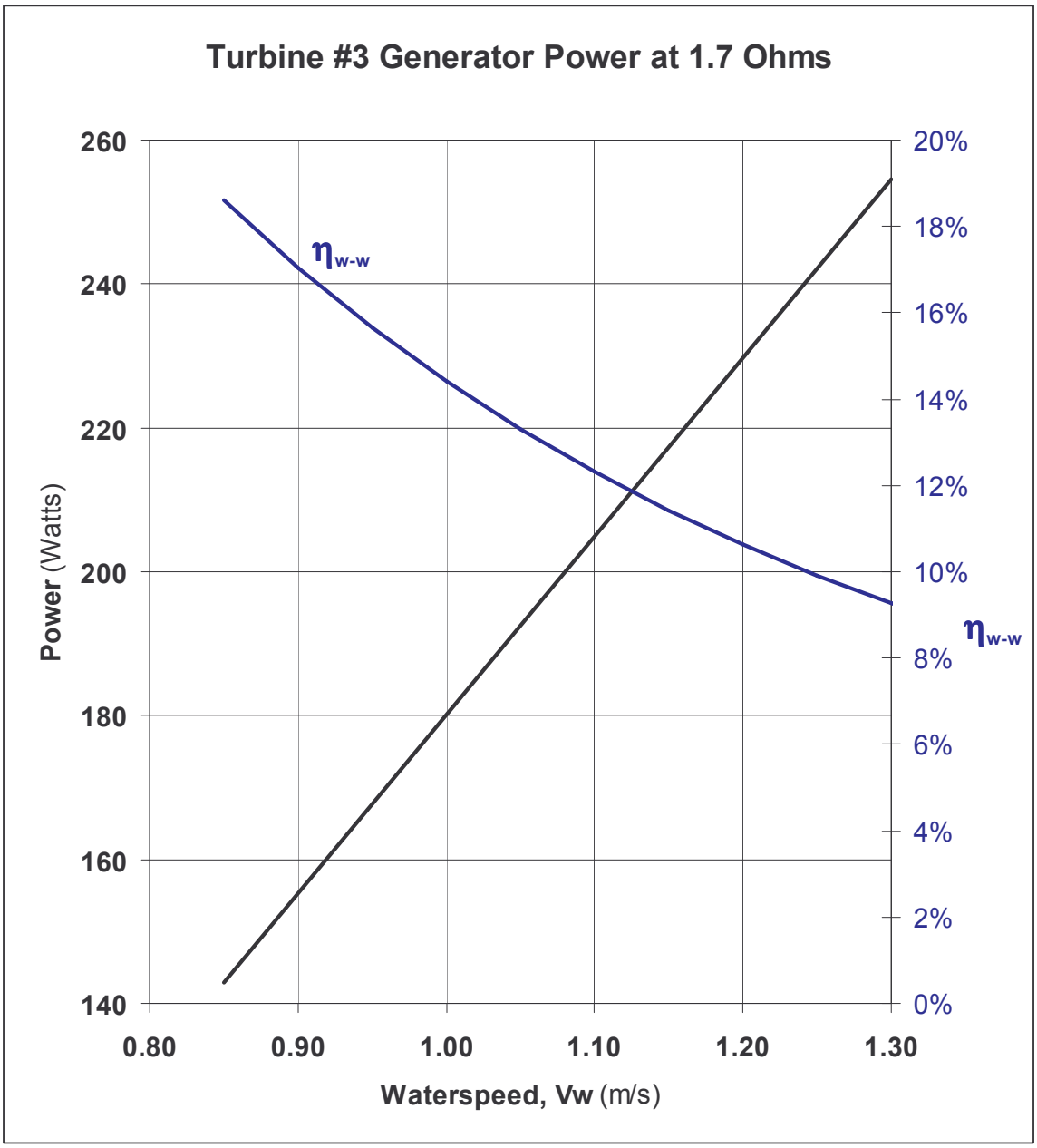

Figure 30. Turbine #3 Electrical Power Output at 1.7 Ohm load

TURBINES #3 AND #4, CROSSWISE SPACING

To examine the effect of crosswise spacing on the performance of the rotors, Turbines #3 and #4 in the sliding side-by-side frames were tested with variable spacing between them. The outermost turbine (#4) was locked at the position farthest from the barge edge, and the inner turbine (#3) was moved in and out on the arm to test at five relative spacings.

Five positions were established for Turbine #3, with spacings between the turbine rotors biased toward the narrower since that is the area of interaction which is of the most interest. The spacings were as follows:

Table 4. Side-bySide Turbine Spacings

Position	**#1**	**#2**	**#3**	**#4**	**#5**
Description	MinNarrow	Narrow	Mid	Wide	MaxWide
Rotor Spacing					
Edge-edge (in)	2	6	12	24	52
(cm)	5.1	15.2	30.5	61.0	132.1
(diameters)	0.051	0.152	0.305	0.610	1.321
Center-center (in)	43	49	55	67	94
(cm)	109	124	140	170	239
(diameters)	1.09	1.24	1.40	1.70	2.39

Turbine #4 power measurements were used for the spacing measurements since this turbine was fixed in position and affected only by the positioning of Turbine #3. As before, electrical power was measured for the turbines at varying waterspeeds and a linear curve-fit was derived for each run. Figure 31 shows one example at the midpoint spacing of 12 inches edge-to-edge.

The crosswise spacing data (Turbine #4 at 2.5 Ohms load) curve-fits are summarized in Figure 32. A clear trend is shown over the range of speeds available, that the power declines with closer crosswise proximity of the two turbines. Apparently, the effected flow from one rotor did not interact constructively with the other.

Figure 33 shows power derating as a function of spacing at the single waterspeed of 1.0 m/s. At the closest spacing, 2 inches (5.1 cm, 0.051 diameters) edge-edge, the power reduced to 72% of that at the widest spacing. This result was similar to that of conventional wind turbines (both Darrieus and axial flow) which lose power as they approach in the crosswise direction on less than the order of a few diameters. However, at a spacing of only 1 rotor diameter (1 meter), which would normally be considered extremely close, the turbine put out about 92% of the power at the widest spacing. Accordingly, even without any enhancement of power at extremely narrow spacing, the turbines may be able to be economically deployed in a dense crosswise manner.

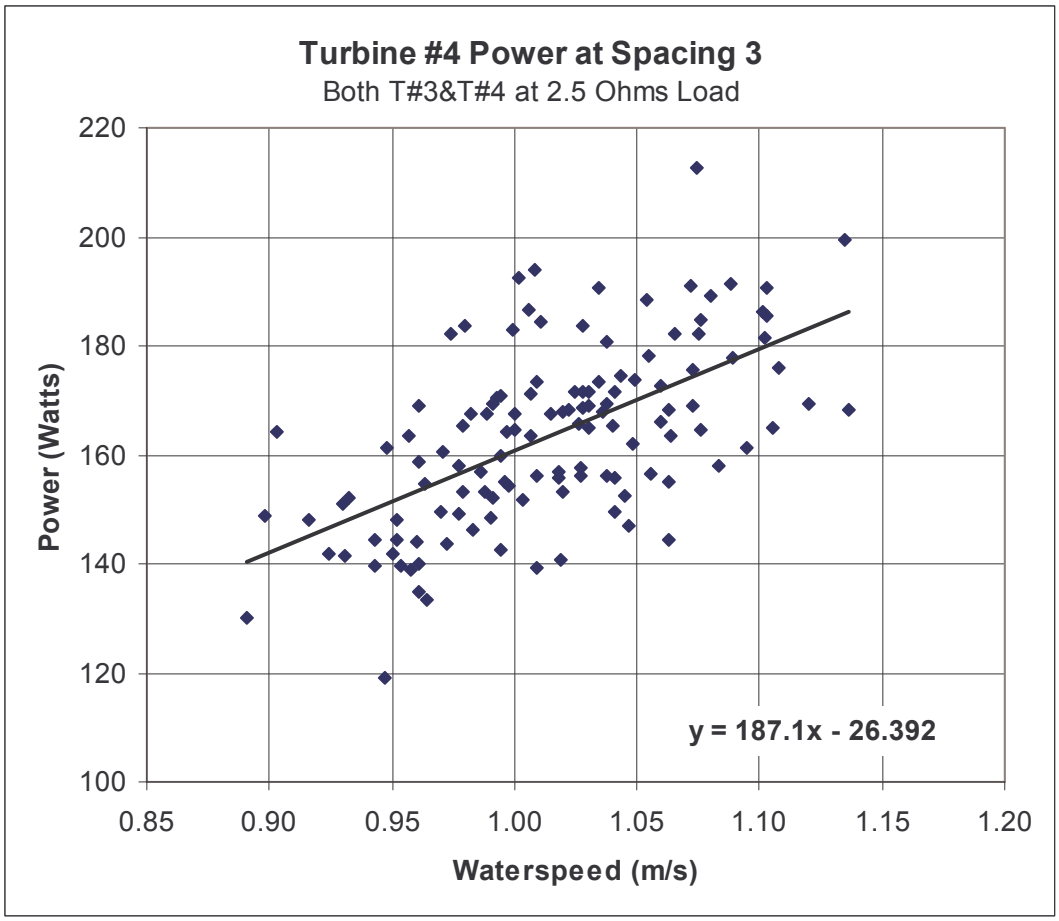

Figure 31. Turbine #4 Power Output with Turbine #3 at Mid Spacing

Furthermore, the arrangement examined here had co-rotating rotors – they turned in the same direction. In this case, since the rotors are turning in the same direction, the closest blade sections of the two rotors are headed in opposite directions, one upstream, and the other downstream. Generally, the power to a rotor could be affected by the proximity of another due to:

1) changed angles of flow relative to the designed,
2) increased flow pressure due to a barrage effect,
3) reduced energy in the flow, and
4) at very close range, even viscous coupling and shearing between the two rotors.

Of these, only the first two effects could contribute to improved performance of nearby rotors, but if this effect could be achieved, it would probably:

1) require very precise geometry of the spacing of the rotors, relative to the individual blade and rotor dimensions,
2) be waterspeed dependent, and
3) be subject to constantly-varying flow conditions due natural waterspeed fluctuations and vortex shedding by nearby rotor blades.

Counter-rotating rotors could be studied, and at very close spacings would be less likely to encounter viscous coupling losses. The use of high-resolution computational fluid dynamics (CFD) analysis would be more appropriate than empirical testing until specific candidate geometries are identified by the CFD.

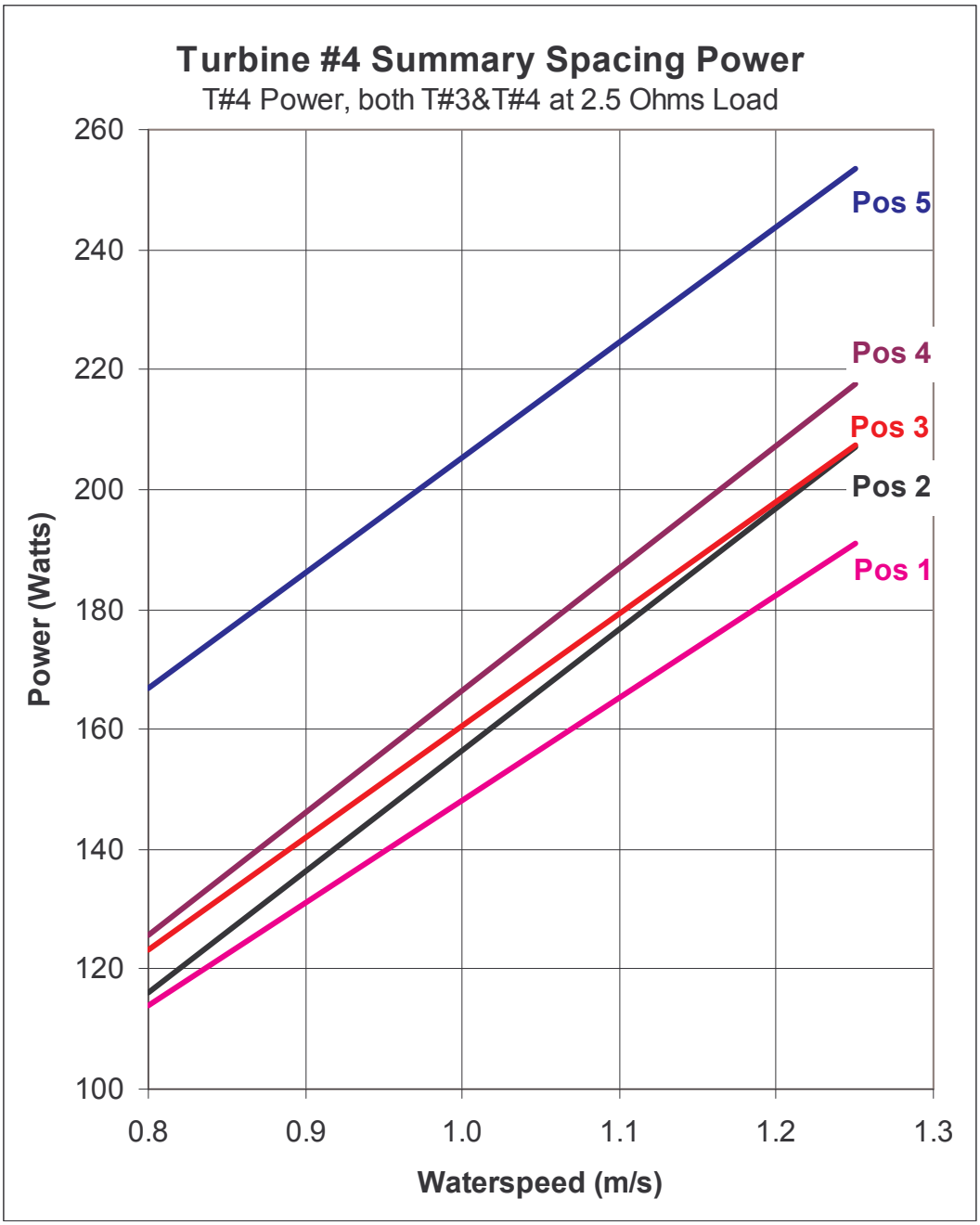

Figure 32. Effect of Turbine #3 Position on Turbine #4 Power Output

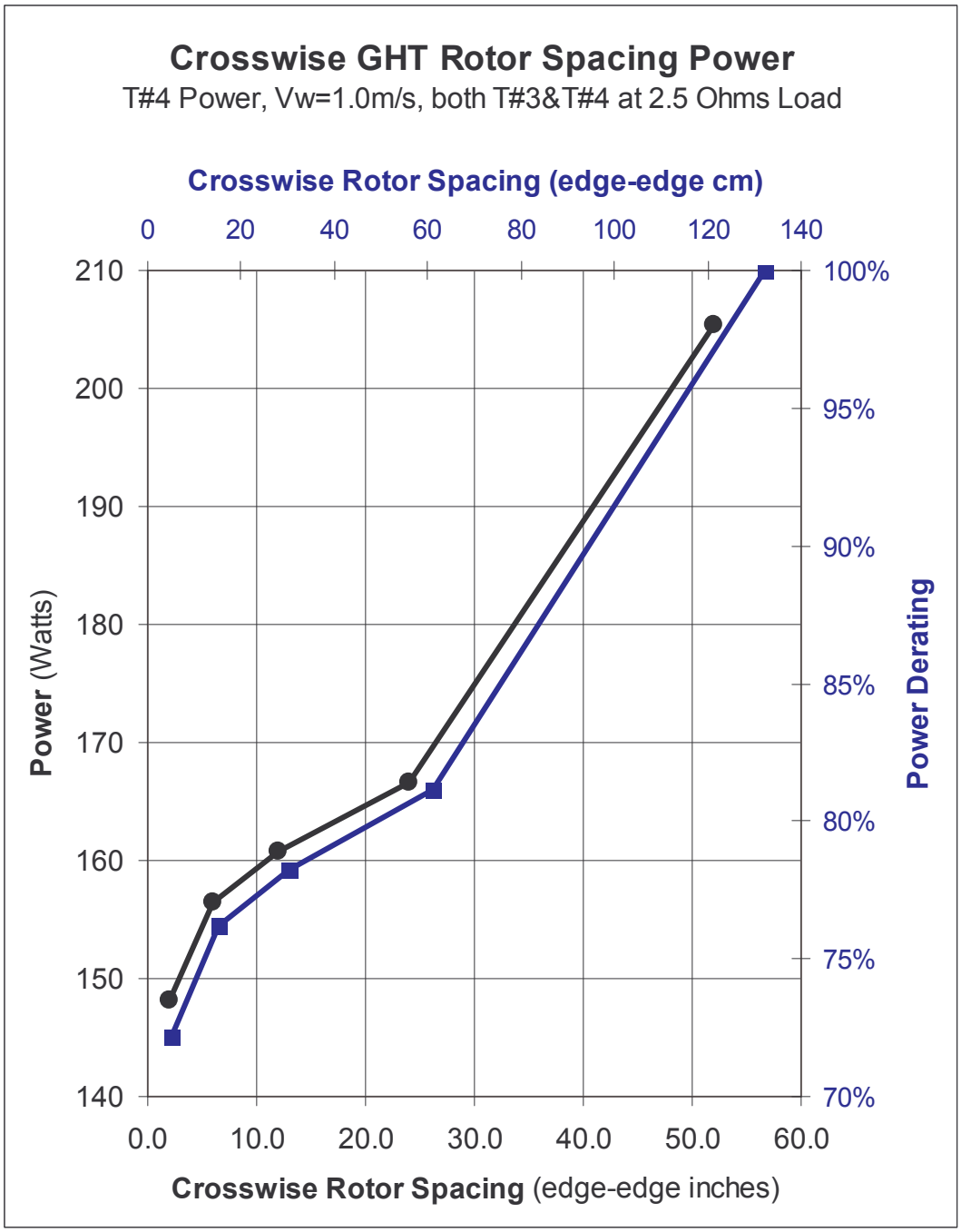

Figure 33. Effect of Turbine Spacing on Power Output

STREAMWISE SPACING EFFECT

In Position 5, Turbine #3 was directly downstream (during ebb flow) of Turbine #1 and farthest from any influence of Turbine #4. In this position it was possible to examine the effect of a relatively closely-spaced upstream turbine on the performance of the downstream turbine.

The streamwise distance from Turbine #1 to Turbine #3 was 4.42 m (14.5 ft) (4.42 diameters) center-to-center, and 3.42 m (11.22 ft) (3.42 diameters) edge-to-edge.

Performance of Turbine #3 with no upstream rotor – Turbine #1 lifted out of the water under three states for Turbine #1:

1) No-Load -- rotating freely)
2) Loaded – rotating under moderate load and power output
3) Locked – braked with no rotation

Anecdotal operator observations during this phase of testing were that numerous times when Turbine #3 was rotating under relatively low **Vw** conditions, releasing the brake on Turbine #1 to allow it to turn would be followed in a few seconds by Turbine #3 stalling. As the waterspeed increased, Turbine #3 could sustain rotation with Turbine #1 rotating, but then stall with Turbine #1 loaded moderately. With yet higher **Vw**, Turbine #3 could maintain rotation even with Turbine #1 loaded.

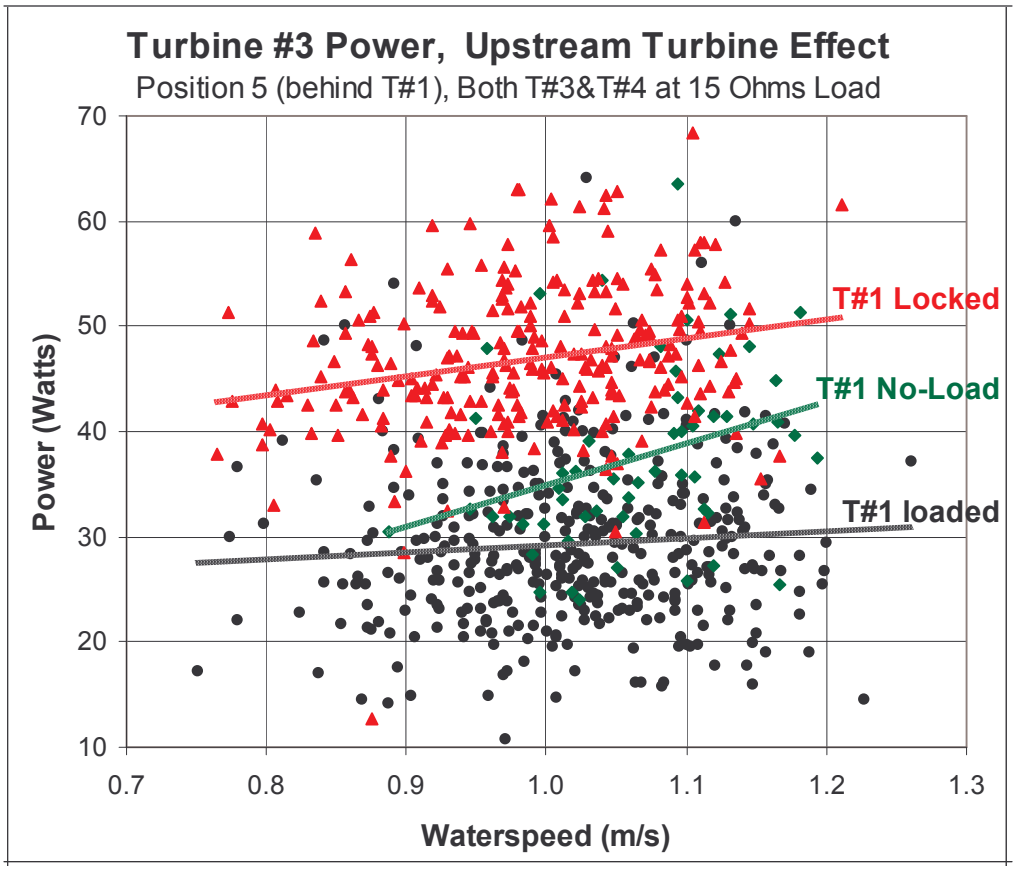

Figure 34. Effect on Power Output of Downstream Turbine

Figure 35 shows the power output of Turbine #3 loaded at 10 Ohms, under the three different operational modes of Turbine #1 upstream. While this data reflects the on-site operator observations, it should be used only as qualitatively illustrative of the phenomenon for two reasons. First, as is noticeable in the graph, the fluctuations in Turbine #3 power were extreme, ostensibly caused by increased fluctuations in **Vw** due to Turbine #1. Second, because of its tendency to stall, Turbine #3 could only be studied in this condition at low loading levels – with high resistance values – so that the power levels are very low, not near optimal or even significant power levels. At 5 Ohms, this relationship showing the loading state of the upstream turbine was not discernable from the data.

Remarkably, when this Turbine #3 power at 10 Ohms is compared with that with no Turbine #1 (lifted out of the water), very little overall power loss, if any is seen from having Turbine #1 upstream at this streamwise spacing of 4.42 diameters center-to-center. A likely explanation for this is that at the fixed resistance, non-optimal loading, the power output is load-match limited, rather than hydrodynamically limited, and is relatively insensitive to waterspeed and structure variations.

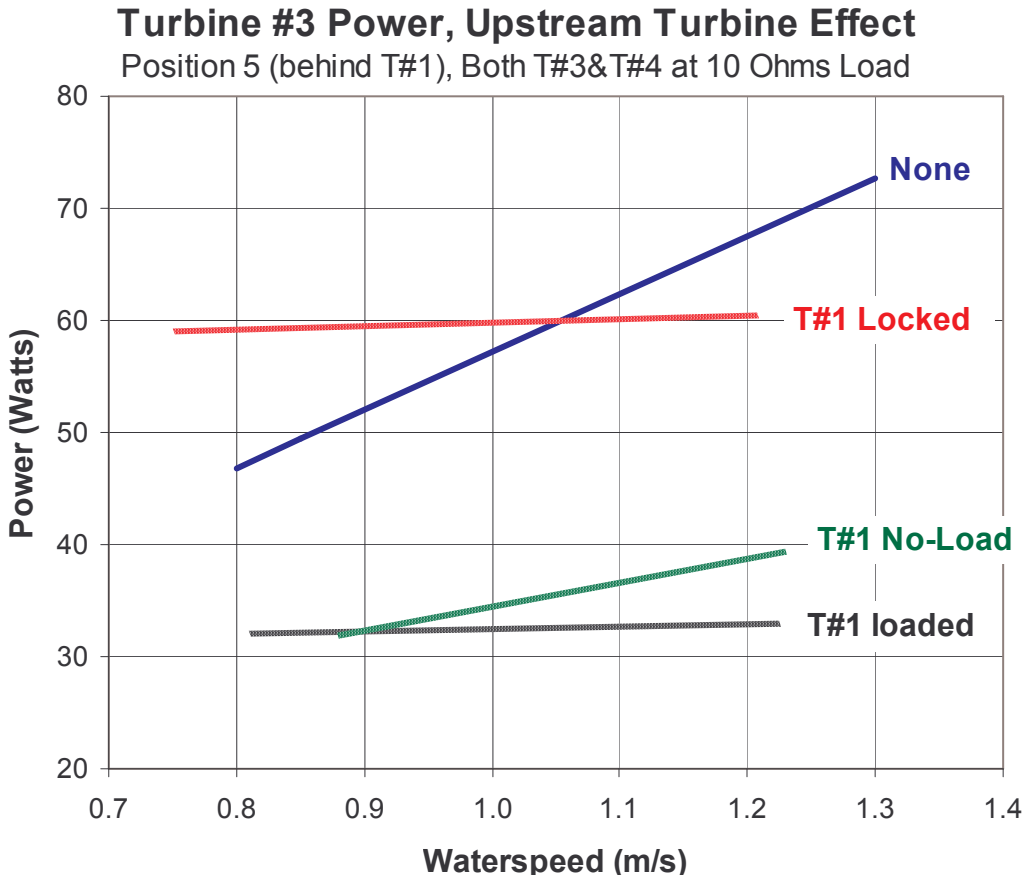

Figure 35. Effect of Upstream Turbine #1 on Turbine #3 Power

This result points to the need to use other techniques to study other streamwise spacings in order to determine power losses (and possibly controllability problems) as a basis for calculating the most cost-effective array spacings for a given site development. Methods could include CFD or using optimally load-matched turbines for spacing comparisons.

CONCLUSIONS AND RECOMMENDATIONS

GHT ROTOR

Performance

As described in previous sections, the efficiency of the GHT rotor is not uniform and presents control issues for automated operation for electricity production.

VP recommends that further research be done to attempt to develop a modified rotor design that combines the starting and torque consistency advantages of the GHT with the higher and more uniform efficiency of the straight-bladed Darrieus rotor.

Approaches to this problem might include:

1) combining GHT and straight-bladed rotor types on a common shaft
2) developing a varying inclination angle shape that transitions from one type to the other
3) developing a rotor than incorporates both types of blades,
4) developing a new hybrid shape

Fabrication

The assembly of the rotor components (shafts, hubs, blades, arms, fasteners) was difficult, labor-intensive, and time consuming. VP had concerns that the bending of the blades necessary to line up the arm/hub mounting holes was putting undesirable stresses into the blades and arm/blade welds, and even potentially quality effecting the hydrodynamic shape. Apparently, the welding and heat-treatment of the blades and arms warped or otherwise distorted the arm/blade assemblies.

A more minor problem was encountered where curved blade airfoil sections had been counter bored as if for socket head cap screw heads, but the screws did not match. Special washers were obtained to solve this problem.

The assembly difficulties may be attributed to the one-off prototype fabrication process, which by nature does not reflect a commercial approach. Therefore, VP concurs with GCK's recommendation that the GHT rotor manufacturing processes be reevaluated with regard to final assembly.

Fouling

Over the test period a significant amount of floating and semi-submerged debris ranging from grasses to full-size trees were observed by VP operators. Despite concerns that a tree or branch could pass through a rotor and become wedged between blades and shaft, at no time did any debris foul a rotor so as to significantly reduce its capabilities. Minor fouling by grasses was easily cleared, as shown in the photo, Figure 36. After the test period, a very small and insignificant amount of biofouling was visible as shown in the photo, Figure 37.

Figure 36. Clearing Minor Fouling By Grasses

Figure 37. Minor Surface Fouling On Rotor and Frame

Corrosion

During the limited test period, only the beginnings of minor surface corrosion from the water (salt on the flood, fresh on the ebb) was observed on the rotor parts that were not anodized or painted. The VP-supplied bearings were made of acetal plastic and stainless steel, and effectively isolated the aluminum rotor assembly from significant galvanic action with the mild steel frame.

Hub/shaft connection

Increasingly with operating time, the turbines vibrated. These vibrations appeared to be about one per revolution, and could be heard and felt when on the frame tops of both turbine #1 and #2 and even near the frame clamp on the barge. Several theories were investigated, and the turbines inspected. It eventually became clear that the vibrations were caused by a wearing and loosening of the connection between the rotor hex shaft and the hubs that hold the rotor arms. These aluminum parts were a slip fit, and before long wore against each other. The resulting horizontal vibrations, which sometimes seemed to be one per revolution and other times two or even three per revolution, began before the wear in these areas was apparent upon inspection. Also, the wearing of the parts apparently accelerated, and if the test period had continued, the rotor hubs would have soon been worn enough to allow the rotor to slip on the shaft and transmit no torque.

VP recommends that this aspect of the GCK rotors should be modified in future rotors to make a positive connection and eliminate relying on the slip fit. Furthermore, a hollow round shaft would be more material efficient and more cost-effective than the solid hex shaft.

BALANCE OF TURBINE SYSTEM

Frames

The one-sided VP frames, both with crosswise arms (Turbines #1 and #2) and with streamwise arms (Turbines #3 and #4) were successful, both structurally and hydrodynamically. They supported the bearings and rotors with adequate strength and rigidity, and presented minimal area to the water flow that could affect the flow entering the rotor itself. In the present case, the mounting of the frames was peculiar to the barge-oriented testing, but they can be readily adapted to any ultimate support structure, whether above the water or on the water bottom.

We recommend that such frames be used with GHT rotors rather than full-cage type frames since they interfere less with the water flow, present less opportunity for fouling (although the rotors are more exposed to potential direct strikes from submerged debris) and use less materials. They therefore have all the benefits of lower-cost handling and shipping, which is further enhanced by the fact that they can be nested while being fully assembled (minus the rotor itself).

Frame Mounts

The barge clamps (Turbines #1 and #2) and cross arm clamps (Turbines #3 and #4) were successful mounts to attach the frames to the barge (to the cross arm structure in the case of

Turbines #3 and #4). As these frame mounts were peculiar to the ATEP study, and further studies or deployments are likely to have different mounting requirements, they serve only as examples of successful approaches to frame attachment.

Bearings

The water-wetted acetal/ stainless steel bearings proved very successful, at least for the 3-month ATEP period. These bearings, when manufactured and installed properly impose little friction, are very rugged and stable (virtually no water absorption and swelling), and require no regular maintenance. Disassembly and inspection of the bearings during and after the test period showed no observable wear, even though the amount of suspended particles in the water was noticeable. An appropriate replacement period for the bearings is thus unknown.

We recommend that such acetal/ stainless steel bearings are a simple, effective, and cost-effective solution to the need for GHT underwater shaft bearings.

Gearing

The belt-and-pulley-transmission provided by VP for Turbine #2 was unsatisfactory, both in terms of residual torque load and overall efficiency, even for manual testing purposes. Meanwhile, the enclosed vertical gearboxes used with Turbines #3and 4 were efficient and reliable.

We strongly recommend using enclosed gear speed increasers in future systems. If it is necessary to use a belt transmission, we would recommend developing a single-stage (despite the large diameter of the large pulley) toothed belt arrangement in which the belt tensioning function is separate from the clutching function. A mechanical clutch that could be used for automated loading/de-loading control would be required, which would add cost, control, and reliability issues.

The combination of an enclosed gearbox with a generator that can be automatically electrically started at the most economical waterspeed point is likely to prove most practical and reliable.

Load Matching and Power Conversion

The load matching efficiency of the rotor is critical to a cost-effective system. The fixed resistance loading used in ATEP was not able to efficiently accommodate the optimal load-matching for the permanent magnet generators over the range of waterspeeds.

In general, due to the sensitivity of the rotor loading and the rapidly-varying waterspeeds in real-world river sites, an active control system based on a simple algorithm using **Ω** and **Vw** inputs is recommended. The drawback with such an approach is the difficulty and expense of implementing and maintaining accurate waterspeed measurements. A large, practical turbine array would likely require multiple ADCP units networked together, both for determining meaningful average values and for redundancy.

Due to the critical nature of load matching the GHT rotor, a desirable approach is a type of maximum power point tracking circuit as has been developed for the solar photovoltaic and wind industries[4]. In one family of devices, an AC-DC-AC converter isolates the apparent load on the generator from the load itself, which may be an inverter for local standalone use or grid connection, or charging a battery bank. A microcontroller programmed with an algorithm based on the rotor's power curve controls the converter to vary the apparent load to the generator so the rotor always operates along its maximum power curve[5]. The brushless permanent magnet generators used here are suited to such a control system and the power capacities and speeds of the key switching components are rapidly increasing as their costs are decreasing. This system would need to accommodate the rapid changes in input power from the water while avoiding stall at all times the **Vw** is above a minimum cut-in value.

Conclusion

These results form useful lessons learned in several technical and practical aspects of the GHT rotor system. However, further progress toward commercialization requires fundamental advances in key areas as discussed below in Areas of Future Research.

[4] Carlin, P.W., Laxson, A.S., Muljadi, E.B., The History and State of the Art of Variable-Speed Wind Turbine Technology, National Renewable Energy Laboratory, NREL/TP-500-28607, February 2001

[5] Marques, J., Pinheiro, H., Gründling, H. A., Pinheiro, J. R. and Hey, H. L., **"A Survey On Variable-Speed Wind Turbine System,"** Federal University of Santa Maria – UFSM. Group of Power Electronics and Control – GEPOC, Santa Maria, RS, Brazil, 2003.

COMMERCIALIZATION

Moving the GHT rotor technology to commercial energy production will require further research and innovation. The most important technical areas are described below in Areas for Future Research. A related issue for GHT commercialization, although not a part of this project, is the availability of water resources as described in section 2.

1) Technical Improvements (Areas of Future Research)
    a. rotor improvements
    b. system improvements

2) Resource Exploration and Qualification
    a. Exploration and accurate qualification of candidate sites
    b. produce inventory

AREAS OF FUTURE RESEARCH

Rotor Development

The characterization of the GHT rotor under the range of conditions in the ATEP study illustrates the need to develop a more comprehensive understanding of the complete set of GHT rotor design variables. Due to the costs, time, and limitations of empirical studies, we recommend a course of detailed computational fluid dynamics (CFD) analyses of the GHT rotor, with specific regard to quantifying the performance with varying values of diameter, height (aspect ratio), chord length, and tipspeed ratio for ranges of waterspeed.

Because of the difficulties of performing them in the field, such analyses should also specifically focus on modeling the effect of the interaction of multiple operating turbines, both cross-stream and streamwise. For example, CFD can provide the flexibility to model counter- rotating turbines in close proximity, and even a cross-stream string of alternating counter-rotating turbines.

Eventual design combinations that exhibit the properties of higher efficiency over a reasonably broad range of **Vw**, could then be subject to a continued program of field testing aimed at commercialization. A reasonable target for such a candidate rotor design would be a **Cp** of at least 30% over a 2:1 range **Vw** such as 1 m/s to 2 m/s.

Load Matching

Once one or more new rotor designs have been accepted, and their power curves generated, a variety of generation, control and power conditioning system topologies should be examined for load-matching to the rotor and for powering specific load types. The efficiencies and costs of these systems should be used to calculate overall system economics.

RESOURCE EXPLORATION AND QUALIFICATION

The Resource Exploration and Qualification of potential sites, includes the following activities:

- quantify power potential
- assess power grid or load interconnection capabilities
- identify competing resource uses
- identify key environmental issues and qualities
- develop inventory of potential sites

In Appendix A is a comprehensive list of information required to determine future site suitability (see "Survey Parameters Table & Log"). Some of this information is readily available with minimal research, while other information may require a field visit and detailed survey work. The relative importance of the information is identified by its color code.

NOMINAL 500KW COMMERCIAL GHT ARRAYS

Appendix G contains a spreadsheet that shows the results of estimates for scenarios of two nominal 500kW total capacity turbine fields using 1 meter diameter by 2.5 meter long GHTs. These scenarios are based on a number of conditions and assumptions including the following:

- The two fields represent two different water velocities that might be found in Massachusetts.
- The first water velocity used is 2.5 meters /second which is the maximum water current for the Cape Cod Canal, and the fastest known velocity in the State. The second is the 1.3 m/s velocity as witnessed during the demonstration period on the Merrimac, during what turned out to be below historical norms for that area.
- We assumed deployment in a unidirectional river that maintains its current velocity at the velocity stated.
- The rivers/fields all have a usable depth greater than or equal to 2.0 meters, the minimum for a 1 meter diameter GHT deployed horizontally. The calculations use a GHT **Cp** (efficiency) of 24%, based on the results of the ATEP tests.
- Efficiencies used for other system components are typical industry values.

Two scenarios are summarized in Table 5, below. The "cost" calculation used the actual costs incurred in the ATEP demonstration, which were largely one-off, custom pieces. It should be assumed that future costs would be dramatically lower due to economies of scale enjoyed by volume production. It is not the purpose of the following graph to explore that element, but to demonstrate the effect that the underlying water resource has on project economics.

The table clearly demonstrates that the difference in water velocity dramatically changes the number of turbines required to make a 500 kW field, and thus the project economics. Thus, for less than a doubling of water velocity, the total cost per kWh decreases to one third of the base-line calculation. The conclusion drawn here is the importance of proper resource assessment and site selection.

Table 5. Summary of Two Nominal 500kW Commercial GHT Array Scenarios

Average Water Velocity		2.5 m/s		1.3 m/s
Turbine Capacity, kW/Unit		3.7		0.5
Number of Turbines		136		964
Total Peak Capacity, kW		502		501
Installed Capital Cost		$4,258,228		$30,183,322
Annual Energy Production, kWh		4,397,482		4,384,471
“Cost” per kWh		$ 0.2253		$ 0.6551

BIBLIOGRAPHY

Gorban, Alexander N., Gorlov, Alexander M., Silantyev, Valentin M., "**Limits of the Turbine Efficiency for Free Fluid Flow",** In Journal of Energy Resources Technology DECEMBER 2001, Vol. 123, pp 311-317.

Gorlov, Alex, **"Harnessing Power from Ocean Currents and Tides**." In *Sea Technology*, July 2004, pp. 40 - 43.

Gorlov, Alexander M., "**Development of the Helical Reaction Hydraulic Turbine,"** Final Technical Report (DE-FG01-96EE 15669), August 1998

Marques, J., Pinheiro, H., Gründling, H. A., Pinheiro, J. R. and Hey, H. L., **"A Survey On Variable-Speed Wind Turbine System,"** Federal University of Santa Maria – UFSM Group of Power Electronics and Control – GEPOC, Santa Maria, RS, Brazil, 2003.

Shiono, Mitsuhiro, Suzuki, Kdsuyuki, Kiho, Sezji, "**Output Characteristics of Darrieus Water Turbine with Helical Blades for Tidal Current Generations,"***,* Department of Electrical Engineering, College of Science & Technology, Nihon University, Tokyo, Japan. In *Proceedings of The Twelfth (2002) International Offshore and Polar Engineering Conference, Kitakyushu, Japan, May 26–31, 2002, ISBN 1-880653-58-3 (Set); ISSN 1098-6189 (Set).*

APPENDIX A

Amesbury Tidal Energy Project

Site Selection and Characteristics

Prepared
by

Jamey Gerlaugh

April 5, 2005
(Rev. 07.26.05)

TABLE OF CONTENTS

Introduction

In support of Verdant Power's Amesbury Tidal Energy Project tidal sites were surveyed from across Massachusetts to determine which would be most suitable for testing the Gorlov Helical Turbine (GHT). Data was gathered with regard to hydrological, social, environmental data that would be relevant to the proper deployment and operation of the GHT from a portable test barge. Information for the test sites was gathered through both on-site visits and offsite research.

The top six sites within the state were identified and evaluated. The data gathered in the summer and fall of 2004 indicated that the site under the Amesbury Swing Bridge on the north side of Deer Island was hydrologically suitable, and was chosen for the short-term GHT test.

Site Selection Procedure

A process to survey and select potential Massachusetts tidal free-flow hydropower sites was created that allowed the site investigation and surveying to occur over multiple stages. This provided for an efficient means to quickly determine whether sites were feasible. The next stage's increased effort and expenses were applied only to sites which passed the previous stage's criteria. Tidal sites were desired in order to test the GHT's bidirectional capability.

The site selection procedure was as follows:

1. Tap existing data sources to create initial list of potential sites
   - **NOAA Tidal Current Tables**. Create an initial list of all tidal sites with maximum ebb and flood velocities greater than 3.0 knots.
   - **NOAA Nautical Charts.** Screen sites to eliminate sites of depth less than 10'

2. Terrestrial visits to top 6 potential sites and perform visual reconnaissance to gather specific hydrological, social, environmental data.
   - **Observe** surface water flow, obstacles
   - **Observe** boat usage, site access, navigation issues. Sites with medium to heavy marine traffic were not selected. Sites with difficult access were not selected
   - **Interview locals-** captains, commercial fishermen, local scientists, and government officials were asked about velocity observations, extent and types of public and commercial use, local project support, fish species of concern
   - **Record with camera and video**

3. Boat visit and acoustic survey of remaining 3 sites
   - **ADCP sonar velocity and depth survey-** Acoustic Doppler Current Profiler (ADCP) to accurately measure 3D velocities from surface to bottom in 3 foot slices.
   - **Further observations** of surface water flow, potential moorings, boat accessibility, fishing usage, navigational issues

4. In-depth data collection of top site, the Merrimack River at Amesbury Swing-Bridge
   - Upstream **USGS river gauge historic flow data** plotted
   - USACE bathymetric and dredging surveys gathered
   - Bridge drawings and specifications
   - Discussion of environmental and fish issues with appropriate agencies
   - Further interviews with boat captains, commercial fisherman, bridge workers for their observations of water velocities throughout year

Site Details and Selection

The list of characteristics which are important to judge a site are listed in the following table, *"Survey Parameters Table & Log"*.

In general, the first stage of the selection process involving researching NOAA Nautical Charts and Tidal Current Tables narrowed the potential state tidal sites down to six candidates. The top six sites and their most important characteristics are listed in the second table, *"Massachusetts. Tidal Site Assessment- Top 6"*

The sites are listed roughly in order of their ranking, with the best sites listed first. Problems that would eliminate a site from the selection process are printed in red text. Maps and photos of the sites follow the table.

By the end of stage 3 the survey information had narrowed the selection down to one site on the Merrimack River. The Amesbury Swing Bridge on the north side of Deer Island appeared hydrologically, environmentally, technically and socially suitable, and was chosen for the short-term GHT test. Details on the chosen Merrimack River site follow in the next section.

Survey Parameters Table & Log

The following "Survey Parameters Table & Log" ("Table & Log") provides the entire list of site information that is needed before a project could proceed to development. The instructions for using the Table & Log sheet are as follows:

1. The Log is used to record Step 1 information. The Step 1 information needs are marked in blue text and represent the information that will need to be gathered first. Site analysis information is shown in green text. If this information is discovered during Step 1, the information, of course, should be recorded in the Table & Log.

2. In general, the order listed is probably the best order for gathering information.

3. Several different survey techniques for obtaining each characteristic are noted next to the characteristic. It is indicated which method will produce the most accurate information by designating that with red text. Methods denoted with pink text will produce slightly less accurate results, but are often much easier, quicker and cheaper than red text methods. Please circle or note the survey technique used.

4. Once the information is determined, record the value using the units specified in the Table & Log, if possible. If a different unit is used, write in that unit.

5. Disqualifying characteristics are listed in the "value" column for a few of the characteristics. Denote any disqualifying characteristics with an "X" in the "Ratings" column. If there are no disqualifiers, the survey proceeds to a site analysis (an in-depth field evaluation and energy analysis) by Verdant Power.

VERDANT POWER

SURVEY PARAMETERS TABLE & LOG

(Page one of two)

TABLE & LOG KEY:

CK = Common Knowledge
LK = Local Knowledge
LTS = Long-Term Study
VP = Verdant Power

Phase 1 Info- Most Valuable Information
Phase 2 Info- More Difficult & Costly Information to obtain
Best Survey Techniques
OK Survey Techniques
Unreliable Techniques

Parameters Most Valuable Information Secondary Information	**Preferred Units, Options** (note if different)	**Survey Techniques** (circle one used) Best Survey Technique OK Survey Technique Unreliable	**Surveyed Value** (write in)	**Rating** A, B, C, X
GEOGRAPHIC DATA				
Body of Water Name		CK		
Site Name		CK		
Country		CK		
State/Providence		CK		
Closest City/Town		CK		
Latitude and Longitude		GPS or Map		
Water Body Resource Type	River, Tidal River, Tidal Strait, Ocean Current, Manmade Channel	CK		
HYDROLOGICAL & GEOLOGIC DATA				
Measured Velocity	m/s; rating: A if > 2.0; B if >1.6; C if > 1.3; X if <1;	ADCP; Speed meter; orange & stopwatch; tables; LK		
Avg Velocity and Velocity Distribution	m/s; rating: A if > 2.0; B if >1.6; C if > 1.3; X if <1;	Long-term study (ADCP; Speed meter; orange & stopwatch; tables); LK		
Max Flood Tide Velocity (if tidal)	m/s; rating: A if > 2.0; B if >1.6; C if > 1.3; X if <1;	Long-term study (ADCP; Speed meter; orange & stopwatch; tables); LK		
Max Ebb Tide Velocity (if tidal)	m/s; rating: A if > 2.0; B if >1.6; C if > 1.3; X if <1;	Long-term study (ADCP; Speed meter; orange & stopwatch; tables); LK		
Peak Velocity	m/s	Long-term study (ADCP; Speed meter; orange & stopwatch; tables); LK		
Length of Section	m	Map; GPS		
Avg Depth	m	ADCP; Depth Sounder; Charts; LK		
Max Depth	m	ADCP; Depth Sounder; Charts; LK		
Min Depth	m	ADCP; Depth Sounder; Charts; LK		
Width	m	GPS; Charts; LK		
Bottom Composition	Sand, Clay, Gravel, Boulders, Organic material, Bedrock	Visual of bank; LK; core sample; depth sounder		
Debris Type	Aquatic Plants, Seaweed, Sticks, Trees, Logs, Rolling Boulders, Trash	Visual; LK; bank survey		

Ice	Never or Surface, Freezes Solid, Bottom ice; note ice thickness and duration	LK;		
Climate	months above freezing (data needed for deployment feasibility)	LK; gov't data		
POWER DEMAND DATA				
Local Peak Power Demand	kW	VP computation		
Local Power Need Projected	kW and Year	VP computation; ask gov't		
Other power currently available	electric grid, wind, solar, diesel generators	LK; ask gov't;		
INFRASTRUCTURE & DEPLOYMENT DATA				
Distance to Transmission Line & of what voltage	km, kV	Map; GPS; ask Power Company		
Local Distribution Network Present	yes/no	LK; ask Power Company		
Nearest Road	m	GPS; Maps; LK		
Nearest Boat ramp or Marina	km	GPS; Maps; LK		
Nearest Airport	km	GPS; Maps; LK		
BIOLOGICAL & ENVIRONMENTAL DATA				
Water Type	Salt, Fresh, Brackish, Polluted	LK; salinity test; hydrometer		
Endangered Species Present	Species name	LK; gov't survey		
Species of Commercial Importance, e.g., Fisheries	Species name	LK; gov't survey		
Biofouling species	Species name			
SOCIAL DATA				
Navigable Waters	no/yes, if yes, type of traffic present (barges, canoes, etc)	Visual; CK; LK; ask gov't		
International Waters	yes/no	CK; LK; ask gov't		
Recreational Uses	fishing, nature tourism, rafting	Visual; CK; LK; ask gov't		
Commercial Fishing	species	Visual; CK; LK; ask gov't		
Dam Plans in works	yes/no	CK; LK; ask gov't		
BUSINESS & ECONOMIC DATA				
Local Utility, if any	Name	LK; ask gov't;		
Site Owner/Governance		LK; ask gov't;		
END OF SURVEY				

(Page two of two)

Verdant Power *ATEP* *Confidential*

Massachusetts Tidal Site Assessment- Top 6

Last Rev: 08-Apr-05 Gerlaugh

Site Name	Nearest City/Town	Data Source	Site Visit	Site Type	Velocity (Fld/Ebb Max if tidal)	Depth	Width	Length of Field	Navig Traffic	Notes
					m/s	m	m		m	
Merrimack River	Amesbury	Verdant ADCP, US Bridge, local marina and captains, NOAA tidal tables	Yes, boat	Fluvial/Tidal	ADCP measured 1.3-1.5 m/s but was dry season; universal locals commonly observe 2.5-3.5 m/s	8	15 m in southern Swingbridge channel	40 m under bridge	heavy near mouth but in Amesbury traffic is minimal and can use adjacent channels	ADCP surveys of 5.5 miles of river from mouth to I95 bridge. The swingbridge site offers great accessibility; high velocity predictions although not observed
Cape Cod Canal	Buzzards Bay	USACE charts and Pilot Books, NOAA tidal tables	Yes, from shore	Tidal	fastest at RR bridge: 2.5/2.5 in middle channel; less on sides	10	135 m but at least 50% needed for nav channel	potentially several miles	heavy navigational use	Met with USACE operators stationed at site. They warned of serious navigation conflict potential
Muskeget Channel	Katama	Local captain, NOAA tidal tables	Yes, from shore	Offshore, Tidal	2.0/1.7	25-45	700	1000	minimal	1 mile offshore southeast Martha's Vineyard, MA
Woods Hole Passage	Woods Hole	Verdant ADCP, local captain, NOAA tidal tables	Yes, boat	Tidal Strait	up to 2.5	6-10	30	700	heavy usage and tricky currents	heavy navigational use, cross currents and shallow depth may prevent usage
Middle Ground Channel	West Chop	Verdant ADCP, local captain, NOAA tidal tables	Yes, boat	Offshore, Tidal	1.6/1.5	13-17	240-300	2000	Fair # of rec. and small commercial fishing boats	appears that ebb may be too weak; along the NW coast of Martha's Vineyard
Blynman Canal	Gloucester	Pilot Books, NOAA tidal tables	Yes, from shore	Fluvial/Tidal	1.5/1.7	Shallow?	10	20	great deal of traffic	under drawbridge is too narrow, and too much traffic; speed in wider part of channel is probably to slow

Map of Cape Cod Canal Site at Rail Road Bridge

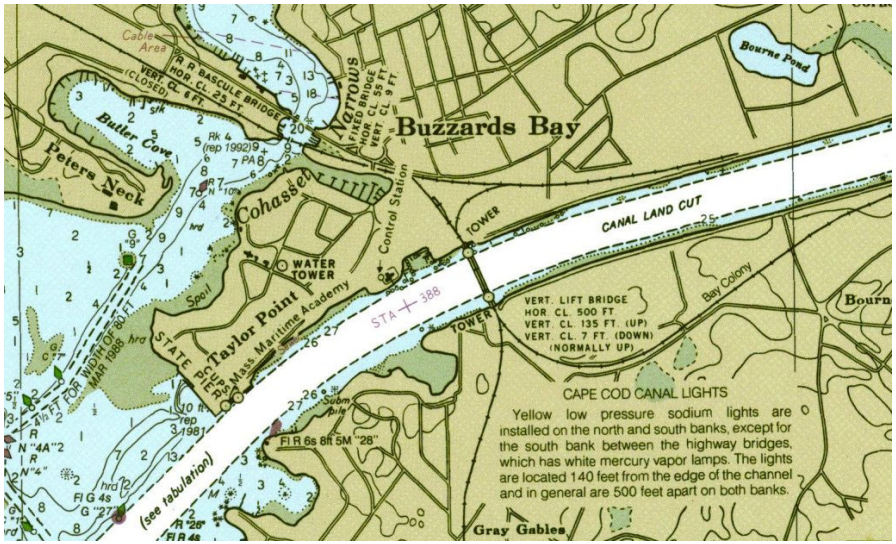

Typical Traffic on Cape Cod Canal

Blynman Canal Map

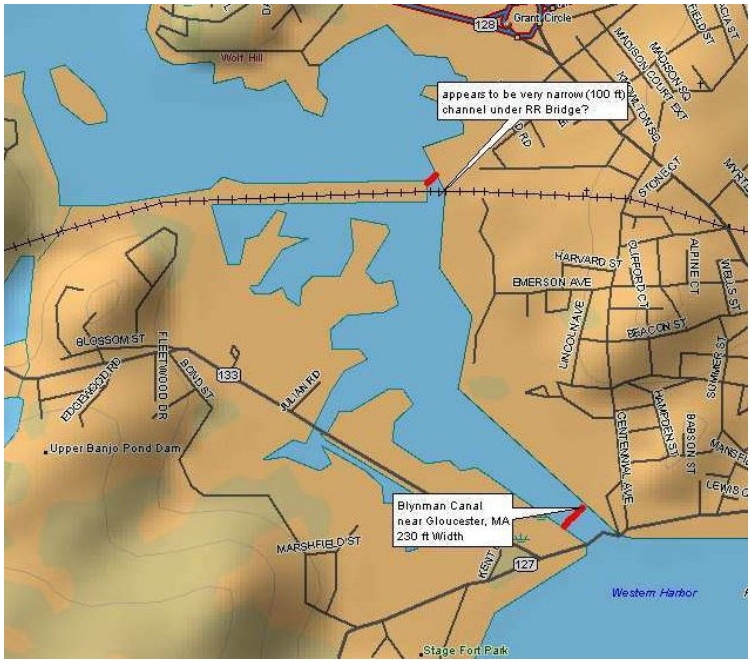

Blynman Canal Railroad Bridge

Woods Hole Passage Chart

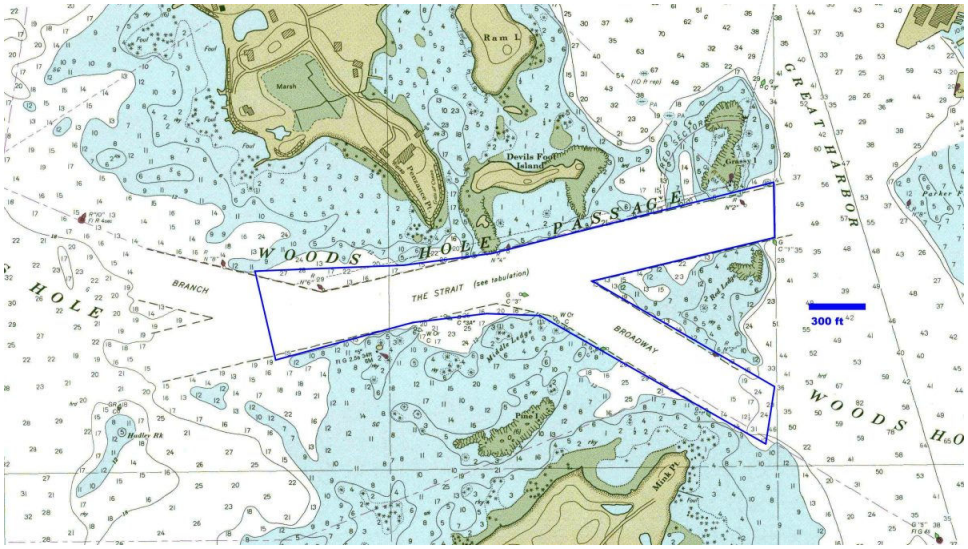

Muskeget Channel Chart

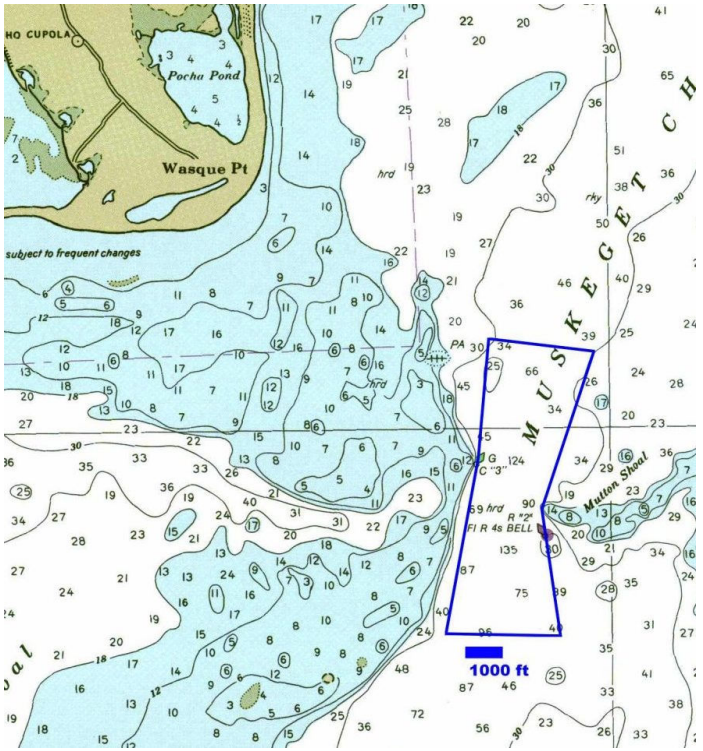

West Chop Chart

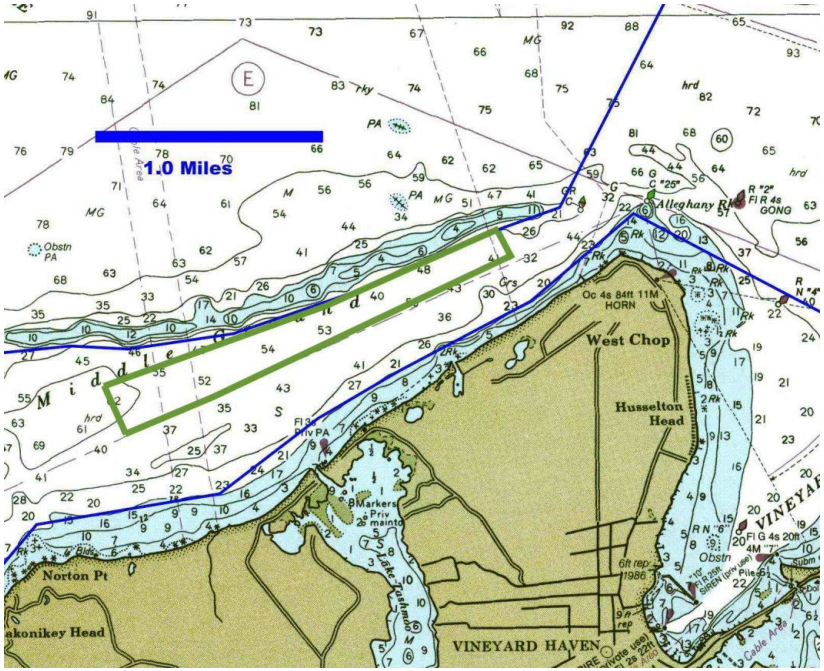

Lowering the ADCP

Merrimack River at Amesbury

Site Description

The chosen site for testing the GHT's is at river mile 5.3 on the Merrimack River, in the town of Amesbury Massachusetts. The site is under the Essex-Merrimack Swing Bridge, which spans between Deer Island to the south and Amesbury on the northern bank. It is located 0.25 downstream of the I-95 Bridge and 5 miles upstream from Newburyport Massachusetts. The site is tidal and the water ranges from fresh to brackish. Deer Island divides the River into a southern and northern channel. Most boat traffic uses the more direct southern channel which is spanned by the fixed Chain Bridge (the oldest suspension bridge in the USA). The northern channel is spanned by a rotating swing bridge, controlled from a station on Deer Island, and opened roughly twice per week to let through sailboats. Most boat traffic does not venture upstream from the bridge since the river quickly shallows.

The channel under the swing bridge is divided by the bridge fender which protects the bridge swing pivot mechanism. The chosen test site is on the southern side of the bridge fender where the channel is approximately 25' deep and has a rock bottom. A test barge can be conveniently moored to the bridge fender. Boats can still have unrestricted passage on the northern side of the fender. Crew access to the fender and barge can be easily gained by a fixed ladder leading down from the bridge's walkway. A public parking lot exists on Deer Island.

Site Map: Lower Merrimack River

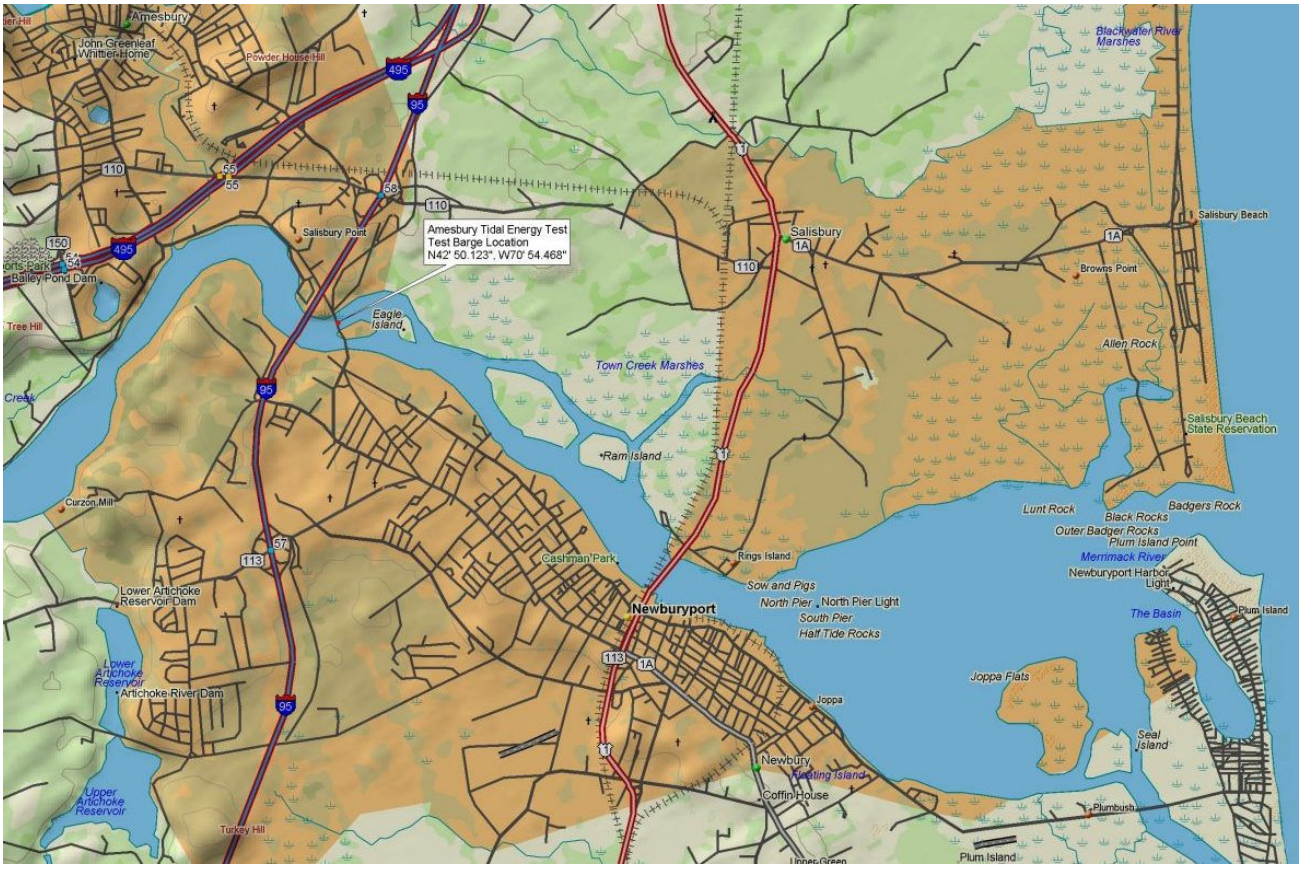

Site Map: Amesbury Bridge Area

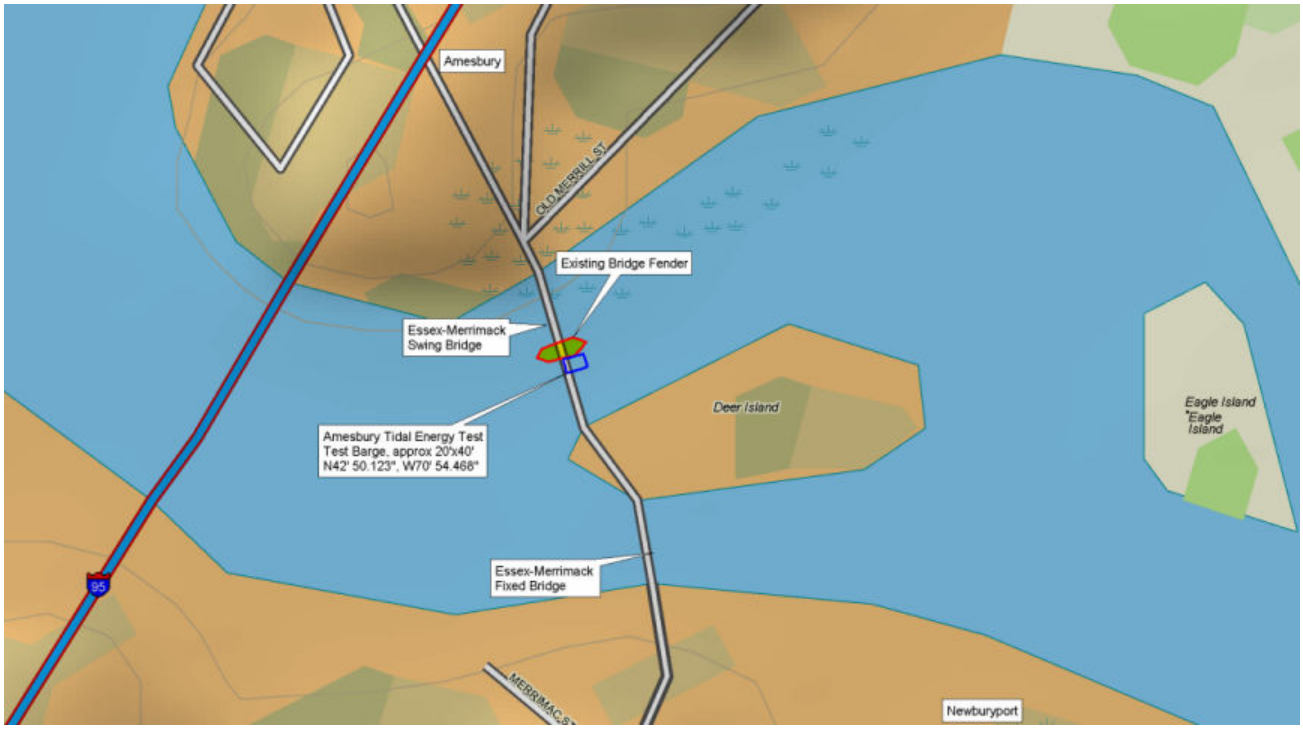

Photo: Bridge Fender from Upstream

Photo: Bridge Fender, looking North from top of Bridge

Photo: Test barge from under Bridge looking upstream

Photo: Looking Downstream from Test Barge at Bridge Fender

Photo: I-95 Bridge as seen from Swing Bridge

Hydrologic Conditions

Merrimack River Flow Components

In determining the water speed of the Merrimack River at the Amesbury swingbridge site of the Amesbury Tidal Energy Test, there are several main factors which come together to determine the velocity. In a tidal river, the water flow will be based on a combination of the following main components:

1. **Base River flow-** The flow contribution from underground sources, snowmelt, average precipitation
2. **Upstream precipitation and snow melt fluctuations-** The flow from recent precipitation events or heavy snow melts.
3. **Daily tidal influence-** The Ocean's water level is affected by the sun and moon's position and subsequent gravitational pull. The flow in a river's tidal zone is based on the difference in heights between the river's water level and the oceans water level.

    - In Ebb tide (during low tide), the River's flow and velocity will increase due to the greater difference between the ocean's and river's height.

    - In Flood tide (during high tide), the River's flow is opposed by the increased ocean's height, decreasing the river's flow toward the ocean. If the ocean's height becomes higher than the river's height, the current reverses direction and flows upstream. Portions of the river can have both up and downstream flows simultaneously.

4. **Wind influenced flows-** The speed and direction of winds can affect the tide's height and also alter the water's velocity at the surface**.**
5. **Dam influenced flows-** Although there are dams upstream they are operated as run-of river facilities. This means that water flow rates entering the dam from upstream equal the water flow being released from the dam and there is no net impact on downstream flows.

Historic River Flow Data from USGS

The closest United States Geologic Survey (USGS) flow station is in Lowell, Massachusetts. The flow would be very similar to the flow at Amesbury since there are no major tributaries to the river between this Station and the Amesbury site. The last major tributary before the Station is the Concord River.

Located downstream of this station in Lawrence Massachusetts is a 14.8 MW dam. Because it is operated strictly as a run-of-river facility (with no varying water storage effect) it does not affect the water flow downstream. The graph below is from the Lowell station[1] displays 365 days of historic mean daily streamflow based on 29 years of data, and last year's actual mean daily

[1]USGS web link: http://nwis.waterdata.usgs.gov/ma/nwis/dv?format=gif&period=365&site_no=01100000

streamflow. Notice that for the last year, there was a huge variation in actual daily flows from the average daily flows.

Discharge, cubic feet per second

Most recent value: 13,300 04-13-2004 13:45

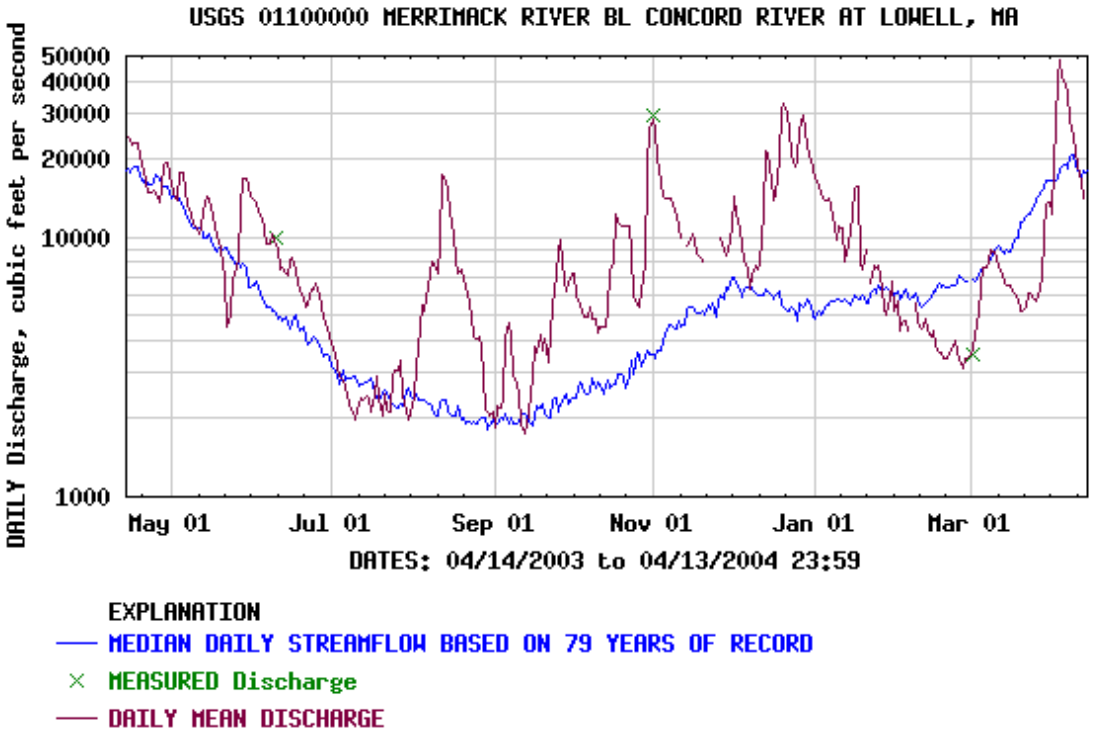

River Flow Reports from Local Observer

John Waitkus, the president of New England Bridge Contractors, is one of the most knowledgeable local people regarding the water flow and velocity around the Amesbury site. He has spent the better part of a year servicing the Amesbury swingbridge from a barge in the main channel. People tend to greatly overestimate water velocities. However in this case, it was based on actual boat water speed observations which can remove much of the measurement's human error. His river velocity observations are from boat speedometer readings taken while maneuvering through the channel at various flows. The following are his observations:

On April 13, 2004, John noted,

> ". . . the River is now flowing 7 knots under the swing bridge as measured by my waterspeed meter on his barge. The water is now unidirectional and there is no flood tide. The water velocity will vary cyclically on a 12 hour cycle from 7 knots down to 4 knots, never reversing. It peaks during the time of the ebb tide and is lowest during the time of the flood tide."
>
> This was echoed by the USCG.
>
> "This flow regime will gradually shift over as spring progresses and the upstream river flow component decreases. By late spring it typically will first drop down in velocity so that the tide is still unidirectional but peaks around 4 knots and down to 0 knots on a 12 hour cycle."
>
> "Then into summer it will shift over to a bidirectional flow which usually maxes at 3-4 knots in each direction at tide peak. Upstream rainfall events can increase the ebb tide and decrease the flood tide."

During the spring, the flows are thus dominated by the influence of the upstream spring rains and the snow melts, which overpower the tidal influence.

Tide Information

The nearest tidal current prediction point is on the Merrimac River in Newburyport. This point is referenced to the NOAA tidal reference station at Boston Harbor at Deer Island Light. A website[2] conveniently and flexibly predicts currents for this site. A sample tidal curve for Newburyport is shown below.

Tidal Current Curve for Newburyport, 17 July 2003

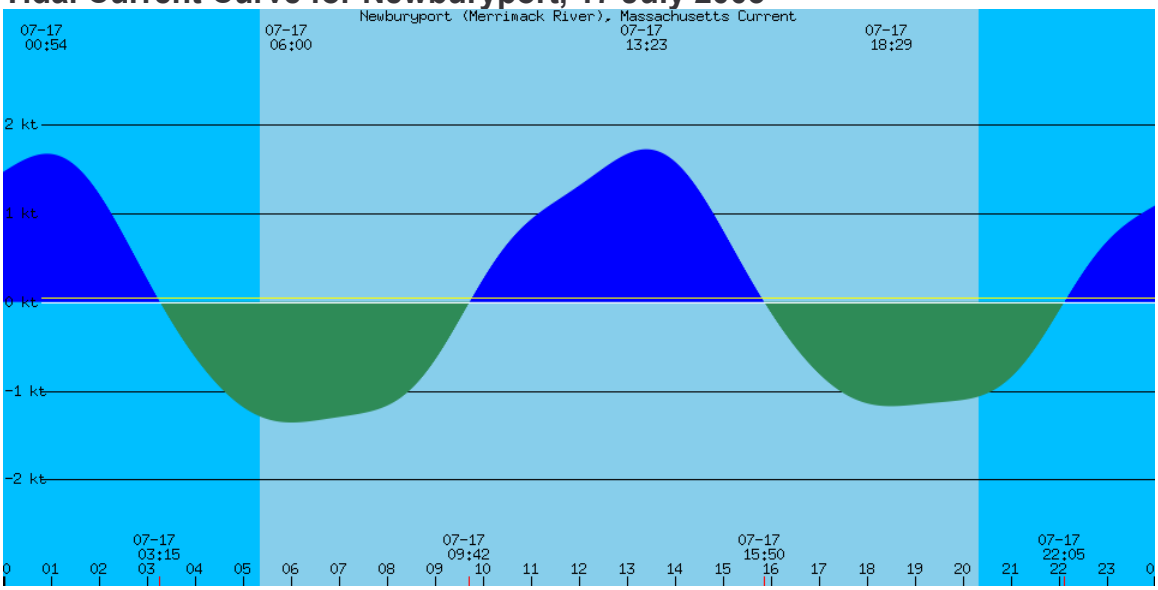

A sample tidal curve for Deer Island Light is shown below.

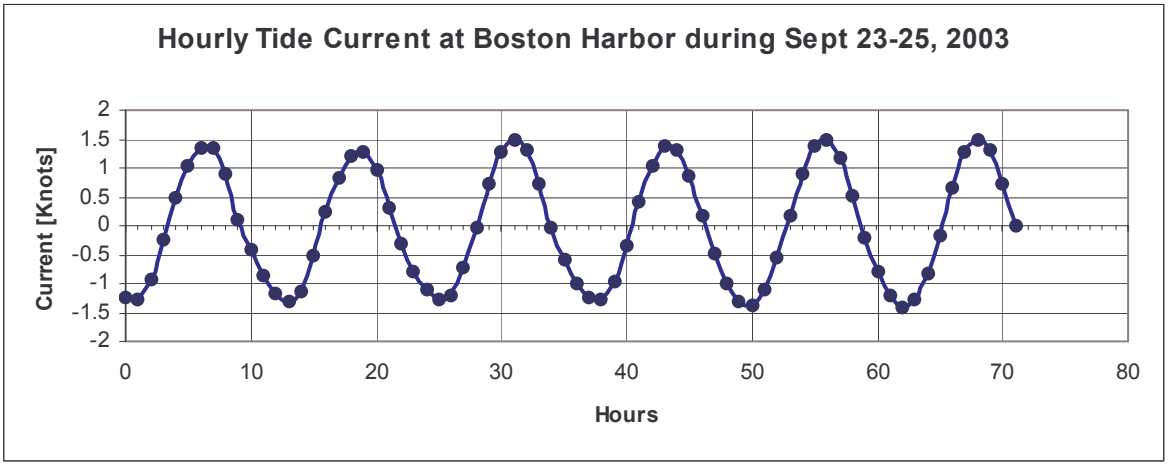

Conversion ratios for converting the tide times and velocities at Deer Island Light to the values for Newburyport are given in the following table. Specific values for July 17, 2003 (the day of the Verdant Power ADCP survey) are also calculated.

[2] http://www2.shore.net/~mcmorran/bin/stateloc.pl?state=MA

Verdant Power Gerlaugh

SURVEY INFORMATION- SITE TIDAL PREDICTIONS

Boston Harbor (Deer Island Light), Massachusetts

Predicted Tidal Current July, 2003

Flood Direction, 254 True. Ebb (-) Direction, 111 True.

NOAA, National Ocean Service

http://www.co-ops.nos.noaa.gov/tab2ac2.html#9

REF STATION: Boston Harbor at Deer Island Light

Tide Type	Date	Time	Tidal Max [knots]
Ebb	7/17/2003	609	-1.4
Flood	7/17/2003	1150	1.3
Ebb	7/17/2003	1838	-1.3

Merrimack River Entrance

Tide Type	Speed Ratio for Boston Harbor to Merrimack Entrance	Corrected Speed for Merrimack Entrance [knots]	Time Correction from Boston Harbor to Merrimack Entrance [knots]	Corrected Time for Merrimack Entrance
Ebb	1.20	-1.68	+115	724
Flood	2.00	2.6	-034	1116
Ebb	1.20	-1.56	+115	1953

Newburyport

Tide Type	Speed Ratio for Boston Harbor to Newburyport ratio	Corrected Speed for Newburyport [knots]	Time Correction from Boston Harbor to Newburyport [knots]	Corrected Time for Newburyport
Ebb	1.2	-1.68	+148	757
Flood	1.4	1.82	+035	1225
Ebb	1.2	-1.56	+148	2026

Verdant Power Measurements

On July 17, 2003, using a boat mounted RD Instruments Workhorse Monitor 1200 KHz ADCP, Verdant Power surveyed potential GHT test sites from Amesbury to the mouth of the River. The following map "ATEP ADCP Survey Cross-sections for 7-20-03" indicates the locations of the cross-sectional survey sites near the Amesbury Swingbridge. For each survey, a subset of the core velocities was measured via the WinADCP software program. All the measurement data shown on that measurement is also shown on the table.

Cross-section MR-12 offers the best ADCP survey of the site. It is the closest measurement to the proposed test site. Note that the map indicates that MR-12 is east of the bridge by 100 feet. In reality, the survey went underneath the bridge. The mapping error has been linked to a GPS measurement error. All ADCP sections on the map need to be shifted west by 100 feet.

The core velocity for MR-12 was approximately 2.97 knots. This would corroborate John Waitkus's description of the velocities during the summer months.

For the tidal component, the daily maximum values for ebb and flood for the Boston Harbor tidal reference station for July 17 were near the maximum peaks for the month. A low contribution from the upstream river components would be expected at this time of year.

From the USGS streamgauge at Lawrence Massachusetts, the flow for July 17, 2003 was measured at approximately 2200 cfs which is near the historical average for that day. The day of our measurements, July 17, was also near the lowest flow for the year.

The depths shown on the ADCP survey appear somewhat shallower (18- 21 feet) than the 25 feet shown on the NOAA depth survey chart. The reason for the discrepancy is not known since the depth chart is referenced to MLLW and the ADCP survey was also done at low tide. There may have been silting since the NOAA chart was created in 1994.

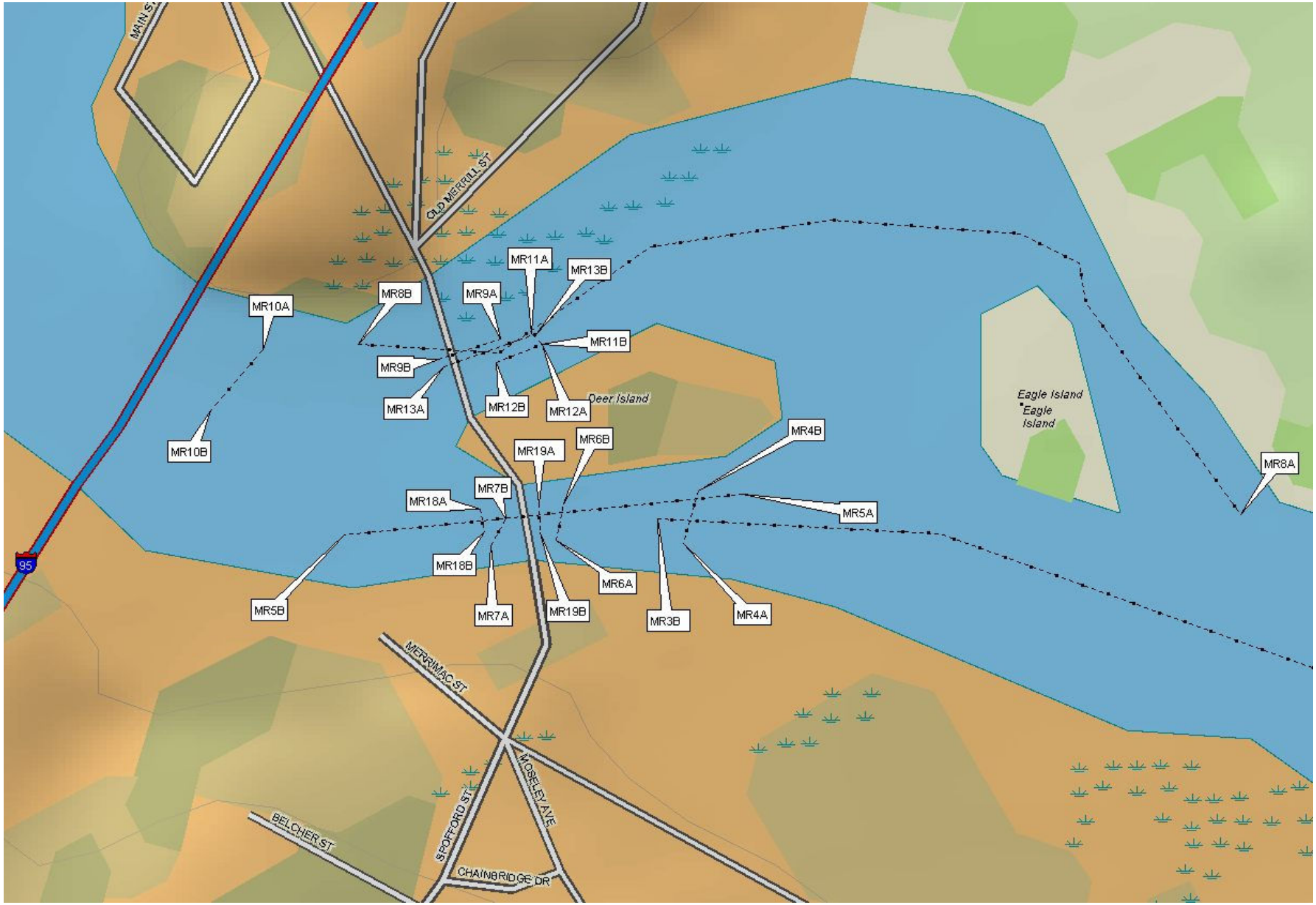
MAIN ST
OLD MERRILL ST
MR11A
MR13B
MR8B
MR9A
MR10A
MR11B
MR9B
MR13A
MR12B
MR12A
Deer Island
Eagle Island
Eagle Island
MR4B
MR6B
MR19A
MR8A
MR7B
MR18A
MR5A
95
MR18B
MR6A
MR5B
MR7A
MR19B
MR3B
MR4A
MERRIMAC ST
MOSELEY AVE
SPOFFORD ST
BELCHER ST
CHAINBRIDGE DR

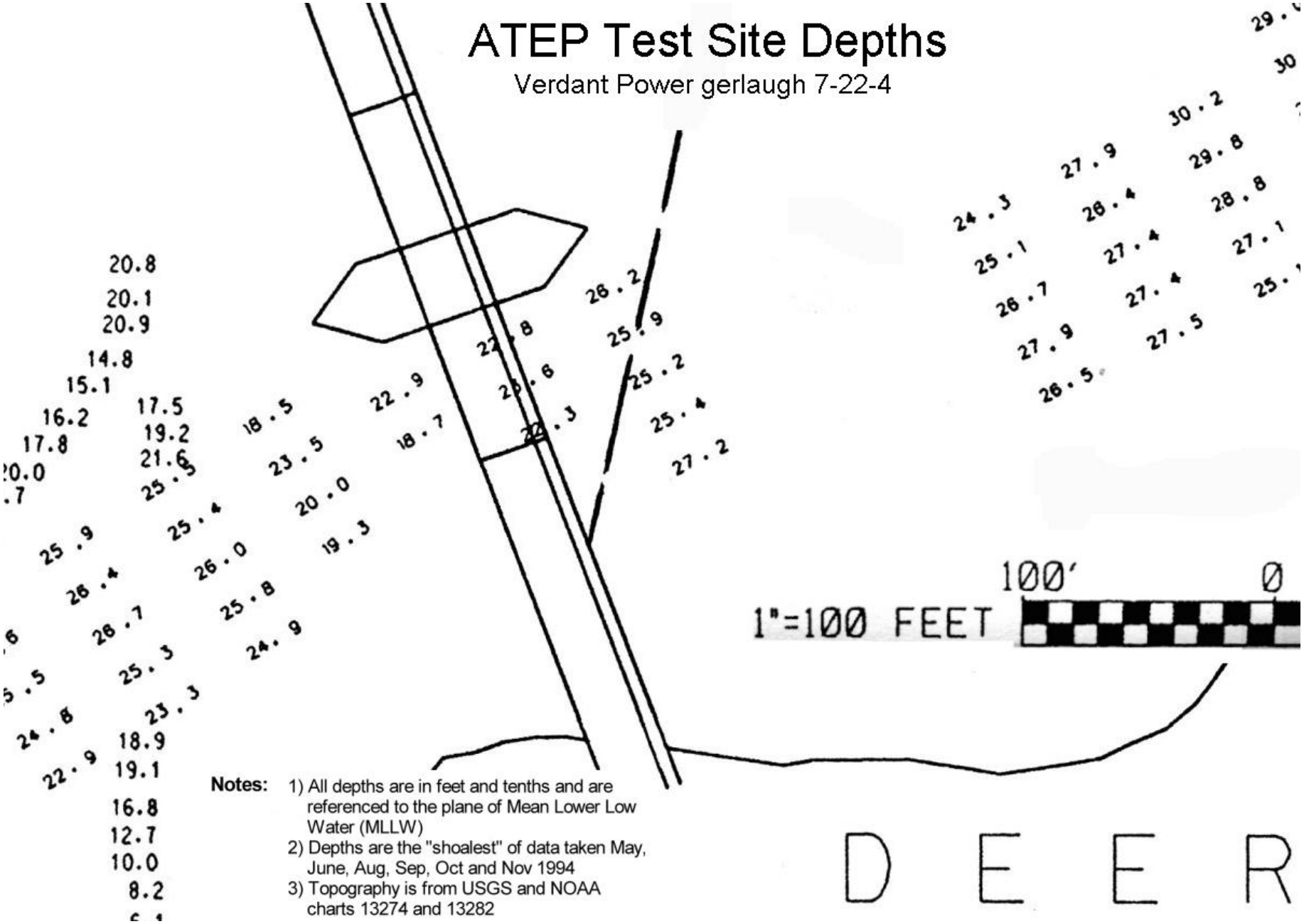
ATEP Test Site Depths
Verdant Power gerlaugh 7-22-4
20.8
20.1
20.9
14.8
15.1
16.2
17.8
17.5
19.2
21.6
25.3
18.5
23.5
20.0
19.3
22.9
18.7
25.4
26.0
25.8
24.9
25.9
26.4
26.7
25.3
23.3
24.8
22.9
18.9
19.1
16.8
12.7
10.0
8.2
26.2
25.9
25.2
25.4
27.2
30.2
29.8
28.8
27.1
27.9
28.4
27.4
27.4
27.5
24.3
25.1
26.7
27.9
26.5
100'
0
1"=100 FEET
Notes:
1) All depths are in feet and tenths and are referenced to the plane of Mean Lower Low Water (MLLW)
2) Depths are the "shoalest" of data taken May, June, Aug, Sep, Oct and Nov 1994
3) Topography is from USGS and NOAA charts 13274 and 13282
D E E R

Verdant Power

Merrimack Project

ADCP Survey Data July 17, 2003

Note: Longitudinal GPS error is approx 100' too far east.

Gerlaugh 10/16/03

				"A" On Map	"A" On Map	"B" On Map	"B" On Map								
X-section Number	Date of Survey (in filename)	Approx File Time (in filename)	Latitude Start	Longitude Start	Latitude Stop	Longitude Stop	Avg Velocity of Rectangular subset m/sec	Avg vel of Subset [knots]	+/- Deviation from avg velocity (m/sec)	Subset Depth Range: [Bin,Bin]	Subset Depth Range: Top [m]	Subset Depth Range: Bottom [m]	Subset ensemble #'s	Subset length [m]	Tide Direction
MR1	7/17/03	713	42-49.042	70-52.382	42-49.004	70-52.410	-								ebb
MR2	7/17/03	726	42-49.034	70-52.394	42-48.986	70-52.440									ebb
MR3	7/17/03	734	42-48.995	70-52.468	42-50.025	70-54.325	1.40	2.72	0.24	1-4	0.5	3.0	2389-2419	69	ebb
MR4	7/17/03	808	42-50.012	70-54.306	42-50.040	70-54.294									ebb
MR5	7/17/03	813	42-50.038	70-54.262	42-50.016	70-54.558	1.45	2.80	0.28	1-5	0.5	3.5	3325-3349	32	ebb
MR6	7/17/03	825	42-50.013	70-54.400	42-50.033	70-54.395									ebb
MR7	7/17/03	829	42-50.010	70-54.449	42-50.025	70-54.438									ebb
MR8	7/17/03	842	42-50.027	70-53.890	42-50.120	70-54.548	1.43	2.78	0.25	1-4	0.5	3.0	5162-5210	65	ebb
MR9	7/17/03	903	42-50.123	70-54.442	42-50.112	70-54.488	1.45	2.81	0.32	1-5	0.5	3.5	5456-5475	25	ebb
MR10	7/17/03	909	42-50.117	70-54.619	42-50.084	70-54.658	1.12	2.28	0.25	1-5	0.5	3.5	5720-5732	16	ebb
MR11	7/17/03	915	42-50.126	70-54.419	42-50.120	70-54.411									ebb
MR12	7/17/03	917	42-50.120	70-54.411	42-50.110	70-54.445	1.53	2.97	0.23	1-6	0.5	4.0	6098-6105	13	ebb
MR13	7/17/03	920	42-50.108	70-54.484	42-50.126	70-54.415	1.35	2.62	0.27	1-6	0.5	4.0	6328-6342	19	ebb
MR14	7/17/03	1218	42-48.910	70-52.248	42-49.051	70-48.138	1.61	3.13	0.27	2-6	1.0	4.0	2634-2777	242	flood
MR15	7/17/03	1321	42-49.120	70-48.258	42-48.987	70-48.267									flood
MR16	7/17/03	1331	42-48.986	70-48.461	42-49.141	70-48.495									flood

ATEP ADCP Cross-section 13

Verdant Power gerlaugh 7-22-4

Survey taken 9:20 AM 7-20-3

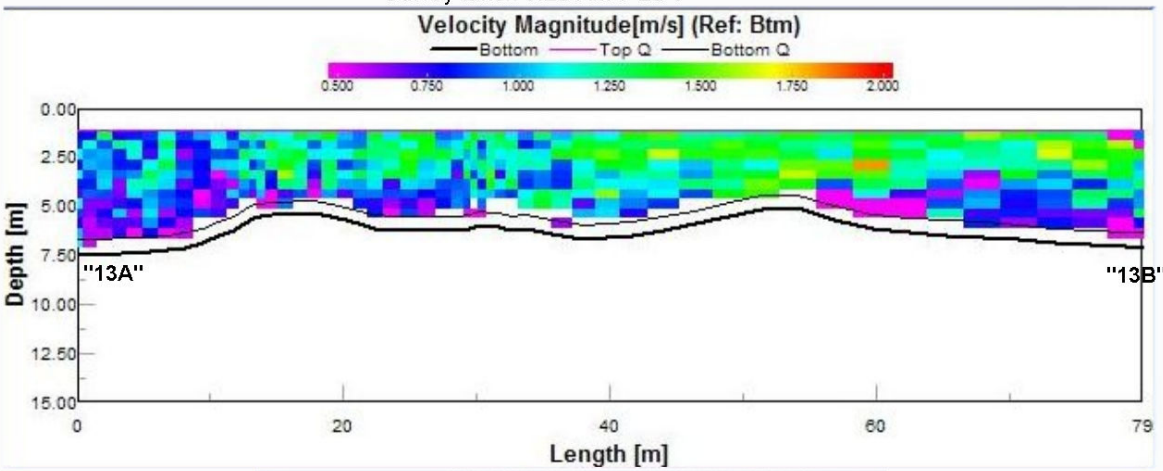

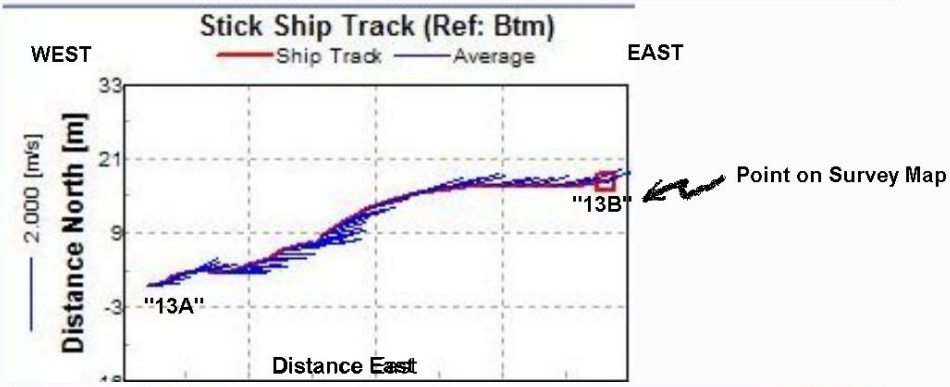

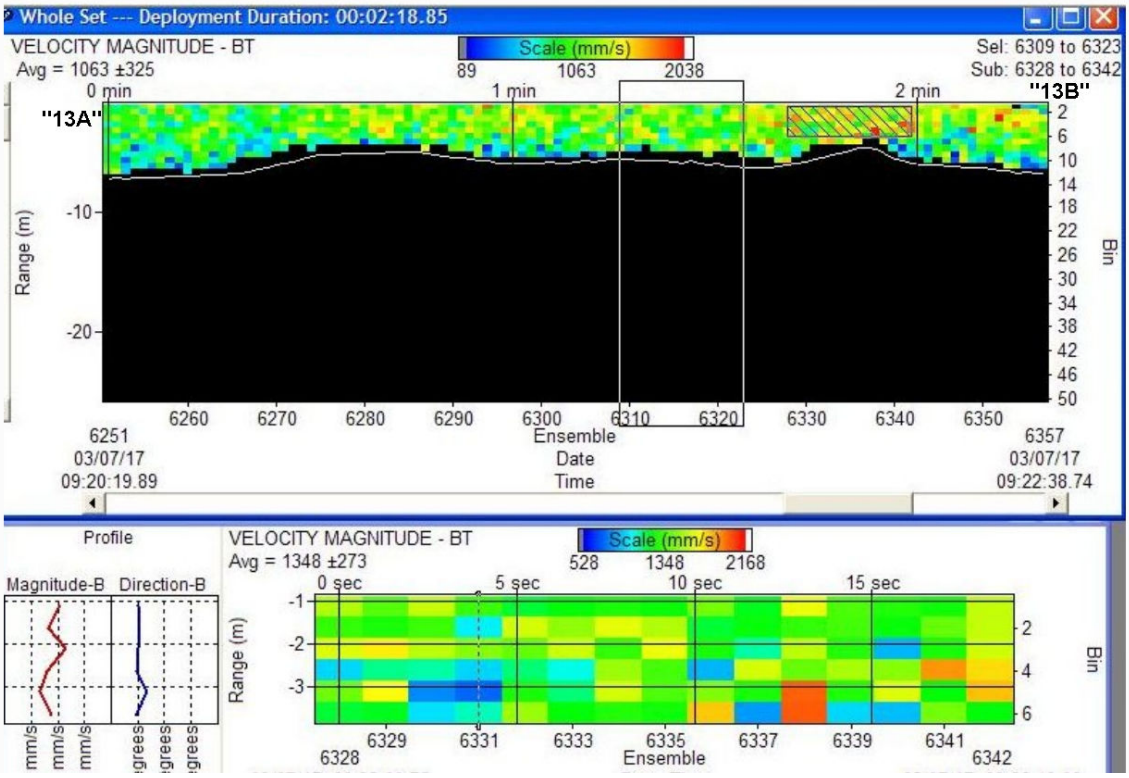

Amesbury Swingbridge Flow & Velocity Predictions

Based on the observations of John Waitkus and Verdant's ADCP readings, a rough estimate was developed of maximum tidal velocities for the swingbridge site, as shown in the table below.

Month	Historic Flow [cfs]*1	Ebb [knots]	Flood [knots]*2
Jan	5300	3.8	1
Feb	6000	4	0
Mar	7000	4.4	-0.5
Apr	15000	7	-5
May	13000	6.4	-4
Jun	6000	4	0
Jul	3100	3	3
Aug	2300	2.7	3
Sep	2000	2.6	3
Oct	2300	2.7	3
Nov	3400	3.2	0
Dec	7000	4.4	-0.5

KEY: Observation of John Waitkus
Estimate from Graph

*1 http://nwis.waterdata.usgs.gov/ma/nwis/dv?format=gif&period=365&site_no=01100000

*2 "-" indicates flood never occurs. Flows in same direction as Ebb

These values are plotted on the following graphs "Ebb Velocity vs River Flowrate" and "Flood Velocity vs River Flowrate".

A rough value for velocities can be determined from these graphs and an estimate of the flowrate from the USGS station data at Lowell. These velocity values are for the river surface.

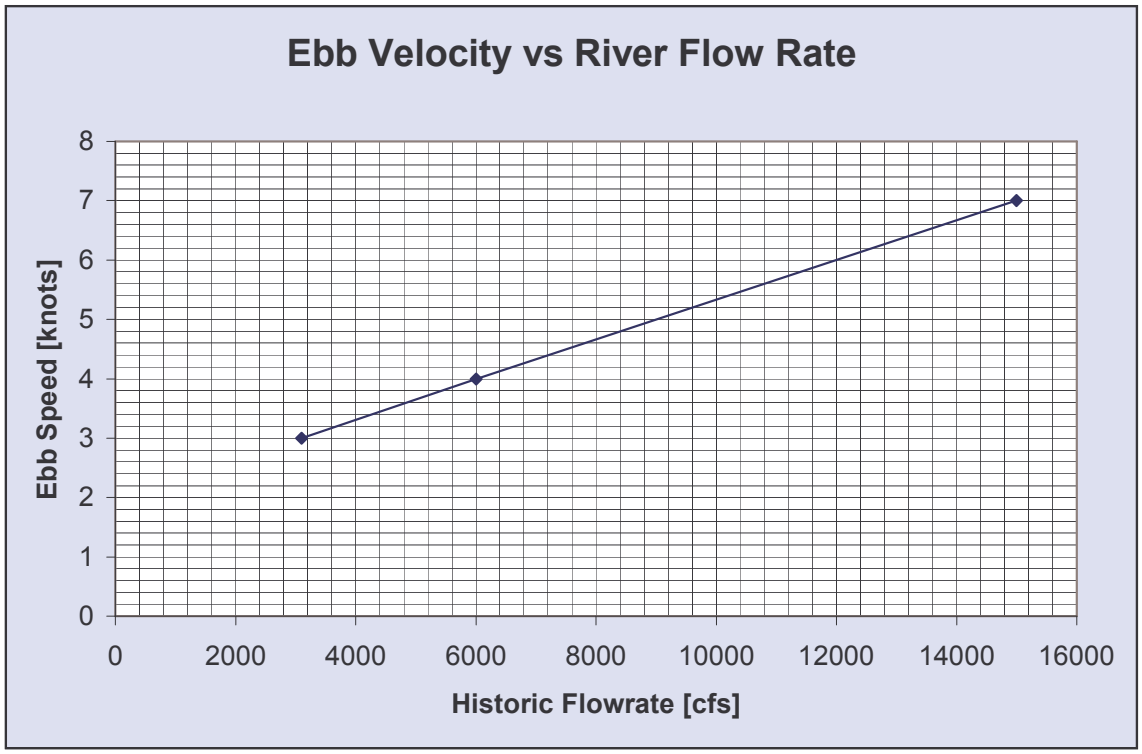
Ebb Velocity vs River Flow Rate
Ebb Speed [knots]
8
7
6
5
4
3
2
1
0
0
2000
4000
6000
8000
10000
12000
14000
16000
Historic Flowrate [cfs]

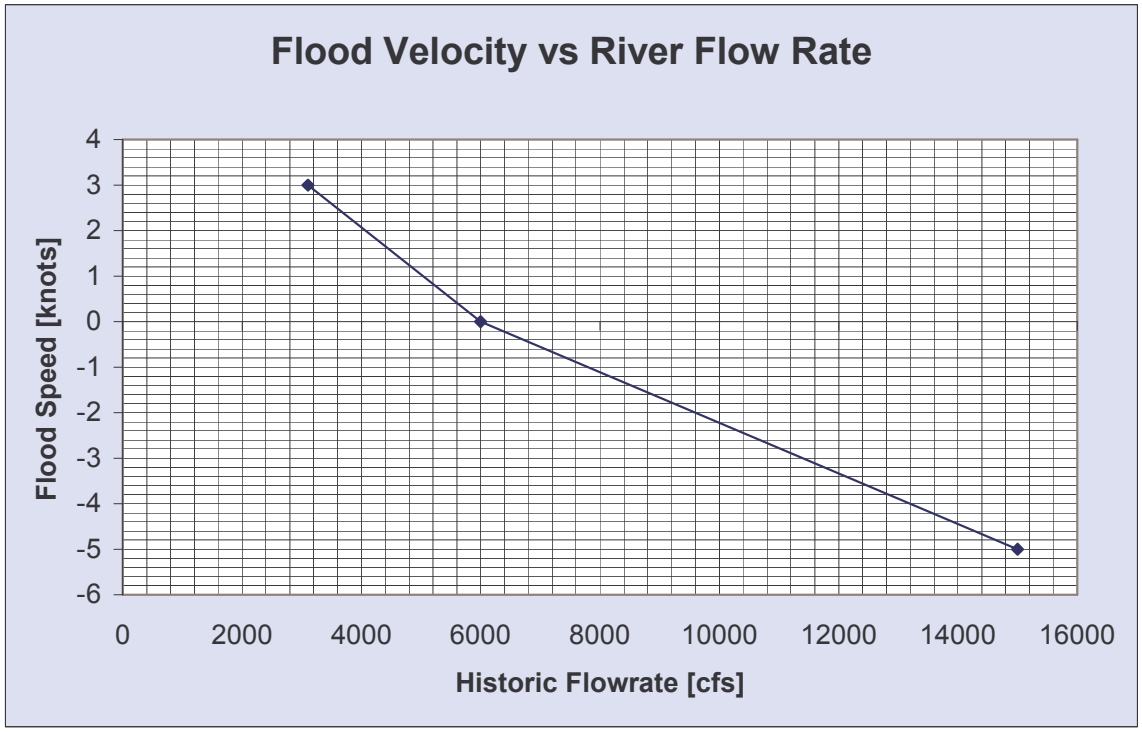
Flood Velocity vs River Flow Rate
Flood Speed [knots]
4
3
2
1
0
-1
-2
-3
-4
-5
-6
0
2000
4000
6000
8000
10000
12000
14000
16000
Historic Flowrate [cfs]

Conclusion

The best indicator of practical velocities at the Amesbury Swingbridge were from the observations of local commercial watermen which indicate that the velocities can reach up to 7 knots in the ebb tide and –5 knots during a flood tide during the spring flows. These values would be very suitable for GHT testing. The ADCP values obtained from a boat survey on July 17, 2003 were taken at a low flow point in the summer and indicated minimal velocities, but helped establish a velocity model for the site based on the flowrate and historic data.

Ideally, the tests would be timed for periods of higher flow which is typically in the spring. However it is noted that the historic data indicates that the flows can vary widely from the long-term averages such that the historic curves cannot be used to accurately determine the flowrates and velocities for a point in the future.

B. GORLOV HELICAL TURBINE ROTOR AND VERDANT POWER TURBINE ASSEMBLIES

APPENDIX
B

ATEP GHT Rotor and Turbine Assemblies

This description of the design and assembly of the GHT rotor turbines is divided into two parts, the rotor provided by GCK Technology, Inc., and the balance of turbine equipment, assembly, installation and deployment provided by Verdant Power, LLC.

I. GCK, INC.

The GHT rotors were provided by GCK Technology, Inc. With a maximum anticipated waterspeed of 4 knots, GCK indicated that the model ASA2, with 1 meter diameter, and 2.5 meter length divided into two sections rigidly connected together, would be appropriate for the ATEP application, as shown in the schematic diagram, Figure 1, GCK sketches, Figure 2, and 3, and in the photo, Figure 4.

The cross-flow rotor has 3 blades, with 5.5" chords, made of extruded aluminum, twisted helically around a solid hexagonal aluminum central shaft with a 2.25" width. The blades have an inclination angle (from the plane of rotation) of about 67 degrees, and a solidity[1] of 0.14. Each blade is held at its ends by welded spokes which are bolted to hubs which slide over the hexagonal turbine shaft. The spokes are aluminum extrusions with full or semi-airfoil cross-sections.

The present rotors have two separate axial sections, using 4 aluminum hubs bolted together on a common shaft, which is held in two bearings, one at each end. A three-bearing version could have been assembled from these rotor parts to accommodate the forces from higher water speeds, in order to keep shaft flexing within reasonable limits. Indeed, the highest waterspeeds actually measured were about 1.5 m/s (3 knots), and two-bearing version used on all four turbines performed well, both in terms of the very light bearing loads and there seemed to be no problems related to shaft deflection.

Typically, the blade and spoke assemblies are heat-treated to T6 and hard anodized, but problems with GCK's vendors resulted in a mixture of anodized, epoxy painted, and unfinished rotor surfaces. Specifically, turbine #1 was anodized, #2 had a black epoxy paint surface, and #3 and #4 were unfinished.

[1] Solidity, σ, (= $\mathbf{NC}/\pi\mathbf{D}$, where **N** is the number of blades, **C** is the blade chord, and **D** is the rotor diameter). Based on the cord length (5.5"), the $\sigma$is 0.14. Based on the chord length in the horizontal direction of flow (6"), the σ is 0.146.

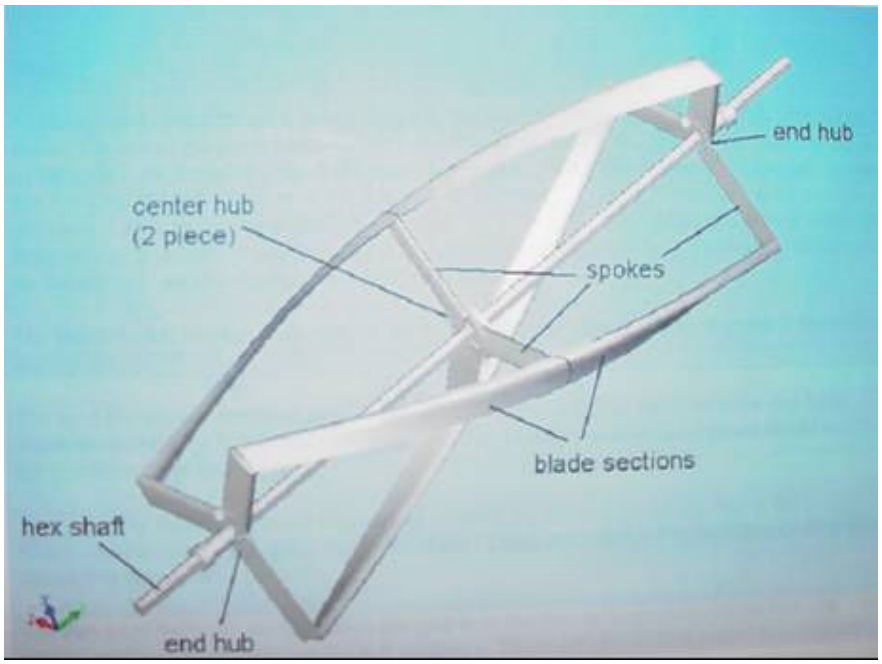

Figure 1. GCK GHT Rotor Schematic

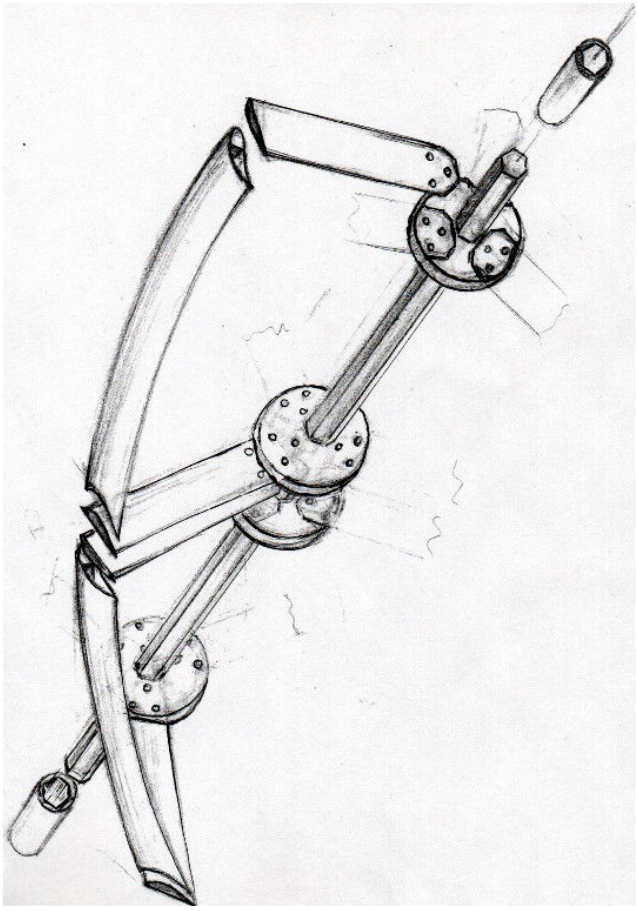

Figure 2. Model ASA2, General view

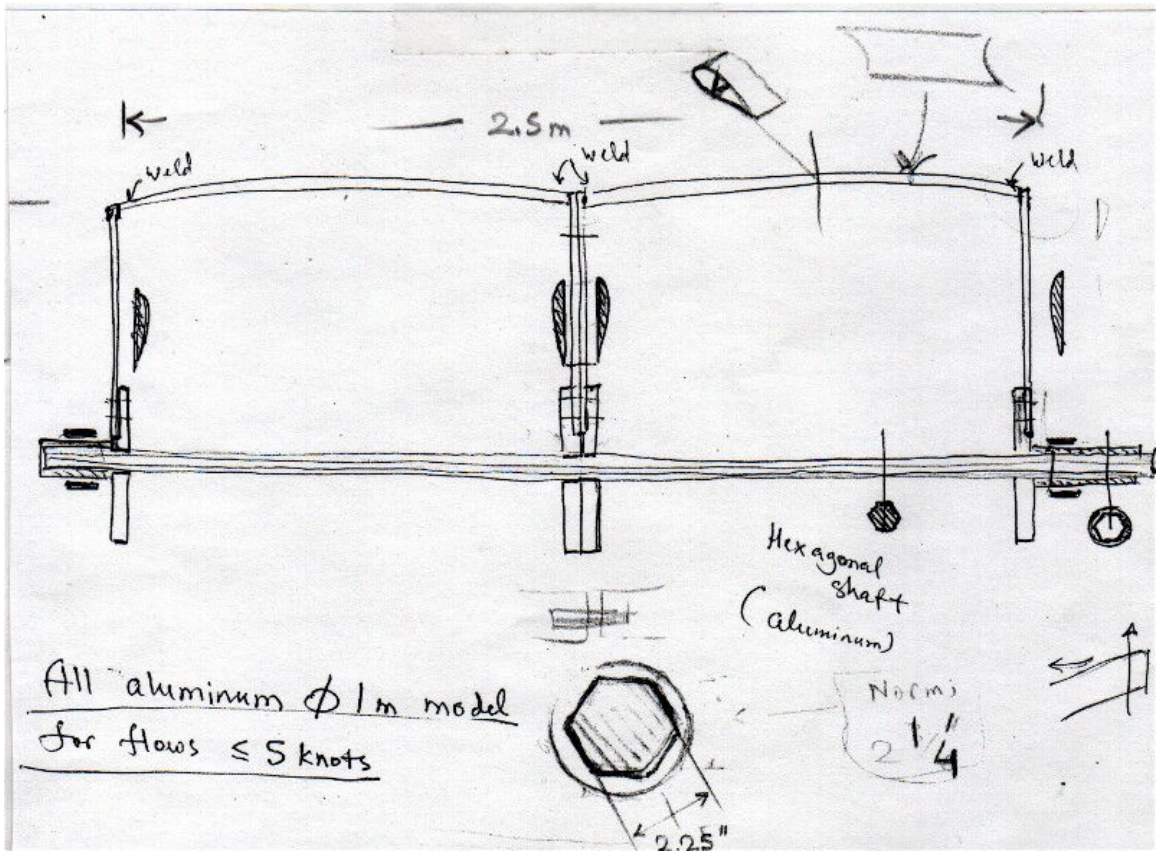

Figure 3. Model ASA2, Side View

Figure 4. Photo of GCK Model ASA2

II. VERDANT POWER, LLC

FRAME DESIGN

Since the performance of the GHT rotor was of primary interest in the study, the VP frames were designed to:

1) hold the rotors with adequate strength and rigidity,
2) present minimal resistance to the flow,
3) neither augment nor detract from the flow entering or leaving the rotor,
4) allow mounting the rotor in suitable low-friction underwater bearings, and
5) provide for strong and convenient mounting to the study barge.

Turbines #1 and #2

Verdant Power has patents pending on the technology described below:

The frames for Turbines #1 and #2 are single-sided, i.e., they do not surround the rotor, but instead have a single column on one side, with a pair of submerged arms that hold the rotor bearings above and below the rotor. Since they were designed to mount along the streamwise edge of the barge, the frames are designed so that the arms extend crosswise to the flow, and there is no support structure upstream or downstream of the rotor. The arms project 1.22 meters (48 inches) crosswise to the stream to hold the shaft bearings on the rotor centerline.

The column and pair of arms are welded of ¼" steel plate and have triangular sections which are oriented horizontal to the flow, presenting very little resistance to water flow while providing for a stiff structure, particularly in the direction of flow.

Figure 5 is a pictorial diagram, and Figure 6 is a photo of Turbine #1 (with the dynamometer stage on top of the frame).

Turbine #1 received a dynamometry top comprised of a manually controlled prony brake and shaft-mounted torque and speed sensor. Made of 2 inch square steel tubing, it held the flange bearings that supported the steel extension shaft and the dynamometry components, as shown in Figures 5 and 6.

Turbine #2 received a frame top, also made of 2 inch square steel tubing, for a generator with belt and pulley transmission, as shown in Figure 7.

These turbine frames were secured to the side of the barge with barge clamps. The barge clamp has upper and lower pairs of arms lined with 2 x 12 inch wood that clamp from the bottom of the barge to the deck as shown in Figure 5. On the outside of the barge clamp are 6 dogs with lockscrews that hold the triangular vertical frame column captive to the clamp. The column can be held to the barge in any vertical position from entirely above the water to fully submerged at which point the top of the rotor is about 18" below the water surface. This permitted the secure mounting of the turbine frames to the barge, followed by the positioning of the barge with the frames out of the water, and subsequent controlled lowering of the frames for turbine testing.

In addition to the clamping action, the clamps were tack-welded in place to the barge deck for additional security.

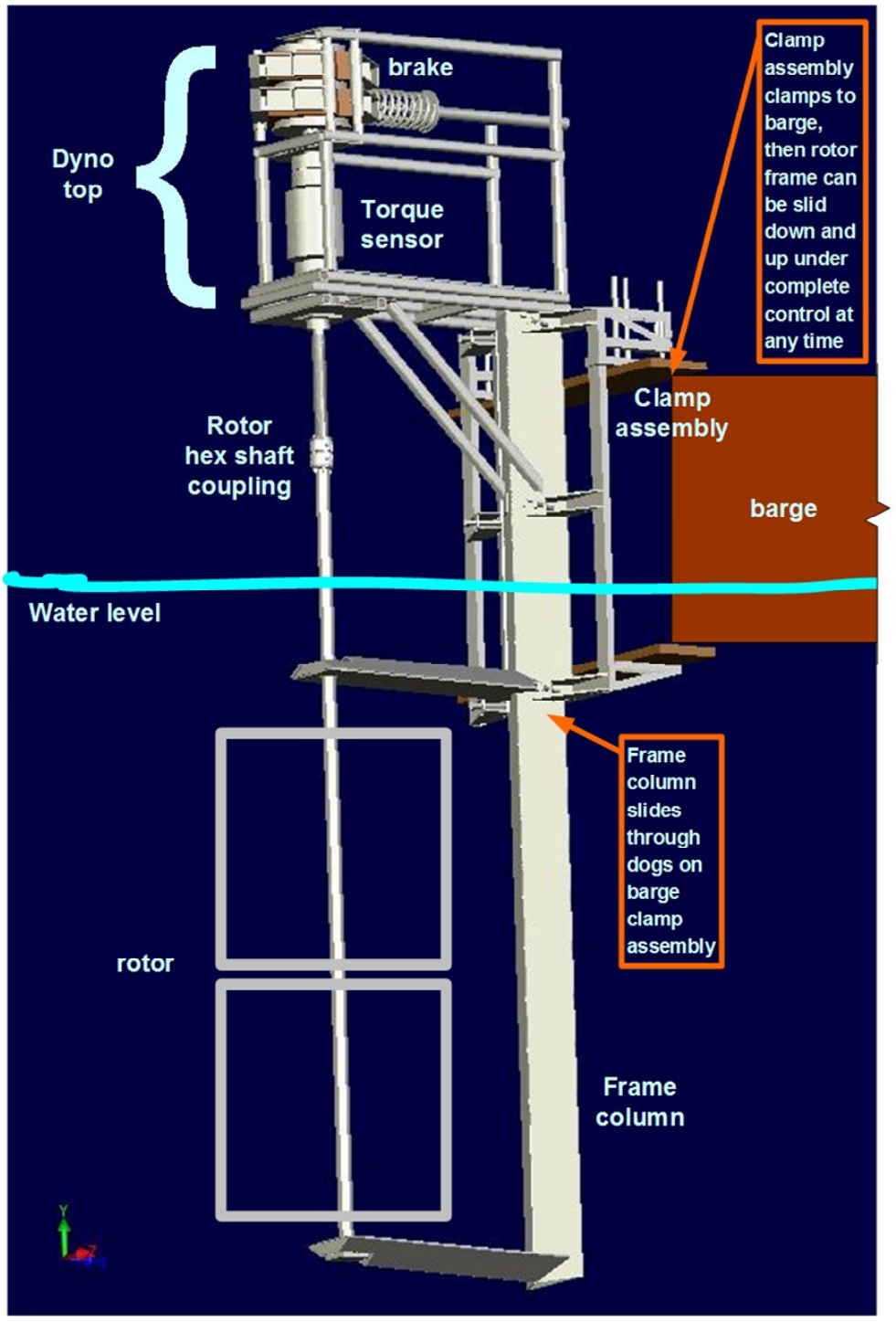

Figure 5. Pictorial Diagram of Turbine #1 Frame (patents pending)

Figure 6. Photo of Turbine #1 in Frame (patents pending)

Figure 7. Photo of Turbine #2 Generator Frame Top Bearings

The two VP-designed bearings which hold the rotors are water-wetted – designed for use underwater without protection from the water. Each is comprised of an acetal plastic radial bushing and a thrust washer secured to the rotor shaft by aluminum blocks that clamp around the hex shaft. The acetal bearing parts run against a stainless steel race and thrust plate, which were bolted to the frame arms, as shown approximately in the drawing in Figure 8 and in the photo in Figure 9. The bushings had axial grooves for sand and debris clearance and the thrust plates had radial grooves. The acetal elements were held to the aluminum shaft clamp blocks by recessed nylon screws. In addition to holding the rotor in a low-friction bearing, the use of the plastic bearing elements provided effective galvanic isolation of the aluminum rotor from the steel support frame.

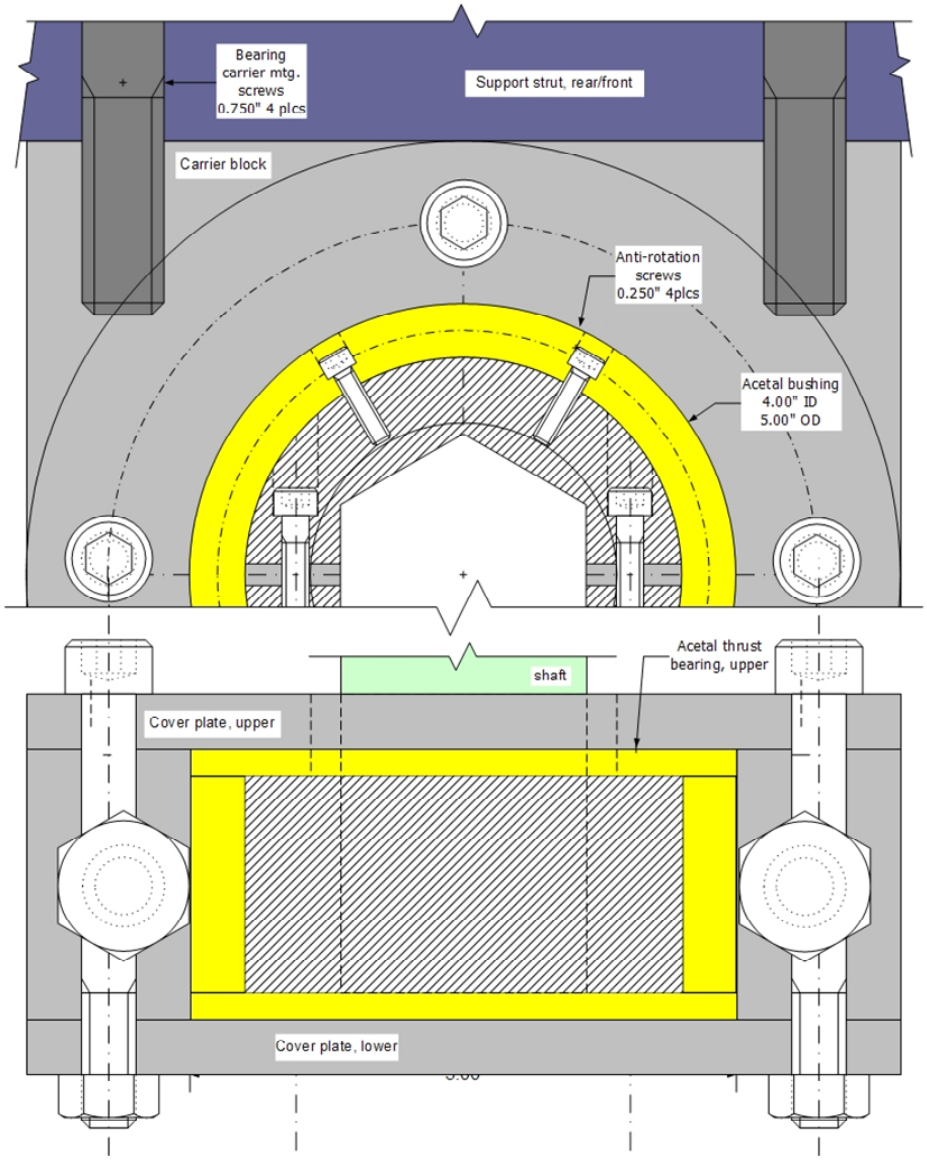

Figure 8. Drawing (approximate) of VP rotor Bearings

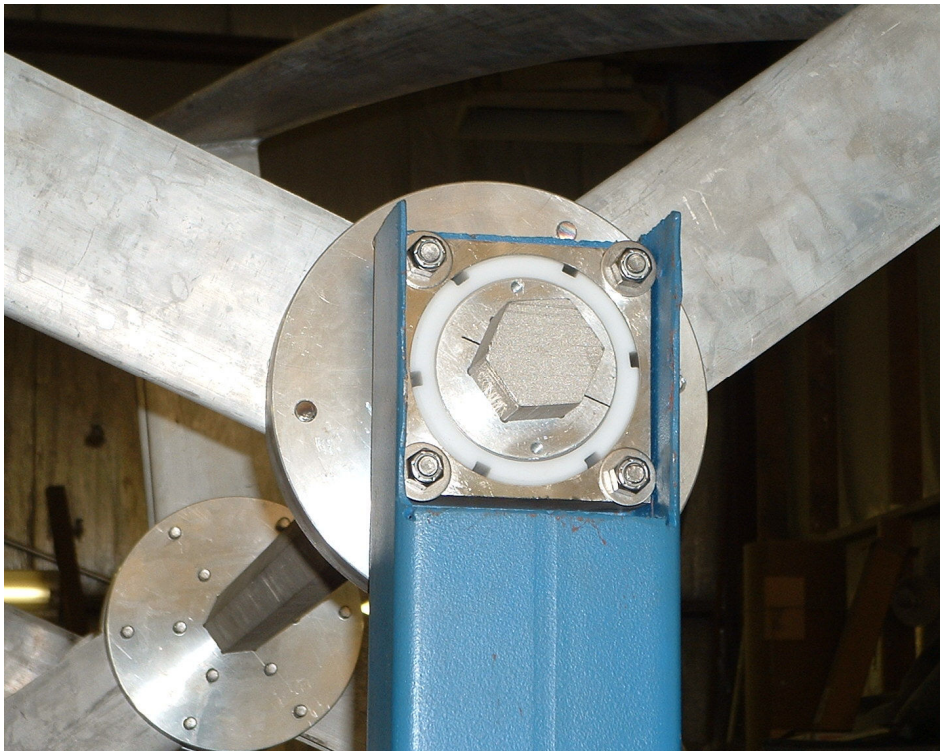

Figure 9. Photo of VP rotor Bearing

Rotor Assembly

VP assembly of the first two GHT rotors began at Larry's Marina in Amesbury, Massachusetts on 8/2/04. The blade components were well crated as shown in the photo in Figure 10 and arrived in good condition along with hex shafts, other hardware, and fasteners.

Figure 10. Photo of GCK, Inc. GHT Rotor in Crate

The assembly of the rotor components (shafts, hubs, blades, arms, fasteners) was intended to be expeditious, but proved difficult, labor-intensive, and time-consuming. Apparently, the welding and heat-treatment of the blades and arms warped or otherwise distorted the arm/blade assemblies so that the angles of the mounting ends of the spokes of many of the blades were not in alignment as shown in Figure 11. VP had concerns that the bending of the blades necessary to line up the arm/hub mounting holes was putting undesirable stresses into the blades and arm/blade welds, and even potentially affecting the quality of the hydrodynamic shape.

Another problem was encountered where curved blade airfoil sections had been counterbored as if for socket head caps screw heads, but hex head screws were supplied. Special washers were obtained to solve this problem.

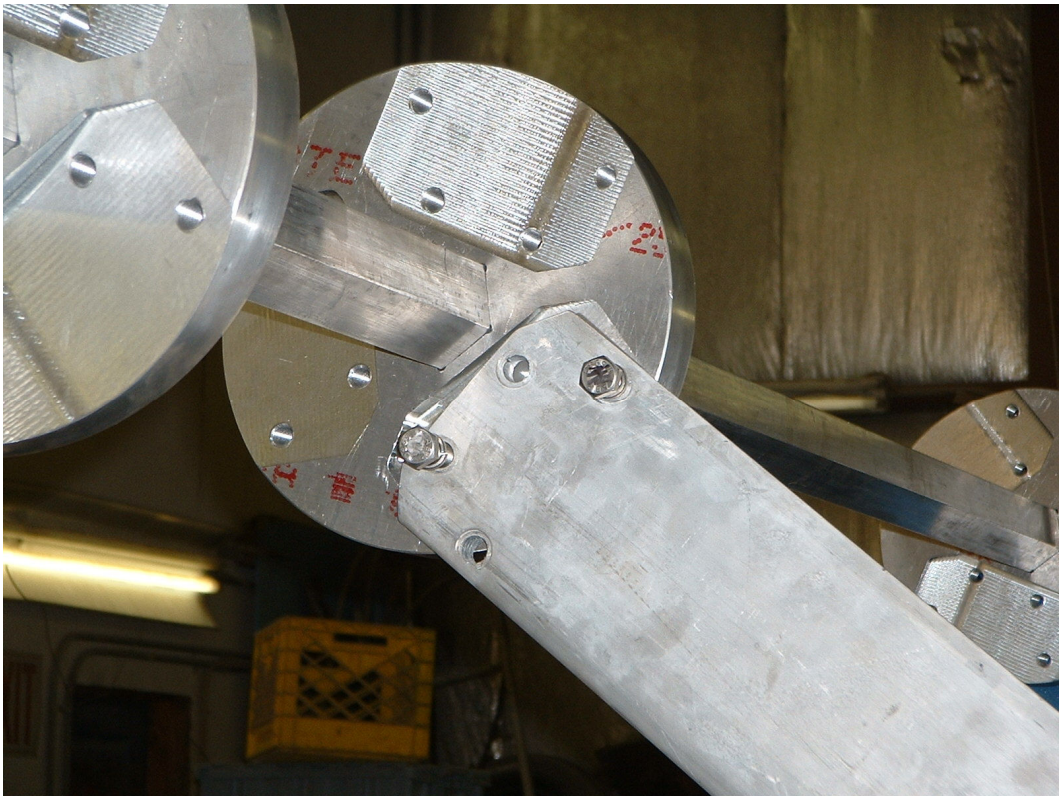

Figure 11. GHT Rotor Blade Assembly Initial Misalignment

The assembly of Turbines #1 and #2 was substantially completed by 8/6/04 and were installed on the barge and deployed to the site on 8/10/04.

SIDE BY SIDE MOUNTING FOR THE ATEP GHT TURBINES #3 AND #4

Purpose

ATEP GHT Turbines #3 and #4 were mounted side by side on frames hung from an arm extending outward, perpendicular to the side of the barge, as diagrammed in Figure 12. This allowed the turbines to be tested with a variable cross-flow spacing, from near-zero separation (2 inches edge to edge) to a separation of almost four feet (more than one turbine diameter of 1m).

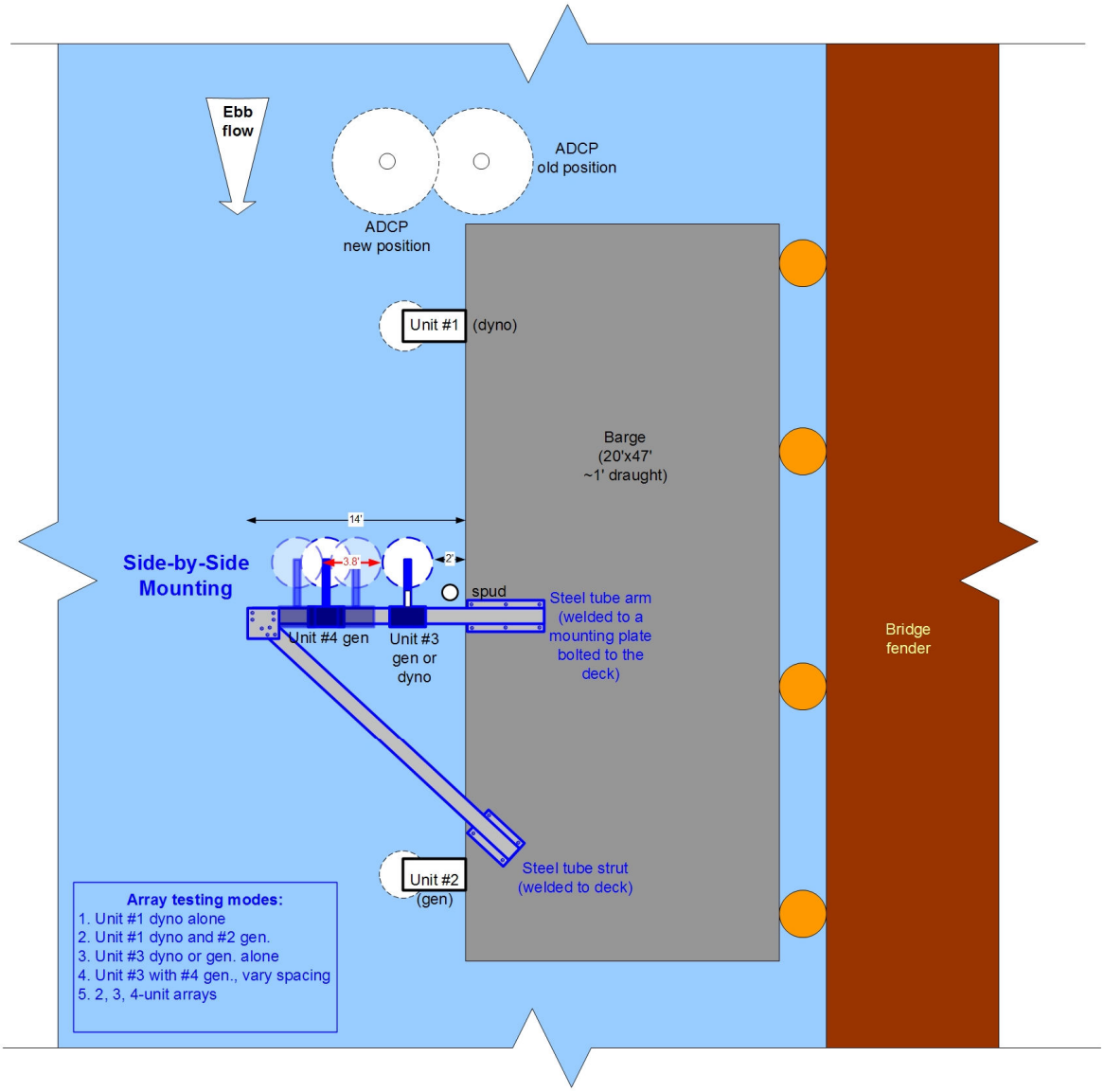

Figure 12. ATEP Turbines #3 and #4 Side-by-Side General Arrangement

Structure

The cross arm for supporting the side-by-side turbine frames extended 14 feet over the water from the side of the barge.

The arm and angled stiffening strut were made from 10” x10” steel tubes welded to angles welded to the barge deck. They were bolted together using steel plates at the outboard end which also held a turning block for a steel cable which was used to pull the turbine frames crosswise, and a mounting for a guy to the raised starboard spud for stiffening and an operator safety line. Each piece of this structure could be lifted by the barge lift.

Because the assembly extended significantly beyond the barge crosswise into the river, the U.S. Coast Guard and Amesbury Harbor Police required a warning sign and automatic flashing light on the end of the arm and two lighted channel markers (buoys) so as to effectively close the adjacent channel under the swing bridge to vessel traffic.

The completed Side-by-Side structure is shown in operation in Figure 13.

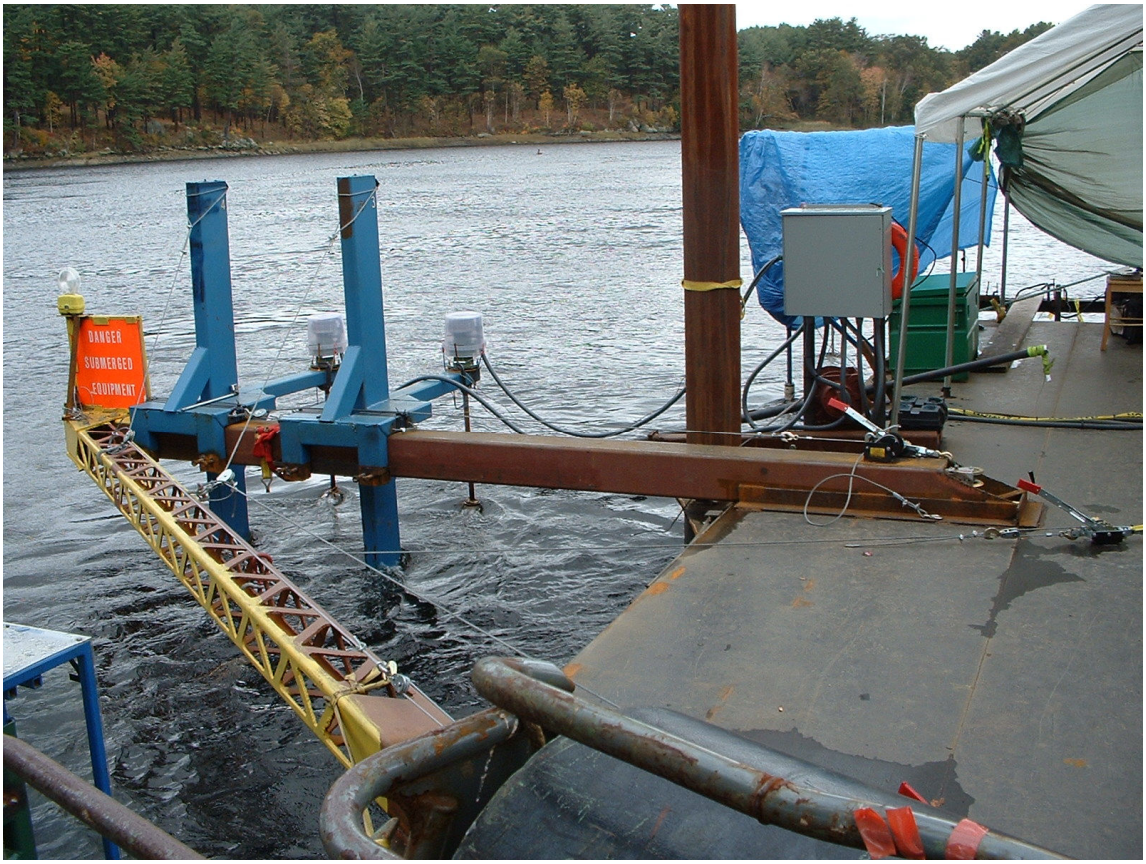

Figure 13. ATEP Turbines #3 and #4 Side-by-Side Structure

Turbine #3 and #4 Frames

The second pair of turbine frames were designed to be mounted on the cross arm, as opposed to the first two turbine units which are mounted to the side of the barge using clamps.

The frames also have single-sided arms supporting the rotor shaft bearings as before, but the bearing support arms point upstream (during ebb flow), rather than across the stream, and because they do not present their sides to the flow, they were made using 4 by 6 inch rectangular steel tube rather than fabricating triangular cross-sections. The frame arms were welded to a column that used 4 x12 inch rectangular steel tubing. Aligned with the flow, the column presented only a 4 inch wide face to the flow, well downstream of the rotor. The column has welded side members that rest on the 10 by 10 inch cross arm, capturing it on three sides, and forming a clamp that can be repositioned and locked at different points along the cross arm.

One further change from turbines #1 and #2 is that both up and down thrust bearings (acetal plastic in stainless steel races) were located with the upper radial bearing rather than having one on each end. This allowed free axial movement of the rotor from the top bearing downward, to reduce any vertical vibration being transmitted from the rotor to the frame structure.

Figure 14 shows the loading of Turbines #3 and #4 Side-by-Side Frames and cross-arm components on a barge to take to deployment on the study barge.

Figure 14. ATEP Turbines #3 and #4 Side-by-Side Frames

Provision was made to stiffen the frames in the pitch moment by using steel cables at their tops and near the waterline running to blocks on the angled cross arm strut; and also to use cables, blocks, and winches to slide the frames in and out on the cross arm. These can be seen in Figure 13.

Balancing

The added weight extending out from the starboard side of the barge required balancing the barge by adding weight to the port side. A frame was built to support up to 20 55-gallon water drums off the port side of the barge to provide up to 12,000 lbs of counterbalance weight, as shown in Figure 15. The weight of the entire Side-by-side assembly and turbines plus the counterbalancing was expected to increase the draft by up to 2.5". The Coast Guard was apprised of and consented to the plan.

Figure 15. ATEP Side-by-Side Balancing Drums

In order to maintain space for the water drums between the barge and bridge fender structure to which it was docked, and to improve the barge's motion with the rising and falling tides, a pair of two-wheeled barge fenders were constructed and installed as shown in Figure 16.

Figure 16. ATEP Rolling Barge Fender

C. ATEP Electrical System Documentation

APPENDIX C

Amesbury Tidal Energy Project

Electrical System

(includes Electric Power Generation, Power Loading, Sensors, Data Acquisition & Control System)

Prepared
by

Jamey Gerlaugh

March 28, 2005

Table of Contents

INTRODUCTION

The Amesbury Tidal Energy Project (ATEP) deployed during the summer and fall of 2004 on the Merrimack River near Amesbury Massachusetts used several different electrical systems connected to the Gorlov Helical Turbines (GHT's) to perform key functions as follows:

- Data Acquisition and Control System (DACS)
  - Measure turbine performance characteristics (power, torque, speed)
  - Measure river conditions (water velocity)
  - Store all collected data for later analysis
- Electrical Generation
  - Produce electricity from river current via generators
  - Provide variable turbine loading via loadbanks
- Monitoring of fish presence and behavior around the turbines
- Maintenance of the test barge's electric power

Details of the implementation of these tasks is described in this report through text explanations, circuit diagrams, block diagrams, 3rd party component descriptions, and photos.

A block diagram of the entire electrical system is provided on the next page.

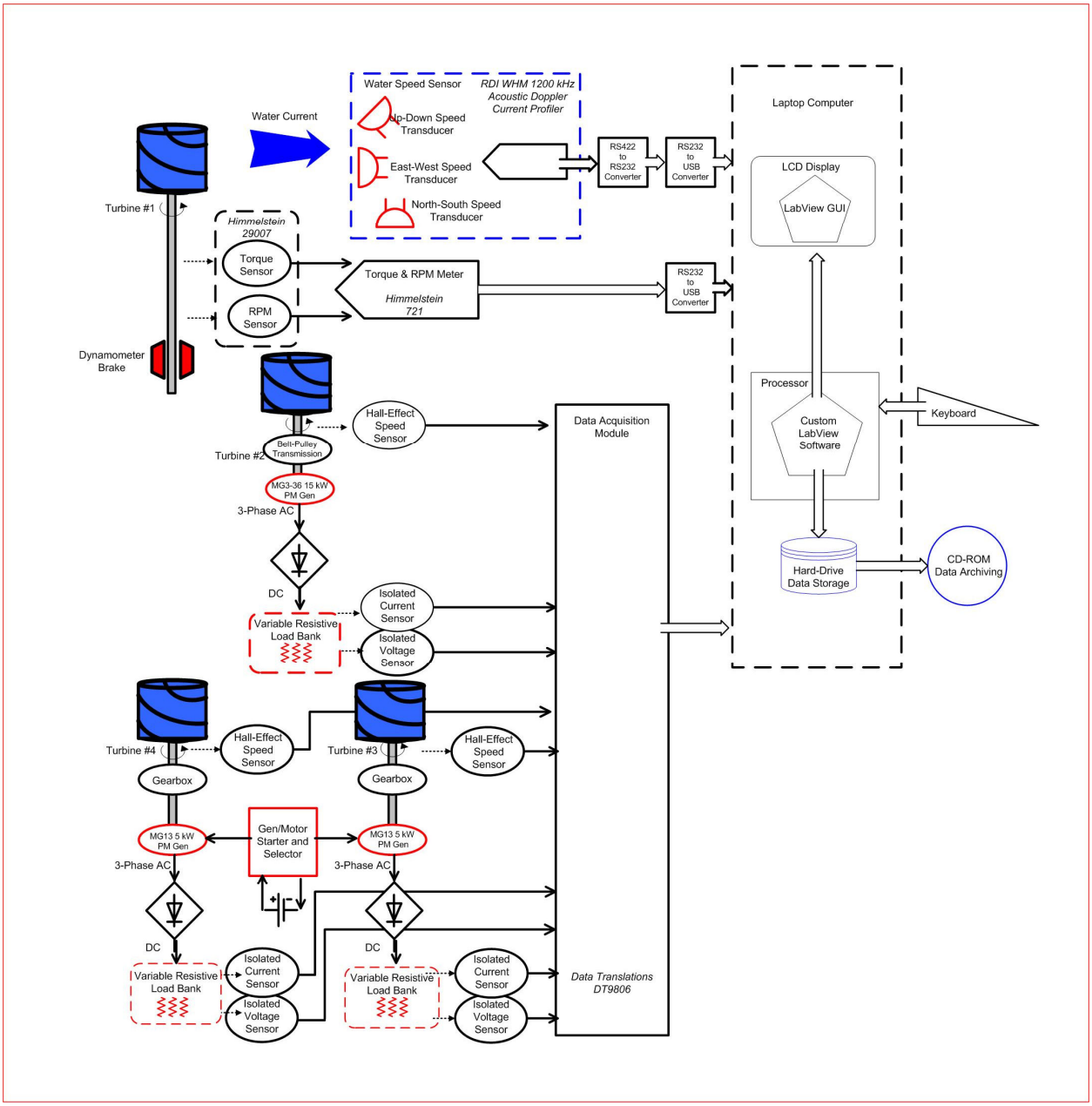

Figure 1 Electrical System Block Diagram

DATA ACQUISITION AND CONTROL SYSTEM

The central nervous system for the ATEP tests was the Data Acquisition and Control System (DACS). The DACS provided all electrical output and input signals. The DACS was physically housed in a watertight Control Room at the upriver end of the Test Barge, roughly 20' from GHT Turbine# 1, 30' from Turbine #3 and 40' from Turbines #2 and #4.

The DACS was used to gather and record all important GHT performance parameters including torque, rotational speed, and generator voltages and currents. It also gathered important environmental information, specifically the river's velocity at various depths along the turbine. From these parameters the DACS can calculate important performance parameters including shaft mechanical power and turbine efficiency.

The DACS has two output functions. First, all sensor data is displayed on laptop Host Computer via the Graphical User Interface (GUI). Secondly, attendants are alerted to any detected DACS problems via an audio alarm.

The DACS last function is as a data storage device. Data was stored on a laptop hard drive with a daily manual backup of data to a CD-ROM.

TURBINE CONFIGURATIONS

The four turbines of the ATEP were outfitted with different sensors to meet the needs of their particular tests.

Turbine #1 was set up for dynamometry experiments with a dynamometer brake, a torque load cell. The Himmelstein model 29007 torque load cell and 721 torque meter provided readings of both torque (τ) and shaft rotational speed (ω). From τ and ω, the turbine's instantaneous shaft output power was recorded and calculated as follows:

$$P_{shaft}\ [kw] = \tau\ [nm] \times \omega\ [rpm]\ /\ 9549$$

When compared with the water's kinetic energy calculated from the water velocity measurements, the turbines performance and efficiency was determined. By covering the full matrix of water velocity and loading combinations, a complete set of "power curves" was created for the turbine, providing a thorough understanding of its performance and potential applications.

Turbines #2-#4 were outfitted with generators. The generators demonstrated the generation of electricity, provide variable loading on the turbines by means of resistive loadbanks, and test the generator-turbine interaction. Isolated Hall-effect voltage and current sensors measured the voltage and current at the loadbank.

- **Turbine #2** was outfitted with a 15 kW Ecycle model MG3-36 Permanent Magnet (PM) 12-pole low-speed 3-phase generator.

- **Turbines #3** & **#4** were each outfitted with 5 kW Ecycle model CMG13 12-pole PM low-speed generators.

DACS TECHNICAL COMPONENTS

The DACS was composed mostly from tried and true components, in order to maximize reliability, control costs, and minimize time to deployment.

Host Computer

A Dell Inspiron 2650 Laptop was used as the Host Computer. The computer has the following specifications:

- 1.70 Ghz Pentium 4 processor
- 384 MB RAM
- 30 GB hard drive
- 3.5" floppy drive
- 14" LED screen
- CD-RW drive
- 10/100 Ethernet port
- 56KB modem

The system has the following accessories:

- PCMCIA RS232 port card
- USB to RS232 port adapter

Software

Programs

The following software programs were installed on the Host Computer

- Microsoft Windows XP Operating System, XP's built-in "Remote Desktop" capability allows the remote control of the DACS and downloading datafiles over an internet connection when one is available.
- LabView for Windows, an object-oriented industrial equipment control programming language. LabView was chosen for its extensive flexibility in acquiring data from various sensors and controlling various interfaces.

Custom Programming

LabView Code (called "Virtual Instruments" or "VI's") was used from an existing VP library. This VI has an excellent Graphical User Interface (GUI) which was customized for use with the ATEP project by Verdant Power and subcontractor, Mink Hollow Systems.

The term "DACS Code" refers to both the LabView Program and to custom VI code. The DACS Code performed data acquisition, limits checking, alarming, data logging, and the display of data on the GUI. DACS Code was written to interface with the following sensors:

- Water Velocity at 0.5m incremental depths from the surface using the ADCP
- Shaft Torque on Turbine #1
- Shaft Speed on Turbine #1, #2, #3, #4

- Generator Voltage on Turbine #2, #3, #4
- Generator Current on Turbine #2, #3, #4

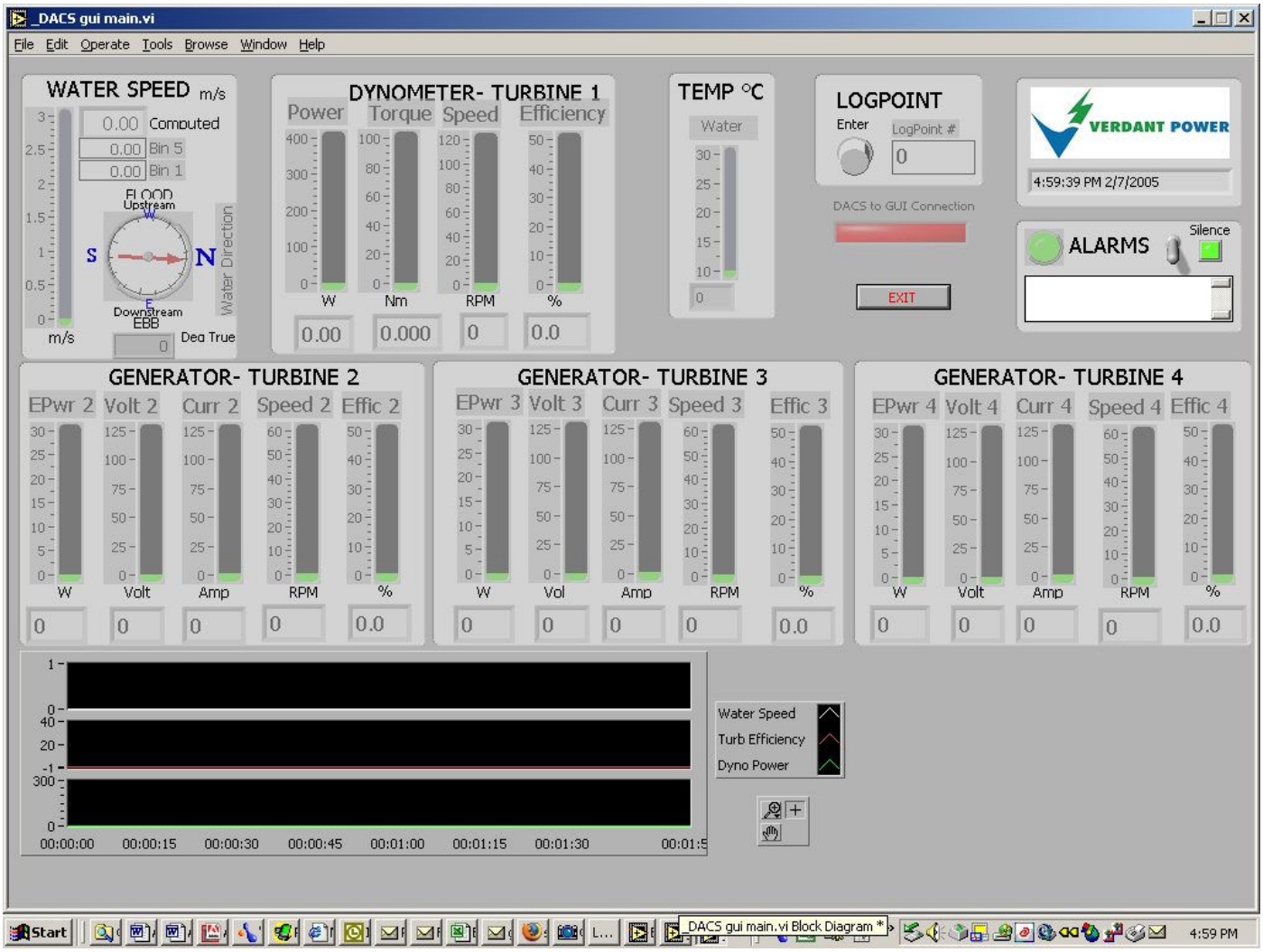

Figure 2 DACS LabView Graphic User Interface (GUI) while System is at Rest

More details are provided in the section 4.5, "Signal Inputs- Sensors"

Data Files

The sensors were read every 2.0 seconds. The resulting data from each read was stored every 2.0 seconds in a datafile. A new datafile was automatically created each day at midnight with the time-stamped filename format "ATEP data Y-MM-DD HH:MM:SS.txt" where "Y" is the year, "MM" is the month, "DD" the date, "HH" the hour, "MM" the minute, and "SS" the second. Data was backed-up on a daily basis by writing to a CD-ROM on the Host Computer.

Data Acquisition and Output Module

The Data Translations DT9806 is an all in one data-acquisition system that provided an interface between sensors and the host computer. Analog signals were converted to digital signals with its 16-bit analog to digital converters. The DT9806 (see diagram below) has the following interface features:

- Support for up to 16 single channel or 8 differential channel analog inputs
- Software support for multiple thermocouple types B, E, J, K, N, R, S, T.
- Thermocouple cold junction compensation
- Programmable gains of 1, 10, 100, and 500 per channel for input ranges of +/-10 V, +/- 1 V, +/- 0.10 V, and +/- 0.020 V.
- USB connectivity to Host Computer
- LabView compatible and available drivers
- Two 16-bit analog output channels
- 8 Digital input channels
- 9 Digital output channels
- Two 16-bit counter/timer channels for event counting & frequency measurements
- 500 Volt galvanic isolation to maximize analog signal integrity and protect the host computer
- Flexible acquisition modes (single value, continuous, and triggered scan)
- Throughputs as high as 50,000 Samples/second (at gains of 1 or 10)

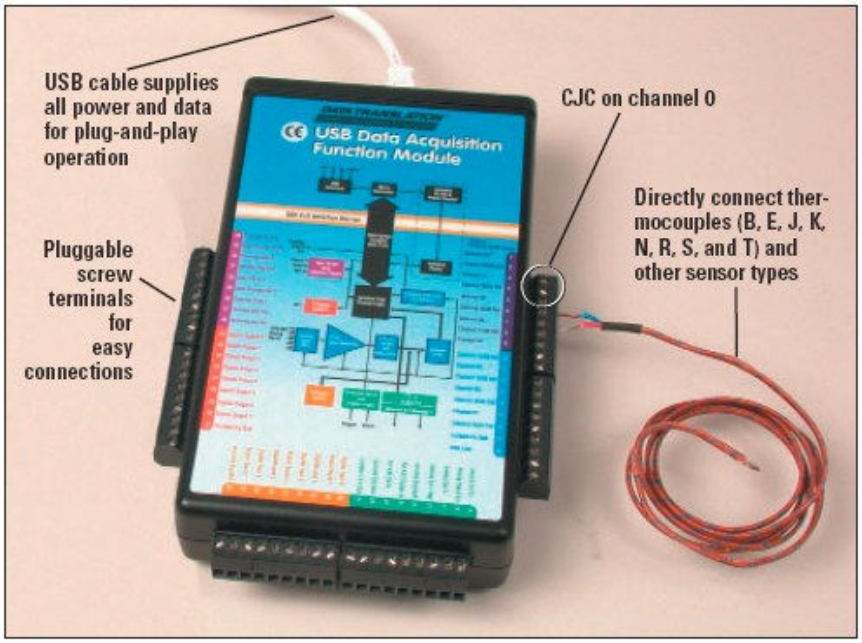

Figure 3 DT 9806 Data Acquisition Module

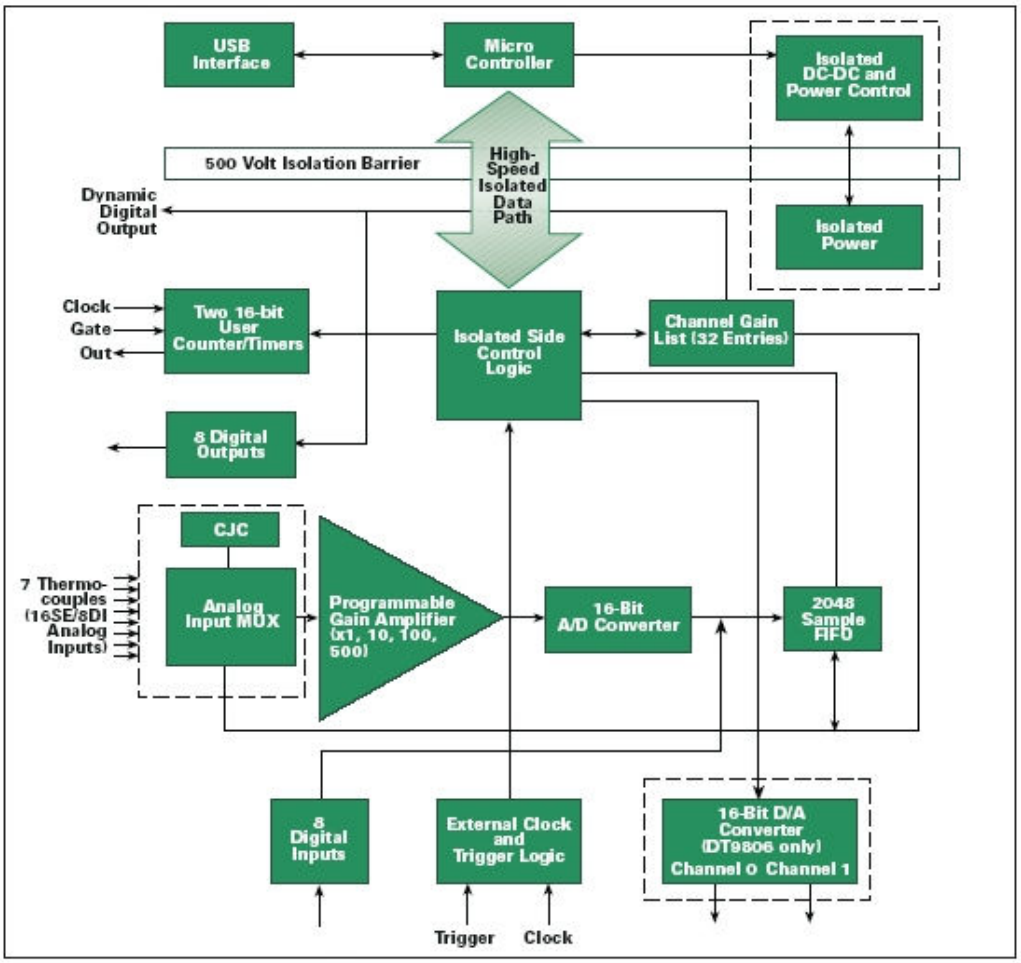

Figure 4 DT9806 Data Acquisition Module Block Diagram

Signal Inputs - Sensors

Shaft Torque and Shaft Speed

Turbine #1

Shaft torque and shaft speed are measured via a Himmelstein 29007 rotating load cell with an integral strain gauge and speed sensor. The load cell interfaces with a Himmelstein 721 Torque Meter which provides excitation and bridge completion, and can display the torque, speed and shaft power directly. The meter connects to the Host Computer through a RS232 link and RS232 PCMCIA card in the Host Computer.

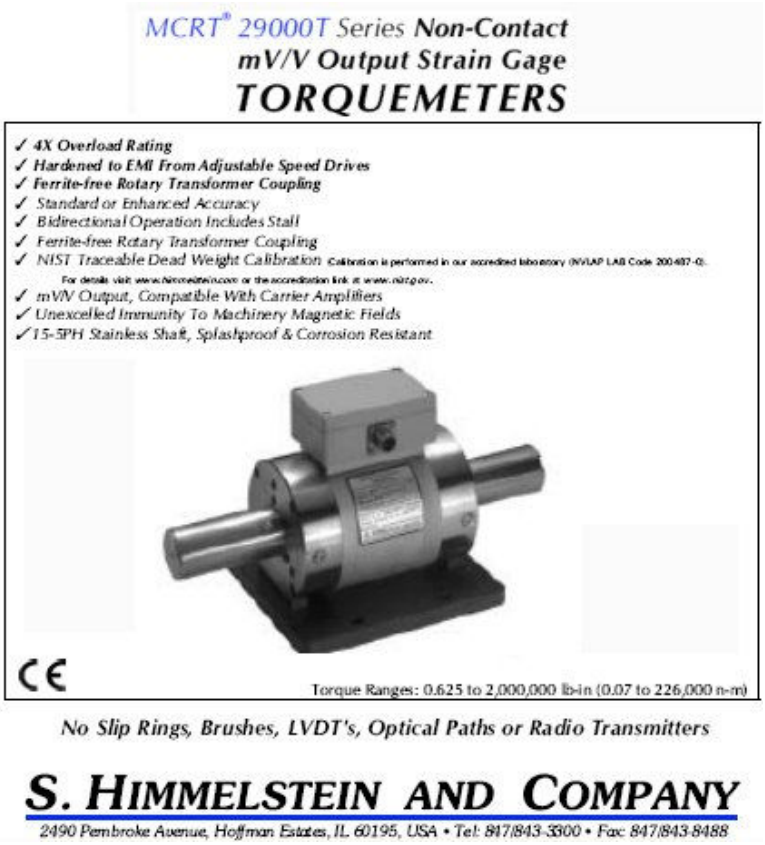

Figure 5 Torque Load Cell

Figure 6 Torque Meter

Turbine #2 – Turbine #4

Shaft speed was measured with a Hall Effect magnetic proximity sensor. The sensor was mounted on a bracket near the turbine axle. Neodium magnets were cemented around the shaft pulley opposite the sensor with a gap of 0.25" to 0.75". The sensor required DC excitation and produced a digital pulse when it encountered the north pole of a magnet. The DT9806 monitored the signal as a Digital Input. The inputs were polled at a high rate and the turbine speed calculated by measuring the time between pulses.

Water Velocity

Water velocities were used to determine the total kinetic energy in the water volume striking the turbine. The power available in the water is:

$$P\ (\text{Watts}) = \tfrac{1}{2}*\rho*A*V^3$$

Where ρ is the water density, which ranged from 1.000 to 1.017 kg/m^3, A is the frontal area of the turbine, nominally 2.5 m^2, and V is the waterspeed in m/s. Turbine efficiency was calculated by dividing the turbine's shaft power, from the product of torque and shaft speed, by the water's kinetic energy. The reported efficiency is derived from averaged data rather than from instantaneous data.

An RD Instruments Workhorse Monitor 1200 Khz Acoustic Doppler Current Profiler (ADCP) was used to determine the water's velocity (see Figure 8). The ADCP uses an RS422 communication link which feeds into the Host computer via a RS422/RS232 converter.

The ADCP monitored water velocities at various depths near the turbines. The bin size (the vertical height of one sample) was set for 0.5 meter so that five velocity readings from the top to the bottom of the turbine were measured. Velocity readings were composed of three velocity magnitudes, East-West, North-South, and Up-Down. Readings were produced by the ADCP every 2.0 seconds based on the averages of approximately 24 individual pings during that 2.0 second period. A single value for horizontal waterspeed approaching the turbine was determined by averaging the bins (with equal weightings since the frontal area of the turbine is a rectangle).

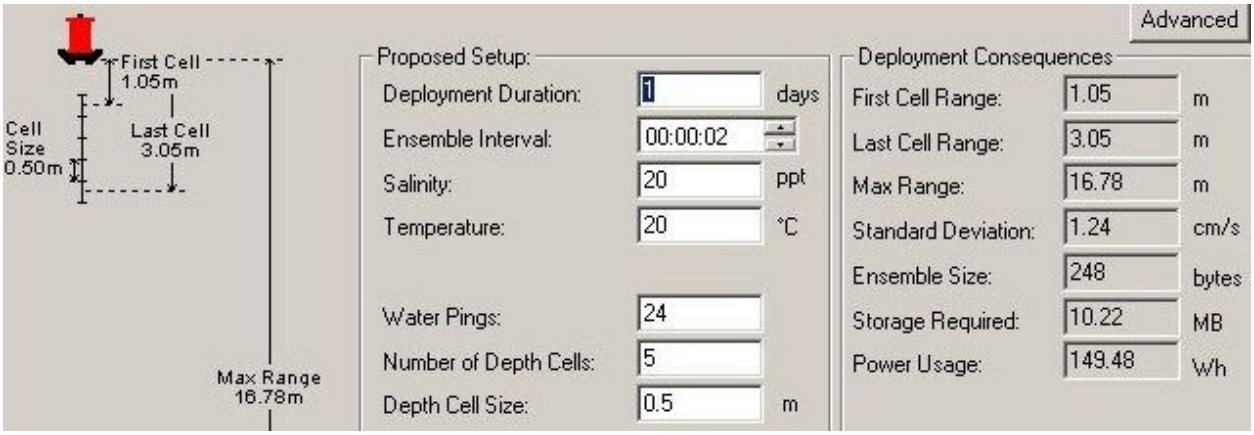

Figure 7 ADCP Setup

Workhorse Monitor ADCP 1200, 600 or 300 kHz

Water Profiling

Depth Cell Size[a]	Nominal range 15m[b] 1200kHz		Nominal range 55m[b] 600kHz		Nominal range 135m[b] 300kHz	
Vertical Resolution	Range (m)	Std. Dev.[c] (mm/s)	Range (m)	Std. Dev.[c] (mm/s)	Range (m)	Std. Dev.[c] (mm/s)
0.25m	12	182				
0.50m	13	66	40	182	see (a)	
1.0m	15	30	45	66	97	182
2.0m	16[b]	18	50	30	110	66
4.0m	see (a)		56[b]	18	123	30
8.0m					138[b]	18

Notes: a) user's choice of depth cell size is not limited to the typical values specified, b) longer ranges available, c) BroadBand mode single-ping standard deviation (Std.Dev.)

Long Range Mode

	Range (m)	Depth Cell Size (m)	Std. Dev. (mm/s)
1200kHz	20	2	35
600kHz	70	4	38
300kHz	175	8	38

Profile Parameters

Velocity accuracy:
- 1200, 600: ± 0.25% of the water velocity relative to the ADCP ± 2.5mm/s
- 300: ± 0.5% of the water velocity relative to the ADCP ± 5 mm/s

Velocity resolution: 1mm/s
Velocity range: ± 5m/s (default): ± 20m/s (maximum)
Number of depth cells: 1-128
Ping rate: 2 Hz (typical)

Echo Intensity Profile

Vertical resolution: depth cell size
Dynamic range: 80 dB
Precision: ± 1.5dB (relative measure)

Transducer and Hardware

Beam angle: 20°
Configuration: 4 beam, convex
Internal memory: Memory card not included. Two PCMCIA card slots available (10-220 Mb each).
Communications: Serial port selectable by switch for RS-232 or RS-422. ASCII or binary output at 1200-115,400 baud.

Standard Sensors

Temperature (mounted on transducer)
- Range: -5° to 45°C
- Precision: ± 0.4°C
- Resolution: 0.01°

Tilt
- Range: ± 15°
- Accuracy : ± 0.5°
- Precision: ± 0.5°
- Resolution: 0.01°

Compass (fluxgate type, includes built-in field calibration feature)
- Accuracy: ± 2° [e]
- Precision: ± 0.5° [e]
- Resolution: 0.01°
- Maximum tilt: ± 15°

Note: e) @ 60° magnetic dip angle, 0.5G total field

Power

DC input: 20 - 60V DC, external supply

Transmit
- 16W @ 35V (1200kHz)
- 37W @ 35V (600kHz)
- 115W @ 35V (300kHz)

Environmental

Standard depth rating: 200m. Optional to 6000m.
Operating temperature: -5° to 45°C
Storage temperature: -30° to 75°C
Weight in air: 7.6kg
Weight in water: 2.2kg

Dimensions

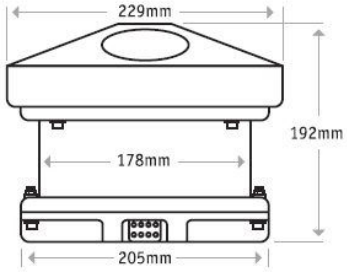

Software

Use RDI's Windows™-based software for the best results:
- WinSC — Data Acquisition
- WinADCP — Data Display and Export

Upgrades Available

- Memory - 10-220Mb PCMCIA cards
- Pressure sensor
- External battery case
- High resolution water profiling modes
- Bottom tracking
- AC/DC power converter, 48V DC output
- Conversion kit for internal power supply and memory

For More Information

Call, e-mail or visit our web page. Ask for our Primer about ADCPs.

Internet: www.rdinstruments.com

RD Instruments
9855 Businesspark Avenue
San Diego, CA 92131 USA
Tel: (858) 693-1178 Fax: (858) 695-1459
E-mail: sales@rdinstruments.com

Figure 8 RDI WHN1200 Acoustic Doppler Current Profiler

ADCP Mounting

The ADCP was generally mounted off the upriver corner of the barge's channel side (as opposed to fender side) using Verdant's ADCP gunwale mounting bracket, oriented vertically with water just covering the top of the unit, and aimed straight down. For the testing of Turbines #3 and #4 the ADCP was relocated to an arm off the end of the side-by-side mounting arm, but due to excessive vibrations, ADCP was returned to the barge corner location. The ADCP mounting locations are shown in Figure 10, on the next page.

Figure 9 ADCP Mounted at the Upriver Position

Generator Power

Generator power for turbines #2 through #4 was determined by measuring the rectified DC output voltage and current of each generator. The equation for generator power is simply:

Power [watt] = Voltage [volt] x Current [amp]

Generator Voltage

The rectified voltages of the three generators was each measured using a galvanically isolated Hall-Effect voltage sensor connected to an analog input channel of the DT9806.

Generator Current

The rectified currents of the three generators were each measured using a galvanically isolated Hall-Effect current sensor connected to an analog input channel of the DT9806.

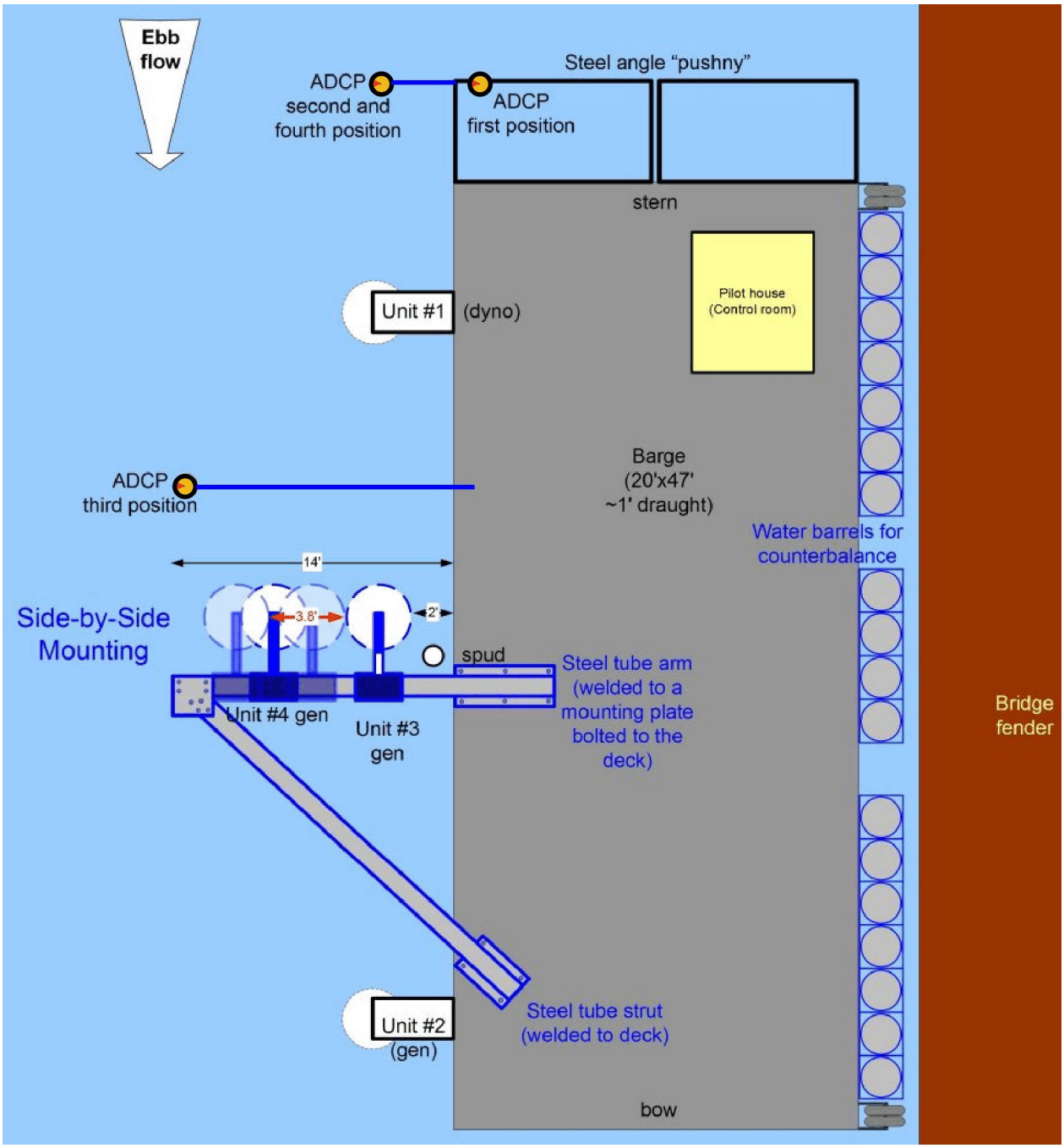

Figure 10 ADCP Mounting Locations

GENERATORS

The main requirements of the ATEP generator were:

- Starts producing power at a water speed of 2.0 knots and a turbine speed of 42 RPM with a generator efficiency of greater than 50%
- Rated for at least 5 kW corresponding nominally to a water speed of 4.5 knots and a turbine speed of 100 RPM
- If possible, be able to accommodate the higher power of 19.3 kW corresponding nominally to a water speed of 7.0 knots and a turbine speed of 148 RPM.

Turbine #2

Turbine #2 was outfitted with an Ecycle MG3-36 permanent magnet, brushless generator/motor (Figure 11)developed for the electric vehicle industry. The MG3-36 is wye-connected, 3-phase, and 12 poles which allows high efficiency at low operating speeds. Rare-earth magnets create a very high power density with a power rating of 18 kW and a weight of 15 kg and dimensions of 203 mm square by 200 mm in length. The geometry is a "triple stack", with three separate pancake motors arranged inside a single housing. An external 3-phase rectifier was used to provide DC power. The specifications are outlined in Table 1.

Figure 11 Ecycle MG3-36 Generator

Table 1 Ecycle MG3-36 Specifications

Ecycle MG3-36 Generator Specifications							
Model	Power Rating (kW)	Gear Ratio	Back EMF (V/RPM)	Torque Constant (nm/A)	Inductance (uH)	Resistance (mOhms)	Max Current (Amps)
MG3-36	18.0	35.5:1	0.038	0.36	136	61	100

Ecycle MG3-36 Power at given Speed and Peak Torque (manufacturer specs)					
Speed (RPM)	Torque (Nm)	Power (kW)	Voltage (V)	Current (A)	Efficiency
500	144	9	24	400	95%
900	90	9	36	250	95%
1300	79	10	48	220	95%
1800	57.6	11	72	160	95%

Turbine #3 & Turbine #4

Turbine #3 and #4 were outfitted with Ecycle MG13 permanent magnet, brushless generator/motors developed for the electric vehicle industry (see Figure 12). They are similar to the MG 3-36 but of smaller power. The MG13 is wye-connected, 3-phase, and 12 poles which allows high efficiency at low operating speeds. Rare-earth magnets create a very high power density with a power rating of 5 kW, a weight of 7kg, and dimensions of 178mm in diameter and 135mm in length.

An internal Hall-Effect position sensor and an external motor driver were used for kick-starting the turbine. When in generator mode, the motor driver functioned as a rectifier to provide DC output power. The specifications following in s.

Figure 12 Ecycle MG13 Generator

Table 2 Ecycle MG13 Specifications

Ecycle MG13 Generator Specifications							
Model	Power Rating (kW)	Gear Ratio	Back EMF (V/RPM)	Torque Constant (nm/A)	Inductance (uH)	Resistance (mOhms)	Max Current (Amps)
MG-13	5.0	43 : 1	0.014	0.13	35	24	100

Ecycle MG13 Power at given Speed and Peak Torque (manufacturer specs)					
Speed (RPM)	Torque (Nm)	Power (kW)	Voltage (V)	Current (A)	Efficiency
1800	49	9	24	400	95%
2700	30.6	9	36	250	95%
3400	27	10	48	220	95%
6500	19.6	11	72	160	95%

GENERATOR/MOTOR "KICKSTART" DRIVER

To start the turbine generators below the speed of spontaneous startup so that useful power could be generated, the design for generator interfaces for Turbines #3 & #4 was updated to include an electronic motor driver circuit and motor phase sensors. To start a turbine, the motor driver, powered by a pair of 12 VDC batteries would be switched in with the load switched out and the motor would start the turbine by using the generator as a motor. Once spun up from its stalled position to a sustainable speed, the motor would be switched into generator mode. As a generator, the three-phase leads were switched to connect to a rectifier for creating DC which was fed to the loadbanks as with Turbine #2. Switching from driver to rectifier mode was done manually. (See Testing Protocols (Appendix V) for generator testing and safety procedures.)

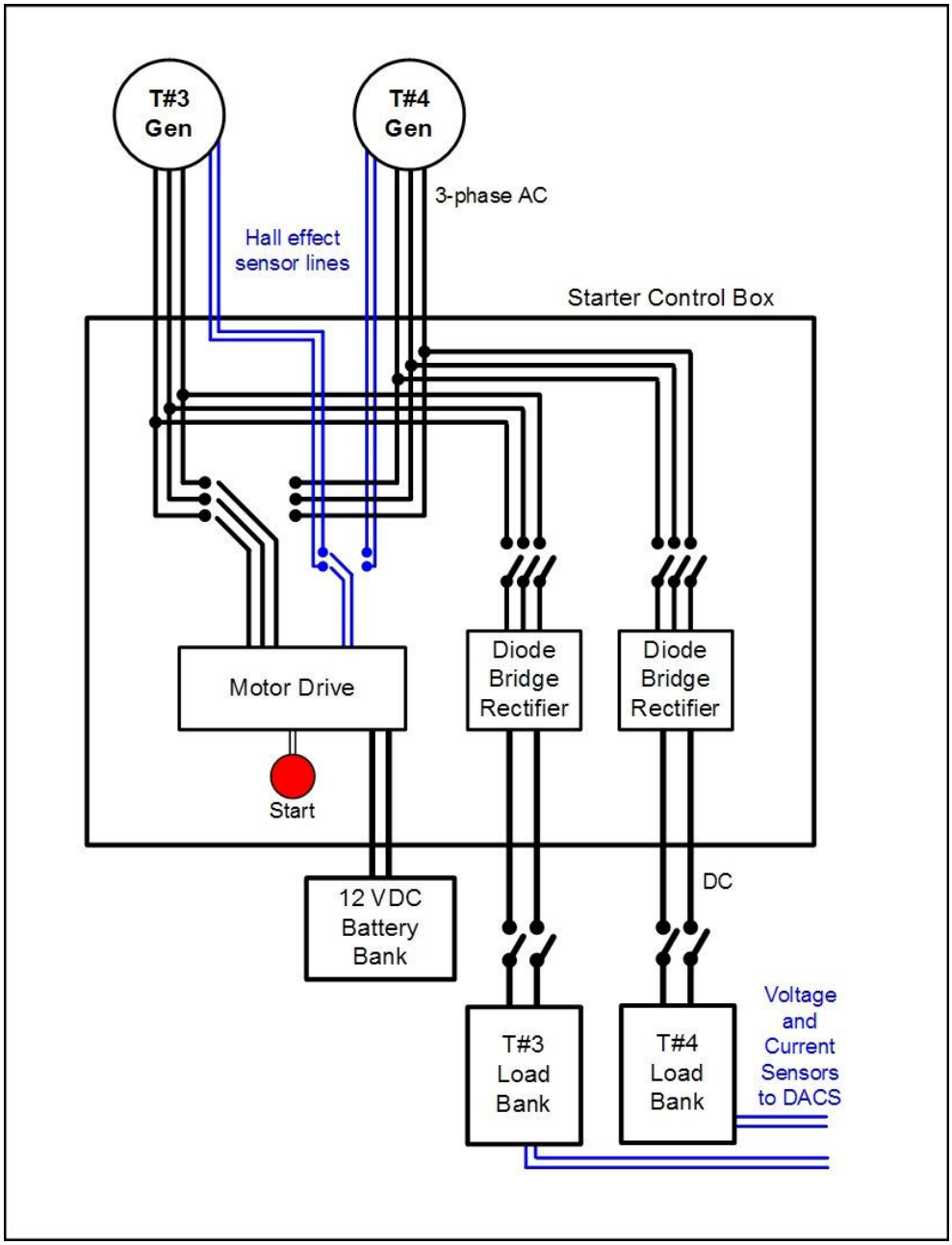

Figure 13 Turbine #3 and #4 Generator Driver and Loadbank

LOADBANKS

Generator power was dissipated in loadbanks built by Verdant Power. Each generator had a dedicated loadbank. The loadbanks were rated for 5.0 kW each and were constructed of Vishay-Dale, 7.5 or 10 ohm, 225 W, HL Series Silicone Fixed Power Resistors mounted in a steel NEMA enclosure 36 ”x 24” x 8” as shown in Figure 15. Patch cables and switches were used to reconfigure the resistance values of the four banks of eight resistors to alter the loading on the generators from 0.040 ohms to 25 ohms. Each loadbank was controlled and protected by a double pole circuit breaker.

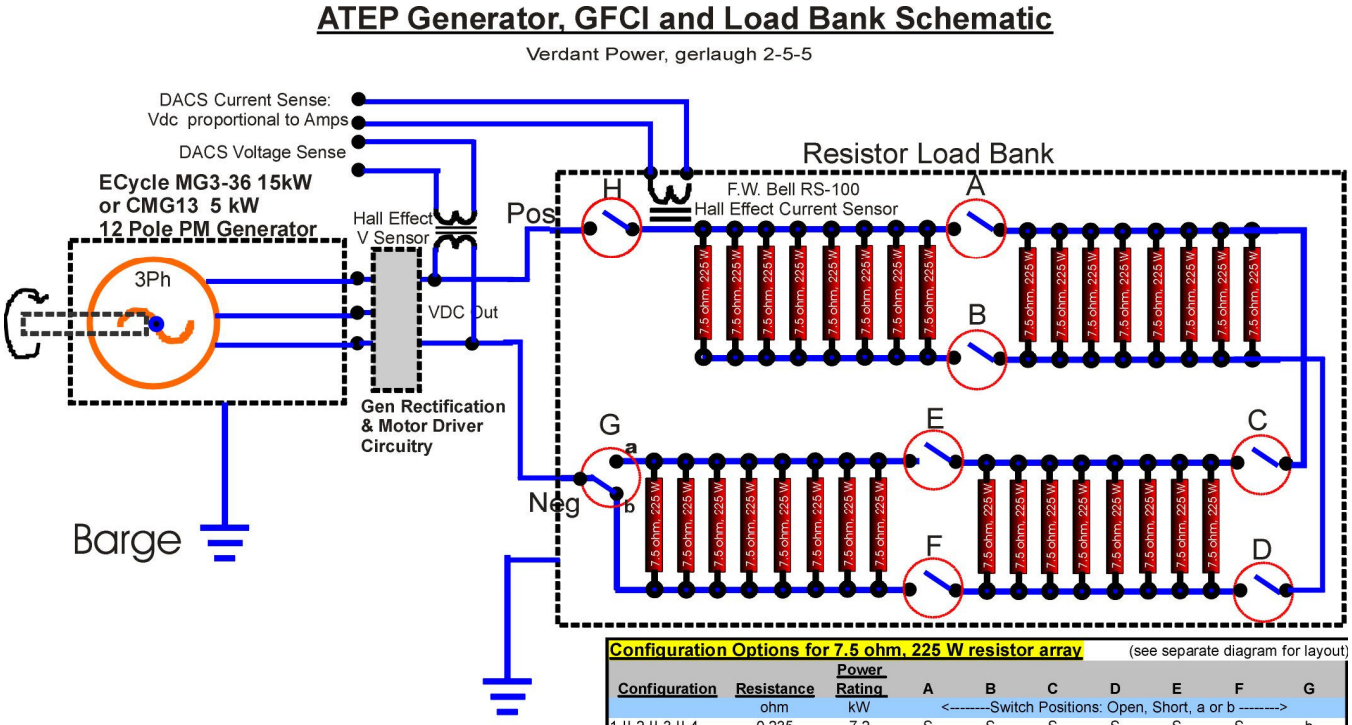

Note: Other resistor values and switching configurations were used for some tests

Configuration Options for 7.5 ohm, 225 W resistor array (see separate diagram for layout)

Configuration	Resistance	Power Rating	A	B	C	D	E	F	G
	ohm	kW	<--------Switch Positions: Open, Short, a or b -------->						
1 !! 2 !! 3 !! 4	0.235	7.2	S	S	S	S	S	S	b
1 !! 2 !! 3	0.313	5.4	S	S	S	S	O	S	b
1 !! 2	0.470	3.6	S	S	O	S	O	S	b
1	0.940	1.8	O	S	O	S	O	S	b
(1 !! 2)-(3 !! 4)	**0.940**	**7.2**	S	S	O	S	S	S	a
1-2	**1.880**	**3.6**	O	S	S	O or S	S	O or S	a
1-2-3	**2.820**	**5.4**	O	S	S	O	O or S	S	b
1-2-3-4	3.760	7.2	O	S	S	O	O	S	a

KEY: POS & NEG are terminals to generator
A,B,C,D,E,F are SPST 125VDC 175 A
G is a SPDT 125VDC 175 A

Key:		
	O	Open Switch
	S	Closed/Shorted Switch
	Bold	Important value & configuration
	!!	Parallel Connection
	-	Series Connection
	a, b	position of SPDT switch
	1, 2, 3, & 4	Block # of 8 Parallel Connected Resistors

Figure 14 Generator Loadbank Schematic

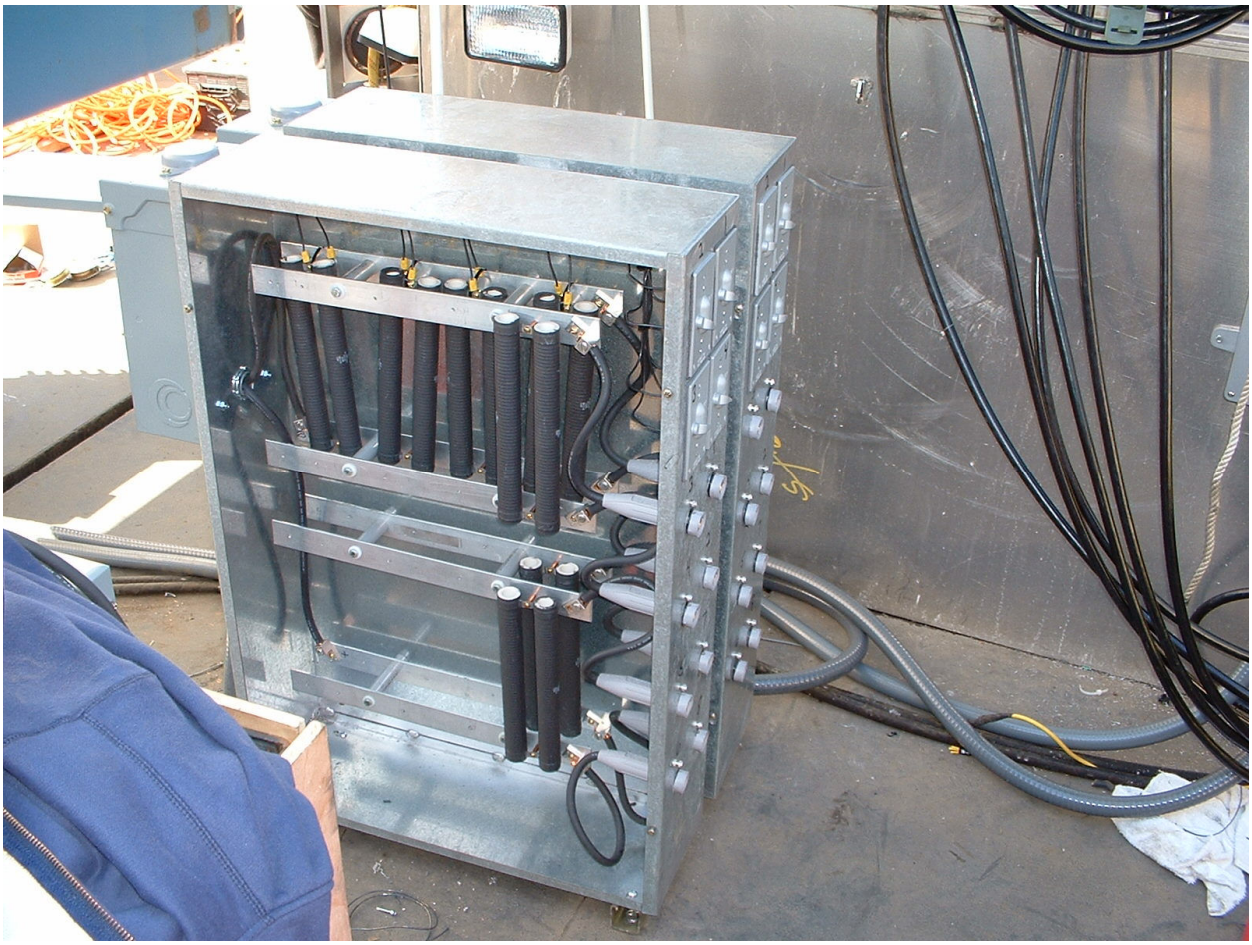

Figure 15 Resistors Mounted Within the Steel NEMA Enclosure

APPENDIX D

Table of Contents

PURPOSE

The Amesbury Tidal Energy Project (ATEP) testing plan conducted by Verdant Power (VP) was undertaken to accomplish several objectives:

1. Fully characterize the performance of the Gorlov Helical Turbine (GHT) rotor under different conditions of waterspeed and loading.
2. Implement the generation of electrical power.
3. Examine the performance of the GHT rotors under different conditions of streamwise spacing and cross-stream spacing.

BACKGROUND

The GHT rotors used in these studies have a 1-meter nominal diameter, and an axial length of approximately 2.5 meters. The GHT rotor is shown in Figure 1. The rotors were used with their axes mounted vertically in the water, supported by underwater bearings, frames and support structures designed, built, and deployed by VP as shown in **Figure 2 (Verdant Power has patents pending on this technology)**. These aspects are described in detail in the full Verdant Power ATEP Report.

Figure 1 GHT 1-m Rotor Test Subject

Figure 2 GHT Rotors #1 and #2 Mounted in VP Frames (patents pending) for Testing

Based on information provided by GCK, the nominal expected performance of the GHT rotor was applied to the range of possible conditions in the Merrimack River, as is shown in Table 1.

Table 1 Nominal GHT Rotor Maximum Power (optimal loading) in Merrimack River

Merrimack River	**Waterspeed**		**Power, max**	**Torque**			**Rotor speed** (@max power)	
flow	kn	fps	kW	Nm	ft-lbs	in-lbs	rpm	rad/s
min	0	0	0	0	0	0	0	0
typical	2	3.4	0.45	102	75	905	42	4.4
nominal	**4**	**6.8**	**3.6**	**408**	**301**	**3611**	**84**	**8.8**
GCK basis	**4.7**	**8.0**	**6.0**	**573**	**423**	**5071**	**100.0**	**10.5**
higher	5	8.4	7.0	636	469	5630	106	11.1
max	7	11.8	19.3	1247	920	11036	148	15.5

Also of importance to the testing of the GHT rotors is that fact that such crossflow rotors are not generally self-starting. Accordingly, provision must be made to unload the rotors and/or provide a manual, electrical, or other mechanism to start the rotors prior to testing.

ATEP GHT TESTING

Four turbines, labeled #1 through #4, were installed in sequence on the ATEP barge. They were located as shown in Figure 3. The turbines were tested in some cases individually, and in combination to explore the above objectives.

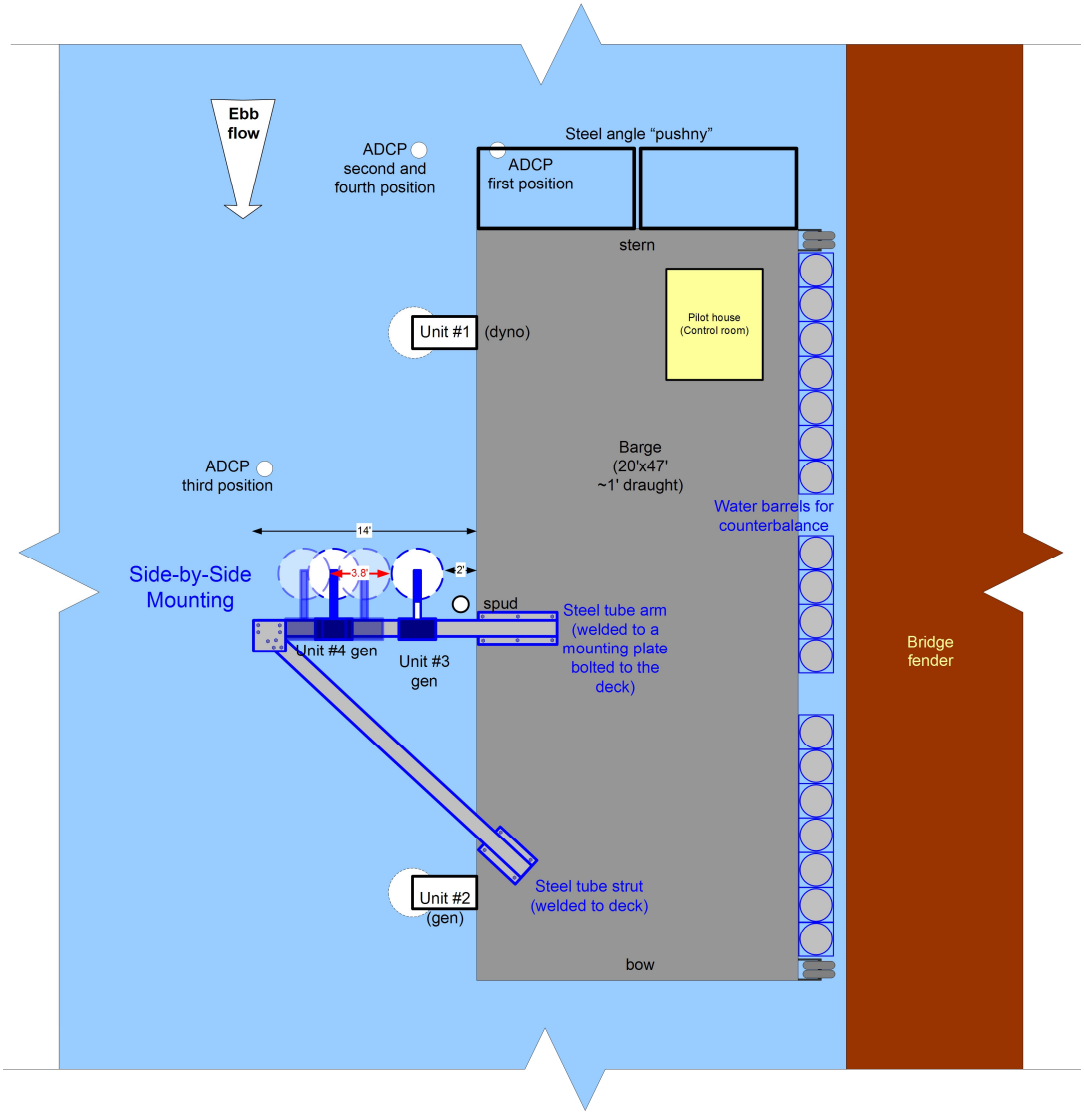

Figure 3 ATEP Barge Turbine Location Layout

Turbine #1, mounted in a side-arm frame held by a clamp on the starboard side of the barge, had a dynamometry loading module on top as shown in the pictorial diagram, **Figure 4 (Verdant Power has patents pending for this technology)**. This turbine was used primarily to perform dynamometry as described in Section IV.I, DYNAMOMETRY.

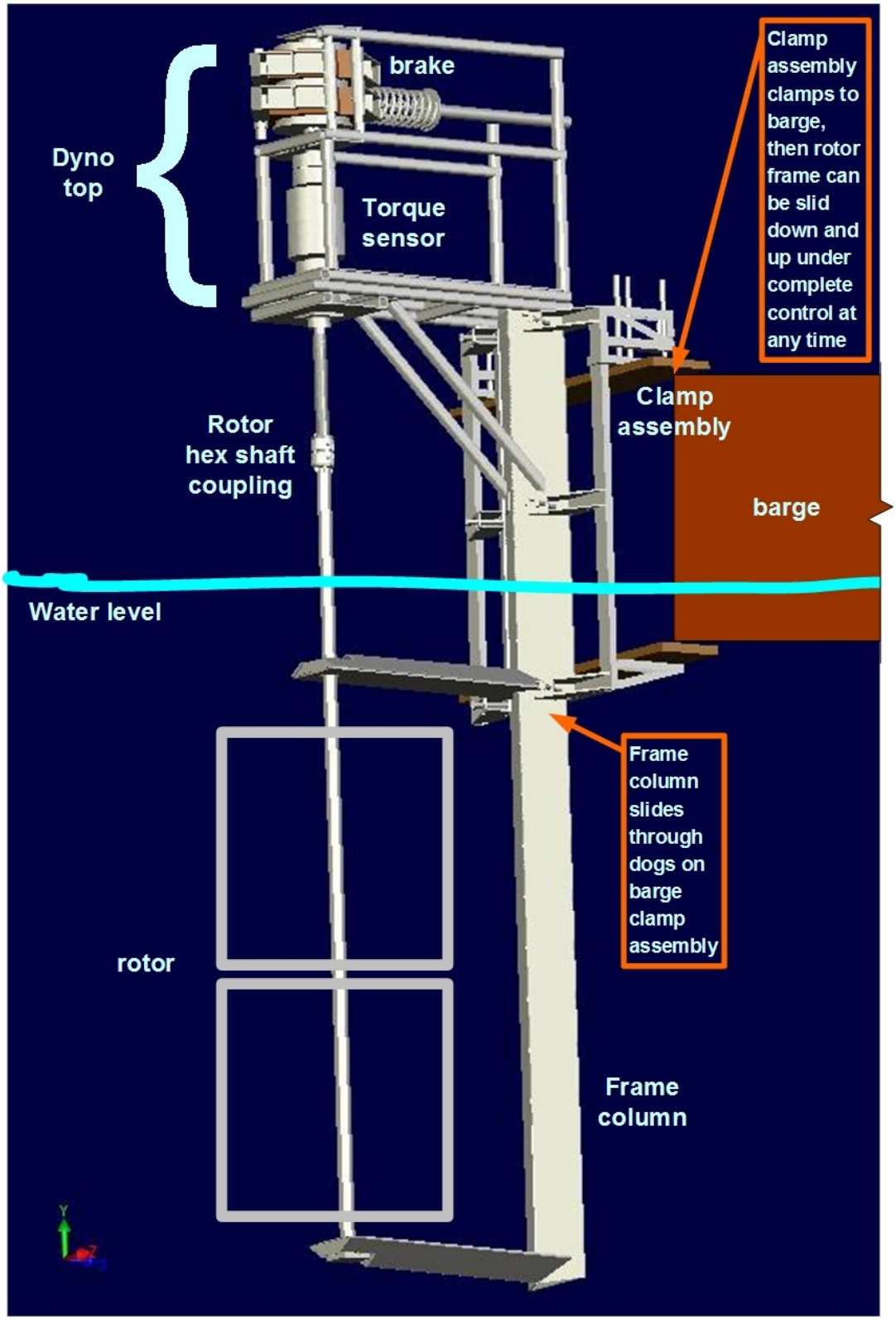

Figure 4 ATEP Turbine #1 with Dynamometry Module (patents pending)

Turbine #2, mounted as with #1, had a frame top with a 35-kW brushless permanent magnet generator driven by a two-stage belt and pulley transmission. This turbine was used to do preliminary electrical generation and transmission tests as described in Electrical Generation testing section II. below. A photograph of Turbine #2 is shown in Figure 5.

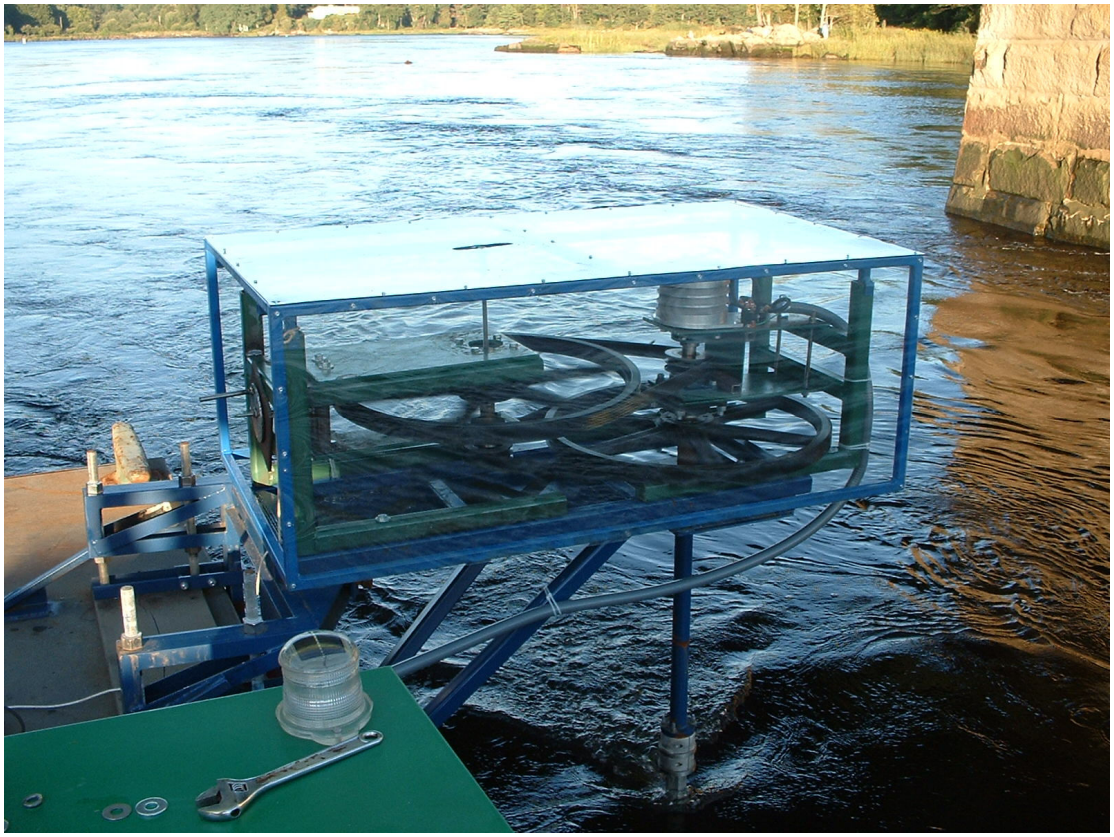

Figure 5 ATEP Turbine #2 with Transmission and Generation Module

Turbines #3 and #4 had rotors mounted in frames with streamwise arms and which were mounted on the upstream side of an arm projecting outward from the starboard side of the barge. These "side-by-side" turbines drove gearboxes and generators on top and were able to be moved transversely across the flow, to study the effect of cross-stream spacing, as described in Section III.

The "side-by-side" turbines #3 and #4 are shown installed on the barge arm in Figure 6.

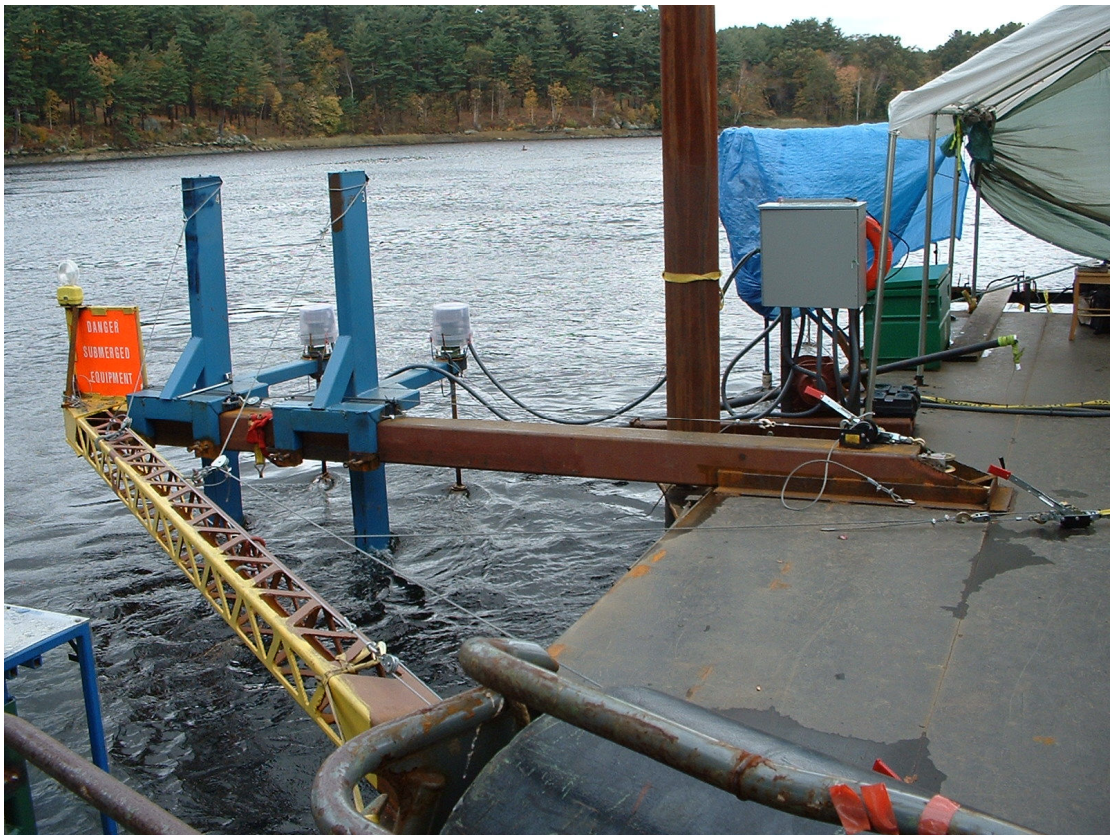

Figure 6 "Side-by-Side" Turbines #3 and #4 Arm with Generator Top Modules

The test apparatus and procedures necessarily evolved dynamically during the course of the ATEP, in respect of the uncontrollable realities of tidal range and timing, waterspeed, and weather. We have attempted to gather the greatest range of useful and valid data

The ATEP turbine testing has four general sections:

I. Dynamometry
II. Electrical Generation
III. Crossflow Spacing
IV. Longitudinal Spacing.

I. DYNAMOMETRY

Turbine #1

The dynamometry data is used to characterize how the rotor converts the **power in flowing water,** $P_{water} = \frac{1}{2} \rho A V^3$ (where ρ is the density of the water, **A** is the frontal or projected area of the device under test, and V is the velocity of the water) into **mechanical energy,** $P_{rotor} = \omega\tau$ **.**

We use the data collected to calculate these and the efficiency**,** or **Coefficient of Performance**, **Cp** of the rotor.

$$Cp = P_{rotor} / P_{water}$$

Combining all of the processed data allows the creation of power curves that show the performance of the rotor under the full range of the input parameters.

To do this, we measure the **waterspeed or velocity, V** continuously using the Acoustic Doppler Current Profiler (ADCP) (along with temperature) and **water density,** ρ manually, while manually varying the load on the rotor via the brake. The torque transducer continuously measures the **rotor speed,** ω and torque, τ**.** The ADCP was located 112 inches (2.8 m).upriver (and upstream during the ebb currents which were used for testing) from the center line (shaft) of Turbine #1.

The computer-based Data Acquisition and Control System (DACS) acquires, converts, calculates, and records the data from the various sensors at 2-second intervals. This results in a large number of datapoints. The basic data reduction method for this stage is to sort and separate the data into bins by waterspeed, and the average the ω and τ data to reduce the effect of natural flow and mechanical fluctuation and system noise. (It should be noted that although instantaneous efficiency is calculated every 2 seconds for use in operational monitoring, such data is not accurately representative due to the water flow fluctuations and angular momentum of the rotor.)

Turbine #1 was hand-started when necessary with a ratcheting and removable crank. Since the brake load could be removed completely, the rotor would self-start with a waterspeed above 0.8 – 1.0 m/s).

The testing operator procedure for acquiring this data is according to *Test Method 1*, as follows:

Test Method 1

Quasi-Constant Water Velocity

The torque is swept from no-load to stall over a period of about 3 to 5 minutes by gradually applying the brake. During such a short period, the waterspeed is relatively constant.

Steps:

1. Verify that the computer and LabView (LV) software is acquiring and logging data.
2. Ensure that the torque is tared properly. If there is any question, re-tare as follows:
    a. Release all tension on the brake by rotating the braking screw CCW. DO NOT release too far, just enough to ensure that the brake shoes are not rubbing on the drum.
    b. Examine the brake to ensure that the shoes are not touching the drum.
    c. Rotor and shaft MAY be turning due to the water current.
    d. Press **Tare** button on front of the Himmelstein Torque Sensor readout unit.
    e. Record **Tare** entry in logbook and LV Logpoint.
3. Measure and record **Water Density** at reasonable periods (see water density section). Enter value (1.000 – 1.020) on log book and as LV logpoint.
4. Record **Torque Sweep** entry in logbook and LV Logpoint, noting approximate water current speed and direction.
5. Begin to apply torque via brake screw with the goal of gradually increasing torque and decreasing rotor speed until the rotor stalls (zero speed) over a period of 3-5 minutes.
    a. Monitor torque and speed readout on the Himmelstein unit or LV screen to see progress of increasing torque, decreasing rotor speed, and computed power.
    b. You may need to turn the screw several turns until the brake shoes engage the drum and the torque begins to rise.
6. Once the rotor stalls, repeat the above steps.

Once an amount of data adequate to characterize the GHT rotor has been collected using Test Method I. above, ***and*** if the conditions exist to allow the brake to provide a reasonably constant torque over prolonged periods of time, we can take some data as per *Test Method 2*, as follows:

Test Method 2

Quasi-Constant Torque

A fixed brake setting is maintained during a tidal cycle such that the waterspeed sweeps from scan beginning (V high enough to sustain rotation) to stall (V drops below level needed to maintain rotation at the given load.)

Steps:

Begin with the first 3 steps in *Test Method 1*, and then:

4. Record **Brake Setting** entry in logbook and LV Logpoint, noting approximate water current speed and direction.
5. While monitoring the torque and speed readout on Himmelstein unit or LV screen, apply a chosen torque via the brake screw.
    a. You may need to turn the screw several turns until the brake shoes engage the drum and the torque begins to rise.
6. Allow the system to remain in this condition until the waterspeed declines enough that the rotor stalls. (If the rotor stalls immediately, try again with a lower torque setting.)
7. Once the rotor stalls, repeat the above steps, with a different torque setting (and lower rotor speed) when the tide cycle next allows.

II. ELECTRICAL GENERATION

Turbine #2

Turbine #2 is located on the starboard side of the barge near to bow (downstream end) as shown in Figure 3.

Mounted identically to Turbine #1, Turbine #2, had a frame top with a two-stage belt-driven transmission with a 40:1 ratio to drive 35-kW brushless permanent magnet generator at about 1500 – 2000 rpm. This turbine and transmission was also hand-started with a crank on the inboard jackshaft which required cranking at a speed approaching 300 rpm. Turbine #2 was used for the preliminary transmission tests as well as electrical generation and loading.

Test Procedure

Quasi-Constant Water Velocity

Generator output is measured into a fixed loadbank resistance during a short test period of about 3-10 minutes.

The generator output is compared to Turbine #1 dynamometry output.

Steps:

1. Set loadbank breaker switch to OFF.
2. Start the turbine using the hand crank. Once the turbine is running...
3. Set the resistance using the loadbank jumper cables.
4. Set loadbank breaker switch to ON.
5. Manually record waterspeed, turbine speed, resistance setting, actual resistance, voltage, and current.
6. Set loadbank breaker switch to OFF.
7. Repeat from Step 3 using R values from near no-load to stall.
8. Repeat from Step 3 as V changes with tidal cycle.

III. CROSSFLOW SPACING

Turbines #3 & #4

One aspect of the use of the GHT is the potential for a constructive interference between GHT rotors operating in close proximity to each other. The developer of the GHT, Dr. Alex Gorlov, has theorized that turbines deployed near each other could increase the power output of both.[1]

In order to study this potential phenomenon, VP designed and built a test apparatus that permitted testing two turbines (#3 and #4) while varying the cross-stream spacing.

Turbines #3 and #4 drove gearboxes and 5kW permanent magnet brushless DC generators. They were started using a motor controller (on the 3-phase motor/generator lines before the DC rectifiers) in an onboard control box that could be switched to start either turbine, and then removed from both generator leads.

For these studies, Turbine #1 was lifted from the water so as not to interfere with the two turbines, especially unit #3 which is directly downstream of Turbine #1 during the ebb flow.

The so-called "Side-by-Side" turbine test structure (See Figure 3) was comprised of a 10-inch square steel tube Arm welded to the barge deck and extending 14 feet crosswise over the river flow. This was supported for thrust force and twisting by a similar tube strut welded to the barge deck and bolted to the end of the arm. (See ATEP Report for full description of the Side-by Side structure.)

Test Setup

The outermost turbine (#4) was locked at the position farthest from the barge edge, and the inner turbine (#3) was moved in and out on the arm. Five positions were established for turbine #3 (see Table 2), with spacing between the turbine rotors biased toward the narrower since that is the area of interaction which is of the most interest.

Table 2 Rotor Position and Spacing Distances for Crossflow Spacing Test

Position	Spacing (inches)
#1	2
#2	6
#3	12
#4	24
#5	52

[1] "Harnessing Power from Ocean Currents and Tides" (Sea Technology, July 2004, pp. 40 - 43).

Due to the substantial forces on the turbine frames, the frames are locked and guyed in position, such that moving Turbine #3 required a coordinated sequence as follows:

Turbine Moving Procedure:

1. Stop both #3 and #4 turbines and remove load.
2. Release tension on #3 bottom guy wire.
3. Unlock #3 turbine clamp lockscrews.
4. Tension in or out winch or come-along as needed to pull turbine frame #3 to new position as marked on arm.
5. Simultaneously observe #3 frame column and adjust upper guy wire to maintain plumbness.
6. Shift upper and lower #3 guy wire attachment points as necessary from inboard to outboard positions.
7. Lock Turbine #3 frame in new position.
8. Adjust Turbine #3 plumbness with upper guy wire.
9. Retension #3 lower guy wire.
10. Restart and reload both #3 and #4 turbines.

All data was collected during ebb flow (stronger, steadier) for which the side-by-side structures and turbines were designed. For this section, data was acquired without Turbine #1 in the water upstream so as to eliminate any effect of the rotor upstream.

Incorporated into the procedures was a strict procedure for starting and loading the turbine/generators using the control box and the loadboxes to avoid any possibility of hazard to the generators or personnel, as follows:

Turbine Starting Procedure:

1. Open Control Panel
2. Place both control toggle switches in the OFF (center) position.
3. Place both 100-Amp starting breakers in the OFF (down) position.
4. Note: Facing the control panel the breaker positions are respective to the turbines, i.e., the right-hand breaker starts the inboard turbine (#3) and the left-hand breaker starts the outboard (#4) turbine.
5. Check that both loadbank 100-Amp breakers are in the OFF (down) position.
6. Place the appropriate starting breaker for the first turbine to start in the ON (up) position.
7. Place both control toggle switches towards the ON starting breaker.
8. Press the red start button until turbine reaches full speed then release button. Note: The “softstart” feature requires at least 1.5 seconds.
9. Place the starting breaker for the first turbine to start (now running) in the OFF position.
10. Place both control toggle switches in the OFF (center) position.
11. Place the other starting breaker for the second turbine to start in the ON position.
12. Place both control toggle switches towards the ON starting breaker for the second turbine to start.
13. Press the red start button until the second turbine reaches full speed then release button.
14. Place the starting breaker for the second turbine to start in the OFF position.

15. Place both control toggle switches in the OFF position.
16. Report an LV logpoint that turbines are started.

Turbine Loading Procedure

1. Once turbines are running, verify that all motor starting controls are all OFF.
2. Check that both loadbox breakers (#3 abd #4) are in the OFF (down) position.
3. Set resistances using loadbox jumpers and switches.
4. Switch loadbox breakers to ON (up) position.
5. Report an LV logpoint that turbines are loaded and report resistance setting.

Test Method

In consideration of the need to take multiple samples at each setting, and due to the time necessary to change the position of the inboard Turbine (#3) between data runs (5-7 minutes), data was acquired over relatively short periods of about 3 to 15 minutes.

Testing was done during periods of reasonable ebb flow, (approximately 0.8 m/s or higher).

A substantial load was applied to both turbines, but one that is not too close to the stall point. (Natural fluctuations in waterspeed on the order of one second can cause a turbine that is otherwise operating at steady-state to stall.) The loads applied by the loadboxes (5, 2.5, 1.7 and 1,3 Ohms) were typically in the ranges of 2.5 to 1.3 Ohms, with resulting (depending on water speed) in powers in the range of 200 – 500 Watts.

Test Procedure

1. Start with the narrowest or widest spacing (Position #1 or #5, usually as left from previous test). Record LV logpoint.
2. Start both turbines. (See *Turbine Starting Procedure*.) Record LV logpoint.
3. Apply load to turbines. (See *Turbine Loading Procedure*.) Record LV logpoint.
4. Acquire data for established period. Record LV logpoint.
5. Remove turbine loads, and stop turbines. Record LV logpoint.
6. Move Turbine # 3 (inner) to the next position. Record LV logpoint.
7. Repeat data acquisition at each location, making at least one full scan of spacings.
8. Repeat, taking data over as wide a range of waterspeeds as practical, adjusting loads as necessary, but with one load fixed for each scan of spacing.

IV. LONGITUDINAL SPACING

Turbines #1 and #3

The last tests conducted examined the upstream/downstream positioning of Turbines #1 and #3. Acquiring empirical data about the performance of a turbine rotor in the proximity of another rotor is essential for developing optimal spacing for practical turbine fields.

In position #5, Turbine #3 is directly (within 2.5 inches) downstream (during ebb flow) of turbine #1. The center-to-center rotor spacing in this position between the two rotors is 174 inches, or about 4.4 rotor diameters. With this spacing, and effect in loss of power would be expected to be measured on the downstream turbine. The degree of the effect will help indicate possible turbine array spacings.

These tests examined the response of Turbine #3 to being downstream of Turbine #1 with Turbine #1 in different loading conditions, since it could be expected that its loading state would have an effect on downstream flow velocity and turbulence. It was also possible to further examine the effect of downstream spacing by moving Turbine #3 laterally outward from the barge and away from being directly downstream of Turbine #1.

In these tests, electric generation data was acquired from units #3 and #4 with Turbine #1 reinstalled in the water. As with the testing in Section III., only ebb flow was used, (approximately 0.8 m/s or higher), and a similar substantial load was applied to both turbines #3 and #4 were given a manageable load. The loads applied by the loadboxes (5, 2.5, 1.7 and 1,3 Ohms) were typically in the ranges of 2.5 to 1.3 Ohms, with resulting (depending on water speed) in powers in the range of 200 – 300 Watts.

Generation data was taken from Turbines #3 and #4 with Turbine #3 in position #5 (downstream of Turbine #1), with Turbine #1 at no-load, at full load, and with a locked rotor. This was followed by taking the same data with Turbine #3 in Positions #4, #3, #2, and #1.

Test Procedure

1. Start with Turbine #3 in Position #1. Record LV logpoint.
2. Start #3 and #4 turbines. (See *Turbine Starting Procedure.*) Record LV logpoint.
3. Apply load to #3 and #4 turbines. (See *Turbine Loading Procedure.*) Record LV logpoint.
4. Set Turbine #1 to no-load. Record LV logpoint.
5. Acquire data for established period. Record LV logpoint.
6. Repeat with Turbine #1 at moderate load. Record LV logpoint.
7. Repeat with Turbine #1 at locked rotor. Record LV logpoint.
8. Remove loads, and stop #3 and #4 turbines. Record LV logpoint.
9. Move Turbine # 3 to the next position. Record LV logpoint.
10. Repeat data acquisition with each loading of Turbine #1 at each Turbine #3 position.
11. Repeat, taking data over as wide a range of waterspeeds as practical, adjusting loads as necessary, but with one load fixed for each scan of spacing.

ADDITIONAL TESTING NOTES

1. It is, of course, critical to know the tide times and heights. These can be conveniently found at several web sites including this site which gives the times and heights of tides:
    i. http://www2.shore.net/~mcmorran/bin/stateloc.pl?state=MA
    ii. *and choose:* Newburyport Merrimac River

2. Because for the vast majority of the time, the water flow is at low velocities, there is a premium on collecting data at high water flows. These occur at this hybrid (both tidal and river flow) site on the ebb flows.
3. Very roughly, the fastest flow per cycle occurs midway in time between the high and low tides (slack water). The fastest flows overall occurs when the tide height difference or range between flood and the subsequent ebb reaches especially high values, e.g. greater than 8 feet.
4. A spreadsheet based on the tide table, annotated to show the current cycles that occur during daylight, their times and ranges, follows for the first month. Note that at the end of August, the highest currents can be expected
5. It is important to be aware of any fouling of the rotor, and since the waterspeed measurement is critical (power is proportional to the cube of the fluid velocity), it is critical to be aware of any fouling of the ADCP that might affect its performance (built-in data checking). Any anomalies or discrepancies are logged in the logbook in conjunction with the DACs.

Sample Tide Chart

See Table 3, following page.

Table 3 Sample Tide Chart

Tide Chart for Newburyport, Merrimack River, MA 08/16/2004 to 09/16/2004 Local Daylight Time											Annotations: During Daylight Hours			
Date	Day	High		Low		High		Low		High		Time of approx peak current	range (ft)	Time of approx peak current	range (ft)
		Time	ft	Time	ft	Time	ft	Time	ft	Time	ft				
8/16/2004	Mon	0:21	8.4	7:21	0.22	12:50	7.57	19:27	0.92					**16:08**	6.7
8/17/2004	Tue	0:58	8.54	7:56	0.16	13:25	7.86	20:04	0.76					**16:44**	7.1
8/18/2004	Wed	1:36	8.6	8:29	0.13	14:02	8.13	20:40	0.59					**17:21**	7.5
8/19/2004	Thu	2:16	8.57	9:02	0.15	14:41	8.36	21:19	0.44					**18:00**	7.9
8/20/2004	Fri	2:59	8.44	9:37	0.22	15:23	8.53	22:02	0.34						
8/21/2004	Sat	3:44	8.23	10:16	0.37	16:08	8.63	22:51	0.3						
8/22/2004	Sun	4:33	7.95	11:02	0.58	16:57	8.67	23:47	0.31						
8/23/2004	Mon	5:27	7.65	11:56	0.83	17:51	8.68								
8/24/2004	Tue			0:51	0.33	6:26	7.39	12:59	1.04	18:50	8.69				
8/25/2004	Wed			1:59	0.28	7:30	7.25	14:08	1.1	19:53	8.77				
8/26/2004	Thu			3:07	0.12	8:37	7.29	15:17	0.98	20:59	8.94				
8/27/2004	Fri			4:10	-0.15	9:44	7.52	16:21	0.69	22:04	9.16				
8/28/2004	Sat			5:08	-0.44	10:47	7.85	17:20	0.34	23:05	9.37				
8/29/2004	Sun			6:02	-0.69	11:44	8.2	18:16	-0.01			**8:53**	8.9	**15:00**	8.2
8/30/2004	Mon	0:01	9.45	6:52	-0.82	12:35	8.47	19:08	-0.26			**9:43**	9.3	**15:51**	8.7
8/31/2004	Tue	0:52	9.36	7:40	-0.81	13:23	8.61	19:58	-0.39			**10:31**	9.4	**16:40**	9.0
9/1/2004	Wed	1:41	9.09	8:27	-0.63	14:07	8.6	20:48	-0.38			**11:17**	9.2	**17:27**	9.0
9/2/2004	Thu	2:28	8.67	9:13	-0.31	14:51	8.44	21:37	-0.23					**18:14**	8.7
9/3/2004	Fri	3:14	8.15	9:59	0.12	15:34	8.19	22:28	0.03						
9/4/2004	Sat	4:01	7.59	10:47	0.61	16:18	7.87	23:21	0.35						
9/5/2004	Sun	4:49	7.07	11:38	1.1	17:05	7.56					**14:21**	6.5		
9/6/2004	Mon			0:16	0.67	5:41	6.63	12:33	1.51	17:56	7.31				
9/7/2004	Tue			1:15	0.93	6:38	6.34	13:31	1.78	18:52	7.17				
9/8/2004	Wed			2:13	1.06	7:39	6.24	14:28	1.87	19:52	7.19				
9/9/2004	Thu			3:10	1.07	8:40	6.33	15:23	1.81	20:50	7.37				
9/10/2004	Fri			4:01	0.96	9:34	6.57	16:13	1.63	21:42	7.64				
9/11/2004	Sat			4:48	0.79	10:20	6.91	16:58	1.36	22:28	7.94				

Cont'd next page

9/12/2004	Sun			5:29	0.58	11:00	7.3	17:39	1.06	23:10	8.22	**8:14**	6.7
9/13/2004	Mon			6:08	0.37	11:37	7.7	18:18	0.73	23:50	8.45	**8:52**	7.3
9/14/2004	Tue			6:43	0.19	12:14	8.1	18:56	0.41			**9:28**	7.9
9/15/2004	Wed	0:28	8.6	7:16	0.07	12:50	8.45	19:32	0.1			**10:03**	8.4
9/16/2004	Thu	1:09	8.65	7:50	0	13:29	8.74	20:11	-0.14			**10:39**	8.7

flood

ebb

APPENDIX E

Amesbury Tidal Energy Project

Data Preparation Steps

Prepared
by

Jamey Gerlaugh

February 15, 2005

General Notes

1. The ATEP Data Acquisition and Control System (DACS), host notebook computer, running National Instrument's LabView (LV) software, saved data in a tab-delineated text file with the format, "YMMDD"D"n.txt" where Y=year, MM= month, DD= day, "D" = Data file, and n = unique number differentiating datafiles on that date. The file consists of a header row and data rows. Each data row consisted of 76 parameters which represent the sensor values at that 2 second interval.
2. A new datafile was automatically created 1) at the startup of the DACS program and 2) at 12:00 AM (midnight) if the DACS program was running at that time. These files were saved to the notebook in the C:/LOG folder

Preparation Steps for All Data

1. All Data files were backed up and placed in a folder "Raw Data." During each subsequent major step of processing, the files were saved and backed up.
2. Text files of less than 8 KB were removed from the "Raw Data" folder and placed in a separate folder, "Non-Test Data Files" since these files would have less then one-minute's worth of data which is not long enough for some of the sensors such as the ADCP to come on line or stabilize.
3. Each remaining text file was opened in Microsoft Excel and saved as a spreadsheet named with the format, "YMMDD"D"n .xls"
4. The "format paint" function was used to format the entire spreadsheet, allowing for maximum readability. Included in this formatting were:
    a) The conversion of the time/date column format from YMMDD HHMMSS to MM/DD/YY HH:MM:SS format.
    b) Displaying the proper number of significant digits
5. Each row of data was checked to make sure that the DACS was running properly and the data was valid. Any data rows exhibiting NAN ("Not A Number") values for the ADCP water velocity data were deleted.
6. Valid data rows for each file were copied and appended into another file named in the format "Y-MM-DD1Day Data.xls" and placed in the folder "One-File-Per-Day Data Files"
7. All files from that one day are processed following steps 3-6 above. Data is added to that day's "One-File-Per-Day" data file.
8. Each "One-File-Per-Day" data file is copied to another file named in the format "Y-MM-DD1Day Data- crunched.xls" and processed as follows:
    a) Columns deemed unnecessary for data analysis are removed.
    b) The data columns are sorted into a more logical and useful order.
    c) Handwritten notes that were recorded in the test log were added to the spreadsheets and the files saved, named in the format "Y-MM-DD1Day

Data-Crunched+fieldnotes.xls." These notes included information such as descriptions of the types of tests being conducted, brake torque scan starts and stops, and torque meter tares. Any anomalous situations that might lead to erroneous data were also noted.

Preparation for Turbine #1- Dynamometer Data Only

1. The data is prepped according to Steps 1-12 described in the above section "Preparation Steps for All Data".
2. "Y-MM-DD1Day Data-Crunched+fieldnotes.xls." files for days with dynamometer testing are copied and renamed in the format "Y-MM-DD 1Day Dyno Data- Step 2.xls" and placed in a separate folder, "Turbine#1- Dyno Tests".
3. All rows with a turbine speed = 0 RPM (stalled or locked) are identified and their speed cells highlighted in red. These denote the periods between torque tests.
4. Valid testing data is identified. A valid torque test contains the following attributes:
    a. When the brake is released and the turbine first starts from a zero speed it ramps up quickly, overshoots, and then settles into a steady-state no-load condition. Data is considered valid only after the speed overshoots, comes back down and then flattens for more than 2 cycles or starts increasing again.
    b. The torque meter is working properly with a minimal offset drift and noise. If immediately before or after the test the no-load torque appears to be drifting more than 10 in-lbs in 3 minutes, that test data was not used. If the torque meter noise appears more than +/- 7.5 in-lbs immediately before the test, that test data was not used
    c. A valid "tare" of the torque meter to zero-out any offsets has to take place while the turbine is spinning with no braking. Thus we looked for a period with the turbine spinning and a tare to 0 in-lbs. A valid "tare" should have taken take place within 5 minutes of the commencement of braking. In most cases the time of tare was also written in the notes.
    d. The dynamometer braking had to be applied in a slow, steady, monotonic manner, slowly and ever increasing in intensity over the course of 2-5 minutes to achieve a quasi-steady state condition while at a near-constant waterspeed. A slow even ramping-up of the torque over this period is an indication of a proper test. Tests lasting less than 2 minutes were not used.
    e. The test ends with a stalling of the turbine. The end of the valid test data is the last row of data before stall is initiated because stall takes place more rapidly than the two-second data logging period and the data during that period is not reliable. The stall initiation is identified as the point at which the turbine speed first started dropping off in a continuous drop to zero speed with no blips of increasing speed.

f. Valid test data was identified by highlighting the time/date cells in green. Unused data before the test and after the stall initiation were marked in red.

5. A master dynamometer data file named "ATEP Total Dyno Data.xls" is created. The valid test rows (with green time/date cells) from each day of dynamometer testing are pasted into this one file. This file is then ready for data analysis.

Preparation for Turbine #2- Generator Data

1. The data is prepared according to the steps described in the above section "Preparation Steps for All Data".
2. "Y-MM-DD1Day Data-Crunched+fieldnotes.xls" files for days with Turbine #2 Generator tests are copied and renamed in the format "Y-MM-DD Gen 1- Step 2.xls" and placed in a separate folder, "Gen-1 Turb-2 Data".
3. Columns deemed unnecessary for Turbine #2 Generator data analysis are removed.
4. Data for Turbine #2 Generator tests were subjected to the following procedure:
    a. The resistive loadbank is removed from the generator (switch opened)
    b. The turbine is hand-cranked to the point it is able to speed up on its own. It is then allowed to ramp up on its own to a stable no-load speed.
    c. A no-load DC voltage reading is taken across the generator's rectifier with a DVM and recorded.
    d. The no-load generator rotational speed is measured and recorded.
    e. A specific nominal resistor load is configured in the loadbank using switches and patch cables. Its actual resistance is measured with an ohmmeter and recorded.
    f. The resistive load is applied by closing the loadbank switch.
    g. The generator voltage and current and turbine rotational speed are recorded.
    h. If the turbine stalled after the application of the load, that is noted.

Preparation for Turbine #3 & #4- Generator Data

1. The data is prepped according to the steps described in the above section "Preparation Steps for All Data".
2. "Y-MM-DD1Day Data-Crunched+fieldnotes.xls." files for days with Turbine #3 and/or #4 Generator tests are copied and renamed in the format "Y-MM-DD T3 & T4 Step2.xls" and placed in a separate folder, "Gen 3-Turb 3 & Gen 4-Turb 4 Data".

3. Columns deemed unnecessary for Turbine #3 and/or #4 Generator data analysis are removed.
4. Data for Turbine #3 & #4 Generator tests were subjected to the following procedure:
    a. The resistive loadbank is removed from the generator (switch opened)
    b. The turbine is kick-started (according to procedures described in the Testing Protocols section) by driving the generator as a motor to the point it is able to maintain speed on its own. It is then allowed to ramp up on its own to a stable no-load speed.
    c. A no-load DC voltage reading is taken across the generator's rectifier with a DVM and recorded.
    d. The no-load generator rotational speed is measured and recorded.
    e. A specific nominal resistor load is configured in the loadbank using switches and patch cables. Its actual resistance is measured with an ohm-meter and recorded.
    f. The resistive load is applied by closing the loadbank switch.
    g. The generator voltage and current and turbine rotational speed are recorded.
    h. If the turbine stalled after the application of the load, that is noted.

F. ATEP Dynamometry Power Curves

APPENDIX
F

ATEP Dynamometry P_T vs. V Graphs

Dynamometry data was generated by loading the GHT at varying waterspeeds with a brake and continuously measuring the waterspeed, **V**, torque, **τ**, and shaft rotation speed, **Ω.**

For details on the methodology, see Appendix D, **ATEP** Summary of Test Protocols.

The following forty-three graphs of $\mathbf{P_T}$ **vs. V** show the operating curves that were generated by grouping all data by **V** into bins 0.04 m/s wide centered at each 0.02 m/s from **V**= 0.66 m/s to 1.50 m/s. The power of the turbine, $\mathbf{P_T}$, is the product of **τ**, and **Ω**. These power curve graphs were used to identify the Practical Peak Power Point for each **V**, identified by the red circle on each graph, and to determine, **τ**, **Ω** and tipspeed ratio, **X,** at each center value **V**. These data were further plotted as shown in the ATEP report to determine the relationships among the parameters and characterize the performance of the GHT rotor across all available waterspeeds including the coefficient of performance, **Cp.**

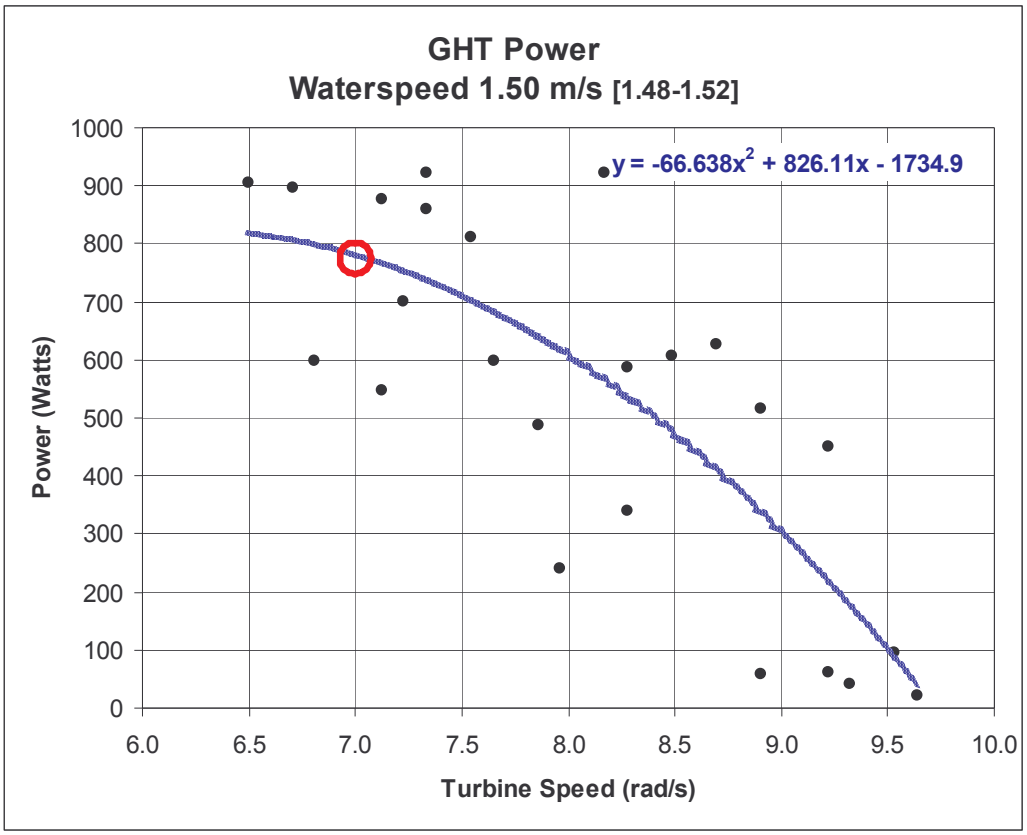

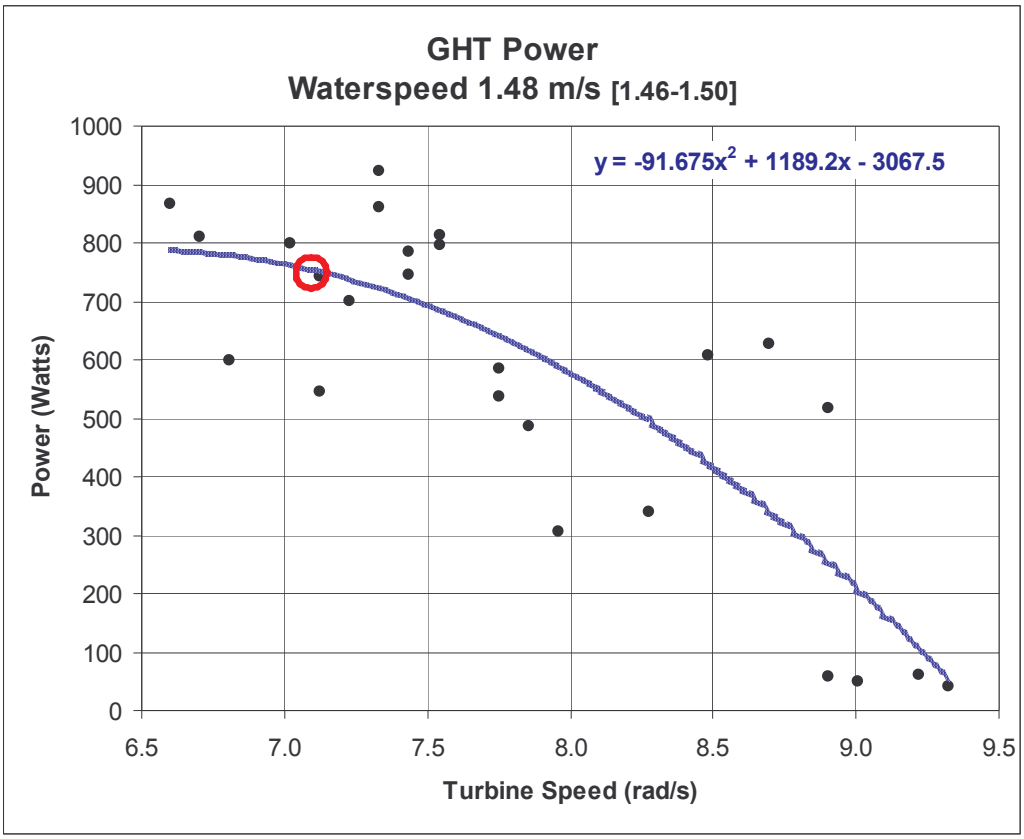
GHT Power
Waterspeed 1.48 m/s [1.46-1.50]
y = -91.675x2 + 1189.2x - 3067.5
Power (Watts)
Turbine Speed (rad/s)
0
100
200
300
400
500
600
700
800
900
1000
6.5
7.0
7.5
8.0
8.5
9.0
9.5

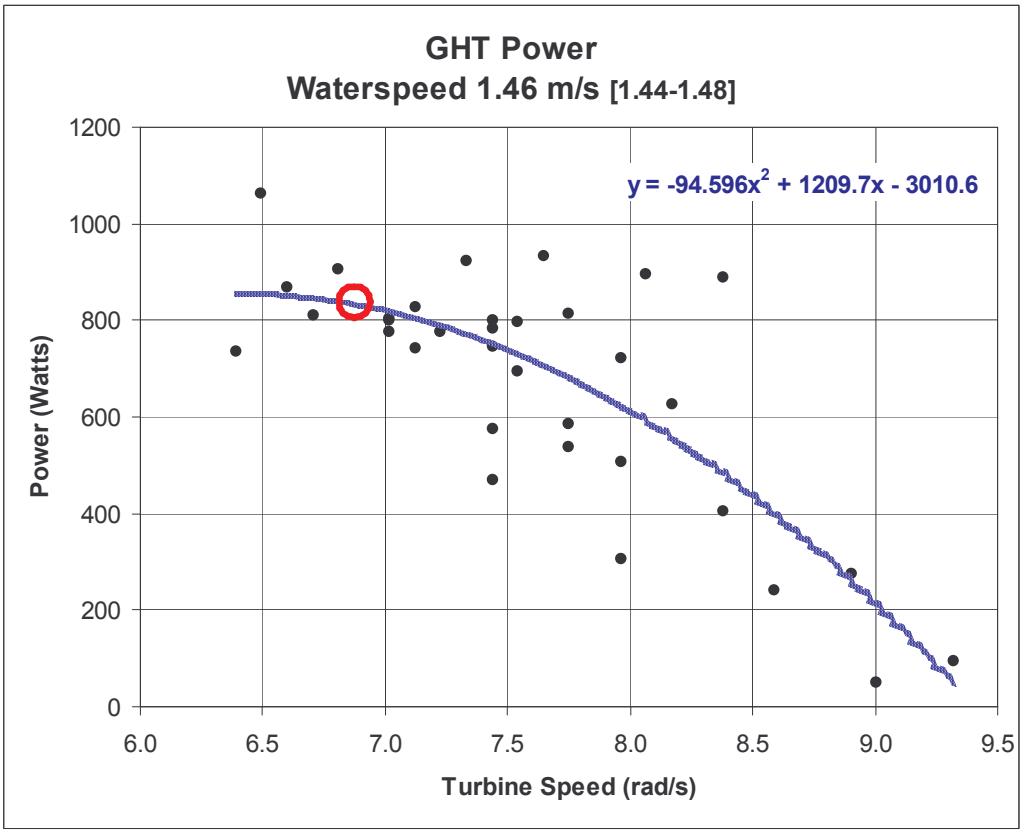
GHT Power
Waterspeed 1.46 m/s [1.44-1.48]
y = -94.596x2 + 1209.7x - 3010.6
Power (Watts)
Turbine Speed (rad/s)
0
200
400
600
800
1000
1200
6.0
6.5
7.0
7.5
8.0
8.5
9.0
9.5

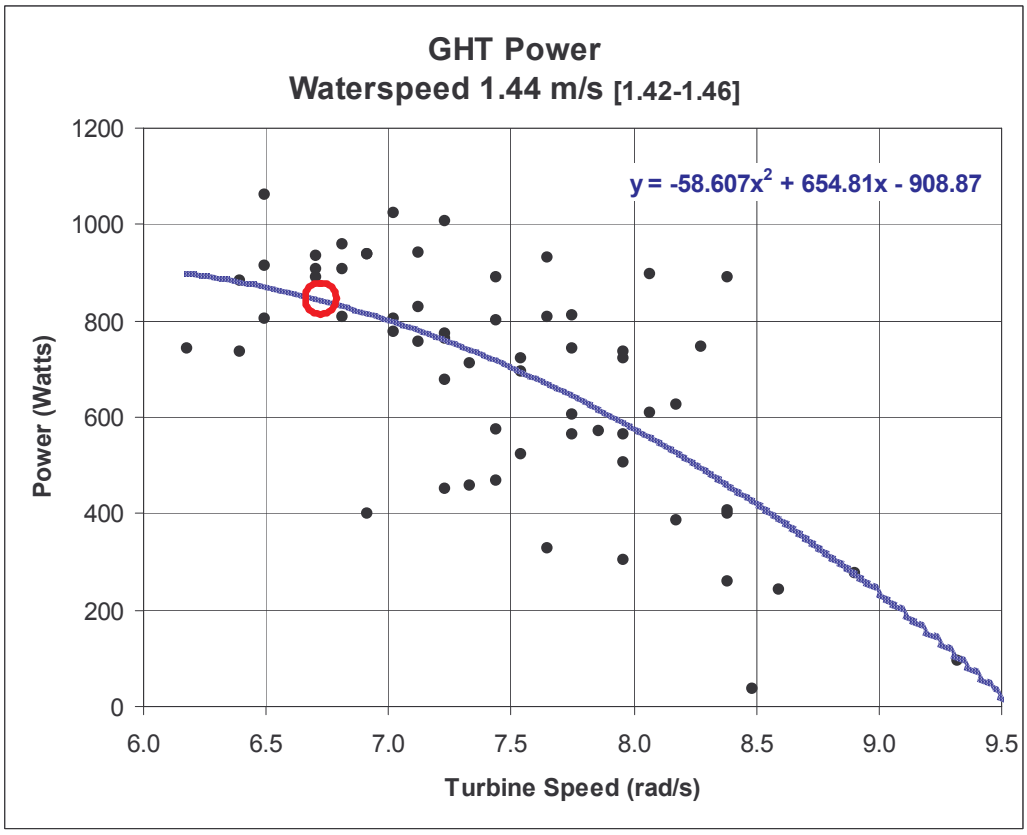
GHT Power
Waterspeed 1.44 m/s [1.42-1.46]
y = -58.607x2 + 654.81x - 908.87
Power (Watts)
Turbine Speed (rad/s)
0
200
400
600
800
1000
1200
6.0
6.5
7.0
7.5
8.0
8.5
9.0
9.5

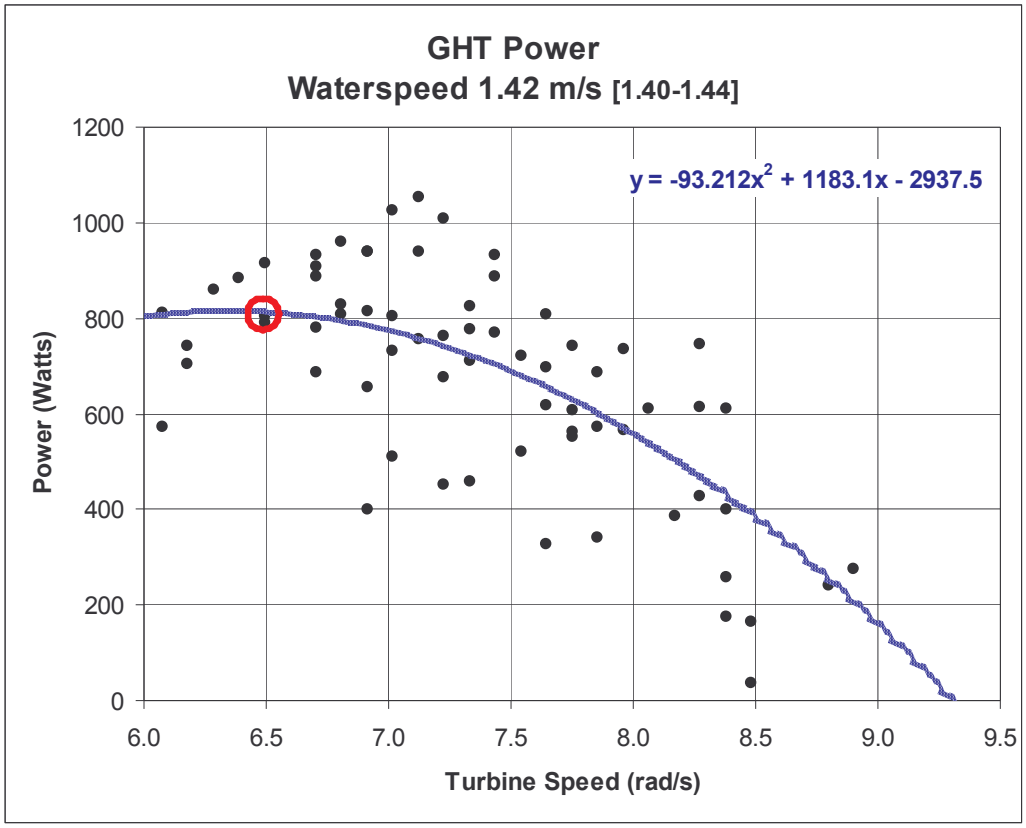
GHT Power
Waterspeed 1.42 m/s [1.40-1.44]
y = -93.212x2 + 1183.1x - 2937.5
Power (Watts)
Turbine Speed (rad/s)
0
200
400
600
800
1000
1200
6.0
6.5
7.0
7.5
8.0
8.5
9.0
9.5

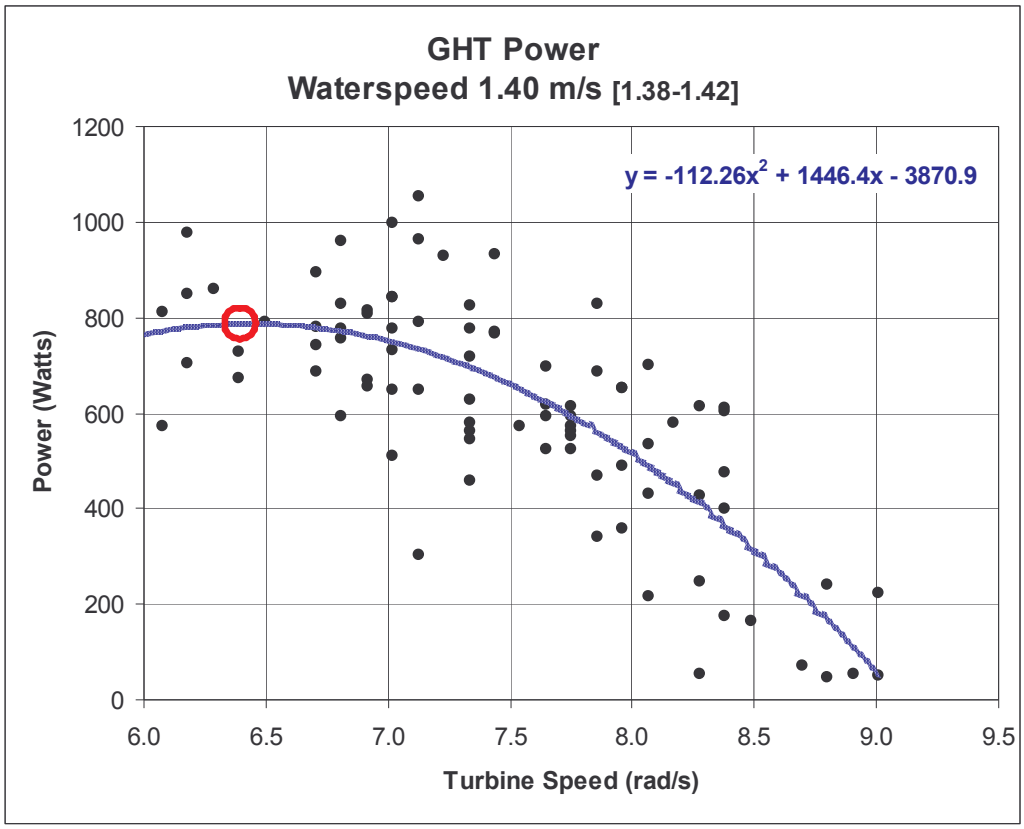
GHT Power
Waterspeed 1.40 m/s [1.38-1.42]
y = -112.26x2 + 1446.4x - 3870.9
Power (Watts)
Turbine Speed (rad/s)
0
200
400
600
800
1000
1200
6.0
6.5
7.0
7.5
8.0
8.5
9.0
9.5

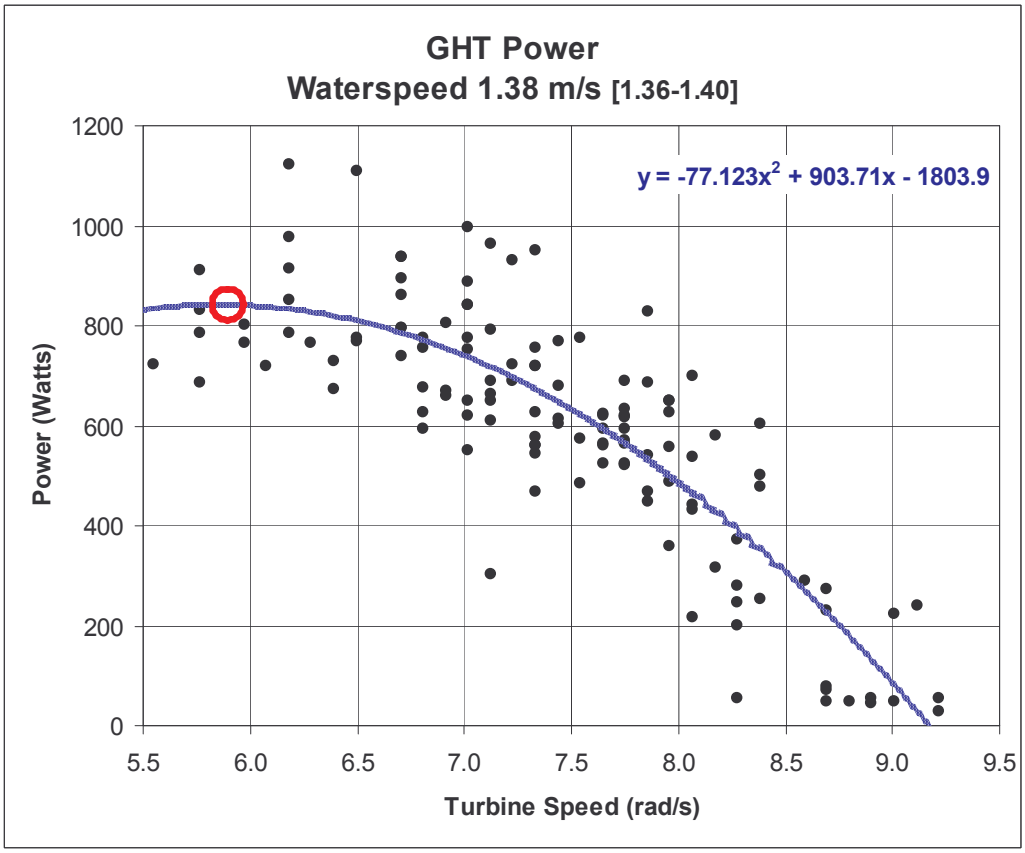
GHT Power
Waterspeed 1.38 m/s [1.36-1.40]
y = -77.123x2 + 903.71x - 1803.9
Power (Watts)
Turbine Speed (rad/s)
0
200
400
600
800
1000
1200
5.5
6.0
6.5
7.0
7.5
8.0
8.5
9.0
9.5

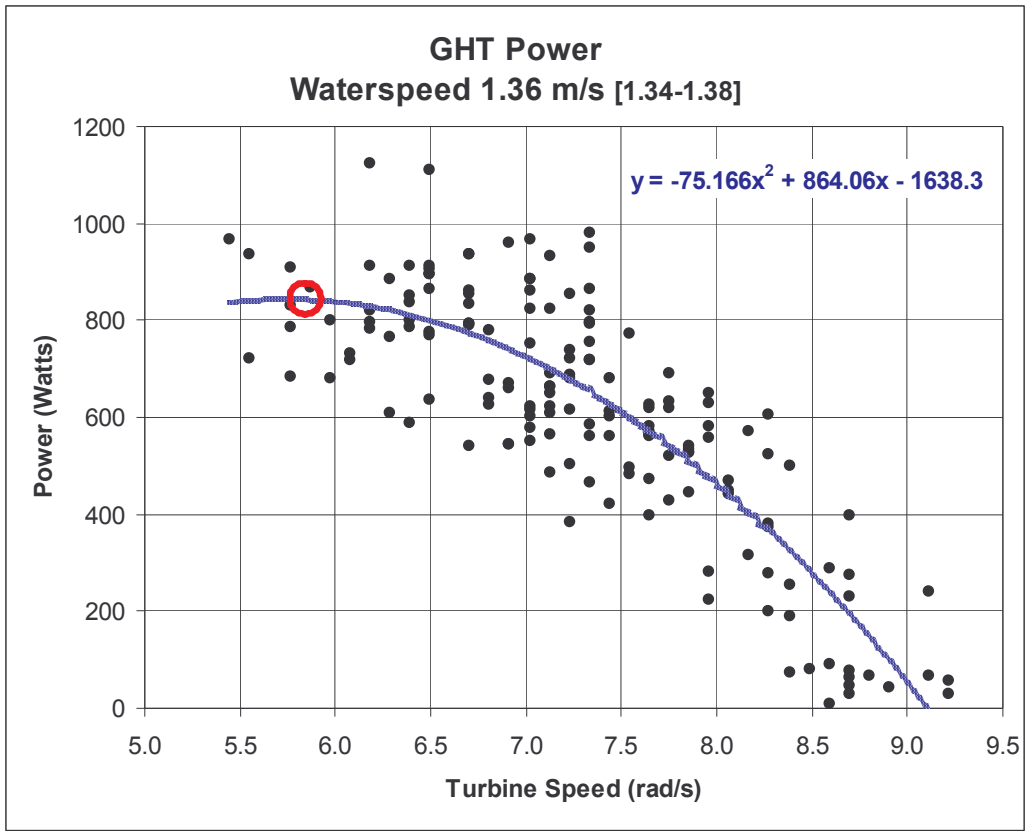
GHT Power
Waterspeed 1.36 m/s [1.34-1.38]
y = -75.166x2 + 864.06x - 1638.3
Power (Watts)
Turbine Speed (rad/s)
0
200
400
600
800
1000
1200
5.0
5.5
6.0
6.5
7.0
7.5
8.0
8.5
9.0
9.5

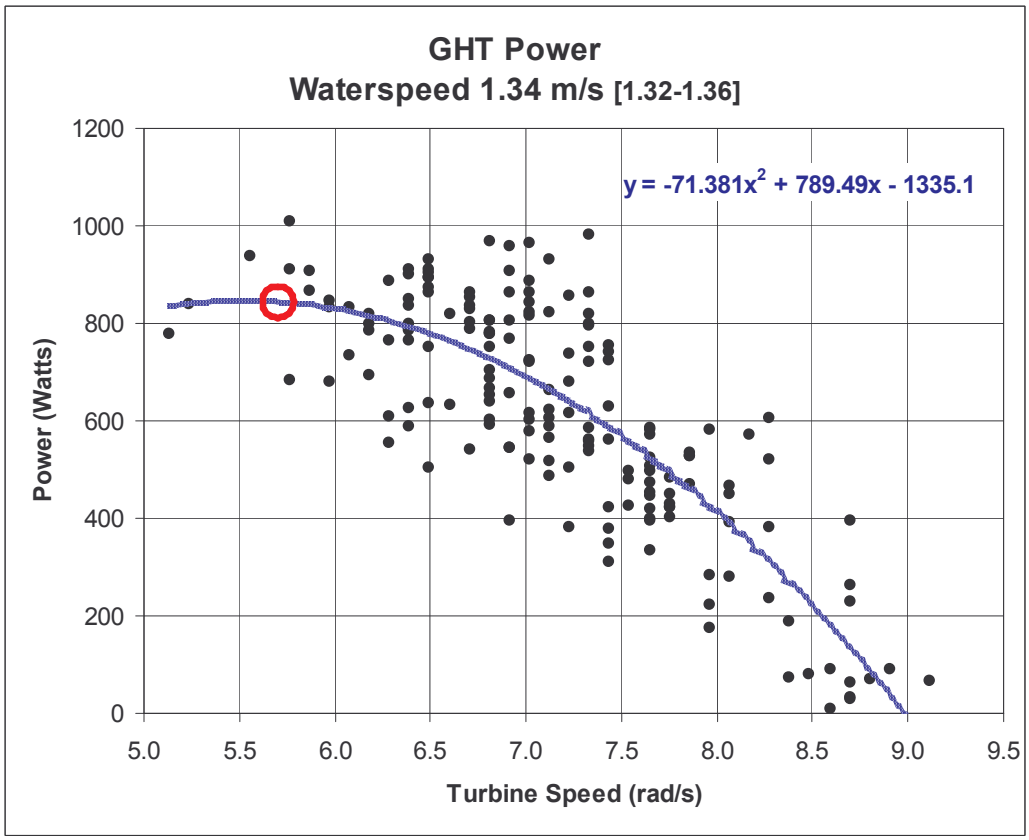
GHT Power
Waterspeed 1.34 m/s [1.32-1.36]
y = -71.381x2 + 789.49x - 1335.1
Power (Watts)
Turbine Speed (rad/s)
0
200
400
600
800
1000
1200
5.0
5.5
6.0
6.5
7.0
7.5
8.0
8.5
9.0
9.5

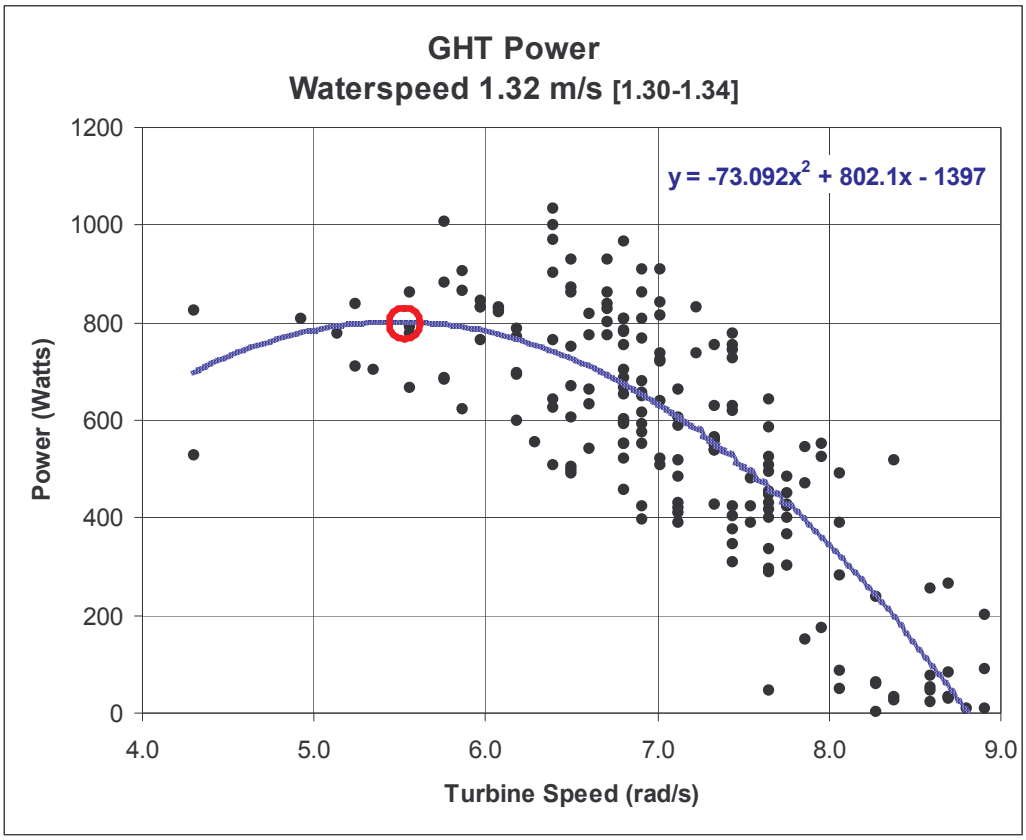
GHT Power
Waterspeed 1.32 m/s [1.30-1.34]
y = -73.092x2 + 802.1x - 1397
Power (Watts)
Turbine Speed (rad/s)
0
200
400
600
800
1000
1200
4.0
5.0
6.0
7.0
8.0
9.0

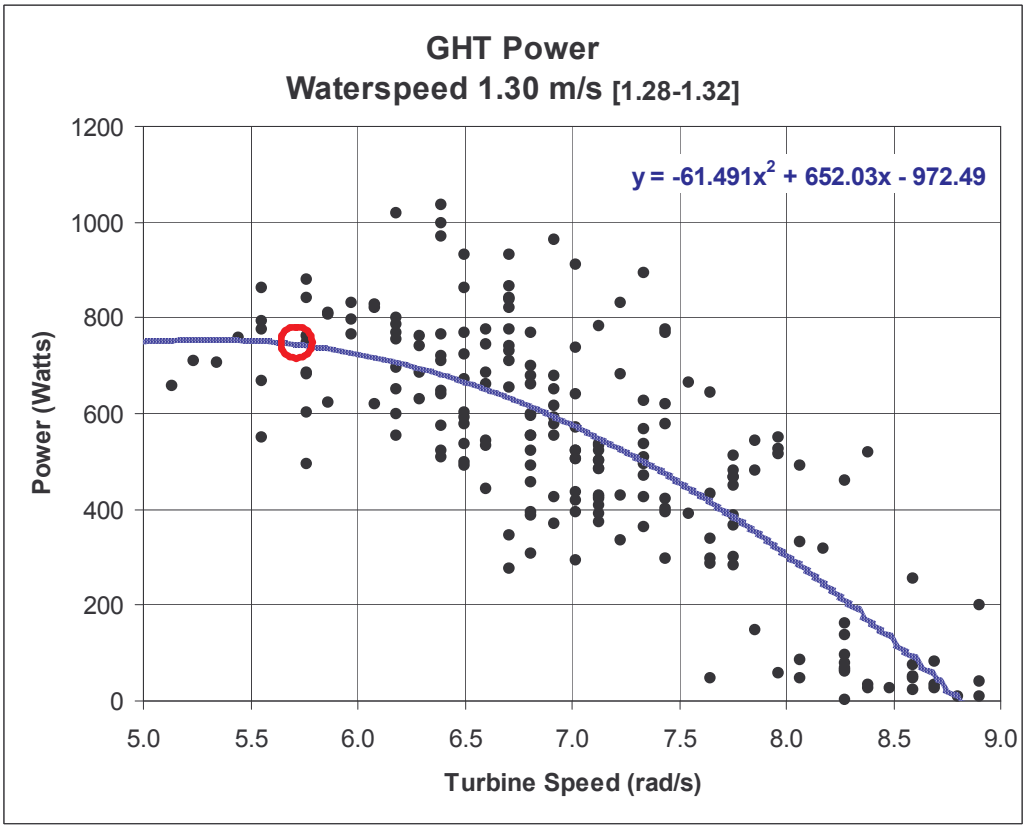
GHT Power
Waterspeed 1.30 m/s [1.28-1.32]
y = -61.491x2 + 652.03x - 972.49
Power (Watts)
Turbine Speed (rad/s)
0
200
400
600
800
1000
1200
5.0
5.5
6.0
6.5
7.0
7.5
8.0
8.5
9.0

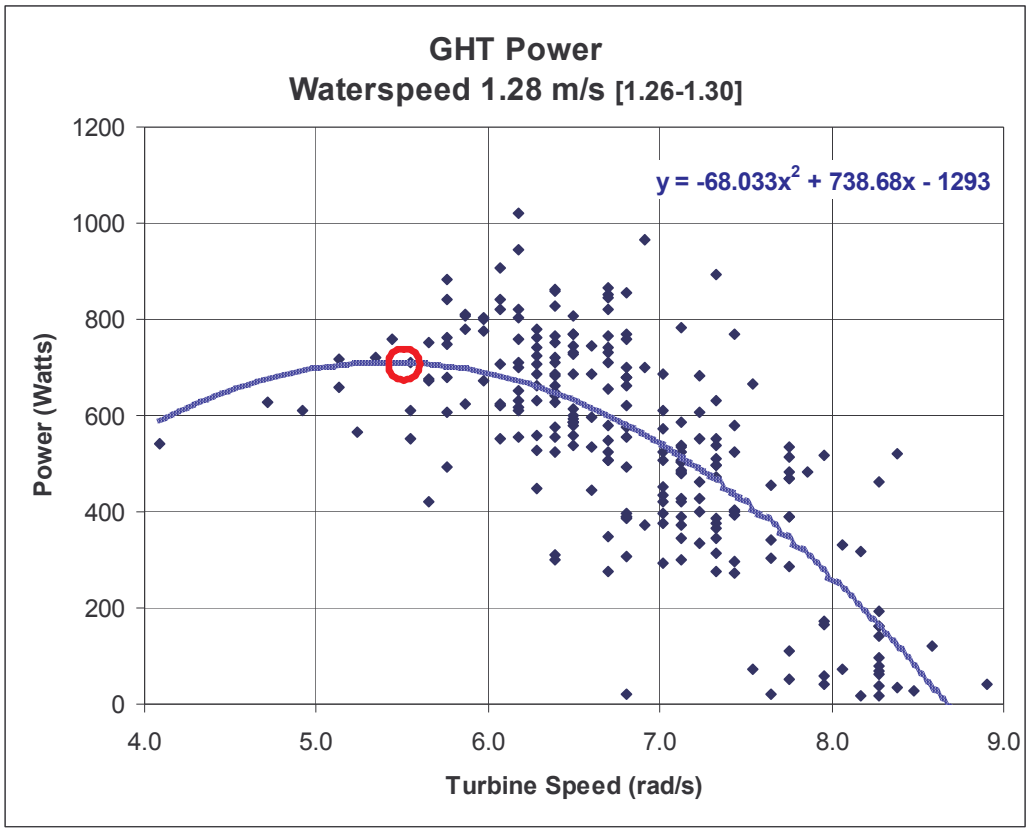
GHT Power
Waterspeed 1.28 m/s [1.26-1.30]
y = -68.033x2 + 738.68x - 1293
Power (Watts)
Turbine Speed (rad/s)
0
200
400
600
800
1000
1200
4.0
5.0
6.0
7.0
8.0
9.0

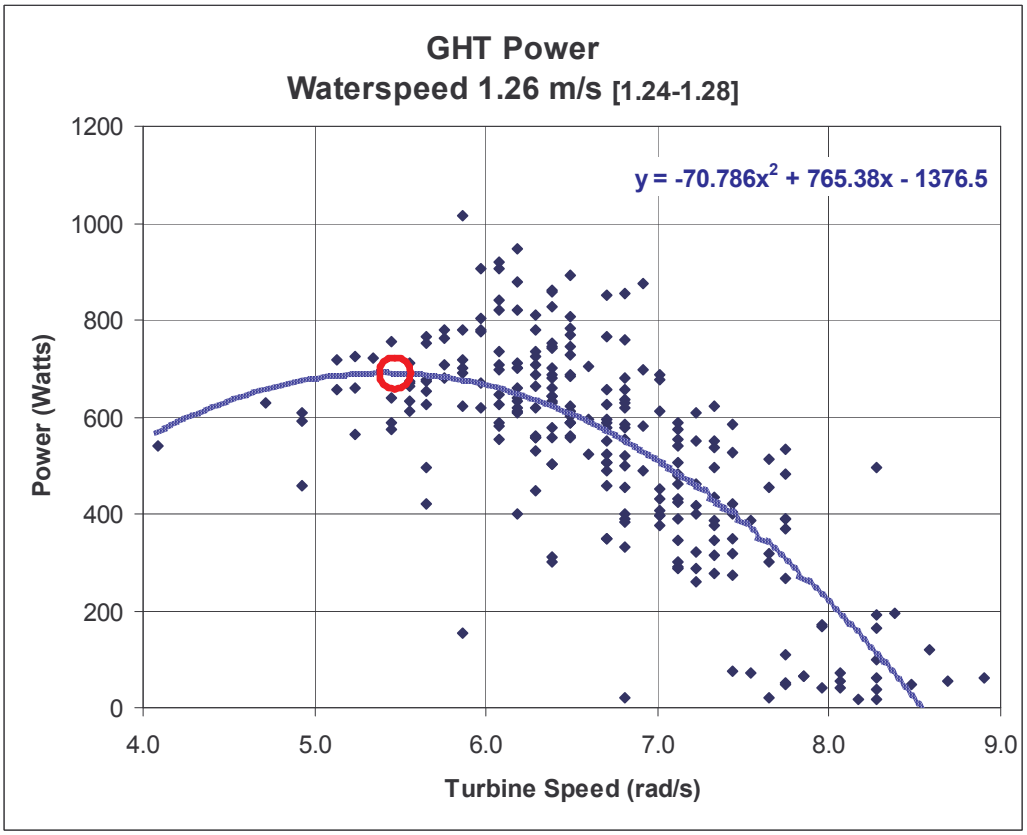
GHT Power
Waterspeed 1.26 m/s [1.24-1.28]
y = -70.786x2 + 765.38x - 1376.5
Power (Watts)
Turbine Speed (rad/s)
0
200
400
600
800
1000
1200
4.0
5.0
6.0
7.0
8.0
9.0

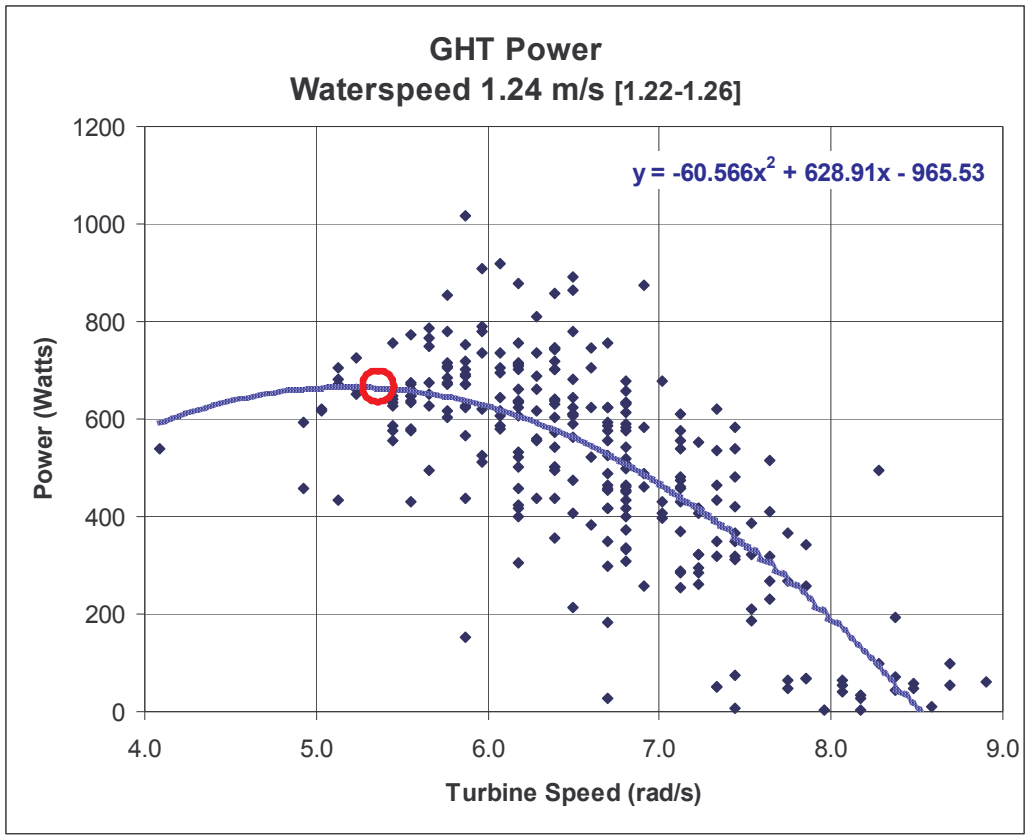
GHT Power
Waterspeed 1.24 m/s [1.22-1.26]
y = -60.566x2 + 628.91x - 965.53
Power (Watts)
Turbine Speed (rad/s)
0
200
400
600
800
1000
1200
4.0
5.0
6.0
7.0
8.0
9.0

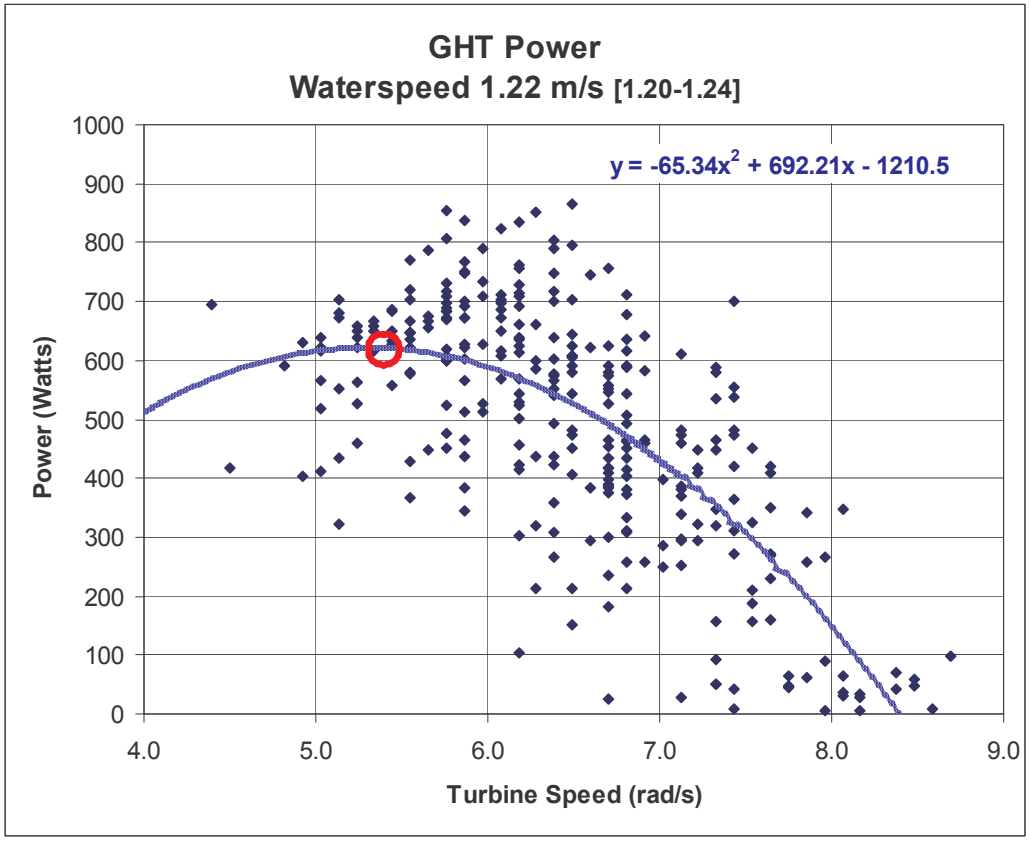
GHT Power
Waterspeed 1.22 m/s [1.20-1.24]
y = -65.34x2 + 692.21x - 1210.5
Power (Watts)
Turbine Speed (rad/s)
0
100
200
300
400
500
600
700
800
900
1000
4.0
5.0
6.0
7.0
8.0
9.0

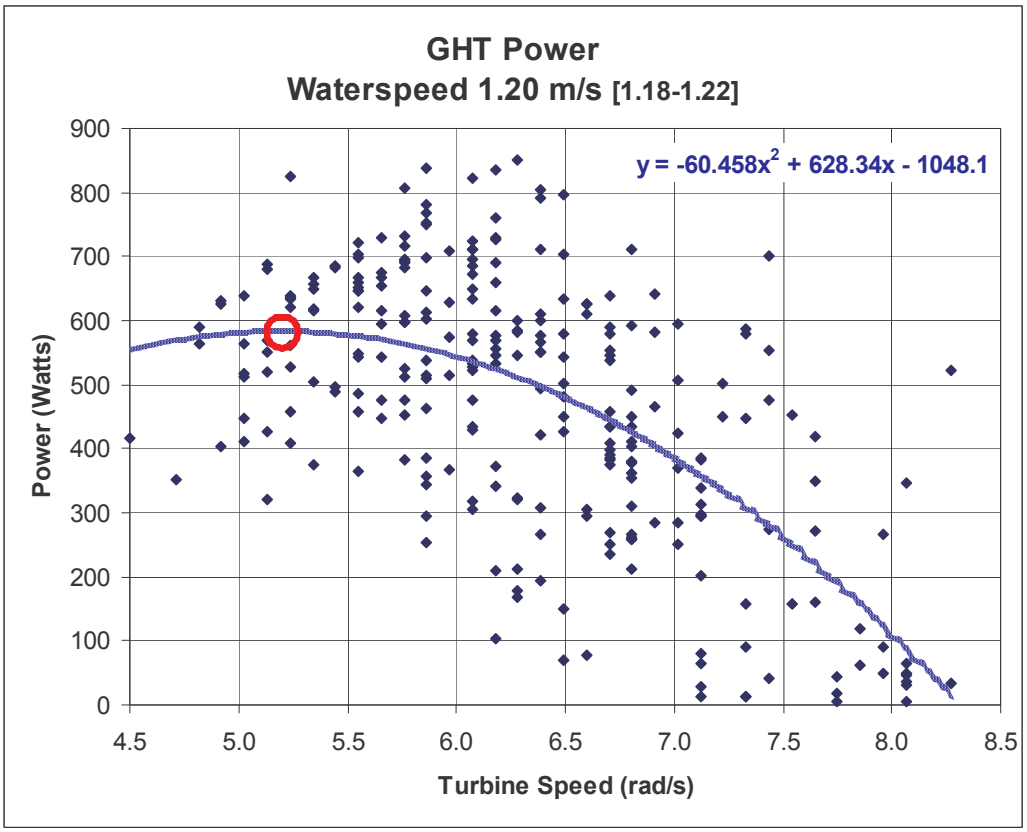
GHT Power
Waterspeed 1.20 m/s [1.18-1.22]
y = -60.458x2 + 628.34x - 1048.1
Power (Watts)
Turbine Speed (rad/s)
900
800
700
600
500
400
300
200
100
0
4.5
5.0
5.5
6.0
6.5
7.0
7.5
8.0
8.5

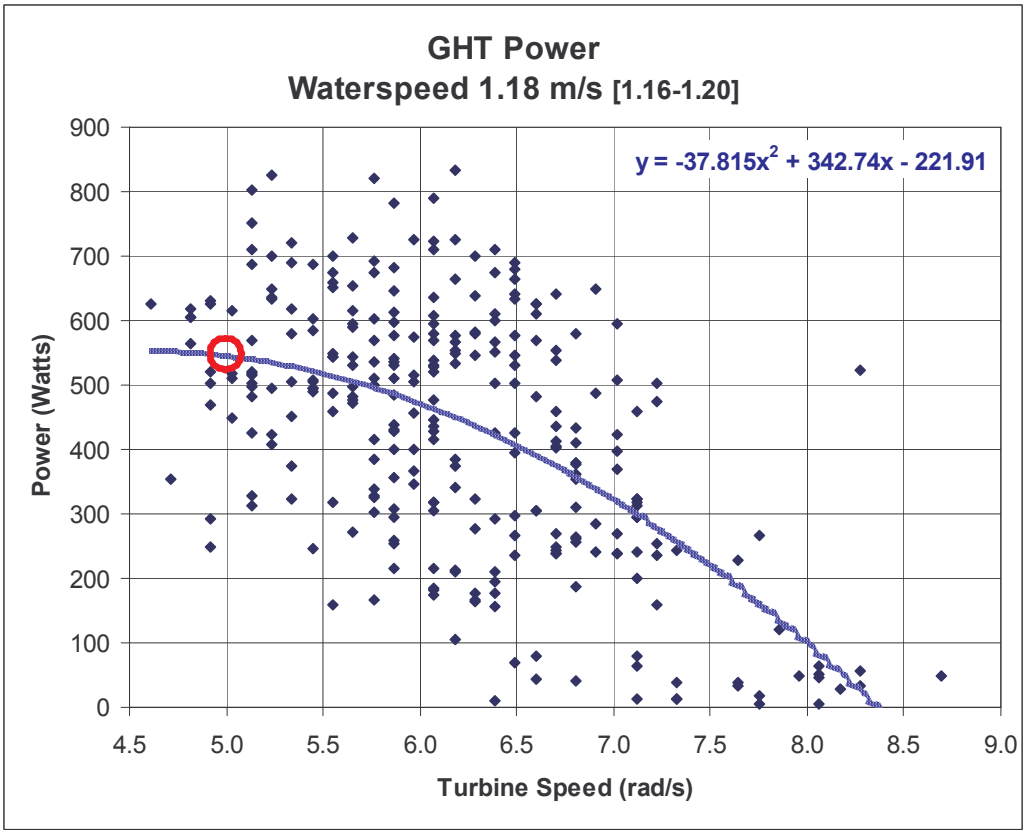
GHT Power
Waterspeed 1.18 m/s [1.16-1.20]
y = -37.815x2 + 342.74x - 221.91
Power (Watts)
Turbine Speed (rad/s)
900
800
700
600
500
400
300
200
100
0
4.5
5.0
5.5
6.0
6.5
7.0
7.5
8.0
8.5
9.0

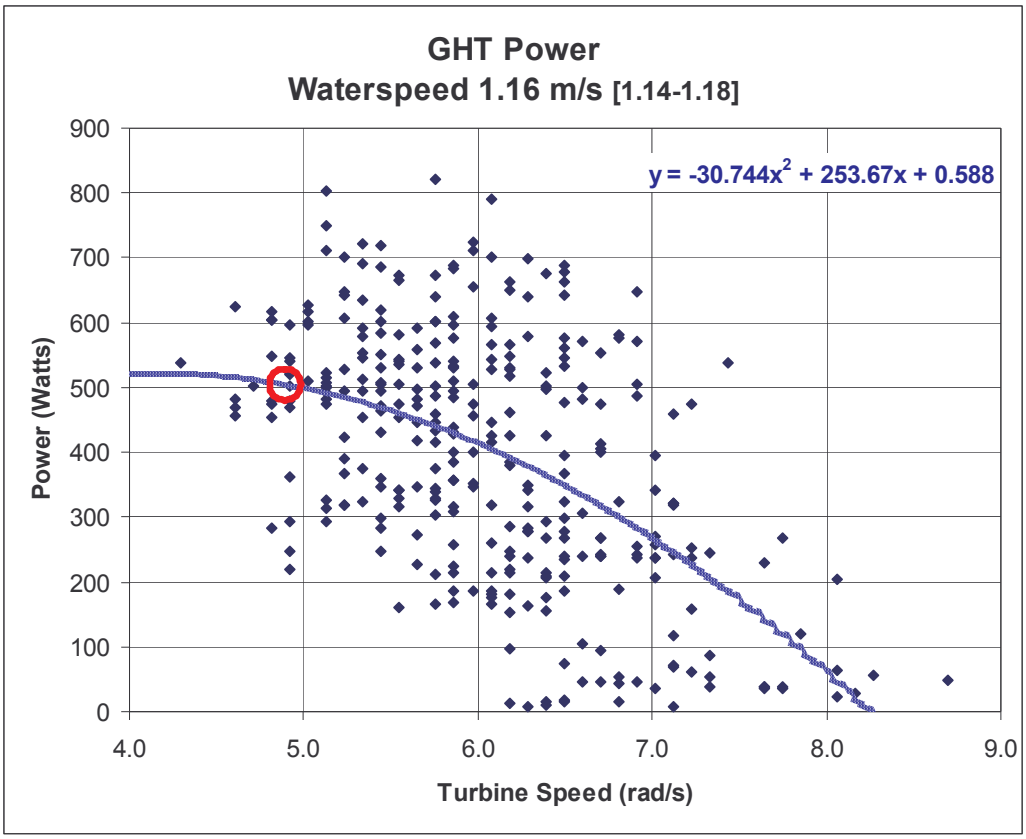
GHT Power
Waterspeed 1.16 m/s [1.14-1.18]
y = -30.744x2 + 253.67x + 0.588
Power (Watts)
Turbine Speed (rad/s)
0
100
200
300
400
500
600
700
800
900
4.0
5.0
6.0
7.0
8.0
9.0

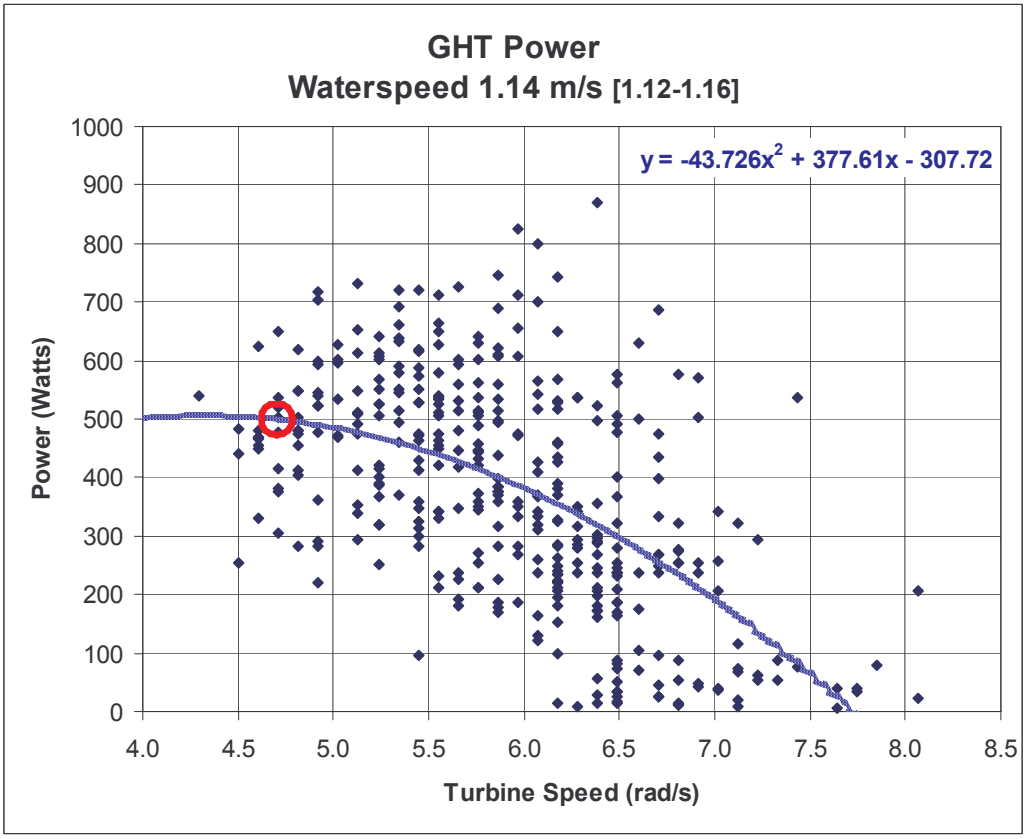
GHT Power
Waterspeed 1.14 m/s [1.12-1.16]
y = -43.726x2 + 377.61x - 307.72
Power (Watts)
Turbine Speed (rad/s)
0
100
200
300
400
500
600
700
800
900
1000
4.0
4.5
5.0
5.5
6.0
6.5
7.0
7.5
8.0
8.5

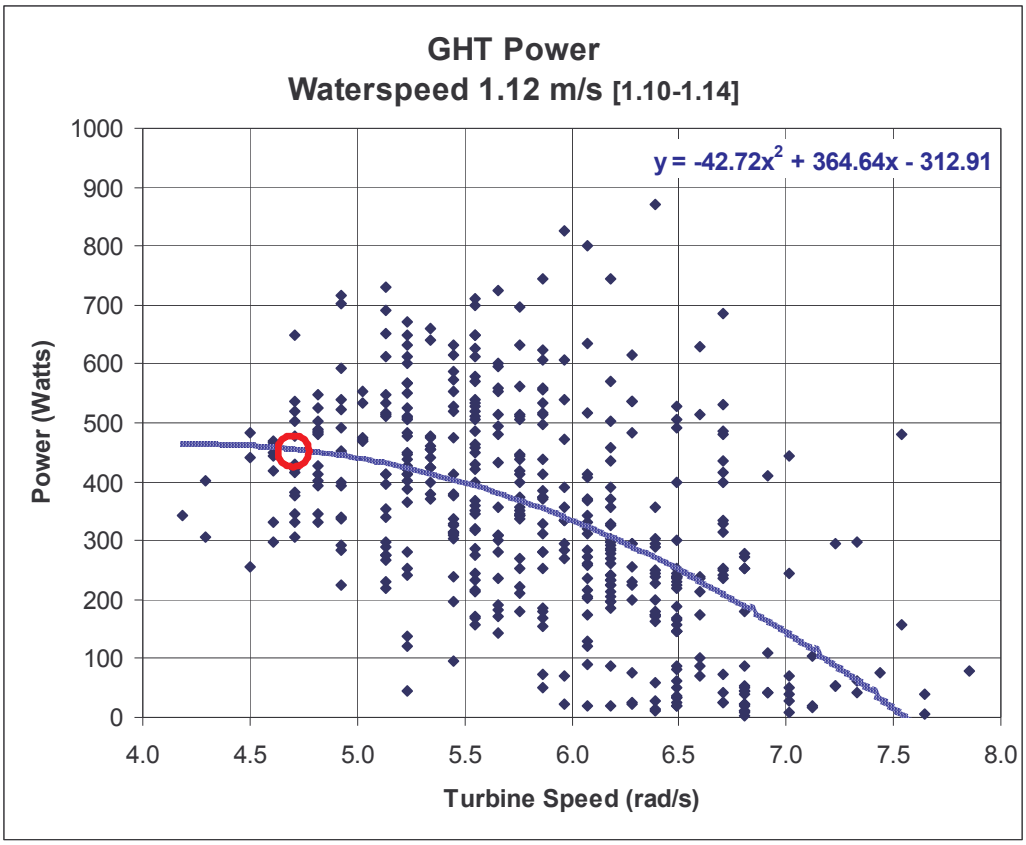
GHT Power
Waterspeed 1.12 m/s [1.10-1.14]
y = -42.72x2 + 364.64x - 312.91
Power (Watts)
Turbine Speed (rad/s)
0
100
200
300
400
500
600
700
800
900
1000
4.0
4.5
5.0
5.5
6.0
6.5
7.0
7.5
8.0

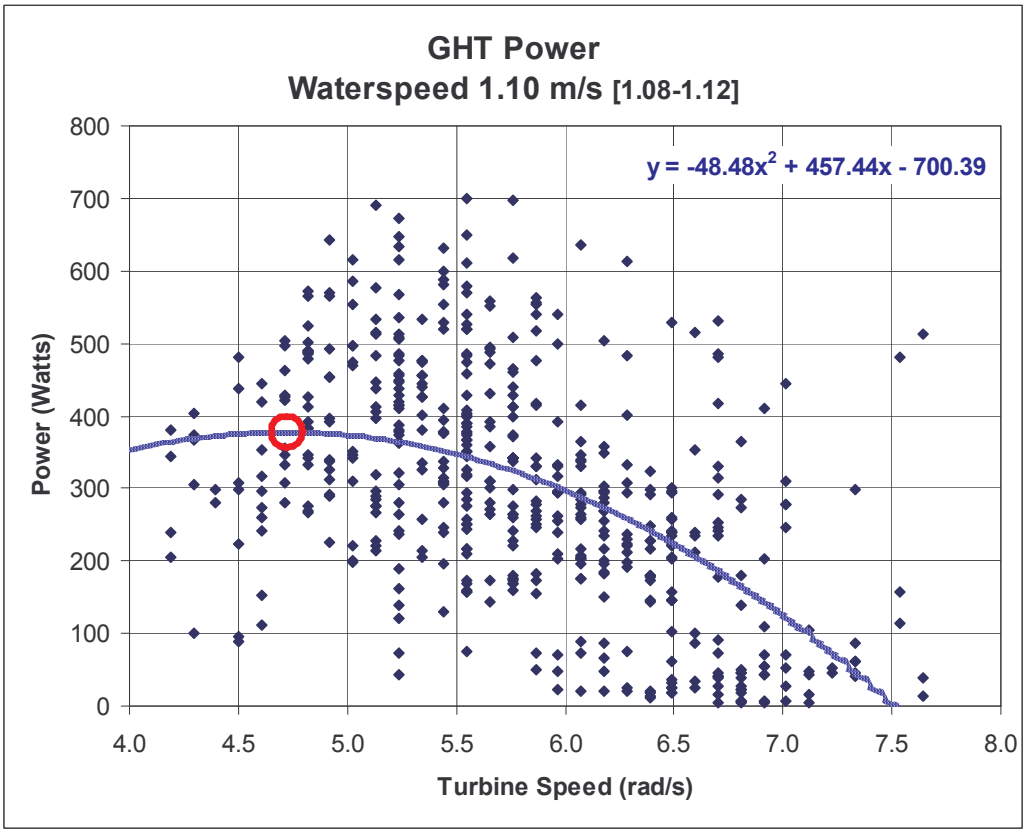
GHT Power
Waterspeed 1.10 m/s [1.08-1.12]
y = -48.48x2 + 457.44x - 700.39
Power (Watts)
Turbine Speed (rad/s)
0
100
200
300
400
500
600
700
800
4.0
4.5
5.0
5.5
6.0
6.5
7.0
7.5
8.0

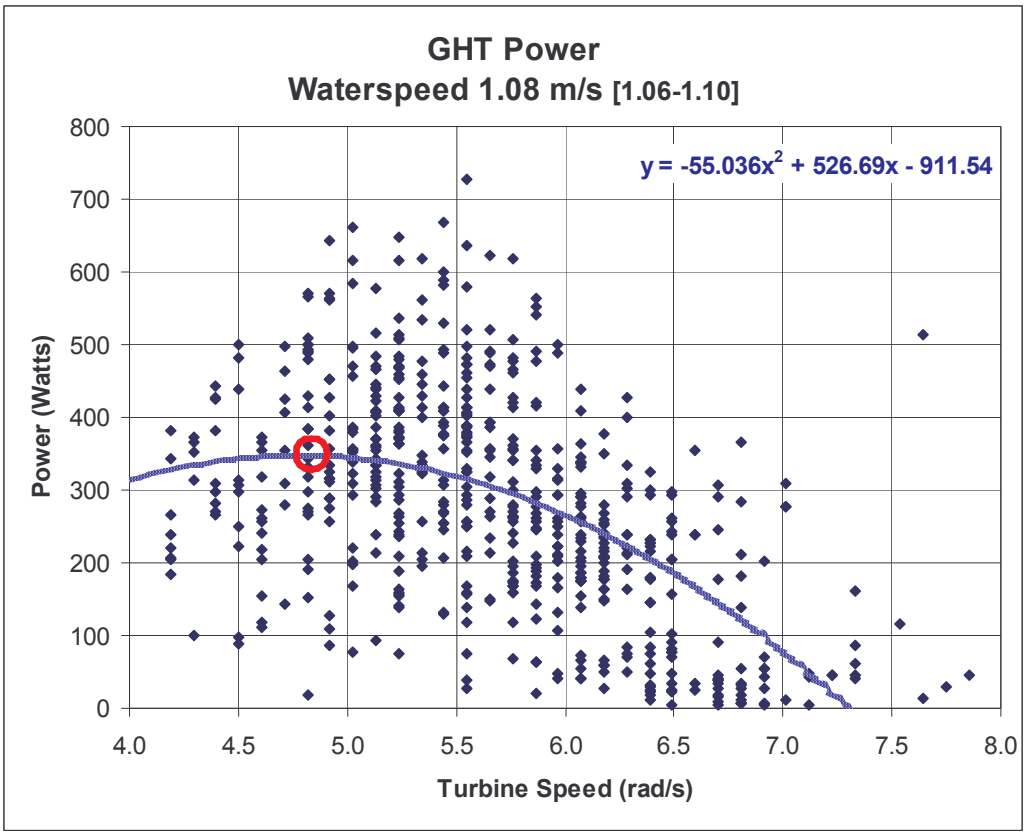
GHT Power
Waterspeed 1.08 m/s [1.06-1.10]
y = -55.036x2 + 526.69x - 911.54
Power (Watts)
Turbine Speed (rad/s)
0
100
200
300
400
500
600
700
800
4.0
4.5
5.0
5.5
6.0
6.5
7.0
7.5
8.0

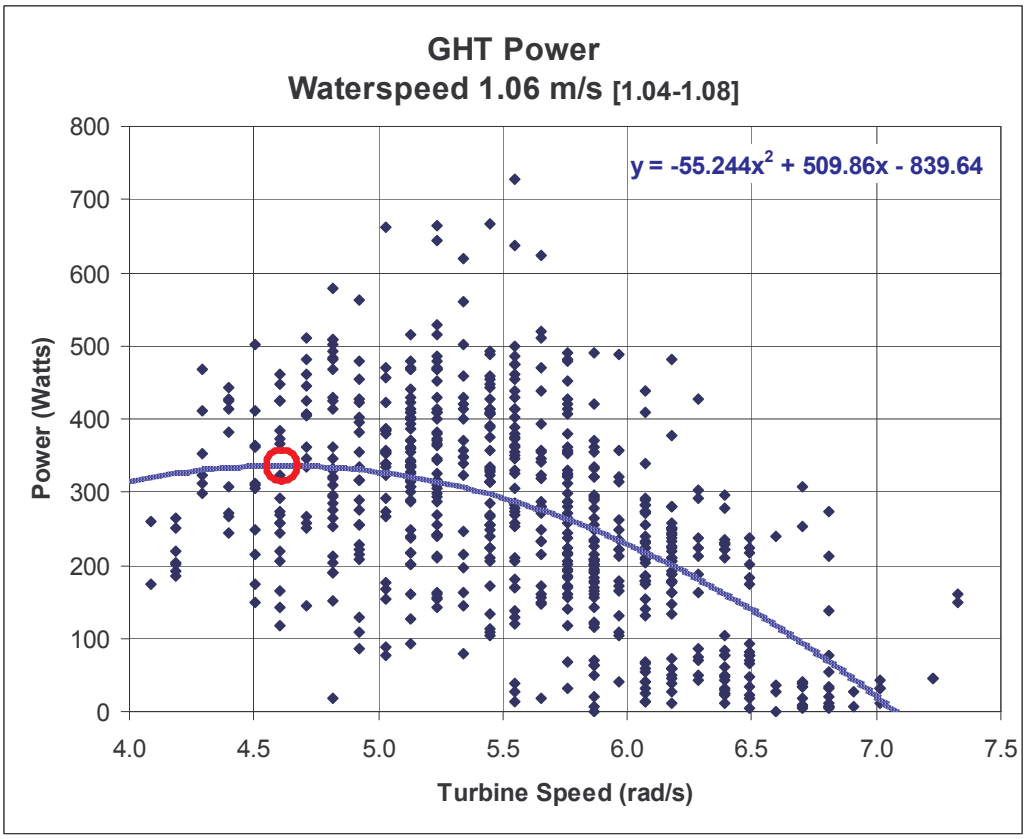
GHT Power
Waterspeed 1.06 m/s [1.04-1.08]
y = -55.244x2 + 509.86x - 839.64
Power (Watts)
Turbine Speed (rad/s)
0
100
200
300
400
500
600
700
800
4.0
4.5
5.0
5.5
6.0
6.5
7.0
7.5

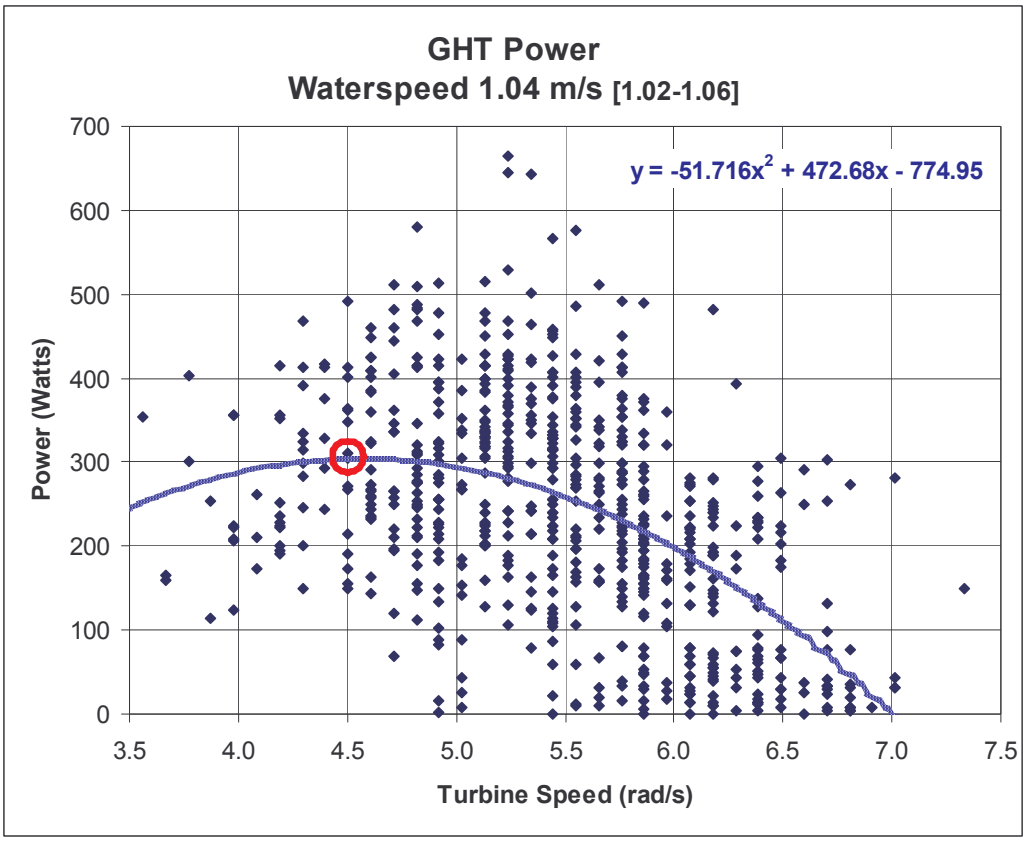
GHT Power
Waterspeed 1.04 m/s [1.02-1.06]
y = -51.716x2 + 472.68x - 774.95
Power (Watts)
Turbine Speed (rad/s)
0
100
200
300
400
500
600
700
3.5
4.0
4.5
5.0
5.5
6.0
6.5
7.0
7.5

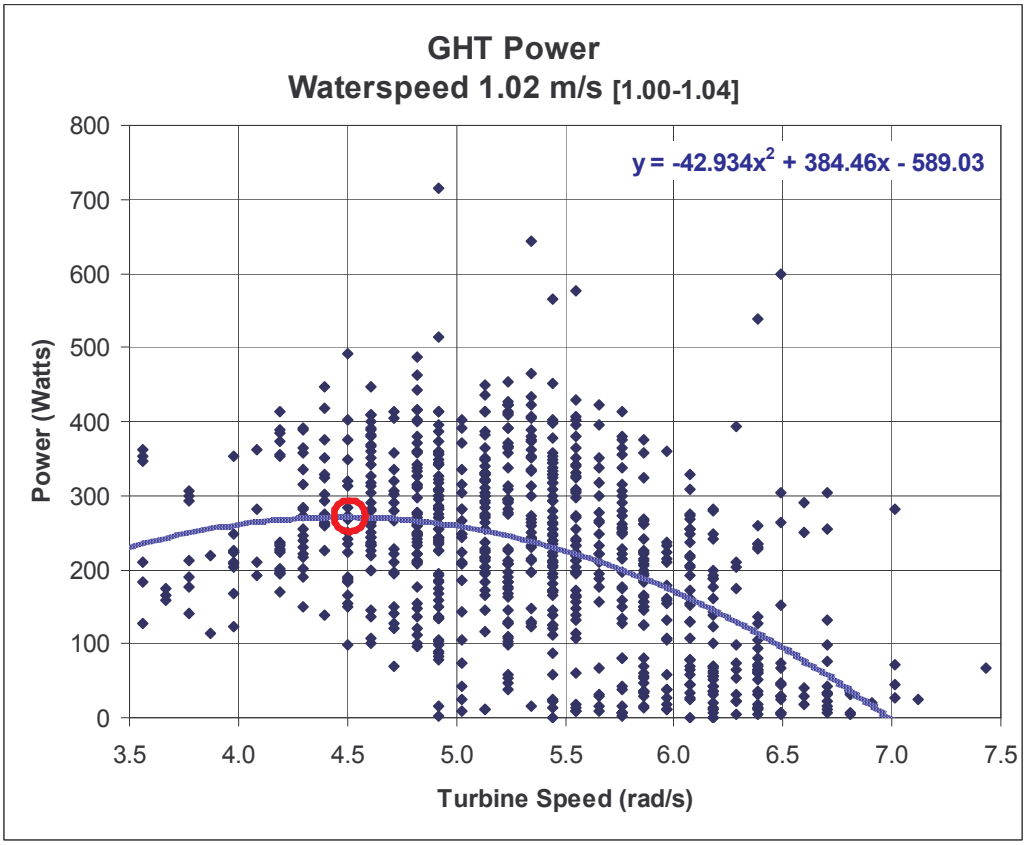
GHT Power
Waterspeed 1.02 m/s [1.00-1.04]
y = -42.934x2 + 384.46x - 589.03
Power (Watts)
Turbine Speed (rad/s)
0
100
200
300
400
500
600
700
800
3.5
4.0
4.5
5.0
5.5
6.0
6.5
7.0
7.5

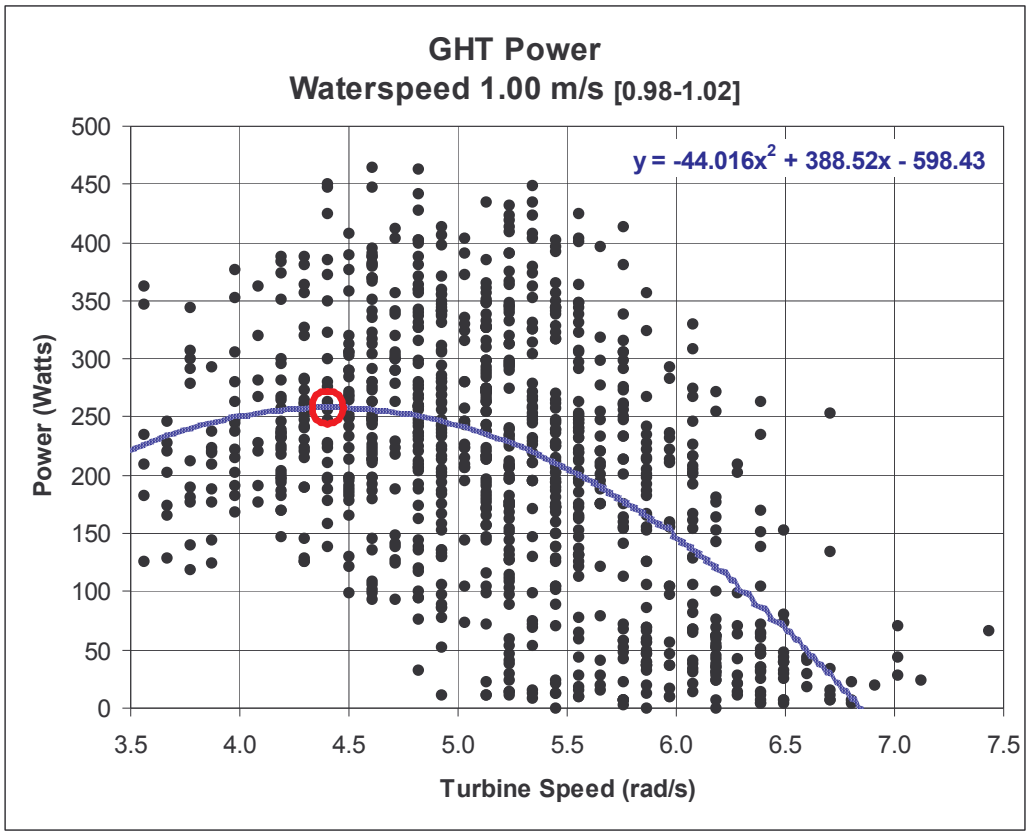
GHT Power
Waterspeed 1.00 m/s [0.98-1.02]
y = -44.016x2 + 388.52x - 598.43
Power (Watts)
Turbine Speed (rad/s)
0
50
100
150
200
250
300
350
400
450
500
3.5
4.0
4.5
5.0
5.5
6.0
6.5
7.0
7.5

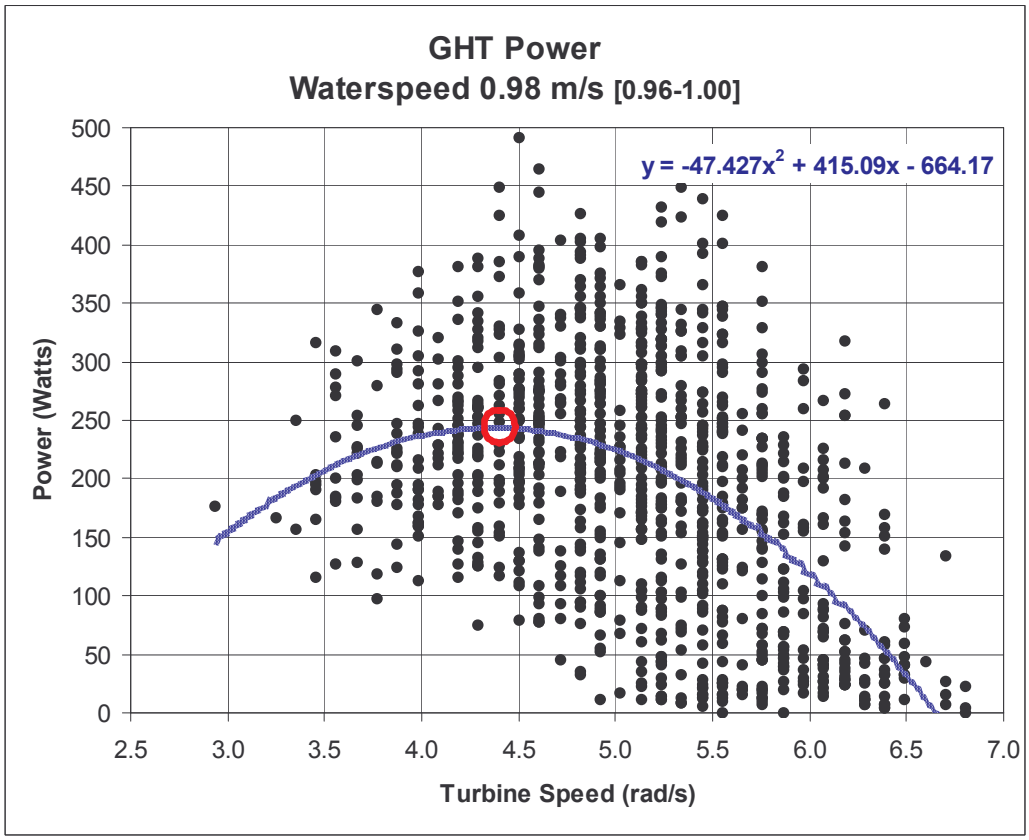
GHT Power
Waterspeed 0.98 m/s [0.96-1.00]
y = -47.427x2 + 415.09x - 664.17
Power (Watts)
Turbine Speed (rad/s)
0
50
100
150
200
250
300
350
400
450
500
2.5
3.0
3.5
4.0
4.5
5.0
5.5
6.0
6.5
7.0

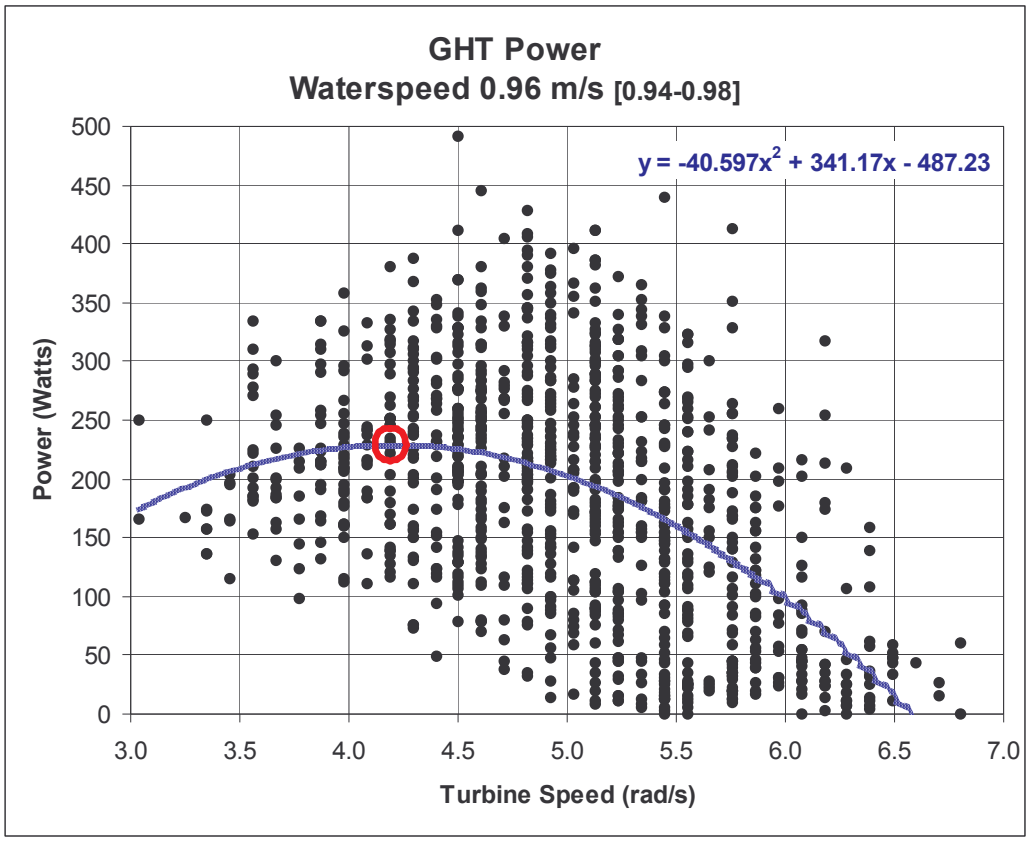
GHT Power
Waterspeed 0.96 m/s [0.94-0.98]
y = -40.597x2 + 341.17x - 487.23
Power (Watts)
Turbine Speed (rad/s)
0
50
100
150
200
250
300
350
400
450
500
3.0
3.5
4.0
4.5
5.0
5.5
6.0
6.5
7.0

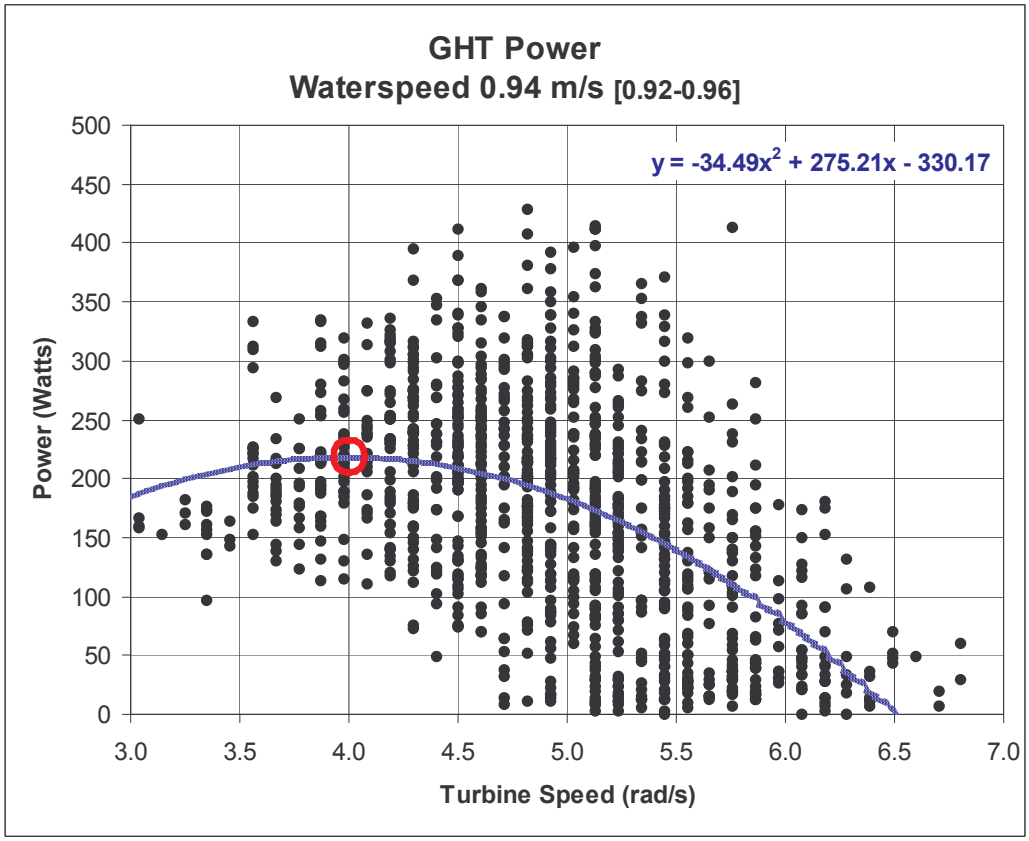
GHT Power
Waterspeed 0.94 m/s [0.92-0.96]
y = -34.49x2 + 275.21x - 330.17
Power (Watts)
Turbine Speed (rad/s)
0
50
100
150
200
250
300
350
400
450
500
3.0
3.5
4.0
4.5
5.0
5.5
6.0
6.5
7.0

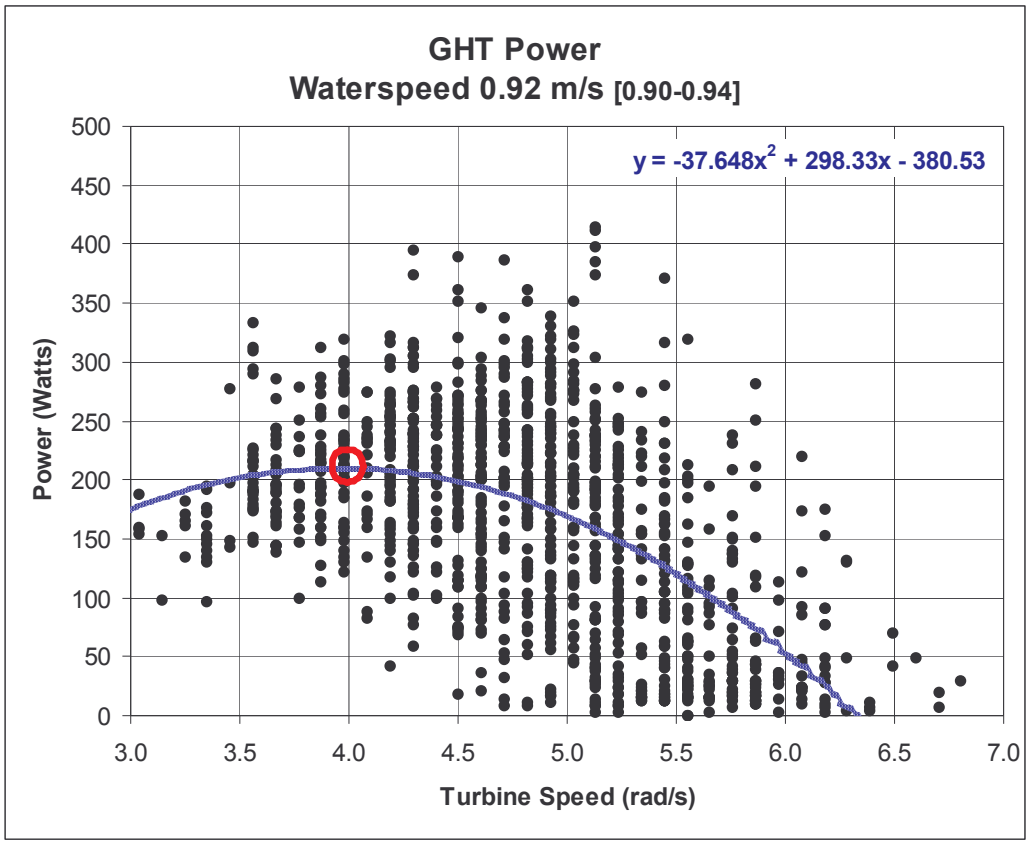
GHT Power
Waterspeed 0.92 m/s [0.90-0.94]
y = -37.648x2 + 298.33x - 380.53
Power (Watts)
Turbine Speed (rad/s)
0
50
100
150
200
250
300
350
400
450
500
3.0
3.5
4.0
4.5
5.0
5.5
6.0
6.5
7.0

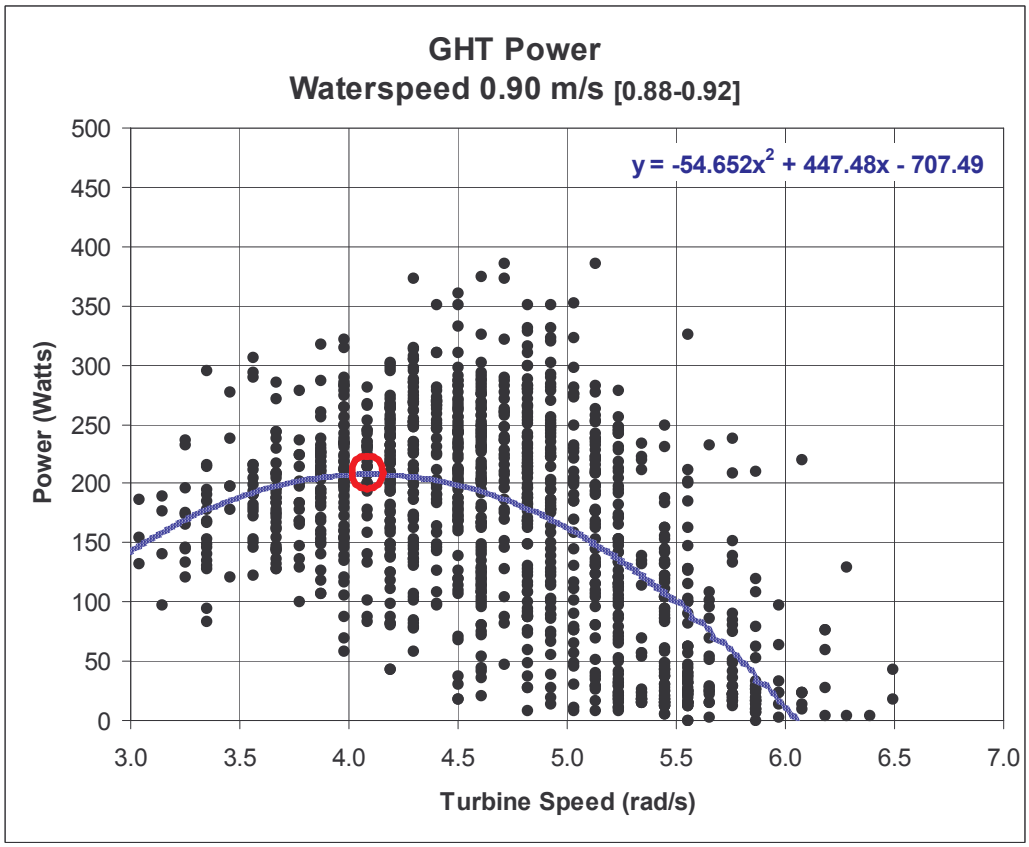
GHT Power
Waterspeed 0.90 m/s [0.88-0.92]
y = -54.652x2 + 447.48x - 707.49
Power (Watts)
Turbine Speed (rad/s)
0
50
100
150
200
250
300
350
400
450
500
3.0
3.5
4.0
4.5
5.0
5.5
6.0
6.5
7.0

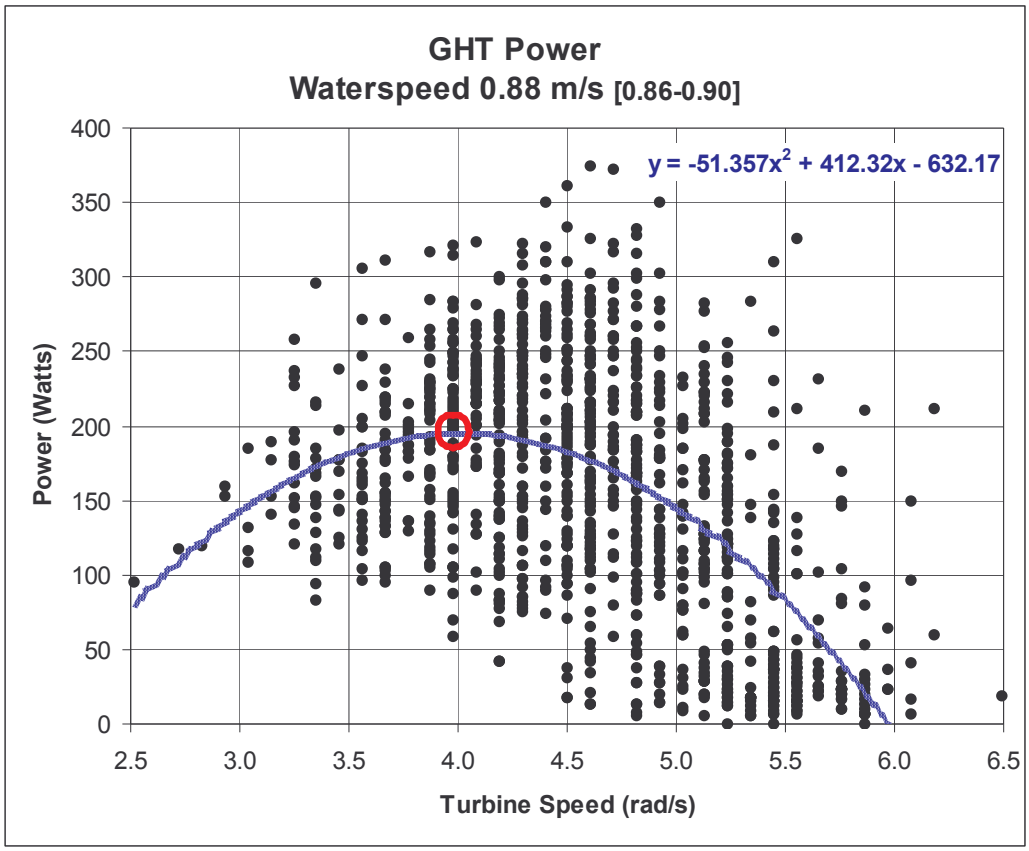
GHT Power
Waterspeed 0.88 m/s [0.86-0.90]
y = -51.357x2 + 412.32x - 632.17
Power (Watts)
Turbine Speed (rad/s)
0
50
100
150
200
250
300
350
400
2.5
3.0
3.5
4.0
4.5
5.0
5.5
6.0
6.5

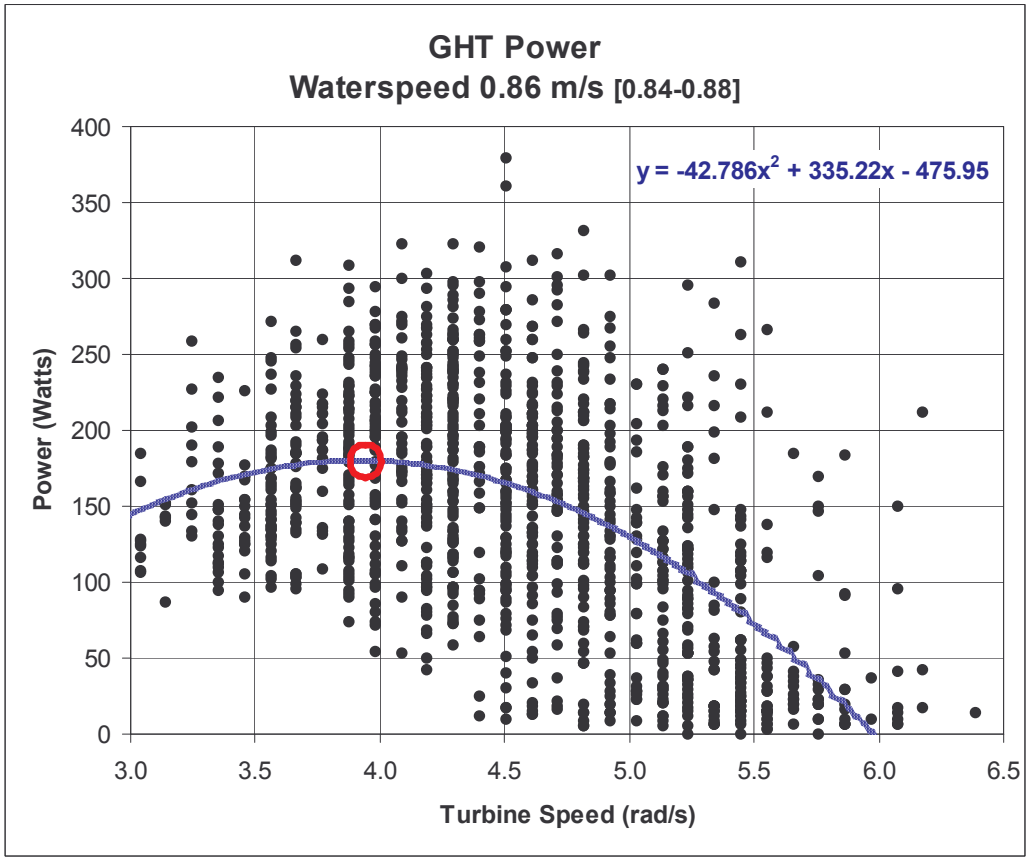
GHT Power
Waterspeed 0.86 m/s [0.84-0.88]
y = -42.786x2 + 335.22x - 475.95
Power (Watts)
Turbine Speed (rad/s)
0
50
100
150
200
250
300
350
400
3.0
3.5
4.0
4.5
5.0
5.5
6.0
6.5

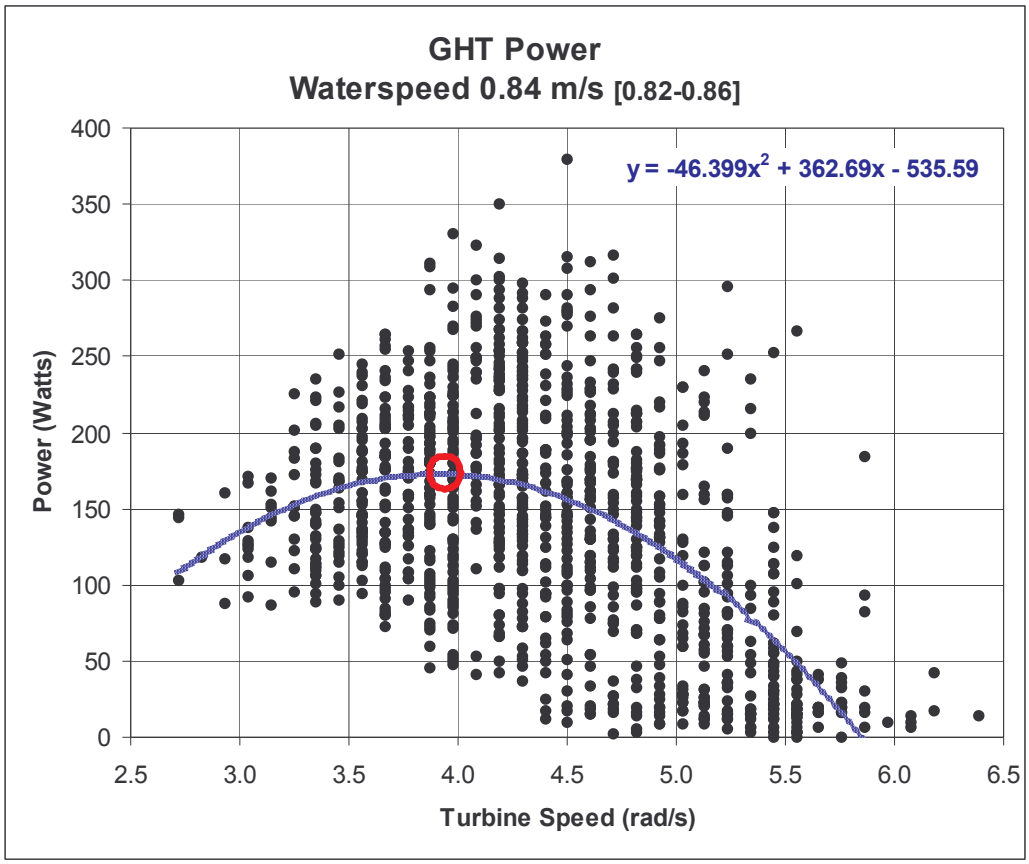
GHT Power
Waterspeed 0.84 m/s [0.82-0.86]
y = -46.399x2 + 362.69x - 535.59
Power (Watts)
Turbine Speed (rad/s)
0
50
100
150
200
250
300
350
400
2.5
3.0
3.5
4.0
4.5
5.0
5.5
6.0
6.5

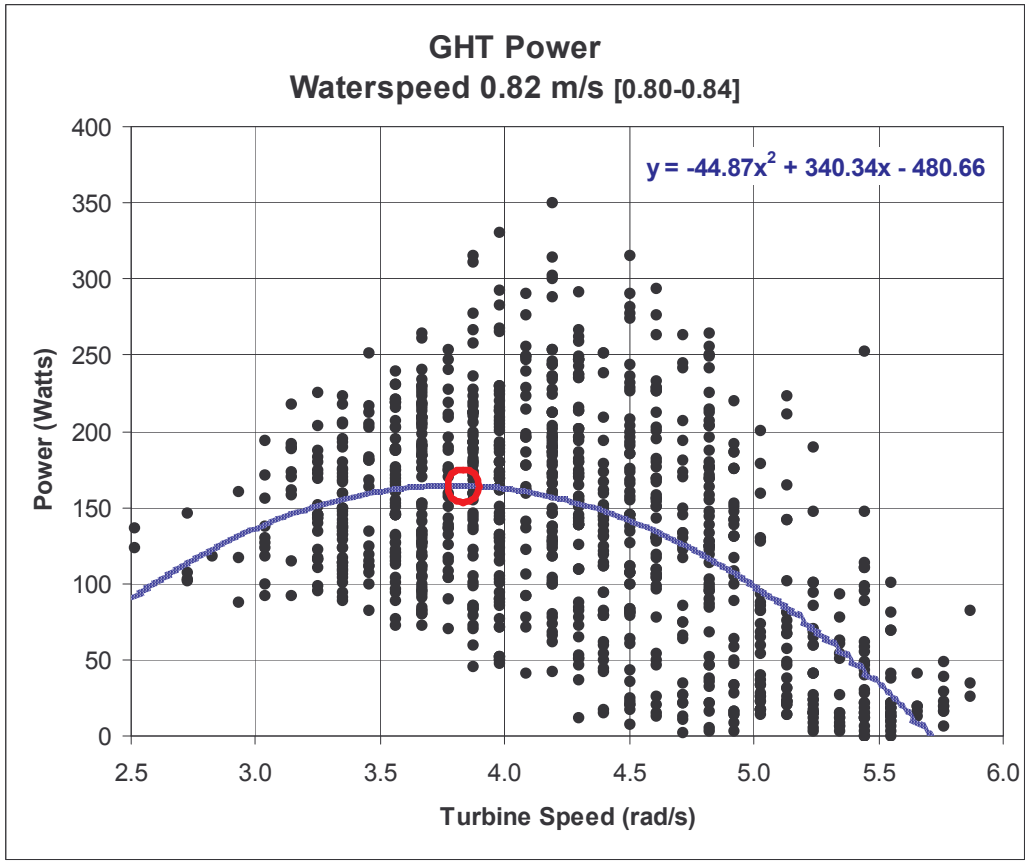
GHT Power
Waterspeed 0.82 m/s [0.80-0.84]
y = -44.87x2 + 340.34x - 480.66
Power (Watts)
Turbine Speed (rad/s)
0
50
100
150
200
250
300
350
400
2.5
3.0
3.5
4.0
4.5
5.0
5.5
6.0

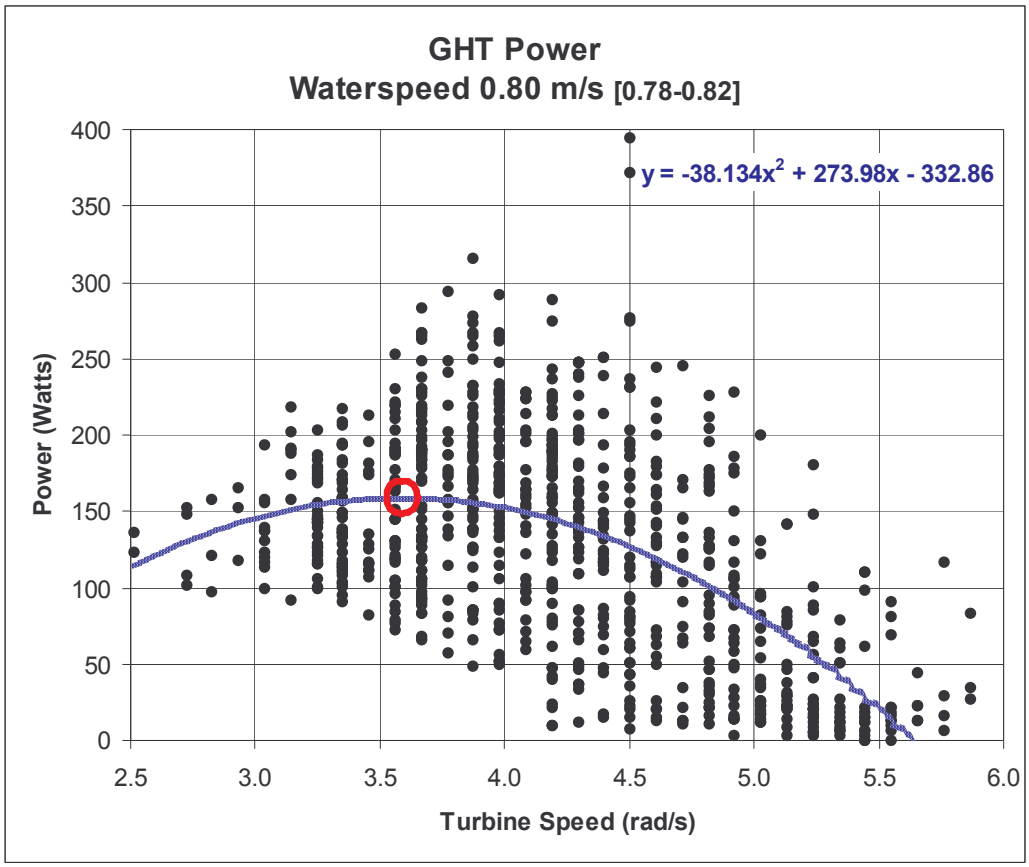
GHT Power
Waterspeed 0.80 m/s [0.78-0.82]
y = -38.134x2 + 273.98x - 332.86
Power (Watts)
Turbine Speed (rad/s)
0
50
100
150
200
250
300
350
400
2.5
3.0
3.5
4.0
4.5
5.0
5.5
6.0

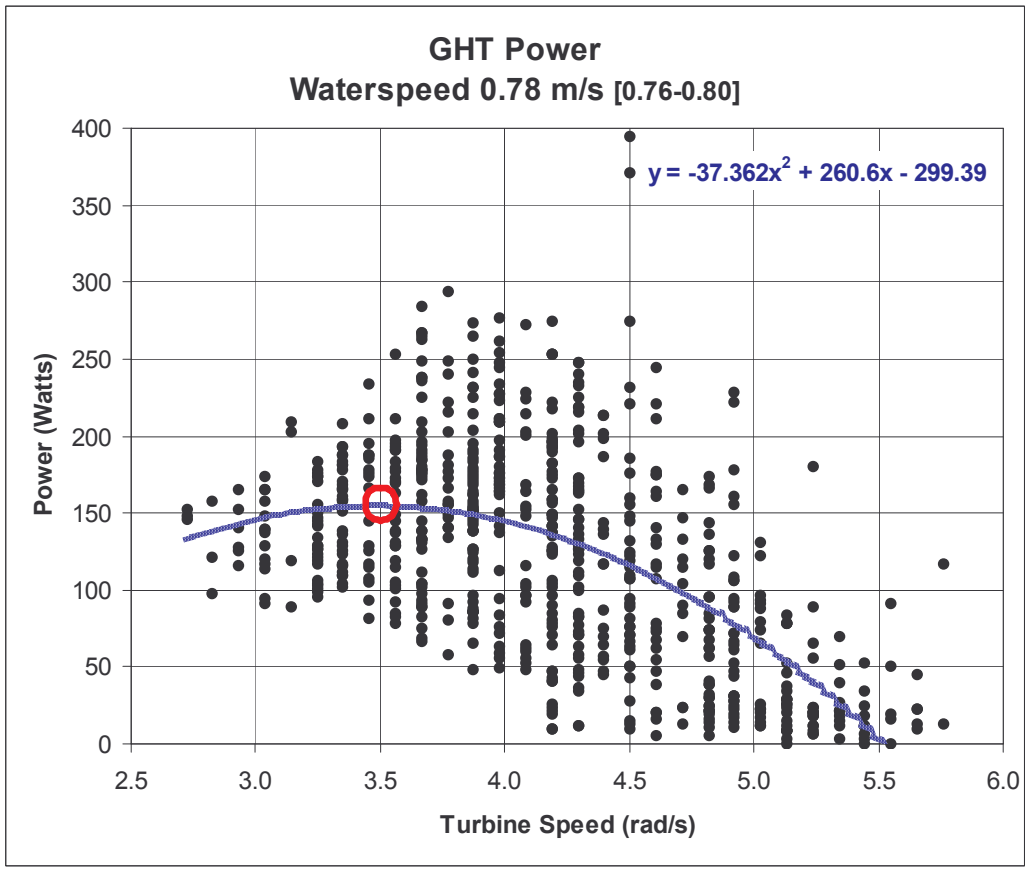
GHT Power
Waterspeed 0.78 m/s [0.76-0.80]
y = -37.362x2 + 260.6x - 299.39
Power (Watts)
Turbine Speed (rad/s)
0
50
100
150
200
250
300
350
400
2.5
3.0
3.5
4.0
4.5
5.0
5.5
6.0

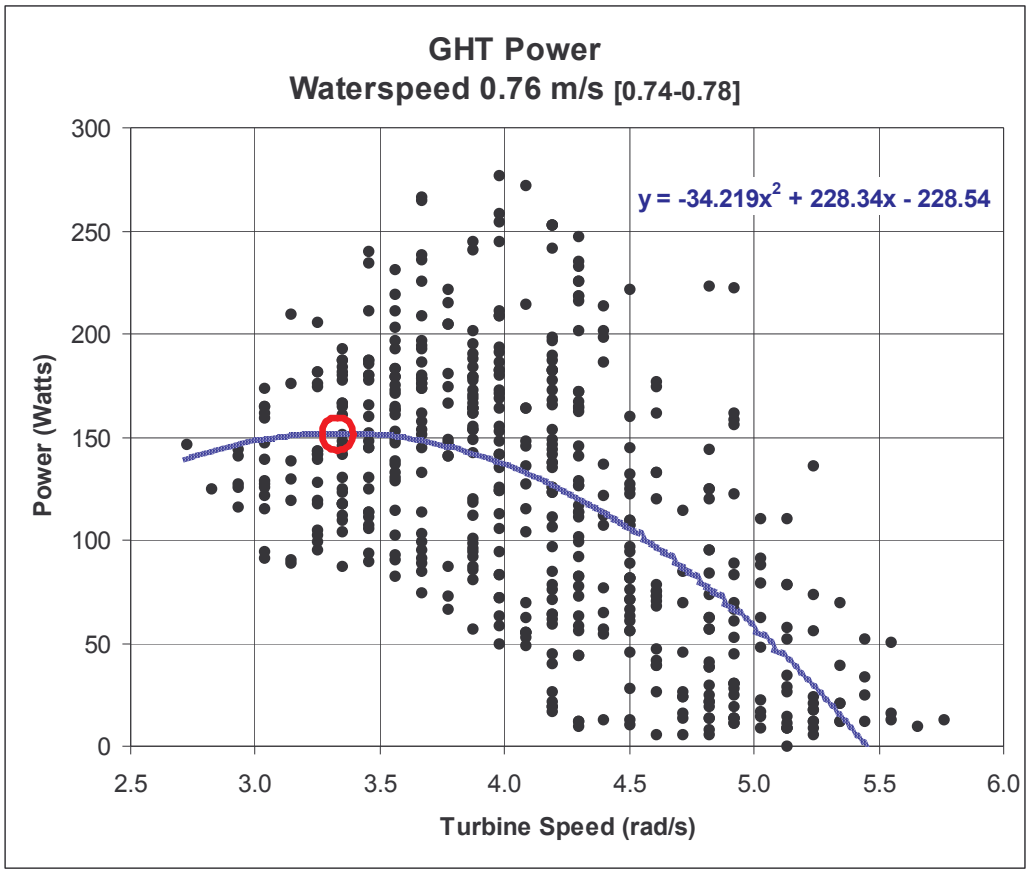
GHT Power
Waterspeed 0.76 m/s [0.74-0.78]
y = -34.219x2 + 228.34x - 228.54
Power (Watts)
Turbine Speed (rad/s)
0
50
100
150
200
250
300
2.5
3.0
3.5
4.0
4.5
5.0
5.5
6.0

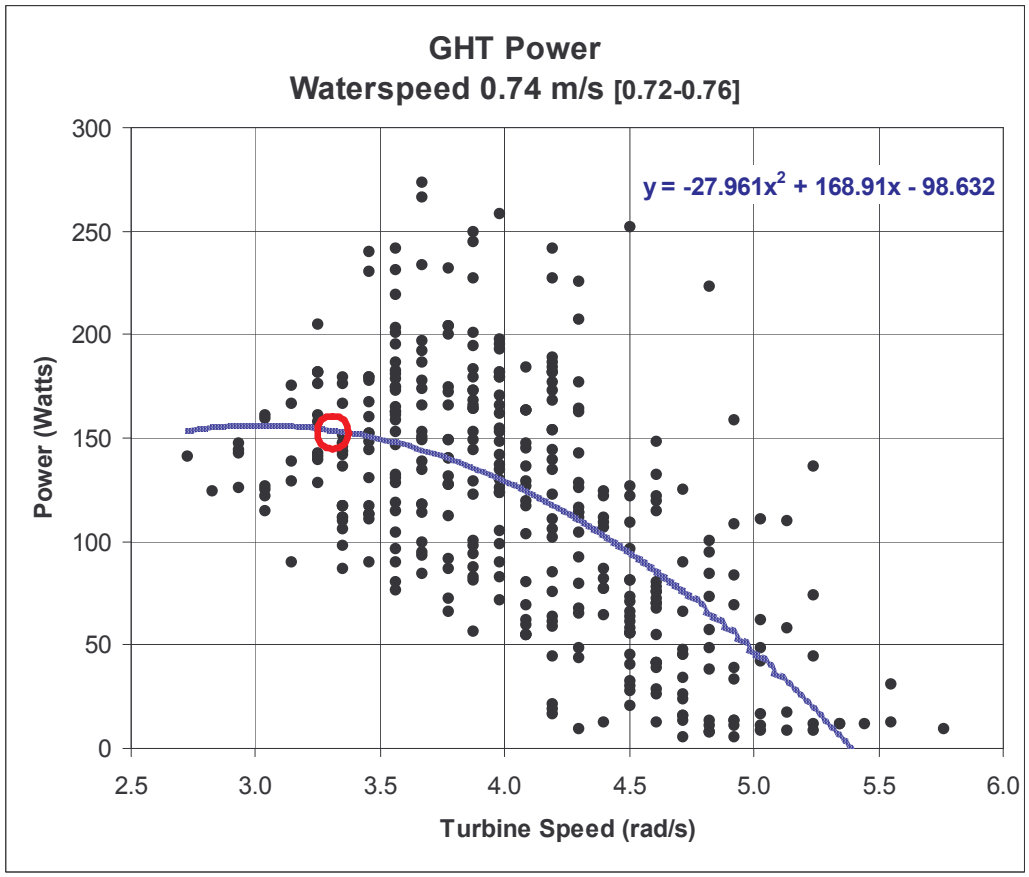
GHT Power
Waterspeed 0.74 m/s [0.72-0.76]
y = -27.961x2 + 168.91x - 98.632
Power (Watts)
Turbine Speed (rad/s)
0
50
100
150
200
250
300
2.5
3.0
3.5
4.0
4.5
5.0
5.5
6.0

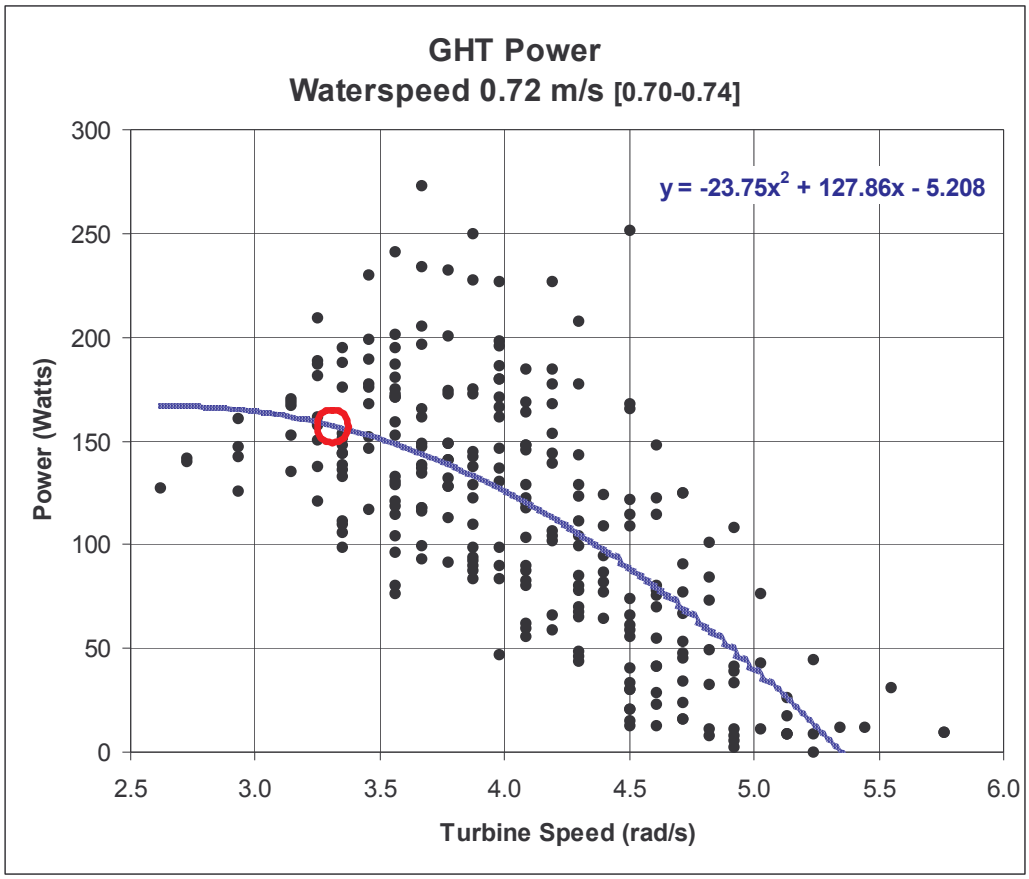
GHT Power
Waterspeed 0.72 m/s [0.70-0.74]
y = -23.75x2 + 127.86x - 5.208
Power (Watts)
Turbine Speed (rad/s)
300
250
200
150
100
50
0
2.5
3.0
3.5
4.0
4.5
5.0
5.5
6.0

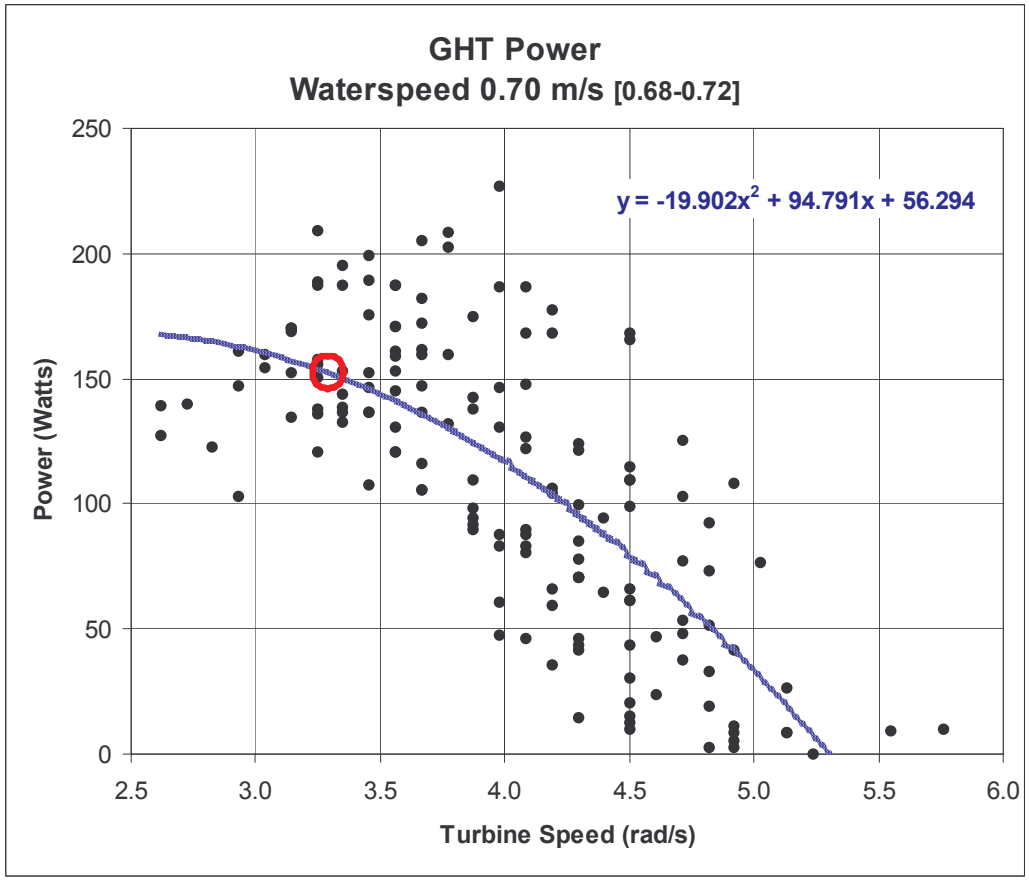
GHT Power
Waterspeed 0.70 m/s [0.68-0.72]
y = -19.902x2 + 94.791x + 56.294
Power (Watts)
Turbine Speed (rad/s)
250
200
150
100
50
0
2.5
3.0
3.5
4.0
4.5
5.0
5.5
6.0

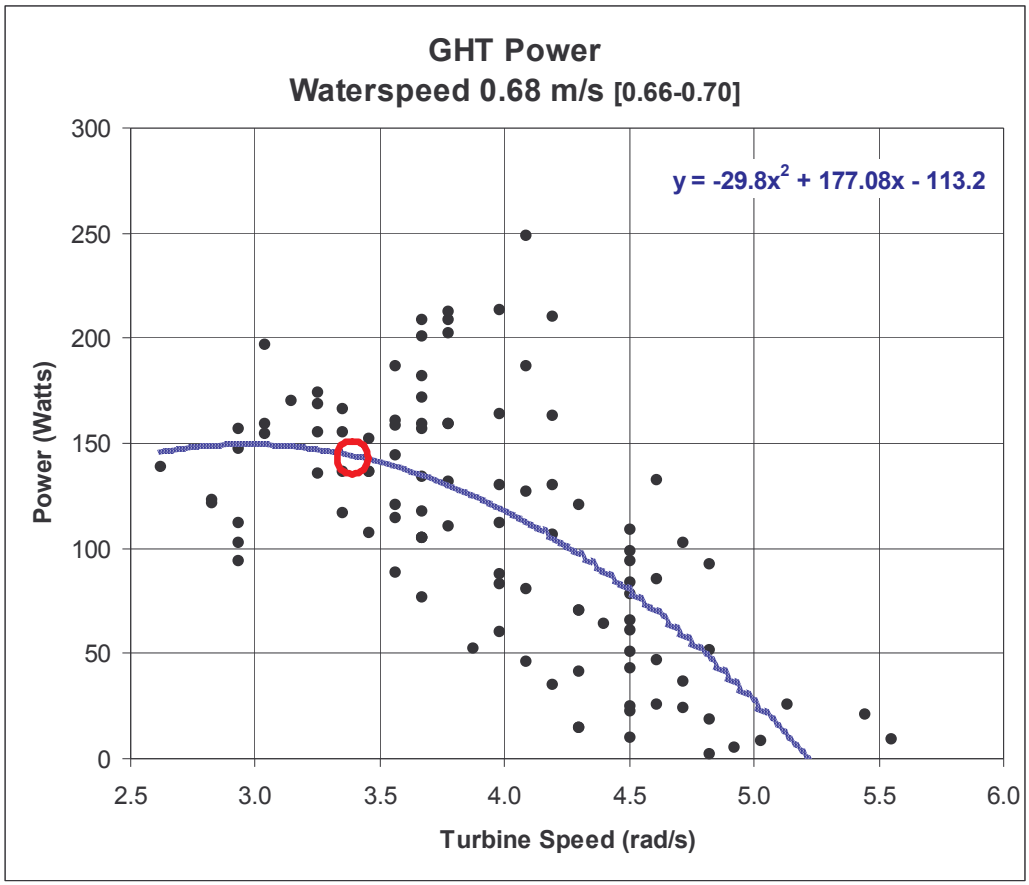
GHT Power
Waterspeed 0.68 m/s [0.66-0.70]
y = -29.8x2 + 177.08x - 113.2
Power (Watts)
Turbine Speed (rad/s)
0
50
100
150
200
250
300
2.5
3.0
3.5
4.0
4.5
5.0
5.5
6.0

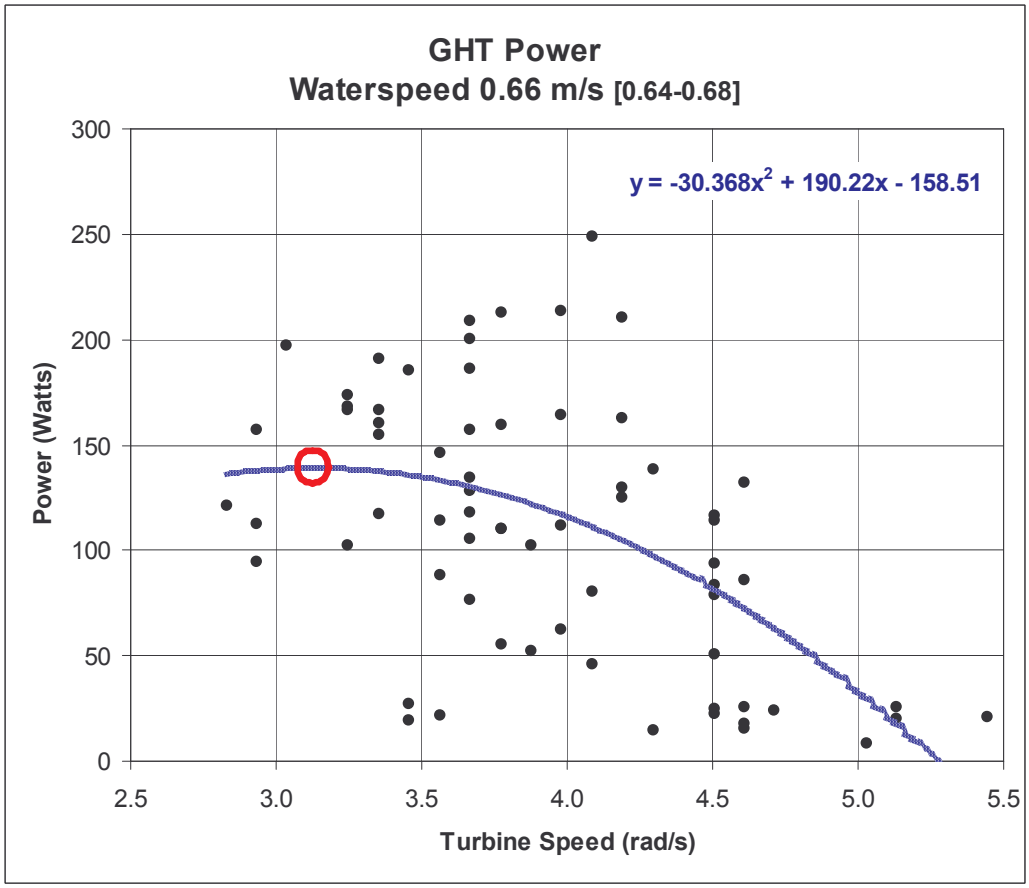
GHT Power
Waterspeed 0.66 m/s [0.64-0.68]
y = -30.368x2 + 190.22x - 158.51
Power (Watts)
Turbine Speed (rad/s)
0
50
100
150
200
250
300
2.5
3.0
3.5
4.0
4.5
5.0
5.5

G. ATEP 500kW Field Example Calculations

APPENDIX G

500 kW Field Examples Calculation Table *Confidential*

Rev. 4/11/05 by J. Gerlaugh

NOTES:
The table below provides four scenarios for 500kW total capacity turbine fields using 1m dia. x 2.5m long GHTs.

These scenarios presuppose a number of basic assumptions as follows:

- The four fields represent four different water velocities that might be found in Massachusetts.
- The greatest water velocity used was 2.5 m/s which is the max water current for the Cape Cod Canal, and the fastest known velocity in the State
- The calculations use a GHT efficiency of 24% which is based on the results of the ATEP tests.
- Efficiencies used for other system components are typical industry values.
- The water velocity changes the number of turbines required to make a 500 kW field. The size of the field changes to accommodate the number of turbines.
- Rough field dimensions have been shown to provide an indication of the field's size.
- To determine the field length, all scenarios assume the same river/field usable width of 15.2 m. This is believed a plausible value for Massachusetts' rivers.
- The rivers/fields all have a usable depth greater than or equal to 2.0 m., the minimum for 1 m diameter GHT deployed horizontally.

Sample Field Calculation Table

Turbine & Field Technical Specifications

Site Name	***Generic Non-Tidal River Site***
Site Location	
Turbine Technology Name	***GHT***
Turbine Technology Company	***GCK & Verdant Power***
Customer	

Note: Calculations assume horizontal axis mounting

System Specifications	Symbol	Equations	Values at specified water velocities 2.5 m/s	1.3 m/s	Units	Notes
Turbine Diameter	*Dturb*		3.28	3.28	ft	3.28 ft = 1.0 m
Turbine Width (Axle Length)	*Wturb*		8.20	8.20	ft	8.20 ft = 2.5 m
Area of Turbine Propeller	*Aturb*	*Dturb x Wturb*	26.9	26.9	ft^2	
Total Package Width	*Wpak*		10.2	10.2	ft	
Lateral Clearance (min) to Adjacent Rotor	*Dpaklat*	*1/4 x Dturb*	0.82	0.82	ft	
Power Recovery Distance	*Xrecovery*	*10 x Dturb*	32.8	32.8	ft	
Screen Efficiency (if present)	*escreen*		100%	100%	%	use 100% for no screen
Turbine Efficiency	*eturb*		24%	24%	%	
Gear & Bearing Efficiency	*egears*		93%	93%	%	
Generator Efficiency	*egen*		92%	92%	%	

Interconnection Efficiency	*econnect*		99%	99%	%	
Power Conditioning Efficiency	*epc*		92%	92%	%	
Total Efficiency	*etotal*		19%	19%	%	

Field Specifications	**Symbol**		**Value**	**Value**	**Units**	**Notes**
Total Length	*Xfield*		1230	8700	ft	
Average Width	*Yfield*		50	50	ft	
Number of Rows	*Nrows*		34	241	#	
Average Number. of Turbines per Row	*Nturbs_row*		4	4	#	
Total Turbines in Field	*Nturbs_fld*		136	964	#	

Water Current Statistics	**Symbol**		**Value**	**Value**	**Units**	**Notes**
Average Peak Velocity	*Vavgpk*		2.50	1.30	m/s	
Tidal Power De-rating	*etide*		100.0%	100.0%	%	42.4% for pure sine wave, 100% for non-tidal river

Power Per Turb Calculations	**Symbol**		**Value**	**Value**	**Units**	**Notes**
Kinetic Power in Water per Aturb @ Vavgpeak constant flow	*Pwater_pk*	*(1/2)rApropVavgpk3*	19.7	2.8	kW	Raw River Power
Grid Ready Power @ Vavgpeak	*Pout_pk*		3.7	0.5	kW	includes power conditioning & interconnect losses
Grid Ready Energy per Year	*Eyr_tidal*		32.3	4.5	MWHrs	

Power Per Field Calculations	**Symbol**		**Value**	**Value**	**Units**	**Notes**
Grid Ready Electric Power @ Vavgpeak	*Pgrid_pk_fld*		502	501	KW	
Grid Ready Energy for Tidal per Year per field	*Eyr_tidal_fld*		4,397	4,384	MWHrs	

APPENDIX H

ATEP FISH MONITORING EQUIPMENT AND PROCEDURES

GOAL

To determine the turbines' effects on Merrimack River marine life.

STRATEGY

BioSonics, a leading fish monitoring firm, was hired to:

- Design the monitoring procedure and physical system
- Supply and install the fish monitoring equipment

EQUIPMENT:

- Commercial 5 beam fish finder for general fish observations
- BioSonics DT6000 split-beam 200 kHz echo sounder attached to a 6-degree transducer attached at the stern of the barge. The transducer is aimed vertically to measure the vertical distribution of fish targets
- BioSonics DT-X scientific echo sounder interrogating three 420 kHz split-beam transducers. The transducers are mounted on poles and aimed horizontally at a depth corresponding to the center of the vertical helix rotor.
- Split-beam technology allows direct measurement of the fish Target Strength (acoustic size), as well as providing the ability to track a target through the sample volume and estimate direction of travel and target velocity.
- A underwater video camera will view the field near the center of the tested turbine to monitor for fish passing through the turbine.

Output

- BioSonics transducer signals are processed in realtime by Biosonics "Visual Acquisition" software.
- Fish and other debris in the water is shown on the Graphical User Interface (GUI) as colored lines. The GUI is observed by an operator any time the turbine is being run.
- The color of the line indicates the echo's intensity and is related to the size of the fish
- The direction of the line indicate the direction of travel of the fish
- The underwater camera image is shown on a TV monitor in the Control Room. The monitor is observed by an operator any time the turbine is being run.

Acoustic Equipment Description

The DT and DT-X scientific echo sounders by BioSonics are some of the most advanced and sophisticated underwater measurements currently available. These systems transmit through focused beams characterized by very low side-lobes. The acoustic echoes are digitized inside the transducer to eliminate the reception of external electrical interference. The digital design

provides for very high dynamic range, meaning that the system can simultaneously measure signals from very large targets and very small targets without saturation or loss of small signals. The calculation of target range is very precise; using the latest published sound velocity equations. The system is adapted to the local conditions by operator entry of water salinity and temperature.

The split-beam technique is implemented into the DT and DT-X systems. The split-beam technique allows the measurement of the angular position of each single fish target inside the acoustic sample volume. Split-beam technology allows direct measurement of the fish Target Strength (acoustic size), as well as providing the ability to track a target through the sample volume and estimate direction of travel and target velocity.

Each split-beam transducer has an intrinsic coordinate system. When viewed from behind or above the transducer, "+Y" is opposite the direction of the transducer connector, and "+X" is 90 degrees clockwise from +Y. This concept is shown in Figure 1.

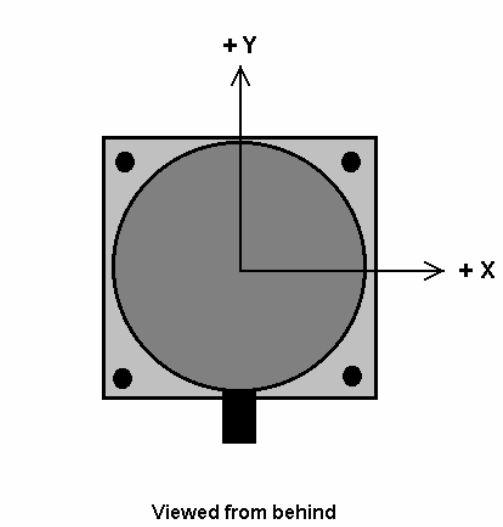

Figure 1. Split-beam Coordinate System

Calibration of Acoustic System

Calibration of acoustic systems used for quantitative measurement focuses on the acoustic performance parameters. Source Level is the amount of sound intensity projected into the water, and Receive Sensitivity is the efficiency of the transducer receiver in converting the returning echo sound pressure into volts. Both of these parameters are carefully measured during calibration of the system, and values are stored into memory chips located inside each transducer. Each cable and transducer was calibrated together. All calibrations are based on standard acoustic hydrophones supplied by the U.S. Navy, and follow rigorous procedures documented and supported by the scientific community.

Additional calibration issues have been introduced by project reviewers, specifically the accuracy of the system in measuring range or distance. The measurement of distance is totally dependent upon the measurement of sound velocity, which is used to convert between time and

distance measurements. Modern digital echo sounders such as the BioSonics DT-X measure time at micro-second levels. Velocity of sound varies with water temperature and salinity, and these values are input by the operator. The DT-X echo sounder automatically calculates sound velocity using a modern peer-reviewed and published equation. It then automatically uses this sound velocity calculation to convert all time measurements to range or distance.

Hydrometer readings at the ATEP barge confirm that salinity differs marginally from that of fresh water. To provide a verification of the measurement capability, we measured the distance from the transducer face to the edge of the rotor blade at 280 inches. We then observed the range on Transducer #1 to the rotor, as shown on the echogram. The "acoustic distance" to the rotor target was 7.1 m.

Distance measurement can be confused if water stratification is present and ray-bending occurs. The dynamic nature of the flow, as demonstrated by the upwelling boils and swells, strongly suggests that no significant stratification can form in the test area.

Acoustic Equipment Installation

A variety of acoustic systems can be found on the barge. A fish finder is mounted near the stern of the barge: its display is mounted in the wheelhouse. A BioSonics DT6000 split-beam 200 kHz echo sounder is attached to a 6-degree transducer attached at the stern of the barge. The transducer is aimed vertically, and the data from this echo sounder provide a measure of the vertical distribution of fish targets at the stern of the barge. A BioSonics DT-X scientific echo sounder is also installed, interrogating three 420 kHz split-beam transducers. The transducers are mounted on poles and aimed horizontally at a depth corresponding to the center of the vertical helix rotor. The plan view in Figure 2 indicates the orientation of the acoustic beams.

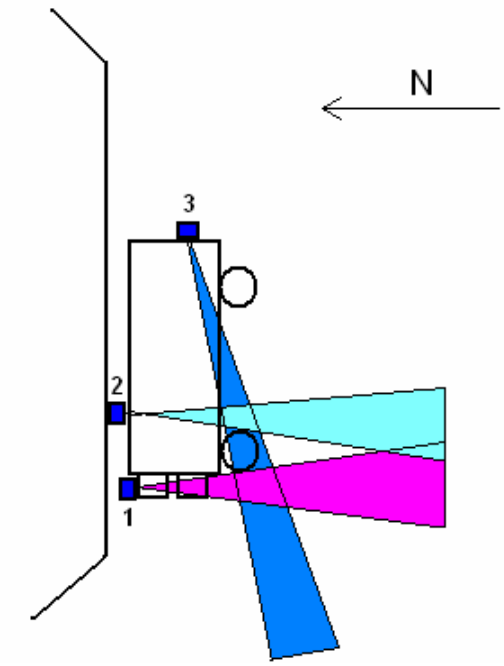

Figure 2. Aiming Directions of Horizontally-Oriented Transducers

Data Collection using DTX system

Acoustic data were collected to 30 minute files on the computer hard drive. File names were coded with time and date to indicate when they were collected. Miscellaneous environmental and engineering observations were typed into a log file resident in the background of the PC display. Additionally, a high-resolution color echogram was displayed in real-time. This display was observed by project personnel, and comments and observations were typed into the log file. The echo sounder transmitted a pulse duration of 0.4 ms at a pulse repetition rate of 5 pings per second per each of the three transducers. All acoustic signals greater than –56 dB were written to file.

Visual Monitoring Interpretation Protocols: Procedures for visually detecting and counting fish with the BioSonics DTX system

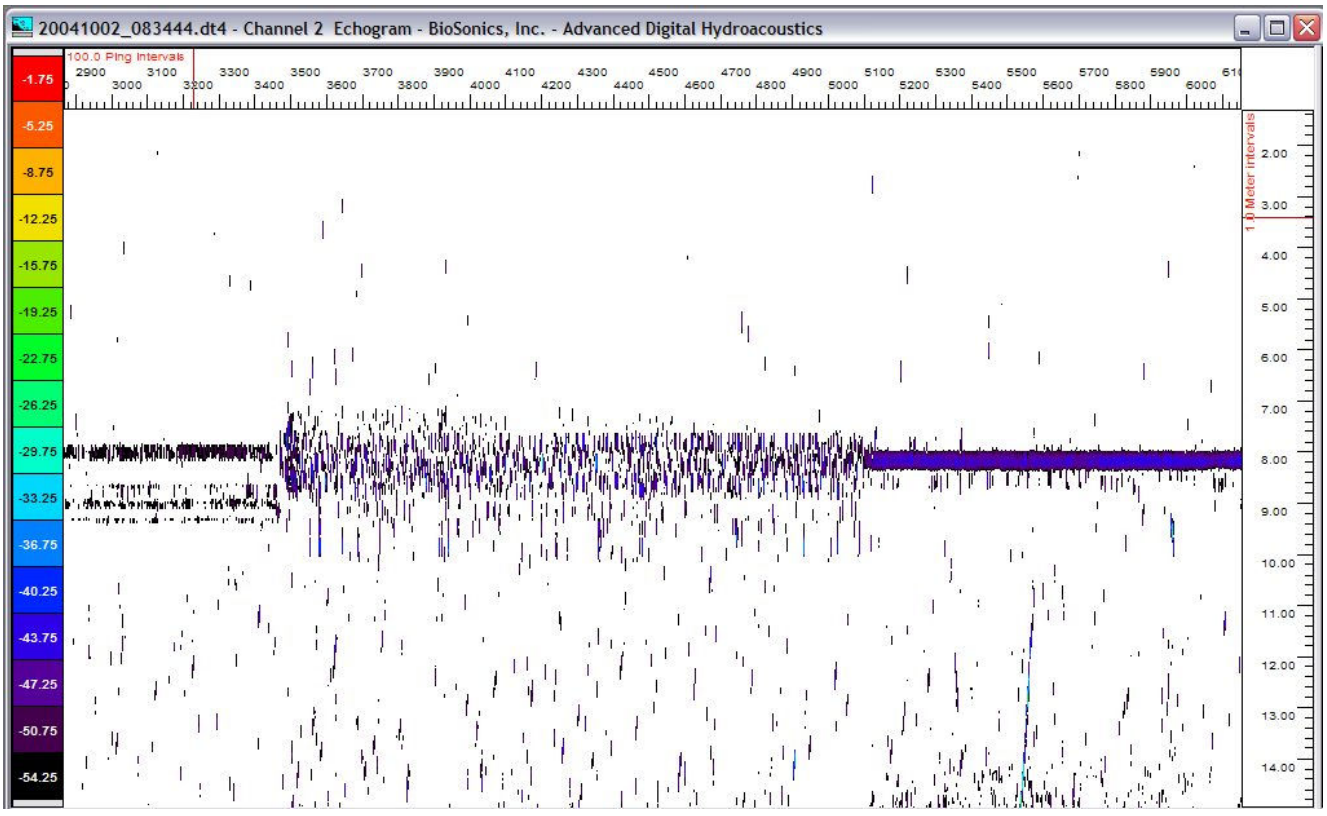

Figure 3. BioSonics "Visual Acquisition" software GUI

What to look for:

A fish is denoted by a connected series of two or more vertical lines of similar size, at least 0.3 to 0.5 meters in length; single lines and groups of lines less than .3 meters in length may be disregarded. Descending patterns indicate the target going away from the transducer. Ascending patterns indicate the target coming towards the transducer. A horizontal block indicates the target is moving parallel to the transducer or is stationary.

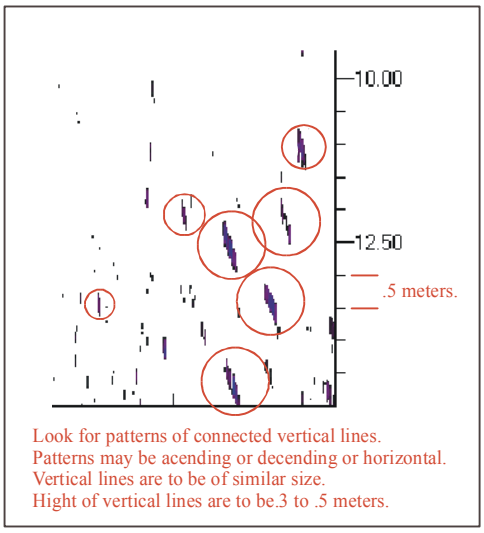

Figure 4. Fish patterns identified

Types of tests:

There are two types of monitoring tests: biological and engineering. The biological test consists of three sections: 10 minutes of baseline data are collected without the turbine spinning; the second part includes a 3 to 15-minute engineering test with the turbine spinning, and the last another 10 minutes of baseline data without the turbine spinning. These tests are designed to evaluate any effects that the spinning turbine might have on the fish movement through the water column before, during, and after turbine use. Ideally, these tests should be performed during full moon night and day and new moon night and day, both at flood and ebb tides because of different fish behavior at these times. Normal monitoring protocols include the collection of a video record; however the biological tests will be conducted at night even though underwater visibility is nil.

The engineering test consists of one ten-minute block of monitoring before and after a continuous series of engineering tests that may consist of the starting and stopping of the turbine.

Counting procedure:

For the purposes of responding to observed impacts, acoustic data are monitored in real time and fish counts from 3 range bins are tallied. The top section of the counting grid represents the region inboard of the rotor, the center region encompasses the rotational width of the rotor and is designated the at-risk area, and the bottom section is outboard of the rotor. During testing, a

count is recorded after each section is filled by the display. At-risk counts are tallied at the end of each test. Two conditions will result in termination of testing. If the mean at-risk count from a test is greater than 1.5 fish per minute, testing is discontinued until a 10-minute baseline test with no rotor rotation indicates that the at-risk numbers have dropped to below 1 fish per minute. Additionally, if any single at-risk observation is greater than 3 fish per minute, turbine rotation is stopped immediately until a 10-minute baseline count indicates that the at-risk value has dropped below 1 fish per minute. A spotter should note any injured or stunned fish downstream of the turbine and increased fish captures by cormorants within 30 meters of the turbine.

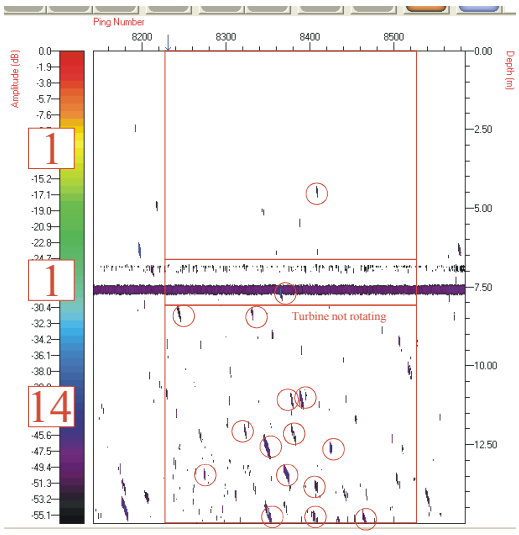

Figure 5. Screen Overlay Indicating Turbine Location

Transducers 1 and 2 of the DTX system are used for this real time monitoring, number one for the region west (inland) of the turbine and number two for the region east (toward ocean) of the turbine. DTX unit three is recording information that may be extracted at a later date with post processing. The statistician recording counts will need to monitor and record both displays. . A second person is required to start and stop the turbine and for monitoring of stunned or damaged fish. This person should also note any increased cormorant feeding activity immediately downflow of the turbine when it is spinning. During preliminary testing, feeding cormorants in the immediate area seemed unaffected by turbine activity.

Underwater Camera Observations

A third person is required to monitor a video display of an underwater camera aimed at the rotor in an attempt to view an actual fish strike. This image is recorded to a VCR for archive purposes. In accordance with U.S. Fish and Wildlife requirements, this person must be actively monitoring the video image from the underwater camera at any time the rotor is turning. Observations are also taken for several minutes pre and post-rotation. The observer will note time and VCR counter display at time of any item passing through the camera's view.

If a fish strike is observed (either by the DTX observer or the underwater camera observer). If a strike occurs the turbines will be shutdown immediately and all personnel will observe the area around the barge, and video system for 10-15 minutes or until there is a visual confirmation of the strike. If there is no indication of a severe strike test will continue as scheduled.

If a sever strike occurs, and the fish is located, a visual assessment of the severity of impact will be determined and a biologist will be contacted (#1 Kipp Powell, #2 Mary McCann, DTA Biologists 207-775-4495). If possible the fish will be collected and saved for assessment by biologist.

Environmental logbook:

An environmental monitoring logbook should be maintained during testing. Entries should start with the date and time of the observation and initials of the person making the entry. Notations of bird and fish activity, weather, temperature, time, name of observer, and turbine status should be entered on a regular basis. Even a lack of activity is notable. Local fishermen could be a source of information regarding fish population, and changes in activity noted or expected.

OBSERVATIONS SUMMARY

The following statements summarize the observations made during the Amesbury Tidal Energy Project.

1. No fish are observed in the video camera entering the turbine
2. In a vertical distribution, more fish are observed below the turbine then at the turbines depth
3. In a horizontal distribution, more fish are seen under the barge than beyond the turbines
4. In a horizontal distribution, a large number of fish are counted in the same plane as the turbine, but these are not corroborated by the video camera. The split-beam transducer is likely miscounting downstream turbulence as fish.